STUDY ON BLACKOUTS OF ETHIOPIAN ELECTRIC POWER NETWORK AND IDENTIFICATION OF SYSTEM VULNERABILITIES

A thesis submitted to Addis Ababa Institute of Technology, School of Graduate Studies, Addis Ababa University in partial fulfilment of the requirements for the ***Degree of Master of Science*** *in Electrical Power Engineering*

By

Moges Alemu

Advisor

Dr.-Ing. Getachew Biru Worku

School of Electrical & Computer Engineering

Addis Ababa Institute of Technology, AAiT

Addis Ababa University

Addis Ababa, October 2017

Addis Ababa University

Addis Ababa Institute of Technology

School of Electrical & Computer Engineering

Study of Blackouts on Ethiopian Electric Power Network and Identification of System Vulnerabilities

APPROVAL BY BOARD OF EXAMINERS

	Signature
1. CHAIRMAN DEPARTMENT OF GRADUATE COMMITTEE	
Mr. AMARE ASSEFA (MSc.)	_____
2. ADVISOR	
Dr.-Ing. GETACHEW BIRU WORKU	_____
3. INTERNAL EXAMINER	
Mr. KIROS TEFAY (MSc)	_____
4. EXTERNAL EXAMINER	
Prof. N. P. SINGH	_____

Declaration

I, the undersigned, declare that this MSc thesis is my original work, has not been submitted in part or in whole, at any other university and all sources, and materials used for the thesis work, and the organizations and individuals who contributed a lot during the development of this study have been acknowledged.

This research was conducted at Addis Ababa Institute of Technology under the supervision of Dr.-Ing. Getachew Biru Worku.

Submitted by:

…….

Moges Alemu Tikuneh

ID No.: GSR/2274/07

APPROVED FOR FINAL SUBMISSION

Dr.-Ing Getachew Biru Worku ……

Advisor's Name Signature

Acknowledgment

The success of this study is from a wide range of contributions. First and foremost, I would like to give all honour and glory to my Lord and Saviour Jesus Christ by Whom and in Whom I am who I am.

I would like to express my deep and sincere gratitude to my advisor, Dr.-Ing. Getachew Biru Worku for his extremely able guidance, constant help, inspiration and positive attitude during my study. Without his unremitting help, I would not have been able to complete this task. In addition, his comments to the entire development of what the research would look like and the contents to be covered in the study were very fruitful for making this thesis to come to be true.

I also wish to express my sincere thanks to Dr.-Ing. Fekadu Shewarega for all his patience, guidance and support. He gladly accepted to support and providing IEEE papers for literature reviewing. His guidance was starting from the inception of the idea. He kindly pushed me to do the best work, and his devotion to patiently guide me throughout the on-going stages of the research is really highly appreciated.

I would also like to thank Mr. Kiros Tesfay (PhD candidate) for providing me where to get the DIgSILENT PowerFactory software. He was not only providing me the technical reference manual of the software but also advised me to be dedicated and deterministic while doing my thesis. I also appreciate his friend Milkiyas (PhD candidate) for cooperating me while I installed the software.

My appreciation and gratitude also goes to the staffs and officials of the Ethiopian Electric Power, especially to those who work at National Load Dispatch Centre (NLDC) for feeding me the required information related to my study. Really, I cannot thank you enough.

I'm indebted to you all.

Abstract

The Ethiopian Electric Power (EEP) has been operating and managing the national interconnected power system with dispersed and geographically isolated generators, complex transmission system and loads. In recent years, with an increasing load demand for rural electrification and industrialization, the Ethiopian power system has faced more frequent, widely spread and long lasting blackouts. To slash the occurrence of such incidents, analysing the reasons and the mechanisms of these blackouts is the first step in this direction.

In this study the causes, mechanism and extent of the past blackouts in the EEP grid are investigated. This is accomplished by collecting the blackouts data from the National Load Dispatch Centre (NLDC) archive. These data are characterized based on four significant indices, namely- number of customers without service, loss of load (MW), duration of blackouts, and their severity level. The investigation is made by considering the following sequential phases of the blackout: system condition prior to the power failure, initiating events, cascading events and the final state of the power system.

Based on analysis of the available data, it is found that the major initiating events for the blackouts of the Ethiopian power grid are short circuits, overloads, loss of generations, protection and communication system failures, switching and temporary transients. It is further observed that 49 blackouts were happened on the national grid from 28th January 2013 to mid of May 2016. It is also found that the highest load loss of 1401.04 MW, which occurred on 28th November 2015. The 27th July 2015 blackout duration was the longest and it lasted for about 22 hours. Furthermore, it is observed that 81.25 % of the blackouts (26/32) are having a severity level of 10 to 100 system-minute. These are classified as “Severe” and the remaining 18.75 % of the blackouts (6/32) are having a severity level of greater than 100 system-minute and are classified as “Very Severe”.

Simulations studies are carried out using DIgSILENT PowerFactory software to further investigate the initiating events resulting in cascaded tripping and subsequent blackouts. In the first stage, power flow simulation studies are carried out to analyse the system performance

under steady state conditions and to determine the voltage magnitude at critical buses and the loadings of lines, transformers and generators prior to the disturbance. In the second stage, time domain Root Mean Square (RMS) simulations are performed to analyse the system performance under transient conditions for the specified initiating and cascading events. A vulnerability analysis was performed using indices called active power performance index (PI_p) and voltage performance index (PI_v). These indices provide a direct means of comparing the relative severity of the different line outages on the system voltage profiles and loadings.

It is found that the line outage of Debre Markos_Sululta 400kV line is the most severe line outage having a line loading performance index of 7.3238 pu. The outage of this line resulted in the overloading of eight components. On the other hand, the outage of Alamata_Combolcha 230kV line is found to be the most severe line with respect to the voltage performance index (PI_v) of 0.1124 pu. Based on this analysis, it is found that the most vulnerable buses of the network in respect of voltage limit violations are Sululta and Gefersa 132kV buses. It is further observed that 11 different line outages led Sululta and Gefersa 132kV buses to have voltage magnitudes of below 0.90 pu. The highest percentage voltage deviations for these buses are -14 % and -13 %, respectively. Furthermore, it is found that the network element's most vulnerable to overload is the transformer at Combolcha II 230/132kV substation, in which 12 different line outages led this transformer to become overloaded.

Finally, from the simulation results and system vulnerability analysis, we identify the remedial steps to coordinate and focus control actions that could mitigate the consequences of the disturbances and reduce the risk of cascading events leading to system blackouts. It is recommended that proper protection system coordination, high-speed fault clearing, proper planned interruptions as well as adhering to the security rules and criterions during planning and operation of the power system are the remedial measures that could be explored by EEP

KEY WORDS: Power system blackouts, Blackout indices, Cascading failures, Transient stability, System vulnerability, Contingency analysis.

Abbreviations and Nomenclatures

AP	Affected Population
DIgSILENT	Digital Simulation of Electrical Networks
EAPP	Eastern Africa Power Pool
EEA	Ethiopian Energy Authority
EEP	Ethiopian Electric Power
EEU	Ethiopian Electric Utility
EF	Earth Fault
EMS	Energy Management System
EPS	Electric Power System
FDRE	Federal Democratic Republic of Ethiopia
GG	Gilgel Gibe
GoE	Government of Ethiopia
GTP	Growth and Transformation Plan
HPP	Hydro power Plant
I/S	in service
NLDC	National Load Dispatch Centre
OC	Overcurrent
OF	Overfrequency
ONAF	Oil Natural Air Forced
ONAN	Oil Natural Air Natural
O/S	out of service
OV	Overvoltage
PI	Performance Indices

PI_p	active power performance index
PI_v	voltage performance index
PLC	Power Line Communication
PLCC	Power Line Carrier Coupling
pu	per unit
RK	Runge-Kutta
RMS	Root Mean Square
RTU	Remote Terminal Unit
SCADA	Supervisory Control and Data Acquisition
SLG	Single Line to Ground
s/s	substation
SVC	Static Var Compensator
SVI	Severity Index
TE	Tripping Event
TSRUP	Transmission and Substation Rehabilitation and Upgrading Project
UF	Underfrequency
UFLS	Underfrequency Load Shedding
UL	Unserved Load
UV	Undervoltage
UVLS	Undervoltage Load Shedding
VI	Vulnerability Index

Table of Contents

List of Figures

List of Tables

Chapter 1

Introduction

1.1. Background

The past decade has witnessed a turnaround in Ethiopia's electricity sector. Between 2005 and 2012, electricity services were spread to 7,000 towns and rural villages from the initial 648, and the number of electricity customers reached over two million from 800,000 at the beginning of the period [1, 2, 3, 4, 5]. Accordingly, demand for electricity grew at more than 15 percent per annum [4]. The steep growth in the electricity sector introduced significant constraints in the Ethiopian Electric Power Corporation (EEPCo)[1], the vertically integrated utility, both with regard to infrastructure development and management. These constraints are of from various points [2, 5]:

- While the Government invested heavily in new power generation capacity, the extension of transmission and distribution infrastructure has not kept pace with demand growth and the scaleup of generation capacity.
- The expansion of the network has not been accompanied by an equal effort to increase connectivity. The GoE defined electricity access targets based on coverage of the network rather than connection to or use of electricity services. Connections have lagged behind for several reasons, including the absence of a robust program and dedicated resources to roll out connections; affordability issues; and capacity constraints at the utility level in handling a growing customer base.
- Such steep growth in electrification can only be pursued in the context of a well-organized and efficient electricity sector, which is not yet the case in Ethiopia. EEP and EEU are overstretched with the implementation demands of numerous large-scale projects and challenging operational issues; they lack critical capacities needed to handle the complex challenges facing the energy sector.

[1] *In 2013, the GoE resolved to unbundle EEPCo into two public enterprises: (a) the Ethiopian Electric Power company (EEP), responsible for the generation and transmission sub-sectors; and (b) the Ethiopian Electric Utility (EEU), responsible for power distribution, sales and implementation of the Universal Electricity Access Program (UEAP) [2]. In addition, the GoE established a federal electricity sector regulator, the Ethiopian Energy Authority (EEA), which replaced the Ethiopian Electricity Agency [2, 4].*

— The electricity tariff, which is among the lowest in the world, compounds the problem and poses a major constraint to scaling up electricity access. Given the significant depreciation of the Ethiopian Birr over the years, the average electricity tariff stands now at US$0.0245/kWh [2].

The government of Ethiopia (GoE) places electrification at the core of its development agenda. Expanded and more reliable access to electricity is instrumental to the structural transformation of Ethiopia's economy and society, including massive poverty reduction and a shift toward higher productivity rates and industrialization. Therefore, the GTP I aimed to reach universal electricity access in the country in the medium term as well as to position Ethiopia as a power hub in the Eastern Africa Region. The Plan included clear and ambitious sector targets, most notably that of doubling the number of electricity customers from two to four million [2, 5]. The GTP II has set an even more ambitious target: to reach seven million customers by 2020 [2]. During the period of GTP I, Ethiopia has made major strides in increasing the national power generation capacity. Large-scale hydropower projects, most notably the Grand Ethiopian Renaissance Dam Project (6,450 MW) and the Genale Hydro Power Project (254 MW), are in advanced stages of construction [1, 2]. Also, wind power projects (Adama 1&2 and Ashegoda), for a total capacity of 324 MW, have started generating electricity, along with Gibe 3 hydropower plant (1870 MW) [2].

The main high voltage levels of the power transmission lines in the EEP grid are 400 kV, 230 kV and 132 kV. Among them, the 400 kV and 230 kV transmission lines are the most important lines, for the power flows and interconnecting seven regional power systems: North, North West, South, South West, West, East, Addis Ababa & Central regions. The electrical network is extended to Djibouti on the East and the Republic of Sudan to the North West and consists of 1071.76 km of 400 kV circuits, 5895.54 km of 230 kV circuits and 4666.79 km of 132 kV circuits [2]. The main high voltage transmission grid of the EEP system is shown in Figure 1-1. The national load dispatch centre (NLDC) has the jurisdiction to control the high voltage substations, transmission lines and the power plants. Currently, the total installed generation capacity is reaching over 4300 MW and the peak load in now come up to 2164 MW.

Because of the high economic development tempo in Ethiopia in recent years, the total load has increased continuously and its power system has been extended accordingly. Nowadays, the Ethiopian power system has suffered partial and total blackouts [6].

Blackouts, which refer to power outages affecting a specific area for a given period of time, are a well-known phenomenon in power systems operation across the world. However, the Ethiopian Electric Power used this term in two ways viz. (1) When this loss of electricity encompasses one or more regions, and (2) when the loss of electricity encompasses the whole parts of the country. The phenomena in (1) is called **"partial blackout"** and in (2) is called **"total blackout"** [6].

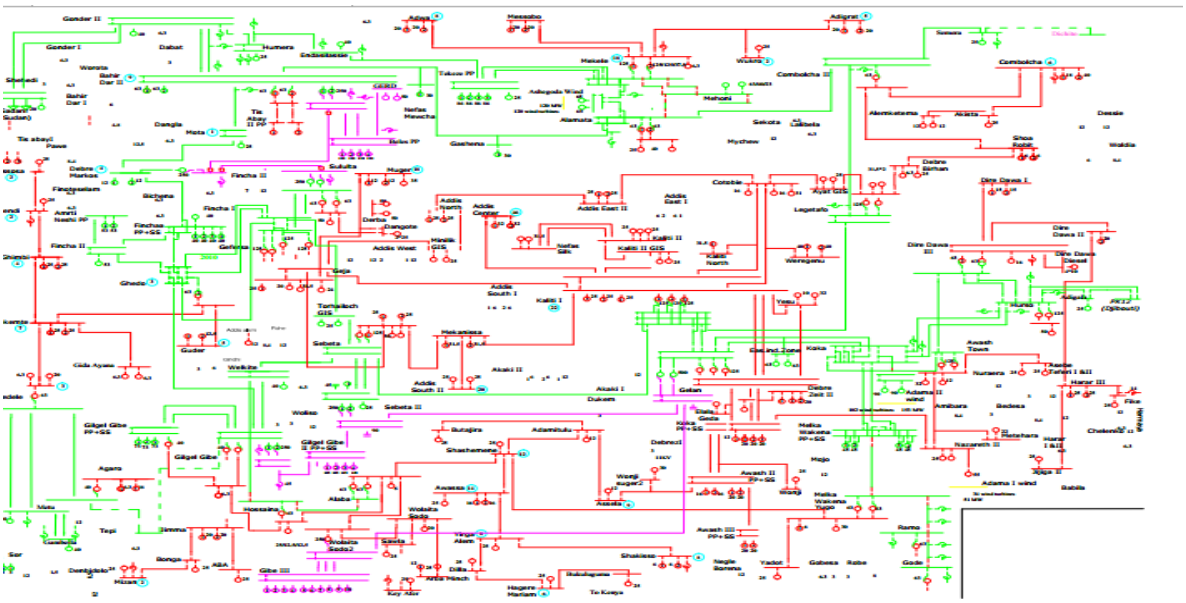

Figure 1-1 The main high voltage transmissions of EEP [7]

In Ethiopia, the system's vulnerability to physical disruptions from technical problems and other causes has not been studied in a concrete way. However, the system vulnerability has increased in recent years because of the explicit and implicit reasons, thereby reducing the system's tolerance against deteriorated, failed, or unavailable system components. In this study, the partial and total blackouts in the Ethiopian electric power network that occurred since 2013 to 2016 are investigated**.** Following this, the system vulnerabilities are highly rectified and from which the mitigation methods of these disturbances are proposed.

In one of the few studies conducted in Ethiopia, the World Bank surveyed on 2011 showed that the frequency of the power outage (number of days per year) was 100 days that lasted an average of about four hours [8]. While this study was completed in 2012 and much has changed since, power outages are still an obstacle for sustainable development that heavily depends on reliable power. The Monitoring and Evaluation bureau of Ethiopia also stated, "Power failure and fluctuations are getting worse even in those industries which the government has allotted mobile power-substation and in those factories that have gotten dedicated power line. And replacing and renovating these will take longer time and huge resources which the country cannot do it within the GTP II period" [9]. Moreover, this report indicated that the power outage would continue to be a challenge for the Ethiopian manufacturing sector under GTP II. Therefore, analyzing and studying the reasons and the mechanisms of these blackouts would be the first step for mitigating blackouts and so, this study aims at evaluating these blackouts in the Ethiopian power grid and draw their common characteristics and propose remedial measures.

1.2. Problem Statement

The Ethiopian Electric Power System has been operating and managing the national interconnected power systems with dispersed and geographically isolated generators, complex transmission lines and loads. These power systems are dynamic in nature, with network topology changing frequently with load demand. Today, however, the aged but scattered infrastructure combined with an increasing demand in domestic electricity consumption and industrialization, ~~e~~xtremely has become vulnerable to even small-scale disturbances, leading to partial or total blackout. Different blackouts have been occurred in Ethiopian electric power system at different times. As obtained from the NLDC archive, there were 49 blackouts happening on the national grid from January 2013 to mid-of May 2016 [6]. During these most severe forms of power outage, tremendous societal consequences and substantial economic loss would have been incurred and therefore, blackouts could affect the industrial and socioeconomic development of the nation and would be the impediments for the country to meet the short and long-term development plans.

This has become a problem that needs to be solved through research. This motivates the idea of investigating and analysing the past blackouts in the Ethiopian electric power network, identifying the system vulnerabilities and proposes methods for mitigating blackouts that may arise in the future.

1.3. Objectives

The general objective of this study is to investigate the major blackouts that occurred in the past and to identify system vulnerabilities and finally to propose the mitigation methods to reduce such disturbances that may cause blackouts in the Ethiopian electric power network.

The specific objectives of this research are as follows:

- To analyse the root cause of these blackouts.
- To identify the sequence of events and linkage of the causes/outages to specific system weaknesses (technical problems like breaker not fast enough, protection coordination problems, incorrect planned interruptions).
- To identify the system vulnerabilities;
- To indicate the severe line outages and weak points of the Ethiopian electric power system.
- To develop methods to cease the possibility of future blackouts and/or system collapses.

1.4. Literatures Review

In recent decades, with the increasing expansion of power system capacity and scale of interconnection, an increasing number of major blackouts caused by unpredictable cascading failures have occurred around the world. These blackouts have attracted increasing attention to cascading events that may cause a serious power system collapse. Cascading failure, usually induced by an initial disturbance such as a short-circuit

line switching or generator tripping; generally, result in a continuous outage of available components in an electrical power system [10].

Cascading failures present severe threats to power grid security, and thus vulnerability assessment of power grids is of significant importance. *Vulnerability* is a measure of the system's weakness with respect to a sequence of cascading events that may include line or generator outages, malfunctions or undesirable operations of protection relays, information or communication system failures, and human errors [10].

In other words, major blackouts often involve a sequence of cascading events. One event may create an operating condition that triggers another event. In an outage scenario, a line fault can cause rerouting of the power flow, leading to overloading of other lines. The overloaded lines may be tripped by impedance relays due to the low voltage and high current operating conditions. Line outages may also cause low voltage and high reactive power demand on nearby generators [11].

As was explored by Dobsona et al [10] occurrence of large blackouts usually results from series of cascading failures. In some cases, a single failure in the system can trigger other failures across the network, pushing beyond operational limits. The protection layer in the power system is designed to prevent these kinds of events, while preventing permanent damage to expensive equipment. However, sometimes the indiscriminate actions of protection schemes remove components out of service that make the system even weaker. Figure 1-2 shows the cycle of cascading failures. Due to overloading, faults, or other circumstances, a particular component is taken out of service. In doing so, power is redistributed based on circuit laws. As a result, other components might get overloaded causing them to be taken out of service by the protection relay signals. The cycle repeats, usually in quick sequence, that operators are not able to manage the situation [10, 12].

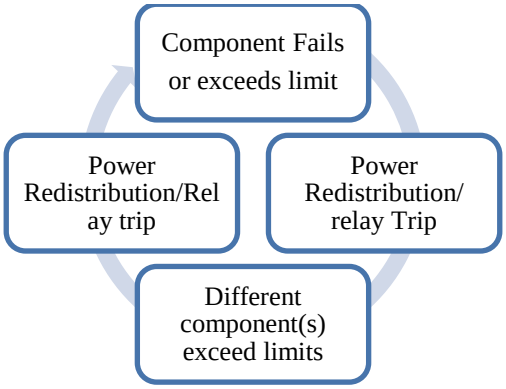

Figure 1-2 Cycle of cascading failure [12]

These types of events most likely occur following sequential outages on a stressed system, when the system is operated marginally in compliance with planning criteria. If a system is stressed and system and equipment are removed without sufficient levels of adjustment or when faults occur, the chain of events

starts. For example, some generators and/or lines are out for maintenance, line trips due to a fault. Other lines get overloaded start to sag, and another line gets in contact with a tree and trips. There is a hidden failure in the protection system (e.g. out-dated settings) that causes another line or generator to trip. At that stage, power system is faced with overloaded equipment, voltage instability, transient instability, and/or small signal instability. Based on the power system condition such as the operating reserves and equipment availability, the severity of the disturbance may cause parts of the power system to be islanded, loose synchronism, and even enter a complete blackout. If fast actions (e.g. load shedding, system separation) are not proactively taken, system cascades into unplanned islands [13].

Evaluation of worldwide disturbances show that protection systems have been involved in 70% of the blackout events [13]. Inadequate or faulty alarm and monitoring equipment, communications, and real-time information processing can further exacerbate disturbances in the system. Human error or slow operator response are also other major contributing factors leading to cascading outages [14].

Arulampalam et al [16] summarizes the history of major and properly reported blackouts in the world. It also discussed the detail analysis on root cause of blackouts and the follow up action, which were taken at the time of occurrences. The paper also discussed some technical information related to how a blackout occurs and which parameters have to be monitored to predict the next possible cascading step of the blackout. It was also noted that events far from each other might cause cascading failures such as the Sweden -Denmark outage [16, 17]. For this reason, studies and recommendations have been made to encourage wide area monitoring systems (WAMS) that report on issues across large areas. WAMS gives operators the ability to view counteracting events that might appear geographically and electrically too far to affect each other [16, 18].

One of the most widely used methods of curbing blackouts is load shedding, in which power is disconnected to some load in a bid to save the rest of the system. However, even load shedding has been found to be ineffective unless it is pre-planned and automatic since cascading events happen too fast for operator action [10, 19]. Automatic actions fall under the control and protection systems, which often might cause more problems. With every component taken out of service, the system is weakened and more susceptible to blackouts [19]. To minimize unnecessary tripping of lines, new protection schemes are being developed and implemented including adaptive protection. Adaptive protection is able to adjust settings in real time based on information from different sensors such that unnecessary trips can be prevented by altering relay settings on the fly [20].

Communication network failures were also blamed for the 2003 US-Canada blackout leading to a call for strengthening and adding redundancy to communication networks as well as putting in place procedures for utilities to act based on failures in neighbouring networks [18]. Redundancy in the communication and

control networks ensure that failures would not go unnoticed and actions would be taken in time to prevent cascading outages.

J. Barkans et al [21] also studied the emergency processes that have occurred in the world‘s power systems since the second half of the 20th century from the viewpoint of adequate protection means to be created. The problem of stability loss caused by short-circuits should be related to the fulfilment of security standards, since the achieved level of transmission grid protection allows for its fast action, practically excluding the occurrence of blackouts (also of those resulting from stability loss due to circuit-breaker and protection failures). In the cases when these standards are not met, this task is delegated to the local and centralized protections with the turbine load relief functions [21]. From the findings of [21], the primary cause of power system blackouts is the transmission grid overload that triggers the development of cascading processes. The authors proposed that momentarily removal of the overload and automatically restoring of the normal system operation are the methods of protecting complex blackouts.
In the 2003 Blackout in the US and Canada, the events started with the outage of a generating Unit in Ohio, whose load was carried by neighbouring generators that were already operating near their limits and producing high reactive power. Further trips of generators and a transmission line pushed the system further towards its limits. Because of a failure in the alarm software, this was not noted in time by the operators to take action, and the next failures cascaded into an unrecoverable blackout that left 63 GW of load unserved [16, 19].

In Sweden and Denmark, their 2003 blackout started with the failure of a nuclear power plant that was taken out of service. Interestingly, an outage on a line 300 kilometres away a few minutes later triggered a cascade of failures due to very high power transfer from the north to the southern regions that overloaded the remaining lines, ultimately leading to voltage collapse with 4700 MW of load lost [19].

In Italy, a tree made contact with a line connecting to Switzerland that caused a fault and tripping of the line. Parallel lines were overloaded and subsequently tripped. This cascaded to more lines, leading to loss of synchronism of the Italian power system to the rest of the Europe. Further outages led to 6400 MW of load losing supply [16, 19].

In light of these and other blackouts, several mechanisms are being put in place to curb the occurrence of similar events. In decentralized energy markets in the West, a lot of geared toward is on policy, standards, and regulation. The committee that reported on the 2003 US-Canada blackout reported that regulations ought to be mandatory and clear as some players had circumvented standards and as such left the system vulnerable [18].

These blackouts have a great impact on citizens, businesses, the economy, and the government. While such blackouts are rare (though, in Ethiopia this phenomenon is occurring on an average of 14 blackouts per year for the study period) [6], they pose a substantial risk to the security and economic health of the country.

In Ethiopia, the government has sought means to alleviate energy shortages and blackouts by constructing new generation plants and by importing and using mobile substations to improve the system reliability. While generation has been at the forefront of energy developments in Ethiopia, attention to the weaknesses in the transmission network are not receiving their due attention. These weaknesses affect the customers, the government and the economy and social welfare of the country as a whole since a poor network is serving it. This fact made the national grid to be vulnerable to blackouts even though generation might increase. The GoE has developed some local generation capacity by installing diesel plants around the capital, Awash 7 killo and Dire Dawa and other renewables in the rural areas funded through the World Bank and ushering in the idea of distributed generation, which uses dispersed generation units close to consumers.

At this point, it is important to reiterate that this study focuses on Ethiopia, whose grid is significantly different from that in the United States or Europe in its size, major concerns, and application. A study of blackouts, being a relatively new field is receiving most attention in developed countries and as such, most of the research and concepts are based on experiences far away and different from Ethiopia's electric power network. Nonetheless, important lessons can be drawn from these various works, and as will be described, can be applied to the specific case of Ethiopia.

1.5. Scope and Significance of the Study

The scope of this study is to investigate the causes of blackouts in the Ethiopian electric power systems and identify the linkage of these causes to specific system weaknesses. With these system weaknesses computer simulations (by using DIgSILENT PowerFactory software package) for some selected blackouts are performed to corroborate whether the suggested causes could possibly have caused the previous system collapses. This in turn helps us to identify the system vulnerabilities and propose solutions to mitigate the occurrence of blackouts. The blackouts that occurred from January 2013 to May 2016 in the Ethiopian power grid are analysed.

The investigations carried out in this thesis may be useful for power system operative personnel in reducing the frequent occurrence of blackouts and thereby improving the reliability and security of the Ethiopian electric power system. Moreover, researchers may use it as a reference for further study in this area and it may be useful to transmission substation personnel and protection engineers of EEP for protection and control of power systems.

1.6. Research Methodology

Study Areas

The areas that are likely included in this study are the high voltage networks, i.e., sub transmission and transmission systems, generation plants and transmission lines under the Ethiopian Electric Power network. The main reason to select these power plants, substations and transmission lines is that the health and power supply security of the national grid greatly depends on the normal and stable running of these circuits.

Data collection

The main data for this research is obtained from the grid disturbance reports of the National Load Dispatch Centre (NLDC) in the Ethiopian Electric Power. The data were collected from February 2016 to mid-of July 2016. Techniques such as interviewing and review of records and/or reports are employed. The sequence of events observed on the SCADA for some disturbances were taken from the NLDC archive. Literature reviewing was also used to get a further insight about the topic and the methodology of analysis of blackouts.

Data Analysis, Modelling and Simulation

The data, in general, was analysed qualitatively and quantitatively through descriptions and simulations. The plan for data analysis was done in two phases as follows:

Phase I: Analysis and systematic collation of blackouts data for the last three and half years

Since the report obtained from NLDC was poorly organized, in this step, the raw data were organized and put it into context. In organizing the raw data, the following procedures were used: For each blackout (specific fault location, type of fault, specific date, time)

- The sequence of events (what exactly happened)
- The effects of the faults (the scope and extent of the disturbance) and
- The causes of the disturbances were examined.

Phase II: Analyses and organizations of blackouts data to make it suitable for modelling and simulations.

- **Modelling**: The modelling of single line diagram (SLD) of the interconnected power system is used. The different components of a power system network (transmission lines, generators, loads, transformers, etc…) were modelled by using DIgSILENT PowerFactory software.

- Computer simulation was performed to analyse the current Ethiopian Interconnected System (ICS) with regard to the physical phenomena (transient instability) for different disturbances and contingency scenarios. Vulnerability analyses were performed and the line loading and bus voltage violations were screened for evaluation of the network weaknesses. Mitigation techniques were also proposed from the technical examination of blackouts and from the vulnerability analyses.

1.7. Organization of Thesis

Chapter 1 gives a general introduction of the study, statements of the problem, the objectives and the research methods and procedures used for this thesis. Chapter 2 focuses on the literatures reviewed. Chapter 3 presents the major grid blackouts of the Ethiopian electric power, their analyses, classification, impacts and the lessons learned from the past blackouts. In this chapter, some international blackouts were also considered to make them as a benchmark for the study of the blackouts of the Ethiopian electric power system. Chapter 4 determined to delve deeper into the details of network models in power factory for power system analysis and simulation results while Chapter 5 discusses about system vulnerability identification methods, and detail contingency analysis of the Ethiopian power system is also explored including comparing the results in tabular and graphical ways to determine the weakest areas of the network and showed ways for mitigating the likelihood of future blackouts. Chapter 6 summarizes the conclusions based on the work carried out and provides suggestions for future work. Finally, a list of bibliographies used, and appendices of network data and simulation details are given.

Chapter 2

Blackouts in Electrical Power Systems

2.1. Introduction

Shahidehpour et al [22] described a blackout as a major incident happening on the power system, which can be characterized by its geographical scale, depth, and duration. The depth is related to the number of not supplied customers, or in other words, to the geographical density of customers. It is then related to the load that is lost during the incident. The combination of geographical scale and depth determines the importance of the blackout: small-scale (partial) blackouts and large-scale (total) blackouts. The duration directly quantifies the severity of the incident and its consequences, particularly in terms of cost. It also gives indications on the difficulty for operators to restore their power system [22, 16]. Moreover, a blackout always results from an initiating event (sometimes more) and worsening factors. Some of these initiating events and worsening factors are:

- Natural Factors. Storm, landslide, lightning, contact between line and tree (lack of trimming), animals, and so on.
- Technical Factors. Short circuit, component failure, heavy load, maintenance of key equipments, breakdown with age, and so on.
- Human Factors. Switching mistakes, erroneous or inadequate communications between operators, lack of training especially for emergencies, and so on.

The combination of some of these factors can lead to a snowball (or domino) effect and then to a catastrophic situation. To avoid this, transmission system operators (TSOs) operate the power system according to different states, as shown in Figure 2-1.

The power system works under two principal types of constraints [23]: constraint of providing electricity to customers and operating constraints. The first type imposes that all the customers must be supplied, and the second type requests that all the system variables (frequency, voltage, line currents, etc.) have to stay in their authorized range.

The system is in normal state if the constraint of providing electricity to customers and the operating constraints are satisfied. The system is in emergency state if some operating constraints are violated. This can be provoked by a perturbation that leads some system variables to go out of the limits. If the intervention

actions of the operator are able to bring back the variables in the limits, the system will preserved and goes to the alarm state. The system is in alarm state when the constraint of providing electricity to customers is not entirely satisfied (a part of the customers is not supplied). The system is in extreme state if both types of constraints are violated.

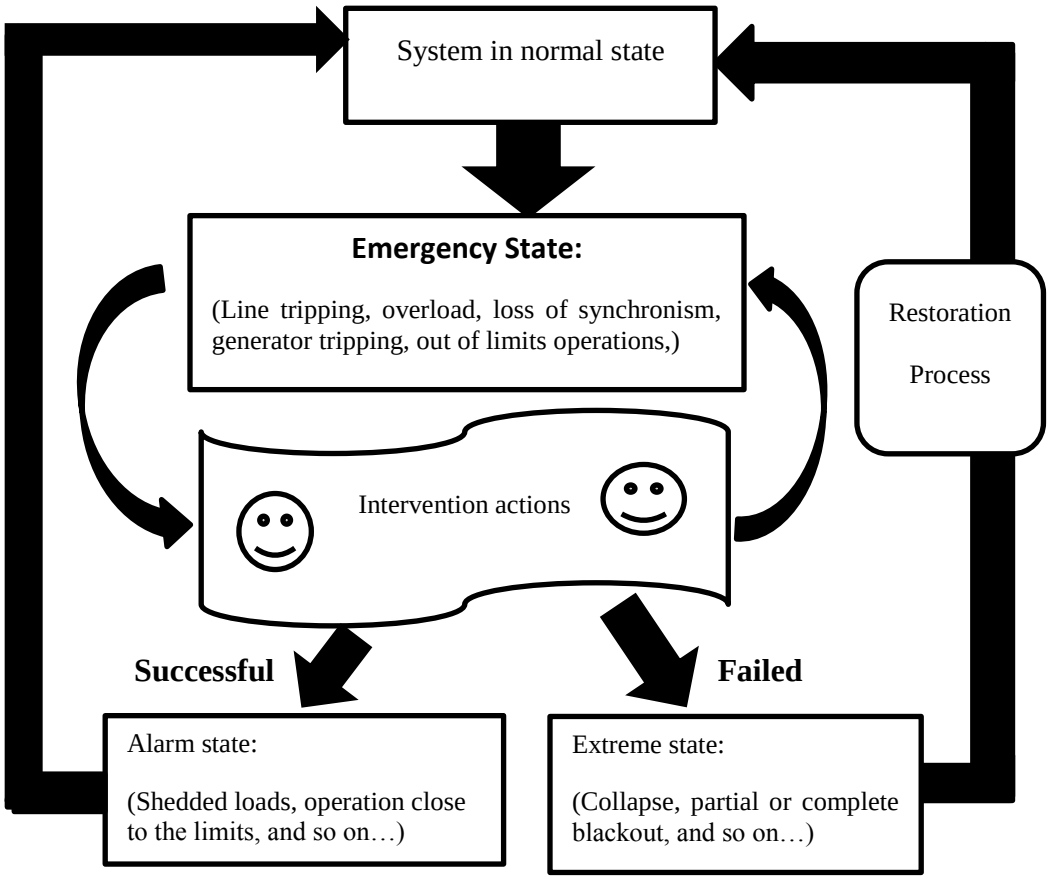

Figure 2-1 Operating states of the power system [23]

Blackouts in electrical grids are not uncommon, especially on small scales. These outages are sometimes considered tolerable if they occur infrequently. This is however changing, as many applications are very sensitive to power loss such as medical, military, telecommunication, or even food processing applications and other businesses as well. Even then, it is not the small outages that have most worries, but the large-scale ones that have dire socio-economic ramifications. In North America, these types of outages are well-documented, the most recent being the blackout of 2003 that took out about 61,800 megawatts (MW) affecting fifty million people, some for days [18].

2.1.1. Reasons and Mechanisms of Blackouts

The power system may enter into an emergency condition due to some critical events that may happen in the system. Usually, the system can be pulled back to normal condition by its protection and control system [22]. However, sometimes, the system cannot return to the normal conditions in a good time and some new events can trigger the cascade incidents, which may interact and rapidly worsen the situation. Finally, blackout can happen.

Veropai et al [24] described the mechanism of blackouts in Figure 2-2. According to this analysis, there are five types of faults that cause blackouts: voltage collapse, frequency collapse, cascading overload, system separation, and loss of synchronism.

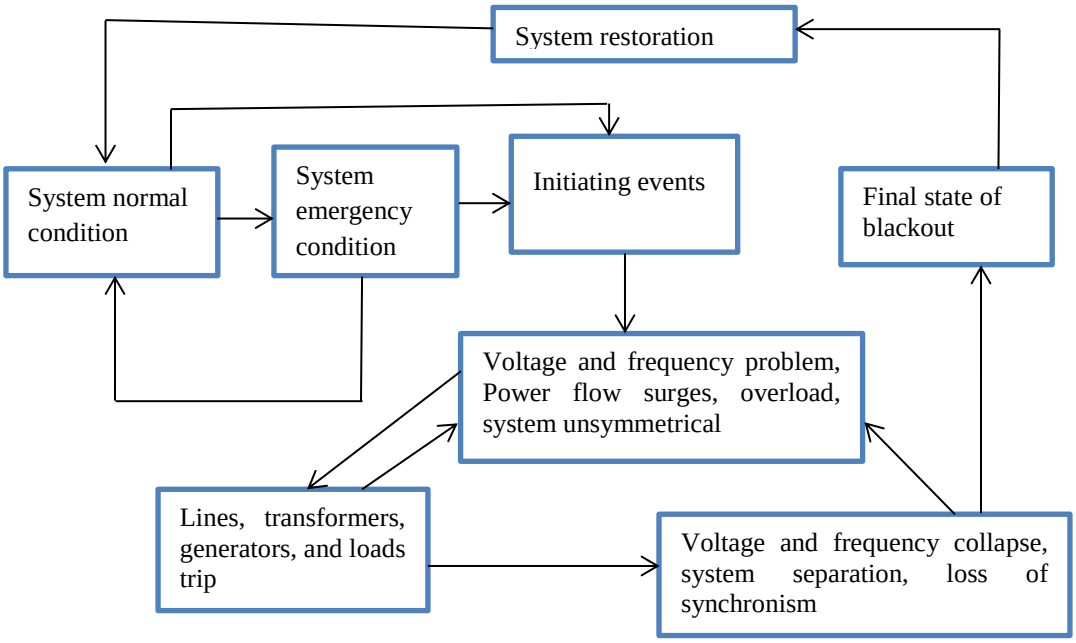

Figure 2-2 Mechanism of blackouts [22]

a) **Voltage collapse:** lines, transformers and/or generators tripping, and consumption disturbance cause the voltage collapse. If there are not enough reactive power reserves in the system, the voltage drops, which cause cascading overload of the lines and transformers and accentuates the voltage to decline.

When the voltage is below the thresholds of under voltage protections of the generators, they trip and the lacks of reactive reserves are worsened. At the same time, overcurrent protections of lines may also trip and the voltage drops more and more: the blackout happens. The duration of voltage collapse is about some

minutes. FACTS, reactive resources and under voltage load shedding, can help voltage return to normal condition (Figure 2-3)

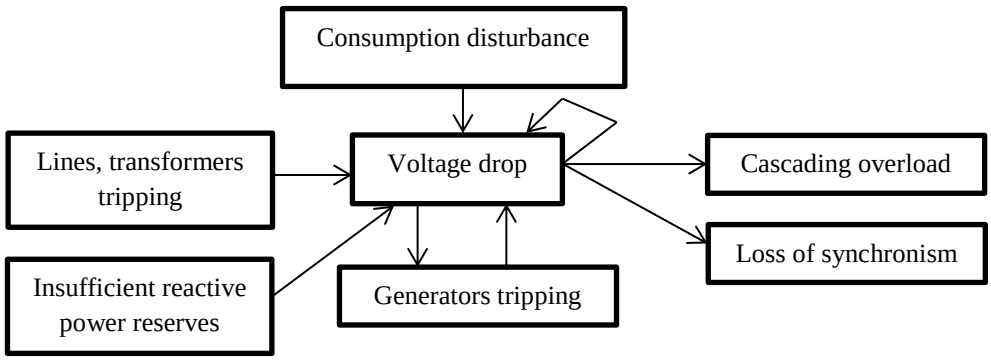

Figure 2-3 The mechanism of voltage collapse [25, 26]

b) Frequency collapse - unbalance between production and consumption appears, insufficient active power reserve in the system and generator tripping cause the frequency collapse. Facing these events, the power system uses the primary active reserve to keep the frequency in the limited operating range. If there is not enough primary reserve, the frequency can go out of the limits. The underfrequency protections of generators provoke their cascade tripping and, consequently, the acceleration of the frequency collapses. It happens in some seconds and can be stopped by underfrequency load shedding (Figure 2-4).

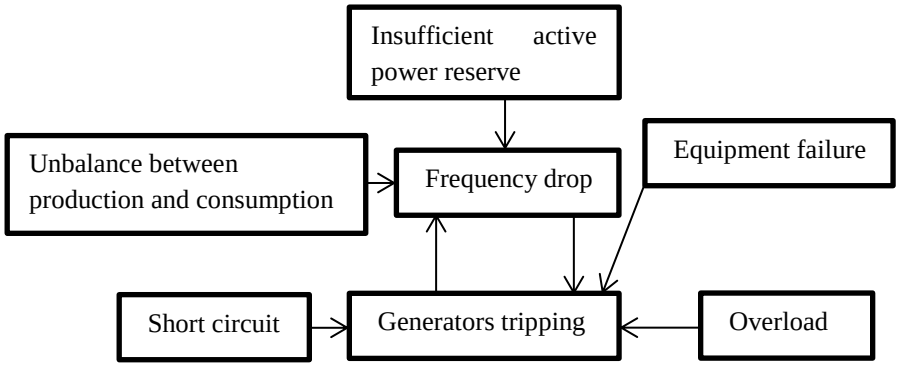

Figure 2-4 The mechanism of frequency collapse [25]

c) Cascading overload. When the power system is stressed, the power flows are close to the limit of the lines transmission capacity. A heavily loaded line can sag close to trees due to overheating, which may, in the long run, provoke a flashover. Therefore, the protection relays of the line disconnect it and its power flow is shifted onto others lines in the neighbourhood.

A line can also be tripped by its overload protection. The power transfer on the other lines may cause them to be overloaded and also tripped by their protection devices and the cascade begins. The system enters into voltage collapse, frequency collapse then loss of synchronism or system separation and finally, the blackout happens. The duration of the cascading overload is from some minutes to some hours. A way to avoid the cascading overload is to use FACTSs, which can change the load flows and relieve the power flows in some critical lines. Load shedding can also help relieve the stress of the system and stop the cascade (Figure 2-5).

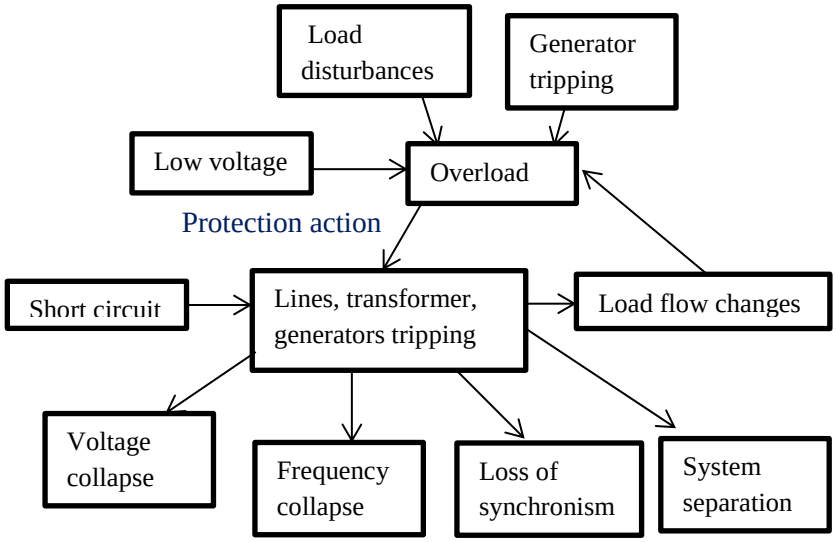

Figure 2-5 The mechanism of cascading overload [22]

d) System separation - When the grid loses some critical lines or transformers, the system is separated. In each isolated subsystem, an unbalance between production and consumption may appear. If the system operator cannot keep the system balance in these subsystems, a voltage or frequency collapse causes a blackout. Load shedding can keep the balance between load and generation in the isolated subsystems (Figure 2-6).

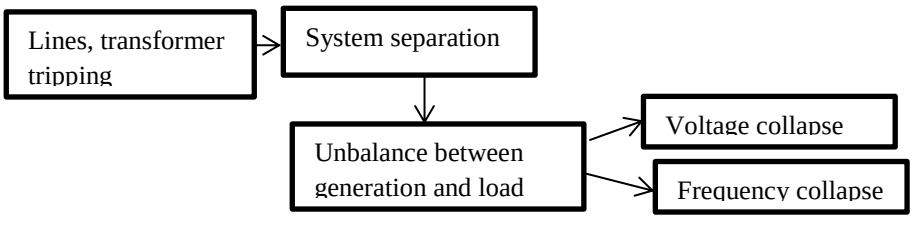

Figure 2-6 The mechanism of system separation [24]

e) Loss of Synchronism- Let us consider two power systems linked by interconnection lines. If one of these lines trips, the others may be overloaded. Unbalance between production and consummation appears and the frequency became different between the power systems. Power oscillations appear on the interconnection lines and the protection system reacts. Finally, the systems split. A short circuit that makes the generators angle exceed 90^0 can also cause the loss of synchronism. To avoid loss of synchronism, load shedding can keep the balance between load and generation and FACTS can be installed in some critical interconnection lines to stop power oscillation spreading (Figure 2-7).

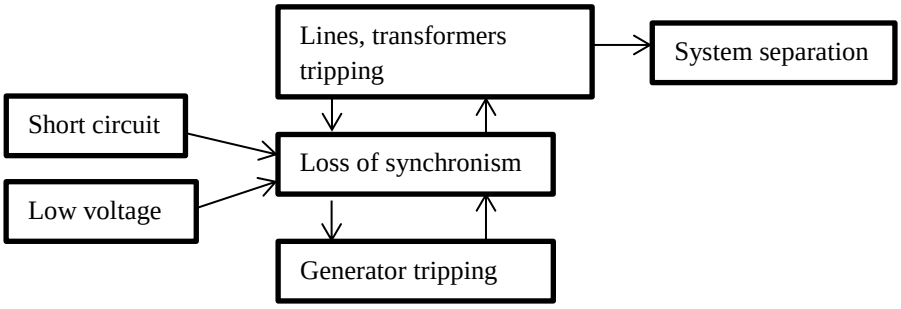

Figure 2-7 The mechanism of loss of synchronism [22]

2.1.2. Method of Analysis of Blackouts

A study by McCalley et al [27] showed that the progression of blackouts after the occurrence of initiating events could be divided into steady-state progression and transient progression. Figure 2-8 clearly describes these phases, which are precondition, initiating events, cascade events, final state, and restoration. Among these five phases, cascade events can be further divided into three phases in the process of some blackouts: steady-state progression, triggering events, and high-speed cascade.

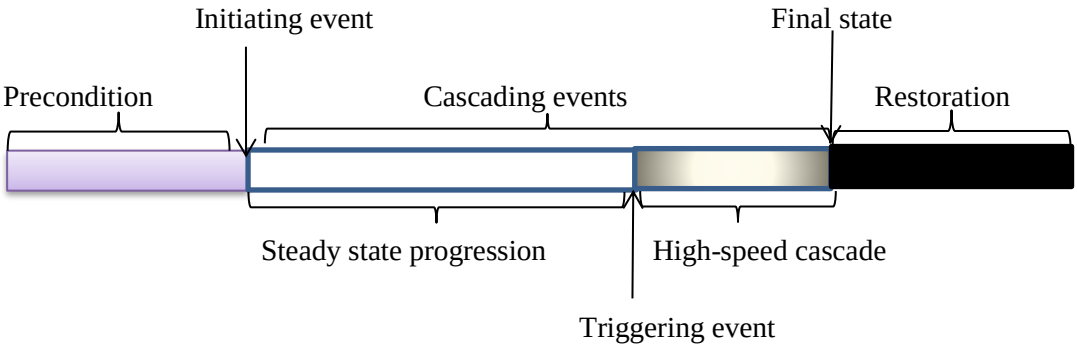

Figure 2-8 Phases of blackout [27]

2.2. Power System Stability Vs Blackouts

Power system stability refers to the ability of synchronous machines to move from one steady-state operating point following a disturbance to another steady-state operating point, without losing synchronism [28]. There are three types of power system stability: steady state, transient, and dynamic.

i) **'Steady state stability'** may be defined as the capability of an electric power system to maintain synchronism between machines within the system and external tie lines following a small slow disturbance (normally load fluctuations, the actions of automatic voltage regulators and turbine governors) [29]. In case the maximum power transfer exceeds under this condition, individual machines or groups of machines will cease to operate in synchronism, violent fluctuations of the voltage will occur and the steady state limit for the system as a whole would have been reached. The steady state limit refers to the maximum power, which can be transferred through the system without loss of stability. The assessment of steady state stability is very important in planning and designing of electrical power systems, in developing special automatic control devices, putting into operation new elements of the system, or modifying its operating conditions (such as interconnection of power systems and commissioning of new power plants, transformer substations, transmission lines, etc.).

ii) **'Transient stability'** involves major disturbances such as loss of generation, line-switching operations, faults, and sudden load changes. Following a disturbance, synchronous machine frequencies undergo transient deviations from synchronous frequency (50 Hz), and machine power angles change. The system response to such disturbance involves large excursions of generator rotor angles, bus voltages, and other system variables. If the resulting angular separation between the machines in the system remains within certain bounds, the system maintains synchronism. Loss of synchronism because of transient instability, if it occurs, will usually be evident within 2 to 3 seconds of the initial disturbance. The objective of a transient stability study is to determine whether or not the machines will return to synchronous frequency with new steady-state power angles [28, 29, 30].

J. P Gupta [29], on the other hand, defined transient stability as the ability of the power system to remain in synchronism during the period following a disturbance and prior to the time that the governors can act.

iii) **'Dynamic Stability'** is the ability of a power system to remain in synchronism after the 'initial swing' (transient stability period) until the system has settled down to the new steady state equilibrium condition [29]. Dynamic stability involves a longer time period than transient stability, typically several minutes. When sufficient time has elapsed after a disturbance, the governors of the prime movers will react to increase or reduce energy input, as may be required, to re-establish a balance between energy input and the existing electrical load. The period between the time the governors begin to react and the

time that steady state equilibrium is re-established is the period when dynamic stability characteristics of a system are effective.

Basic Concepts of Transient Stability

Consider the system shown in Figure 2-9, consisting of a generator delivering to a large system represented by an infinite bus through two transmission circuits. An infinite bus represents a voltage source of constant voltage magnitude and constant frequency [11]. All resistances are neglected to simplify the analysis.

The corresponding system representation is shown in Figure 2-10 (a). X_E is the equivalent reactance of the transformer and the transmission lines. The voltage behind the transient reactance (X'_d) is denoted by E'. The rotor angle δ represents the rotor angle by which E' leads E_B. When the system is perturbed, the magnitude of E' remains constant at its pre-disturbance value and δ changes as the generator rotor speed deviates from synchronous speed ω_0.

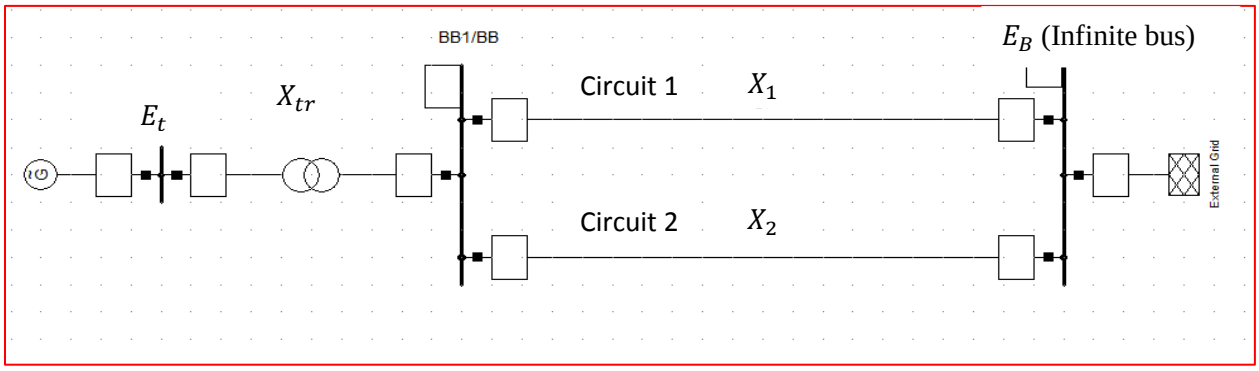

Figure 2-9 Single machine infinite bus system [11]

(a) Equivalent circuit (b) Reduced equivalent circuit

Figure 2-10 Corresponding system representation [11]

$$E' = E_{to} + jX'_d I_{t0} \quad (2.1)$$

$$X_T = X'_d + X_E \quad (2.2)$$

Where,

E_{to} the terminal voltage of the generator prior to disturbance

X_E the equivalent reactance of the transformer and lines

I_{t0} the currents flowing through the terminals of the generator

The generators electrical power output (P_e) is:

$$P_e = \frac{E'E_B}{X_T}\sin\delta \quad = P_{Max}\sin\delta \tag{2.3}$$

Where

$$P_{Max} = \frac{E'E_B}{X_T} \tag{2.4}$$

The power angle relationship with both transmission circuits in service (I/S) is shown graphically in Figure 2-11 as curve 1. With a mechanical power input of P_m, the steady state electrical power output P_e is equal to P_m, and the operating condition is represented by point *a* on the curve. The corresponding rotor angle is δ_a. If one of the circuits is out of service (O/S), the effective reactance X_T is higher. The power angle relationship with circuit 2 out of service is shown in Figure 2-11 as curve 2. The maximum power is now lower. With a mechanical power input of P_m, the rotor angle is now δ_b corresponding to the operating point *b* on curve 2; with a higher reactance, the rotor angle is higher in order to transmit the same steady state power.

During a disturbance, the oscillation of δ is superimposed on the synchronous speed ω_0, but the speed deviation $\left(\Delta\omega_r = \frac{d\delta}{dt}\right)$ is very much smaller than ω_0. Therefore, the generator speed is practically equal to ω_0, and the per unit (pu) air gap torque may be considered to be equal to the pu air gap power. Therefore, when referring to the swing equation, torque and power can be used interchangeably.

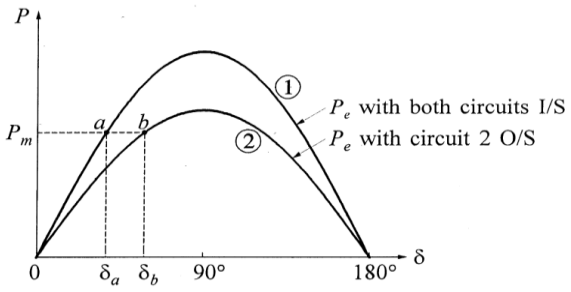

Figure 2-11 Power- angle relationship [11]

The swing equation can be written as [29, 30]:

$$P_m - P_{Max}\sin\delta = \frac{2H}{\omega_0}\frac{d^2\delta}{dt^2} \tag{2.5}$$

Where,

P_m is the mechanical (turbine) power input, in pu

P_{Max} maximum electrical power output, in pu

H inertia constant, in MW. s/MVA

δ rotor angle, in elec. Rad

t time, in s

Let us consider the response of the system to a three-phase fault at location F on transmission circuit 2 as shown in Figure 2-12 (a). The corresponding equivalent circuit is also shown in Figure 2-12 (b). The fault is cleared by opening the circuit breakers at both ends of the faulted circuit, the fault clearing time depending on the relaying time and breaker time.

If the fault location F is at the sending end bus (BB1/BB) of the faulted circuit, no power is transmitted to the infinite bus. The short circuit current from the generator flows through pure reactances to the fault. Hence, only reactive power flows and the active power P_e and the corresponding electrical torque T_e at the air gap are zero during the fault. If the fault location F is at some distance away from the sending end as shown in Figure 2-12 (a) & (b), some active power is transmitted to the infinite bus while the fault is still on. Figures 2-12 (c) & (d) show $P_e - \delta$ plot for three network conditions:

(i) Prefault (both circuits in service)

(ii) A three phase fault on circuit 2 at a location some distance from the sending end

(iii) Post fault (circuit 2 out of service)

Figure 2-12 (c) considers the system performance with a fault clearing time of t_{c1} and represents a stable case. Figure 2-12 (d) a longer fault clearing time (t_{c2}) such that the system is unstable. In both cases P_m assumed to be constant as the mechanical power cannot be increased or decreased instantly as the fault occurs.

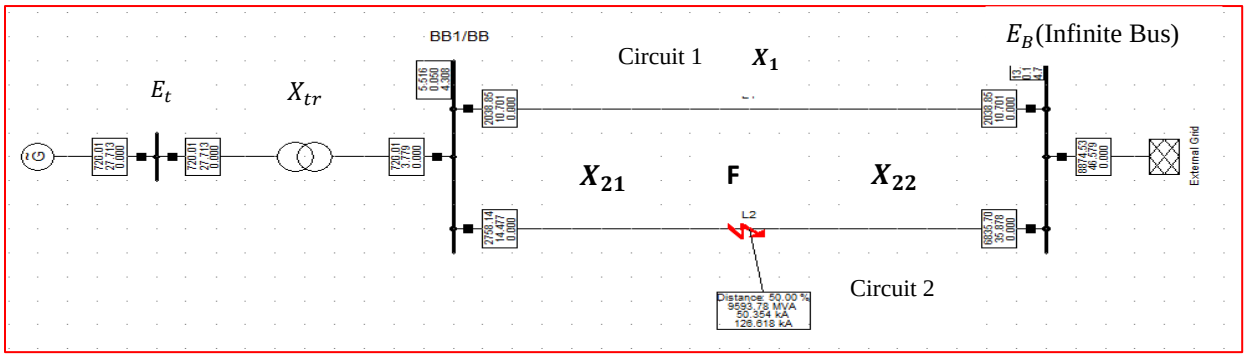

a) Single line diagram

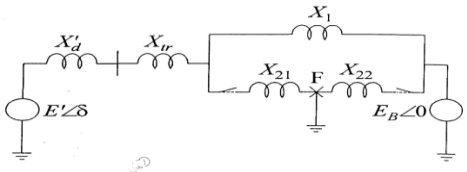

b) Equivalent circuit

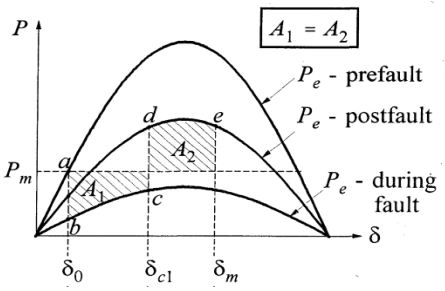

c) Response to a fault cleared in t_{c1} seconds-stable case

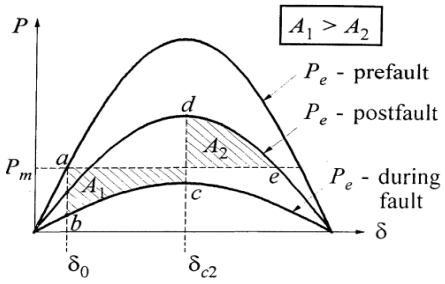

d) Response to a fault cleared in t_{c2} seconds – unstable case

Figure 2-12 Illustration of transient stability phenomenon **[11]**

The two areas can be calculated using equation (2.6) & (2.7) as shown below [11, 29, 30, 31]:

$$area\ A_1 = \int_{\delta_0}^{\delta_{c1}} (P_m - P_e)\, d\delta \qquad (2.6)$$

$$area\ A_2 = \int_{\delta_{c1}}^{\delta_m} (P_e - P_m)\, d\delta \qquad (2.7)$$

The area A_1 is the kinetic energy gained by the rotor during acceleration when δ changes from δ_0 to δ_{c1}. On the other hand, area A_2 represents the energy lost during deceleration when δ changes from δ_{c1} to δ_m.

In the stable case which is depicted by Figure 2-12 (c), the system is initially operating with both circuits in service such that $P_e = P_m$ and $\delta = \delta_0$. When the fault occurs the operating point suddenly changes from a to b. owing to inertia, the angle δ cannot change instantly. Since P_m is now greater than P_e, the rotor accelerates until the operating point reaches c, when the fault is cleared by isolating circuit 2 from the system. The operating point now suddenly shifts to d. Now P_e is greater than P_m, causing deceleration of the rotor. Since the rotor speed is greater than the synchronous speed ω_0, δ continues to increase until the kinetic energy gained during the period of acceleration (represented by area A_1) is expended by transferring the energy to the system. The operating point moves from d to e, such that area A_2 is equal to area A_1. At point e, the speed is equal to ω_0 and δ has reached its maximum value δ_m. Since P_e is still greater than P_m, the rotor continues to retard with the speed dropping below ω_0. The rotor angle δ decreases, and the operating point retraces the path from e to d and follows the $P_e - \delta$ curve for the post-fault system farther

down. The minimum value of δ is such that it satisfies the equal area criterion for the post-fault system. In the absence of any source of damping, the rotor continues to oscillate with constant amplitude.

With a delayed fault clearing, as shown in Figure 2-12 (d), area A_2 above P_m is less than A_1. When the operating point reaches e, the kinetic energy gained during the accelerating period has not yet been completely expended; consequently, the speed is still greater than ω_0 and δ continues to increase. Beyond point e, P_e is less than P_m, and the rotor begins to accelerate again. The rotor speed and angle continue to increase, leading to loss of synchronism.

It is to be noted that the equal-area criterion is applicable to one machine and an infinite bus or to two machines. For multi-machine stability problems, however, numerical integration techniques can be employed to solve the swing equation for each machine [29, 30]. Among the numerical integration methods, Euler and Runge-Kutta (R-K) methods are the most commonly used methods. In this thesis, the transient simulation is performed by DIgSILENT PowerFactory software package and this software uses R-K method of numerical integration techniques.

2.3. Vulnerability Assessment of Power System

In recent years, "vulnerability" has been a hot topic in the study of complex networks [32, 33, 34]. The degree of the vulnerability of a node or line is defined to be the decrease in the level of network performances after the node or line is removed intentionally from the network. This notion has its origin in the research on computer networks [35], and has been introduced into the study on complex networks to assess from different angles the consequences of attacks using various complex network models [36]. The aim is to identify the most critical faults threatening the operation of the system, and thus to take effective actions for preventions and adjustments.

Performance Index (PI) was first proposed to evaluate the line loading and voltage performance for the automatic contingency selection algorithm [37]. Various vulnerability analysis techniques for power systems are used by different researchers, viz., performance indices with contingency analysis in [37, 38, 39], transient energy function method is used in [40], a fast sensitivity type algorithm in [41], and many mores in [42, 43, 44].

This thesis presents an approach for assessing vulnerability of the Ethiopian Electric Power System by using two indices, called performance indices (PIs) which reflect the health of the system. The combination of these indices yields a vulnerability index (VI). The indices allow assessing two different symptoms of system stress such as voltage instability and overloads.

Chapter 3

Analysis of Blackouts of the Ethiopian Electric Power Network

3.1. Introduction

This chapter mainly focuses on the analysis of blackouts of the Ethiopian electric power network that were happening from January 2013 to mid-of May 2016. The analysis begins by first reviewing the policy guidelines of EEP. These policy guidelines include the network security, system operation and restoration procedures that are currently undertaken by EEP. Thereafter, the analysis of blackouts is done based on the pre-disturbance conditions, the type of initiating event(s), the sequence of events observed on the SCADA, and the final state of the system. Some international blackouts are also considered in this chapter, to make them as a benchmark for the study. Finally, the impacts and the lessons learned from the blackouts are discussed in detail.

3.2. Operating Procedures of National Load Dispatch Centre of EEP

The national load dispatch centre (NLDC) of the EEP has developed the first operation procedure on 30th April 2014, which was approved by Humble Board of Directors. The importance of such operational policy increases manifold as the power system operation & control in the country is becoming more complex day by day not only with the rapidly rising demand growth but also with the intricate Extra High Voltage (EHV) transmission network within the country & across the East African Region. To operate the grid in a desired manner in line with the operating policies, the role of each player in the grid viz. a mix of Generating and Transmission Divisions, Distribution Zones, System Operators and other departments become important and inter dependent. It has thus become necessary not only to draft the internal operating procedures but also implementing these operating policies which lay down the rules and guidelines for operation and maintenance of the national grid in an efficient, reliable and economic manner.

The NLDC operating procedure describes the actions required on the part of the system operator to keep the network secured at all times against contingencies. It also describes the actions required to maintain system variables (voltage, frequency, current) close to nominal values in day-to-day operation [23].

The system planner must generally designs & provides a power system, which complies with the various transmission security standards and associated criteria mentioned in the Operating Policy Guidelines. However, under certain conditions, system may operate beyond the assumptions made during planning [23]. These deviations are classified as:

(i) Those amenable to some optimization during operational stage
(ii) Those outside the operator's control.

The first category includes planned maintenance programs on the generators & transmission lines. Attempts must be made to ensure that these planned maintenance programs are properly coordinated & do not result in weakened network configuration not envisaged during system planning [14]. The second category of events, are those outside the operator's control such as extreme weather conditions either affecting the reliability of transmission system (e.g. thunderstorm, cyclones, Silt formation, floating Islands etc.) or resulting in uneven demand growth (e.g. widespread flood/drought in certain pockets of the system or unexpected or emergency outage of transmission system and generating units).

It is necessary to carry out power system studies in order to assess the grid security and network stability while finalizing the annual, monthly, weekly and daily outage plan of the important elements of the power system. The operating procedure enforces the one-line diagram of each of the generating station (10 MW and above) and substations above 132 kV along with National level Grid maps to be made available in the SCADA system by System Logistic (SCADA) team for the quick access of network configuration during day to day operation and under emergency condition. Generally, various security rules are stated in [23].

The other main assumptions of the power system planner is that the system parameters viz. frequency, voltage, etc.; remain close to nominal values. The operating procedures of NLDC states that the frequency should be maintained as far as possible in different system conditions as per the limits specified in the connection code of EAPP as mentioned in Table 3-1 below:

Table 3-1 Frequency Limits in the EAPP Interconnected Transmission System [23].

Operating conditions	**Frequency limits**
Under Normal Operation	49.50 Hz to 50.5 Hz
Under System Disturbance	49.0 Hz to 51.0 Hz
Maximum band under system fault	48.75 Hz to 51.25 Hz
Under extreme system operation or fault conditions	$f < 47.5\ Hz\ or\ f > 51.5\ Hz\ \ for\ upto\ 20\ sec$

This frequency limit is ensured by perfoming some actions as was described in [23]. In addition, the high voltage networks (above 132KV level); the operating range of the voltage at various voltage levels of the grid is as follows:

Table 3-2 Voltage operating ranges of EEP [23]

Network voltage level (kV)	Normal Operating Condition (kV)		Single contingency (kV)	
Nominal	Maximum	minimum	maximum	minimum
400	420	380	440	360
230	242	218	253	207
132	138	125	145	119

- **In the event of high voltage** (e.g., 400kV bus voltages above 420kV), the respective grid substations / generating station operators switched in the reactors, and taken out the capacitor banks [23]. The generating units connected on the busbars are also made to absorb reactive power. In the event of low voltage (e.g., 400kV bus voltages going down below 380kV), the reverse is true.

In addition to the network security and operation procedures, the NLDC has developed system restoration procedures. The objective of this policy procedure is to achieve restoration and re-synchronisation of systems effected, in case of a grid disturbance, in the shortest possible time, taking into consideration all essential requirements like traction loads, water pumping, hospitals, airport, core sector industrial loads, generation capabilities and the operational constraints of national transmission system.

As defined in [23], a 'Grid Disturbance' denotes the situation under which a set of generating units / transmission elements trip in an abrupt and unplanned manner affecting the power supply in a large area and / or causing the system parameters to deviate from the normal values in a wide range. In the event of a grid disturbance, utmost priority is to be accorded to early restoration / revival of the system.

The power system in different regions is being interconnected and very often, an incident initiated in one region can lead to a disturbance in other region. The classification of grid disturbances in the Ethiopian power system is based on [23]:

i. Category 'A **'Major grid disturbance:** if the disturbance affects generation / load of greater than 80% of the total generation.
ii. Category 'B' **Minor grid disturbance**: if the disturbance affects generation / load of greater than 40% but less than 80% of the total generation.
iii. Category 'C' **Grid Incident**: if the disturbance affects generation/load of greater than 20% but less than 40% of the total generation.

3.3. Analysis of the Past Blackouts on the Ethiopian Electric Power Grid

In this section, the analysis of blackouts are made in the same way for each blackout, considering the following sequential phases: antecedent condition (system condition prior to the initiating incident), initiating events, cascading events, and final state of the system. The techinical analyses using computer simulations of some selected blackouts is also given in Chapter 4.

As obtained from the NLDC archive, a total of 49 blackouts (on average 14 blackouts per year, or 1.167 blackouts per month) were reported from 28th January 2013 to mid of May 2016 and are indicated in Appendix C, Table C-1 to Table C-4.

3.3.1. Analysis of the 2013 Blackouts

3.3.1.1. May 22, 2013 Blackout

On May 22, 2013, a partial blackout was happened on the Ethiopian electric power network. According to the NLDC report, 868.1 MW of power was scheduled to supply the total load prior to the incident. However, there was a weak point (cracked conductor due to loosely re-joined conductors during previous maintenance) on Kality I_ Sebeta I 230 kV line near to Kality I substation. The system frequency at 6:00 Hrs. was 49.1 Hz. The power plants status prior to the blackout was indicated in Table 3-3 below.

Table 3-3 Power plants status at 6:00 hrs.

No.	Power Plant	Available units	Total generations (MW)
1	Beles HPP	all	277.1
2	G/Gibe II HPP	U_2, U_3 & U_4	130
3	Fincha HPP	all	80
4	Tekeze HPP	all	210
5	Melka Wakena HPP	U_1, U_3, & U_4	30
6	G/Gibe I HPP	all	30
7	Koka HPP	U_1	10
8	Awash II HPP	U_2	13
9	Awash III HPP	U_1, U_2	22
10	Amerti Neshe	U_1	35
11	Adama Wind I		31
		Total	**868.1 MW**

At 6:01 hrs, Koka & Awash III HPP generators were tripped by under frequency relays due to overloads in the Eastern Region. This incident caused the major line of the grid to be stressed. Sebeta I_ Kality I 230 kV line interconnected the Southern, Southwestern and Western HPPs with the Eastern region through Kality I 230/132kV substation. This overload together with loosely re-joined conductors forced the line to be interrupted and fallen to the ground and finally a short circuit fault was occurred on this line near to Kality

I substation and the line tripped at 6:05 hrs. Similarly, autotransformers 1 & 2 at Gefersa 230/132 kV substation were tripped at 6:05 Hrs by sensing this earth fault.

The outage of Kality I_ Sebeta I 230 kV line caused major disturbance on the power system and led to the cascade tripping of other lines, transformers and power plants. The following transmission lines and transformers fault records were taken according to the available data at NLDC archive.

At Kality I Substation:

i. Kaliti I_ Sebeta I 230 kV line
- Fault current $I_a = 3.52kA$, faulted phase = AC.
- Time at 6:05
- Acted relay – distance protection relay

At Sebeta I substation:

ii. Sebeta I_Kaliti I 230 kV line
- Fault = overvoltage
- Time at 6:05
- Acted relay- distance protection relay.

At Gefersa_ Substation:

iii. Gefersa_ Sululta 230kV line 1& 2
- Fault type = overvoltage
- Time at 6:06
- Acted relay- Distance relay

iv. Gefersa Auto transformers 1 & 2
- Fault type = overload
- Current magnitude = 606 A
- Time at 6:05
- Acted relay- MiCOM P127 overcurrent protection

The power system equipments that were out due to the cascade tripping are indicated in Table 3-4 below. Finally, the cascaded outage of the transmission lines and power plants resulted 54.8% of the total load to be disconnected from the grid, which caused a partial blackout to the Ethiopian power network. Most of the loads at Addis Ababa region were restored within 30 minutes. However, the complete restoration of the power system took more than 6 hours.

Table 3-4 Power plants status, reason of outage & outage time of generating units

No.	Power plant	Tripped Unit	Total outage (MW)	Outage time	Reason of outage	Resynchronization time
1	Beles HPP	No	0	-	Load rejection	-
2	G/Gibe II HPP	U_2, U_3 &U_4	130	6:06	Over frequency	6:19
3	Tekeze HPP	all	210	6:05	Over frequency	8:27
4	Fincha HPP	No	0	-	Load rejection	
5	G/gibe I HPP	U_1	30	6:06	Load rejection	6:48
6	Melka Wakena HPP	U_1, U_3 & U_4	30	6:05	Overload	12:30
7	Koka HPP	U_1, U_2	10	6:01	Under frequency	6:45
8	Awash II HPP	U_2	13	6:05	Under frequency	7:15
9	Awash III HPP	U_1, U_2	22	6:01	Under frequency	6:45
10	Adama Wind I	No	31	6:02		
Total MW outage			**476 MW**			

3.3.1.2. Other Blackouts of the Year 2013

The reports of NLDC for the 2013 blackouts is summarised[2] in Table 3-5.

Table 3-5 Analysis of the 2013 blackouts

Blackout	Preconditions	Cascading events
28th January	- System load was 1108.68MW - The transnational exchange was 40 MW exported to Sudan - One major line (Sebeta I-Kality I 230kV line) and Adama Wind plant were out of service - Normal load level - Normal temperature	- GG II_Sebeta II 400kV line tripped by EF at 16:57 hr - GG II HPP tripped at 16:57 hr by OF - 400/230kV transformers 1 & 2 at Sekoru s/s tripped by EF (50/51- backup) at 16:58 hr. - 230/132kV transformer at Sebeta I s/s tripped by EF at 16:58 hr. (Diff. relay) - Sebeta I _wolkite 230kV line tripped by EF - Melkewakena HPP tripped by OC at 17:06 hr. - Koka_kality 230kV tripped by EF at 17:07hr. - Fincha HPP tripped by UF at 17:08 hr. - Tekeze HPP tripped by OF at 17:09 hr. - Awash II & III HPPs tripped by UF at 17:09 hr. - Alamata_B/Dar 230kV tripped by OC at 17:10 hr.
2nd March	- High load conditions - Normal weather conditions - Generation limitations due to unavailability of the following generating units: 2 units of Melka Wakena, 1 unit of Awash II, 2 Units of Amertinesh, 1 unit of Tekeze HPPs	- Koka & Awash II HPPs tripped by underfrequency at 16:31hr. - Ghedo_Gefersa 230kV line tripped by overload at 16:31 hr. - Fincha HPP was tripped by overvoltage at 16:31hr. - System collapsed by overload & overvoltage at 16:58 hr.
6th March	- System was in stressed condition - High load level - Beles HPP was continuously interrupted - Gilgel Gibe I & Melka Wakena HPPs were out of service - Protection coordination was poor	- Gefersa_Ghedo 230kV line was tripped by earth fault. - This fault has caused a cascade outage of both Ghedo & Gefersa which made the system to lose the major power plants: Beles HPP, Tekeze HPP, and Fincha HPP which was 73% of the total system generation.
27th July	- Total system load was 1140.68 MW - High load conditions - Normal weather conditions - Two power plants were out of service	- B/Dar II_ Alamata 230kV tripped by EF at 14:58 hr. - Tekeze HPP was tripped at 15:02 hr by OF - Ashegoda_Alamata 230kV line tripped at 15:03 hr. - Gondar II_Shehedi 230kV line tripped by UV at 15:04 hr. - System wide system collapse arised.
13th September	- System was at stressed condition (peak load was 1254.11 MW) - Total generation was 1247.82 MW - High load level - Normal weather conditions	- Gefersa_Addis North 132kV line was tripped by earth fault at 20:25 hr. - Ghedo_Gefersa 230kv line, Gefersa_Sululta 230kV line &Sebeta I_Kality I 230kV line were tripped by overvoltage. - Sebeta I 230/132kV auto transformer tripped by overcurrent. - Sebeta I_Sebeta II 230kV transmission lines I & II tripped by overvoltage. - Alamata_B/Dar 230kV line, Combolcha _Legetafo 230kV lines tripped by overcurrent protection
24th October	- System load was 680MW while the generation was 702 MW - Light load level (off-peak hour) - Normal weather	- Fincha HPP_D/Markos 230kV line was tripped by EF (SLG fault) at 23:55:27 hrs. - Combolcha II_ Legetafo 230kV tripped by OC at 23:56 hrs. - Combolcha II_Alamata 230kV tripped by OC at 23:56 hrs. - Fincha HPP tripped by UF at 23:59 hrs.

[2] *The initiating events and restoration times of the 2013 blackouts are indicated in Appendix C, Table C-1*

	- Some units of the generation plants were out of service	- Tekeze & Koka HPPs tripped by OF & UF respectively at 00:00 hr. - GG II & Awash II HPPs tripped by UF at 00:02 hr. - GG I HPP tripped by UV at 00:04 hr. - Beles HPP tripped by load rejection at 00:07 hr.
6th December	- System was in normal condition - System load was 959.97 MW and generation was 1105.74MW - Normal weather condition	- Combolcha II_Alamata 230kV line tripped by SLG fault - D/Markos_Fincha 230kV line tripped by OC - Awash III HPP was tripped by UF at 8:06 hr. - Fincha & Melkewakena HPPs by UF at 8:10 hr. - Tekeze & GG I HPPs tripped by UV at 8:11hr. - GG II & Beles HPPs tripped by UF at 8:12 hr.

3.3.2. Analysis of the 2014 Blackouts

3.3.2.1. November 5, 2014 Blackout

1. **Preconditions:** all the transmission lines were in the system and according to the Ethiopian Electric utility operation point of view, the system was at normal and stable state. The total system load was over 1.3 GW and the transnational exchange was with the Republic of Sudan and Djibouti with a power interchange of 40 MW and 29 MW respectively. The power plant status during pre-disturbance conditions is indicated in Table 3-6. The PLC system installed at Beles HPP was not functional. The 110 V DC (battery) systems was defective at this power plant; there was abnormal AC fail signal initiated by a controller card in the battery charger and AC supply to the rectifier was interrupted frequently and it was found that there was a design problem on 110V DC system of the plant. The operators and the power plant maintenance crew did not respond to these problems. However, until the initiating event was observed, the power system status observed on the EMS/SCADA was normal.

Table 3-6 Power plant status before the incident

Power Plant	Available units	Total generation (MW)	Time (Hrs)
Beles HPP	U_1, U_2, U_3 & U_4	359	12:18
G/Gibe II HPP	U_1, U_2, U_3 & U_4	340	12:18
Tekeze HPP	U_4	50	12:18
Fincha HPP	U_1, U_2, U_3 & U_4	118	12:18
G/Gibe I HPP	U_1, U_2 &U_3	160	12:18
Melka Wakena HPP	U_1, U_3 & U_4	90	12:18
Koka HPP	U_1 & U_2	20	12:18
Awash II HPP	U_2	12	12:18
Awash III HPP	U_1 & U_2	10	12:18
Amertinesh	U_2	47	12:18
Adama I Wind plant	All	29.11	12:18
Ashegoda Wind plant	All	44	12:18
Tis Abay	U_2	30	12:18
	TOTAL	**1309.11**	

2. **Initiating Events:** the first incident on the Ethiopian electric grid was observed when the Alamata - Combolchaa 230 kV line tripped by main protection trip at 12:19 hrs due to load unbalance. However, this could not create disturbance since, the power flow could have an alternate path though Alamata - Bahir Dar-Mota-D/Markos-Fincha-Ghedo-Geferssa 230 kV line and B/Dar - D/Markos- Sululta 400 kV lines. However, since the alternate paths are much longer than the tripped line, the generators in the Eastern region (near to the load) became stressed and resulted for the following generation plants to trip:
    - Unit 2 of Awash II HPP was tripped at 12:22 hrs by overcurrent/overload protection.
    - All units of the Awash III HPP were tripped at 12:22 hrs by under frequency protections.

Immediately following the outage of these power plants the following lines were tripped:

- Koka- Awash II 132 kV line I& II were tripped at 12:22 hrs with no signal (the reason was not identified). This means that there was a problem on the protection relays settings and/or the malfunctioning of the communication system between the bay control unit (BCU) and the remote terminal unit (RTU).
- Similarly, the Awash II- Awash III 132 kV line I was tripped at 12:22 hrs with the same reason as Koka- Awash II 132 kV lines.

3. **Cascading events:** when the initiating events were happened, the system became further overloaded and stressed as the power flow routes changed to other lines and power plants. At 12:29 hrs most of the transmission lines in the East, South & South West regions were tripped. Following this

- Sokoru-Gibe II 400 kV line tripped by bus bar backup protection and Sebeta II – Gibe II 400 kV line also tripped at 12:29 hrs which isolated Gilgel Gibe II HPP from the grid.
- Wolkite – Sekoru 230 kV line tripped by CBF (circuit breaker failure protection) and isolated Gilgel Gibe I from the grid.
- All power plants except Beles were isolated from the system by over load, under frequency and over speed protections.
- The loading of Beles was 440 MW and it was running for about 25min with a frequency of 44.6 Hz.
- The system voltage kept on increasing and the whole system was collapsed at 12:59 hrs.

The detail time line of the cascading events is shown in Table 3-7 and 3-8**.**

Table 3-7 Time line of the November 5, 2014 blackout

	Transmission line	Outage time	Reason of outage	Revival time
1	400kv bahirdar – beles line l	12:58	Over voltage	…….
2	400kv bahirdar – beles line ll	12:58	Over voltage	15:35
3	400kv D.Markos_Bahirdar	12:58	Over voltage	12:17(next day)
4	400kv D.Markos_Sululta	12:59	Over voltage	14:27(next day)
5	400kv Gelgel Gibe II_Sebeta II	12:29	NO	16:56
6	400kV Sekoru_Gelgel Gibe II	12:29	Busbar protection and main protection	15:55
7	400kv Gelan –Sebeta ll	12:59	Over voltage	16:45
8	230kv Gelgel Gibe I_Sekoru Line 1	12:29	NO SIGNAL	15:56
9	230kv Gelgel Gibe I_Sekoru Line 2	12:29	NO SIGNAL	15:56
10	230kv Gelgel Gibe I_Gehedo	12:29	NO SIGNAL	17:30
11	230kv Sekoru_Welkite	12:29	CB fault	15:52
12	230kv Welkite_Sebeta I	12:57	NO SIGNAL	15:47
13	230kv Sebeta I_ Kality I	12:37	Over voltage	15:31
14	230kv Kality I_Gelan Line 1	12:59	Over voltage	16:41
15	230kv Kality I_Gelan Line 2	12:59	Over voltage	16:41
16	230kv Koka_Dire Dawa IIl	12:59	NO SIGNAL	18:50
17	230kv Dire Dawa II_Adigala	12:59	NO SIGNAL	11:07(next day)
18	230kv Gelan_Koka Line 1	12:59	Over voltage	16:42
19	230kv Gelan_Koka Line 2	12;59	Over voltage	16:45
20	230kv Dire Dawa II_PK12	12:59	NO SIGNAL	……..
21	230kv adigala_PK12	12:59	NO SIGNAL	14:00(next day)
22	230kv Kality I_Legetafo	12:58	NO SIGNAL	16:23
23	230kv Legetafo_Combolcha	12:59	NO SIGNAL	16:23
24	230kv Combolcha_Alamata	12:19	Main protection trip	17:59
30	230kv Bahirdar II_Gonder line ll	12:58	Over voltage	21:24
31	230kv Gonder_Shehide	12:58	NO SIGNAL	21:17
32	230kv Sheidi_Sudan	12:30	Under voltage	21:25
33	230kv Sebeta I_Gefersa	12:58	NO SIGNAL	12:44(after two days)
36	230kv Gefersa_Gehedo	12:58	NO SIGNAL	14:10
37	230kv Ghedo_Finchaa	12:30	Over current and earth fault	14:11
38	230kv Finchaa_D. Markos	12:30	Over current	17:16
39	230kv Finchaa_Fincha II	12:30	NO SIGNAL	17:09
40	230kv D.Markos_Mota	12:58	NO SIGNAL	17:18
41	230kv Mota_Bahirdar II	12:58	NO SIGNAL	17:22
42	230kv Koka_Melkawakena line 1	12:35	NO SIGNAL	15:36(next day)
43	230kv Koka_Melkawakena line 2	12:35	NO SIGNAL	17:05
44	230kv Sebeta I _Sebeta II line 1	12:57	NO SIGNAL	16:33
45	230kv Sebeta I _Sebeta II line 2	12:57	NO SIGNAL	16:33
47	132kv Kality I_Gefersa	12:58	NO SIGNAL	15:03
48	132kv Kality I_Mekanisa	12:58	NO SIGNAL	15:20
49	132kv Mekanisa_Sebeta I	12:35	NO SIGNAL	15:20
50	132kv Gefersa_Sebeta I	12:58	NO SIGNAL	15:20
51	132kv Legetafo_Cottobie	12:59	NO SIGNAL	16:43
53	132kv Koka_Awash II line 1	12:22	NO SIGNAL	13:35
54	132kv Koka_Awash II line II	12:22	NO SIGNAL	13:50
55	132kv Awash II_Awash IIl line 1	12:22	NO SIGNAL	13:35
58	132kv Adamitulu_Shashemene	12:29	NO SIGNAL	23:55
59	132kv Shashemene_Alaba	12:29	NO SIGNAL	21:20

60	132kv Shashemene_Yego	12:29	NO SIGNAL	23:54
61	132kv Melkawakena_Yego	12:29	NO SIGNAL	23:54
63	132kv Hossina_old Gibe	12:29	NO SIGNAL	19:09
65	132kv Sekoru _ Jimma	12:29	NO SIGNAL	15:55
66	132kv Koka –gelan line l	12:59	NO SIGNAL	13:31
67	132kv Koka –gelan line ll	12:59	NO SIGNAL	17:09

There are some points that should be noticed:

- The power system lacks a real time simulation tool for unpredictable events. For example, if the Ethiopian power system has got a real time simulation tool, the NLDC operators could know that the system would enter into a danger condition. An effective load shedding could be made before the cascading events had happened.

Table 3-8 Time line of Power plant status, reason & outage time of generating units

	Power plant	Tripped units	Total outage (MW)	Outage time	Reason of outage	Resynchronization time
1	Beles HPP	U1,U2,U3&U 4	359	13:01 12:58 12:58 12:58	Over voltage	U1=13:05 U2=12:05 U3=11:53 (Next day)
2	GGII HPP	U1,U2,U3&U 4	340	12:29	Over frequency	U1=19:44; U2=19:17 U3=19:10 U4=18:49
3	Tekeze HPP	U3	50	12:32	Under voltage	U4=14:30 U2=15:00
4	Finchaa HPP	U1,U2,U3&U 4	118	12:30	Under frequency	U1=15:11 U2=14:09 U3=13:54 U4=15:16
5	GGI HPP	U1,U2& U3	160	12:31 12:40 13:22	Under voltage and Over current	U1=16:20 U2=16:16 U3=16:07
6	Melka Wakena HPP	U1, U2 & U3	90	12:35	Over current and over voltage	U1=14:05 U3=13:40 U4=13:42
7	Koka HPP	U1 & U2	20	12:33	Under frequency	U1=13:25 U2=13:13
8	Awash II HPP	U2	12	12:22	Over current	U2=16:15
9	Awash III HPP	U1&U2	10	12:22	Under frequency	U1=13:53 U2=14:09
10	Amerti Neshi HPP	U1	47	12:29	Over frequency	U1=17:12
11	Adama Wind	All	29.11	12:59		17:28

- There was no effective defence plan for the emergency condition, even if NLDC has monitored some critical sections. For example, the overloads in the interconnection lines could be reduced by intelligent load shedding plan before the protection devices action took place.
- The under frequency protection of generating units of Beles HPP was not operating correctly (the setting should be reviewed seriously), which is dangerous for the power plant. It was operating at 44.5 Hz at the time.
- The over-voltage tripping of the shunt capacitors at Sebeta II was not implemented as this capacitor bank is a mechanically switched capacitor (MSC); this was one of the factors that aggravate the system collapse by over-voltage.
- The 110V DC system of Beles HPP was defective, and there was no reaction to solve the problem before the incident (negligence).

In the November 5, 2015 blackout, we can clearly see the period of the steady state progression and the period of the high speed cascade. The triggering events tripped G/Gibe II- Sebeta II 400kV line, Sekoru_G/Gibe II 400kV line, G/Gibe I- Sekoru 230kV line I &II, and Ghedo- G/Gibe I 230kV line. The time of the cascade progression was around 40 minutes. The blackout mechanism of the November 5, 2014 blackout is shown in Figure 3-1.

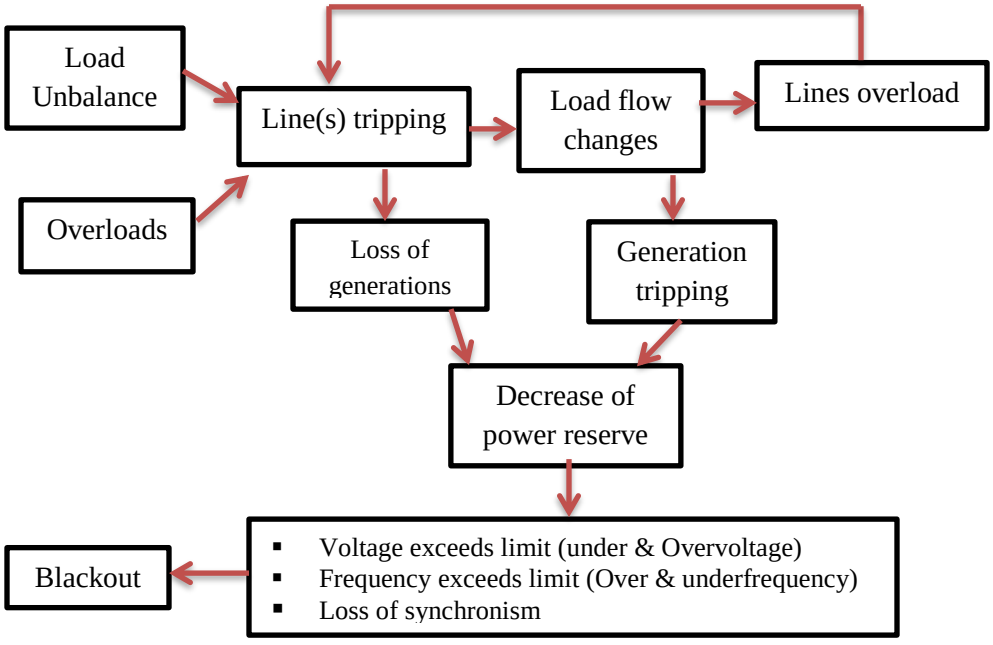

Figure 3-1 The mechanism of the November 5, 2014 blackout

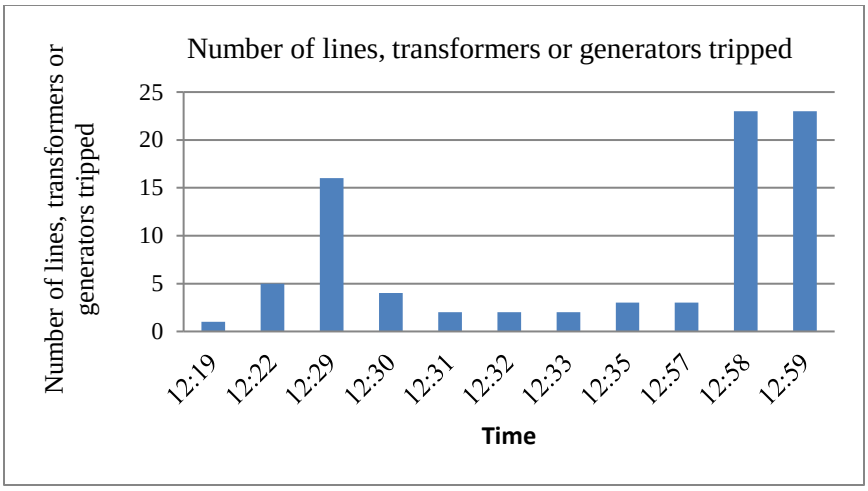

Figure 3-2 Accumulated lines, transformers and generators tripping during the cascade in the November 5, 2014 blackout

4. **Final state of the system**: this blackout affected the whole country and the load was not supplied for a time interval ranging from 26 minute to over 22 hours.

3.3.2.2. Other Blackouts of the Year 2014

The preconditions and cascading events of some of the blackouts of 2014 are summarised in Table 3-9.

Table 3-9 Analysis of the 2014 blackouts[3]

Blackout	preconditions	Cascading events
5th April	- Normal weather condition - Every HV transmission lines were in the system and the system parameters were within the acceptable limits - Normal load level	- Kality I_Sebeta I 230kV line tripped by EF at 9:24 hr. - Melkewakena, Koka, Awash II & III HPPs tripped by overload at 9:25 hr. - GG II HPP tripped by UF at 9:25 hr. - Tekeze HPP tripped at 9:25 hr. by OF - Sululta _Gefersa 230kV line tripped by backup EF at 9:30 hr. - Sebeta II_Sebeta I 230kV tripped at 9:30 hr. - Sebeta I _Wolkite 230kV tripped at 9:30 hr.
13th April	- Normal load level - Adama & Ashegoda wind plants were out of service - Time synchronization problem was observed on the EMS - Ghedo – Gefersa 230kV line was out at Ghedo. - Ghedo – Finchaa I/II 230kV lines were out of service - Ghedo – Sekoru 230kV line was out of service - Time synchronization problem was observed on the EMS	- Gefersa_Addis North 132kV line tripped by EF (the EF was due to conductor broken and fallen to ground) at 12:02 hr. - Gefersa – Sebeta I and Gefersa – MekanisaTP tripped by over load at 12:02 hr. - Gefersa – Sululta lines I&II 230kV lines tripped by over voltage at 12:02 hr. - 230/132kV Transformer at Sebeta I S/s tripped on both side by earth fault at 12:02 hr. - Sebeta- Kaliti I 230kV tripped by Over Voltage at 12:02 hr. - D/Markos_Sululta 400kV line tripped by over voltage at 12:02 hr.
11th May	- Every HV transmission lines were in the system and the power grid	- Gelan 400/230kV tripped by differential relay (external fault) at 7:24 - B/Dar II _Gondar II 230kV line tripped by OC at 7:24 hr.

[3] *The initiating events and restoration times of these blackouts are stated in Appendix C, Table C-2.*

	parameters were within acceptable limits - Normal load level - Normal weather conditions	- Tekeze HPP tripped by OF by 7:24 hr. - Sebeta l 230/132 kV transformer tripped by EF at 07:25 hr. - Melkawakena HPP tripped by OC at 7:25 hr. - Alamata – B/Dar II 230KV tripped with back up protection at 07:26 - Geferssa- Sululta L1 & L2 230KV, Geferssa – Sebeta I 132KV, Geferssa – Kaliti l 132kV tripped by OV at 7:27 hr. - Makanissa – Sebeta I tripped by EF fault at 07:28 hr. - Mekenissa 132/15 kV transformer tripped by EF at 07:28 hr. - Sebeta l- Kaliti l 230 kV tripped due to OV at 07:30 hr. - D/markos_Sululta 230kV line tripped by OV at 07:30 hr.
8th August	- High load level - Fincha HPP – D/ Markos 230kV line was out of service due to collapse of tower, - Sebeta II – G/Gibe II 400kV line was out due to OV at 22:51 and - Beles HPP – B/Dar II 400kV line I out of service due to OV at 22:51 - Normal weather condition	- Beles HPPs_B/Dar II 400kV line II tripped at 23:17 hr with distance protection device fail and tele protection fail signal - B/Dar II_Gondar II 230kV line tripped at 23:17 hr by lockout relay signal - Sekoru_GG I HPP 230kV line tripped without signal at 23:17 hr - Tekeze_Mekele 230kV lines tripped at 23:19 hr by OV. - Wakena_Koka 230kV L1& 2 tripped by OC at 23:19 hr - Koka _D/Dawa III 230kv Line tripped at 23:20 hr - Koka –Gelan 230 kV line l tripped at 23:20 hr
24th October	- All HV transmission lines were in the system and the electric power network was in normal state and relatively stable - Normal weather condition - Over voltage was observed on the system (high reactive power generation was observed in the system)	- Beles HPP_B/Dar II 400kV lines tripped by OV at 16:16 hr. - B/Dar II_Tis Abay II 132kV lines tripped by OV at 16:16 hr. - Beles HPP tripped at 16:16 hr. - G/Gibe I_Sekoru 230kV lines and GG I HPP were tripped by UV & OC at 16:16 hr. - Fincha, Koka & GG II HPPs were tripped by UF at 16:16 hr. - Tekeze HPP tripped at 16:17 hr with no signal - All the 230kV & 400kV lines tripped at 16:17 hr with no signal - Melkawakena HPP was tripped by OC at 16:20 hr.
6th November	- Fincha & Amertinesh HPPs ware out of service - Beles HPP – B/Dar II 400kV line I, Ghedo – Gefersa 230kV line II, B/Dar II – D/Markos 400kV line, and Sebeta I – Gefersa 230kV lines were out of service - System was overloaded	- Gefersa_Sebeta I 132kV line tripped by OC at 18:00 hr. - Ghedo_Sekoru 230kV line tripped at 18:06 hr with no signal. - B/Dar II_Alamata 230kV line tripped by OC at 18:06 hr. - Gefersa _Kality I 132kV line tripped by OC at 18:10 hr. - BELES, FINCHA, TIS ABAY and AMERTINESH HPPs tripped at 18:30 hr by order of NLDC to prevent them from damage.

3.3.3. Analysis of the 2015 Blackouts

3.3.3.1. The December 25, 2015 Blackout

a) Pre-disturbance conditions

Before the incident, the system was in normal operating condition. Most areas of the country were highly affected by drought and therefore, there was lack of water at the reservoirs of some HPPs. The Tekeze HPP was generating only 10 MW; Melka Wakena, Awash II &III and Koka areas were also highly affected by the drought and their energy production was lessened. With the aim of better voltage regulation and reservoir water management, Bahir Dar II – D/ Markos and Sebeta II – G/Gibe II 400kV lines were interrupted at the night time. In addition, for rehabilitation and extension purpose, G/Gibe II power plant was out of service at the time. However, the power system was at its normal conditions.

At 4:00 hrs, the total generation was able to feed the load demand and the system operating frequency was 50 Hz. The total power production was around 839 MW from which 16 % (137 MW) of it was from the wind power plants (Ashegoda, Adama I & II) and the rest was from the hydro power plants. The voltages at the crucial substations, i.e., Gelan, B/Dar II and Sululta 400/230 kV substations were declining as it is indicated in the Table 3-10. The voltage declining was due to the insufficient reactive power reserve in the system as the major HPP (G/Gibe II) was not serving the grid.

Table 3-10 Voltages of important substations at 4:00 hrs

Substation	Kality I 230/132kV	Sululta 400/230kV	Sebeta I 230/132kV	B/Dar II 400/230kV	Gelan 400/230kV	Combolcha II 230/132kV	Ghedo 230/132kV
Voltage (kV)	231/132	388/229	230/130	404/220	373/230	232/133	232/131

Table 3-11 Power flows on important lines at 4:00 hrs

No.	Transmission line (s) name	MVA
1	B/Dar II – Alamata 230 KV line	$90 + j50$
2	Sululta - D/Markos 400kV line	$115 + j64$
3	Sululta – Gefersa 230 kV line I	$38 + j5.5$
4	Sululta – Gefersa 230 kV line II	$38 + j3.6$
5	Sebeta I – Kality I 230 kV line	$100 + j134$
6	Sebeta II – Gelan 400kV line	$25.6 + j95.3$
7	Gefersa – Ghedo 230kV line I	$82 + j12$
8	Gefersa – Ghedo 230 kV line II	$62 + j16$
9	Sekoru – Ghedo 230kV line	$39 + j34$

From the company's point of view, the power system operation was normal and the voltage declining that was observed at the important substations was in the acceptable range.

b) Initiating event(s)

At 4:34 hrs, the first incident on the Ethiopian Electric Power system was seen on B/Dar II 400/230 kV and 230/132 kV transformers as B/Dar II – D/Markos 400kV line was reconnected to the system. B/Dar II 400/230kV transformer I and 230/132kV transformer I &II were tripped by overvoltage protection relays. This overvoltage happened because of the transmission line-switching transient and this transient propagated to other lines and transformers.

c) Cascading event(s)

Immediately after the initiating events, B/Dar II – Gondar II 230 kV line was tripped by overvoltage protection and this had initiated a remedial action scheme that disconnected 19 generators. All the four units of Fincha HPP were overloaded and finally tripped by under frequency protection at 4:35 hrs. This further aggravated the system condition and as a result, the system voltage degraded drastically. G/Gibe I and G/Gibe III HPPs were unable to feed the required reactive power and hence, they tripped by overcurrent and under voltage protections. The power flow changed its route to other lines and power plants. These lines and power plants became overloaded and were unable to supply the power demanded by the load. Within 2 minutes' interval, more than 80% of the transmission lines and generators tripped. Generally, the December 25, 2015 blackout constituted only by a high-speed cascade, which led to the collapse of the entire system.

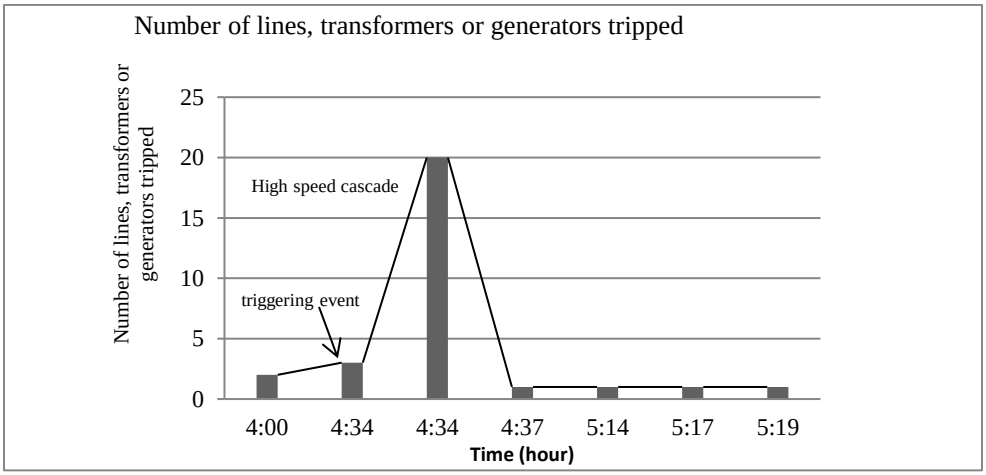

Figure 3-3 Accumulated line, transformers and generators tripping during the cascade in EEP grid on December 25, 2015 blackout

d) Final State

Finally, the Ethiopian electric power system collapsed and left all the customers in the dark. All the plants and equipments were out of service and all network areas of the country were affected.

e) System restoration

The restoration time for the important loads of the Capital took 40 minutes and most of the substations were restored within 3:30 hours. Customers sustained power cuts lasting between 31 min to 5.5 hrs.

f) Process of the December 25, 2015 blackout

The process of this blackout is shown in Figure 3-4 below.

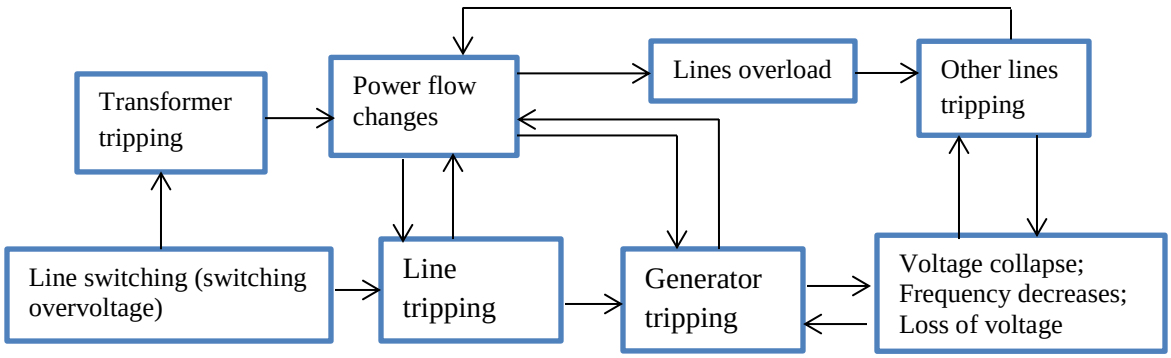

Figure 3-4 Mechanism of the December 25, 2015 blackout

3.3.4. Analysis of the 2016 Blackouts

3.3.4.1. January 17, 2016 Blackout

a) System condition prior to disturbance

The system operating condition at 7:45 hrs was normal and the total generation was around 1323 MW of power. From the total power production, 37.49 MW of electric power was exported to Djibouti. Beles HPP was supplying 432 MW (more than 32% the total demand) of power to the system. The total system load was around 1322.61 MW. The system frequency was observed to be 50 Hz. The voltages at B/Dar II 400/230 kV, Combolcha II 230/132 kV, and Gelan 400/230 kV substations were increased (3%, 4.34 % and 1% respectively) above their corresponding nominal voltages. However, these increments were in the acceptable range. The voltages of important substations are indicated in Table 3-12.

Table 3-12 Voltages of important substations

Substation	Kaliti I 230/132kV	Sululta 400/230kV	Sebeta I 230/132kV	B/ Dar II 400/230kV	Gelan 400/230kV	Combolcha II 230/132 kV	Ghedo 230/132 kV
Voltage (kV)	230/130	399/233	237/132	412/233	403/233	240/131	231/130

According to the Ethiopian Electric Power (EEP) point of view, the system operation was normal.

b) Initiating events

The event triggering incident was observed at 7:59 hrs as all units of Beles HPP was tripped due to force majeure when the power plant maintenance team shifted the 110 V DC supply from battery bank A to battery bank B.

c) Cascading event

Immediately after the initial event, all the power plants of the country shut down with a time interval of less than 60 s. All units of Fincha HPP tripped at 7:59 hrs by under frequency protections. Unit I, II & III of G/Gibe I HPP tripped by under voltage protection devices. The outage displayed on the SCADA/EMS was only the generation unit outages. There was no reserve power at the time that can compensate the outage of Beles HPP and therefore it was impossible to stop the high-speed cascade.

a) Final state of the system

The existing system defence mechanism could not help to recover the system frequency and following the outage of Beles HPP, most units of the system tripped by under frequency relays. The underfrequency load shedding (UFLS) defence mechanism was unable to prevent the frequency collapse. The reason is that the outage of Beles HPP led to the outage of 32% of the system generation. However, the UFLS relays installed at 26 selected sites could only shed 16% of the system load and therefore they were unable to recover the frequency collapse. As a result, the system finally collapsed and left all the customers of EEP without electricity.

3.4. Ethiopian Power Blackouts vs. International Blackouts

Though this study is focusing on the blackouts that were happening in the Ethiopian power grid, the blackouts of the advanced countries are also considered here to make them as abenchmark for the study. This is done based on the blackout trends and blackout indices.

Blackout Trend Analysis

As was listed in Appendix C, Table C-1 to Table C-4, there were 49 blackouts happening on the Ethiopian electric power grid during the period from 28th January 2013 to May 2016. The blackouts that were happening before the year 2013 were not documented in the NLDC archive. Accordingly, the blackout trend for the Ethiopian power grid is 14 blackouts per year.

E. Bombard et al [45] had analysed the blackout trends of some countries that had happened during the period from 1965 to 2011. Based on the analysis, the blackouts trend of the United States is 1.13 blackouts per year and that of the UCTE[4] (Union for the Co-ordination of Transmission of Electricty) countries is 0.81 blackouts per year. Therefore, the frequency of blackouts happening on the Ethiopian power grid is much greater than that of the United States and the UCTE grid.

[4] *The UCTE grid consisted of 25 European countries.*

Blackout Indices

The blackouts data are also analysed based on four significant indices. These indices correspond to the numbers of customers without service, lost load (MW), blackout time duration, and severity (System-minute). Table 3-13 and Table 3-14 shows the indicators corresponding to the first three indices for each one of the Ethiopian Blackouts and the nine incidents of the world respectively.

It is observed that the blackouts of the year 2016 and 2015 affected the largest number of customers. The 28th November 2015 blackout was the event in which the largest amount of load was lost and took eight hours to completely restore the interrupted load. The lost load recorded was 1401.04 MW. The April 22nd 2015 blackout caused the second largest amount of load (1308.95 MW) to be unserved. The blackout that took the longest duration was 27th July 2015 blackout and it was reported that it took 22 hours to completely restore the interrupted load.

Table 3-13 Indicators (Ethiopian blackouts- Part I) [6]

Blackouts	Numbers of customers interrupted (in millions)	Lost load (MW)	Time duration
January 28th 2013	1.6	746	23 minutes to 3 hrs.
March 2nd 2013	1.38	542	2.5 hours to 3.5 hrs.
March 6th 2013	2.4	737	40 minutes to 2 hrs.
April 22nd 2013	2.1	713	45 minutes to 2 hrs.
April 26th 2013	2.08	694	3o minutes to 3.5 hrs.
May 22nd 2013	1.32	476	15minutes to 6 hrs.
May 25th 2013	2.1	930	12 minutes to 3.5 hrs.
July 27th 2013	2.4	1104.62	15 minutes to 2.25 hrs.
September 13th 2013	2.35	967	45 minutes to 2.75hrs.
October 7th 2013	2.35	967	15 minutes to 3 hrs.
October 24th 2013	1.5	684	48 minutes to 2.25 hrs.
November 12th 2013	1.2	522.2	25 minutes to 45 min.
December 6th 2013	2.19	959.97	50 minutes to 2 hrs.
February 2nd 2014	3.01	1279.71	40 min. to 2 hrs.
April 5th 2014	1.23	593.9	30 min. to 3.5 hrs.
April 13th 2014	2.9	1169.21	38 min. to 4 hrs.
March 8th 2014	3.01	980.82	18 min. to 2 hrs.
May 7th 2014	2.73	989.25	37 min. to 2.5 hrs.
May 11th 2014	1.42	542.12	27 min. to 3.5 hrs.
June 17th 2014	2.5	1127.43	31 min. to 4.25 hrs.
August 8th 2014	3.1	872.07	56 min. to 8.75 hrs.
September 3rd 2014	3.1	948.14	21 min. to 11 hrs.
October 24th 2014	3.1	1079.71	26 min to 3.75 hrs.
November 6th 2014	3.1	789.68	1hr. to 7 hrs.
January 15th 2015	1.6	455	15 min. to 4 hrs.
March 15th 2015	4.0	983.31	50 min. to 4 hrs.
April 22nd 2015	4.0	1308.95	1hr. to 8 hrs.
May 8th 2015	4.0	745.38	1.25 hrs. to 8 hrs.
May 26th 2015	2.4	509.1	43 min. to 5 hrs.
July 27th 2015	4.2	1175.11	44 min. to 22 hrs.

August 14th 2015	4.0	1029	28 min. to 3.75 hrs.
November 28th 2015	4.2	1401.04	35 min. to 8 hrs.
November 29th 2015	4.0	988.32	38 min. to 13.5 hrs.
December 25th 2015	4.0	874.05	31 min. to 5.5 hrs.
January 6th 2016	3.2	975	20 min. to 2.5 hrs.
January 17th 2016	4.2	1300.18	20 min. to 3 hrs.

When we look at the world blackouts, it is observed that the blackout that affected the largest amount of customers occurred in Brazil, followed by the blackout of Italy, and the blackout of North America on August 14, 2003. This last incident was the event in which the largest amount of load was lost and is also the one reporting the longest duration. The more localized blackout with fewer customers affected, smaller loss of load and smaller duration was the blackout occurred in London in the same year.

Table 3-14 Indicators (World blackouts- Part I) [46, 47]

Blackout	Customers without service (Number)	Lost Load (MW)	Time Duration
Brazil March 11, 1999	75, 000, 000	24,731	Up to 4 hours
Iran March 31, 2003	22, 000, 000	7,063	8 hours
London August 28, 2003	410, 000	724	37 minutes (0.62 hours)
Denmark & Sweden September 23, 2003	4, 000, 000	6,550	5 hours
Italy September 28, 2003	57, 000, 000	24,000	5 to 9 hours
North America & Canada August 14, 2003	50, 000, 000	61,800	16 to 72 hours in U.S and up to 192 hours in Canada

The other index used to study the incidents was Severity (System - minute) **[47]**. This is calculated as,

$$Severity\ (System-Minute) = \frac{Energy\ not\ served\ (MWh)}{Base\ of\ Power\ (MW)} \quad (3.1)$$

The classification of incidents according to the severity level is as following:

Table 3-15 Disturbance Severity Classification [47]

Classification (Level)	Severity (System-minute)	Interpretation
0	<1	Acceptable
1	1 to 10	Not severe
2	10 to 100	Severe
3	100 to 1000	Very severe
4	>1000	Catastrophic

Table 3-16 shows the calculated indices for each one of the blackouts on the Ethiopian Electric Power grid, and the blackouts classification as per Table 3-15. From the calculated indices, it is clear that the blackouts of 13th April 2014, 17th June 2014, 8th August 2014, 27th October 2014, 22nd April 2015, 27th July 2015 and 28th November 2015 were the most severe, with a severity level of 3, ranking them as "Very severe". The remaining blackouts had a severity level of 2, ranking them as "Severe". More than 81.25 % of the blackouts were "severe" and the remaining 18.75% of the blackouts were "very severe".

Table 3-16 Indicators (Ethiopian blackouts) (Part II)

Blackout	Energy not served (MWh)	Severity (System-minute)	Level
28-Jan-13	1026.88	41.0752	2
3/2/2013	1498.9	59.956	2
6-Mar-13	677.7	27.108	2
22-Apr-13	2028.53	81.1412	2
26-Apr-13	1710.98	68.4392	2
22-May-13	839.73	33.5892	2
25-May-13	961.267	38.45068	2
27-Jul-13	970.31	38.8124	2
13-Sep-13	1428.53	57.1412	2
7-Oct-13	1428.53	57.1412	2
24-Oct-13	887.867	35.51468	2
12-Nov-13	582.79	23.3116	2
6-Dec-13	1440.268	49.38062	2
2-Feb-14	1403.62	48.12411	2
5-Apr-14	1011.83	34.69131	2
13-Apr-14	3268.99	112.0797	3
8-Mar-14	1088.33	37.31417	2
7-May-14	1286.03	44.09246	2
11-May-14	863.83	29.61703	2
17-Jun-14	6192.73	212.3222	3
8-Aug-14	5079.81	160.4151	3
3-Sep-14	2337.87	73.82747	2
27-Oct-14	3593.99	113.4944	3
6-Nov-14	2286.82	72.21537	2
15-Jan-15	640.083	20.21315	2
15-Mar-15	2250.177	71.05822	2
22-Apr-15	3690.71	116.5487	3
8-May-15	3026.55	88.97256	2
26-May-15	1077.36	31.67153	2
27-Jul-15	4504.46	132.4192	3
14-Aug-15	2002.023	55.50896	2
28-Nov-15	6219.71	172.4504	3
29-Nov-15	1723.58	47.78872	2
11-Dec-15	2021.74	56.05564	2
22-Dec-15	1493.22	41.40166	2
25-Dec-15	2158.19	59.83891	2
6-Jan-16	1224.87	33.96128	2
17-Jan-16	3394.91	94.12874	2

3.5. Classification of Blackouts

From the review of the blackout reports in section 3.3 and Appendix C, different preconditions were observed, initiating events were various, and the two severity levels were seen. Therefore, the classification of blackouts on the Ethiopian electric power network can be carriedout based on:

(1) Pre-disturbance conditions

The following pre-disturbance conditions are identified from the review of blackout records:

i. System condition is stressful during peak hours: Most of the 2013 blackouts were happened during the peak hours. The total generation capacity was lower than the peak load demand at the time.

ii. Some important equipments out of service and/or poor planned outages: Before the blackout on December 11th 2015, the critical lines (Sululta_Gefersa 230kV line II, Fincha HHP_Ghedo230kV line, Ghedo_Gefersa 230kV Line II & III) of EEP were out of service. The 400kV and 230kV busbars of Gelan substation were also out of service. This led the system to a stressful condition.

iii. Aging equipments, loosely reconnect conductors & out-dated relay settings: The breakers and transformers of most of the substations, especially at Addis Ababa & Central regions were working over their lifetime and such system became unstable during the emergency condition. Appendix C gives a clear description of the causes of each blackout.

iv. Natural reasons such as drought, contact with tree, fire, landslide, etc…

Generally, most of the 2015 blackouts were tested by such natural disasters.

(2) Initiating Events

These events can directly cause blackout or can worsen the system condition, which may indirectly lead to blackout. Short circuit, overload, and protection-hidden failure, loss of generators, and switching and temporary transients are the usual initiating events for most of the blackouts. Table 3-17 depicted these classifications.

Table 3-17 Initiating events of blackouts

Blackouts	Initiating events				
	1	2	3	4	5
January 28th 2013	√				
January 17th 2016			√		
December 25th 2015					√
January 6th 2016	√				
November 5th 2014		√			
December 6th 2013	√				
November 17th 2013	√				
November 6th 2014		√			
February 2th 2014	√				
July 27th 2015	√				

May 8th 2015					√
April 22nd 2015	√				
March 15th 2015	√				
August 14th 2015	√				
November 29th 2015			√		
April 26th 2013			√		
March 6th 2013					√
November 28th 2015	√				
May 11th 2014	√				
August 8th 2014				√	
February 13th 2013	√				
April 22nd 2013	√				
October 24th 2013	√				
November 12th 2013	√				
November 17th 2013	√				
October 24th 2014					√
May 25th 2013		√			
October 7th 2013		√			
March 8th 2013		√			
March 2nd 2013			√		
November 29th 2015			√		
January 17th 2016			√		
June 17th 2014				√	
September 3rd 2014				√	
May 26th 2015	√				
December 11th 2015	√				
December 22nd 2015	√				

1- Short circuit (51.35 %), 2. Overloads (13.51 %), 3. Loss of power plants (16.22 %), 4. Protection and communication failure (8.11 %), 5. Switching & temporary transients (10.81 %)

(3) Severity of the Incident

By referring to Section 3.4, the blackouts of the Ethiopian Electric power can be classified based on the severity level as indicated in Table 3-18 below.

Table 3-18 Severity of the Incident

Blackouts	Severity of the incident				
	0 (acceptable)	1 (Not severe)	2 (Severe)	3 (Very severe)	4 (Catastrophic)
28-Jan-13			√		
2-Mar-13			√		
6-Mar-13			√		
22-Apr-13			√		
22-May-13			√		
27-Jul-13			√		
13-Sep-13			√		
6-Dec-13			√		
2-Feb-14			√		
13-Apr-14				√	
8-Mar-14			√		
7-May-14			√		

11-May-14	√	
17-Jun-14		√
8-Aug-14		√
3-Sep-14	√	
27-Oct-14		√
6-Nov-14	√	
15-Jan-15	√	
15-Mar-15	√	
22-Apr-15	√	
8-May-15	√	
26-May-15	√	
27-Jul-15		√
14-Aug-15	√	
28-Nov-15		√
29-Nov-15	√	
11-Dec-15	√	
22-Dec-15	√	
25-Dec-15	√	
6-Jan-16	√	
17-Jan-16	√	

3.6. Impacts of Blackouts

This work was not intended to be a definitive and detailed assessment of the blackout impacts. Detailed assessment of the impacts of blackouts need a more rigorous survey and it will stand as a big national project and requires collaborations of various entities and researchers. Therefore, this work only shows the cost of the unserved energy due to the past blackouts.

The blackout affected businesses, individuals, government agencies, environment and electric utility company itself. The impacts were complex and included economic, environmental and social costs [18]. Given the significant depreciation of the Ethiopian Birr over the years, the average electricity tariff stands now at US$0.0245/kWh [5] [2]. By using this electricity tariff, the principal economic costs of the blackout with respect to the cost of unserved energy, developed during the course of this study are shown in Table 3-19.

The cost with respect to the userved energy of the 28th November 2015 blackout was the highest among the other blackouts and costed US$ 152, 382.895. The second costliest blackout was the 17th June 2014, which has a cost of US$ 151, 721.885 as depicted in Table 3-21. Among the 38 blackouts indicated in Table 3-

[5] *The feasibility study prepared by the Ethiopian Electric Power for investments indicates that the average tariff should increase to cost-recovery level (11.3 USc/kWh) during 2021-2023 and further to 12.6 USc/kWh from 2024 onwards. While such increases may be difficult to be implemented in the timeframe indicated, the Ethiopian Electric Power has prepared a proposal for a significant tariff increase that is currently under discussion and whose details remain to be confirmed [3, 4].*

21, the least cost with respect to the unserved energy was the 12th November 2013 blackout, which costed US$ 14, 278.355. To sum up, there was a huge economic loss due to the unserved energy, which accounts for **1,943,431.018 USD** for the 38 blackouts of the last three and half years on the Ethiopian Electric Power network.

Table 3-19 Cost of unserved energy

Blackout	Energy not served (MWh)	Cost (USD)
28-Jan-13	1026.88	25158.56
3/2/2013	1498.9	36723.05
6-Mar-13	677.7	16603.65
22-Apr-13	2028.53	49698.985
26-Apr-13	1710.98	41919.01
22-May-13	839.73	20573.385
25-May-13	961.267	23551.0415
27-Jul-13	970.31	23772.595
13-Sep-13	1428.53	34998.985
7-Oct-13	1428.53	34998.985
24-Oct-13	887.867	21752.7415
12-Nov-13	582.79	14278.355
6-Dec-13	1440.268	35286.566
2-Feb-14	1403.62	34388.69
5-Apr-14	1011.83	24789.835
13-Apr-14	3268.99	80090.255
8-Mar-14	1088.33	26664.085
7-May-14	1286.03	31507.735
11-May-14	863.83	21163.835
17-Jun-14	6192.73	151721.885
8-Aug-14	5079.81	124455.345
3-Sep-14	2337.87	57277.815
27-Oct-14	3593.99	88052.755
6-Nov-14	2286.82	56027.09
15-Jan-15	640.083	15682.0335
15-Mar-15	2250.177	55129.3365
22-Apr-15	3690.71	90422.395
8-May-15	3026.55	74150.475
26-May-15	1077.36	26395.32
27-Jul-15	4504.46	110359.27
14-Aug-15	2002.023	49049.5635
28-Nov-15	6219.71	152382.895
29-Nov-15	1723.58	42227.71
11-Dec-15	2021.74	49532.63
22-Dec-15	1493.22	36583.89
25-Dec-15	2158.19	52875.655
6-Jan-16	1224.87	30009.315
17-Jan-16	3394.91	83175.295
	Total Cost (USD)	**1, 943, 431.018**

3.7. Lessons Learned from the Blackouts

Taking a look at most of the major disturbances as indicated in Section 3.3, Section 4.6 and Appendix C, common denominators could be highlighted as follows:

a. The inappropriate estimation of the situation leading to non-respect of the security rules (negligence);
b. The weakness of the inter-transmission and substation operators' coordination;
c. Bad planned outage decisions in critical situations
d. Lack of communication infrastructures for the power system and poor protection system coordination (poor data communication and teleprotection systems, relay setting too long); etc…

Organisational Response

In 2015 alone, 16 blackouts were happened on EEP's network. These blackouts imposed a great impact on citizens, businesses, and the government. In December 2015 alone, three large scale blackouts were occurred (December 11th, 22nd &25th) and after these blackouts, the board of directors of the Ethiopian Electric Power (EEP) decided to organize a new department called "**System Study**", whose mandate is to investigate the previous blackouts and assess the vulnerabilities of the power grid, and to find the possible ways that can reduce the size and the frequency of the disturbance that will arise in the network.

In addition, a committee was appointed to technically help and strengthen the new department. The committee members are from senior engineers and are experts of power system protection, teleprotection and signalling, communication and PLCC, RTU and SCADA systems. They generally called as "**Advisors**".

Technical Response

On the other side, technically, various under frequency load shedding (UFLS) relays were installed at 26 selected sites to prevent the frequency collapse during the disturbance and balancing the load demand with the power generated by the power plants. A shunt reactor was also installed at Wolaita Sodo 400kV substation to protect the network from over voltages during off-peak hours by absorbing the excess reactive power of the system.

Chapter 4

Network Models and Simulation Studies

4.1. Introduction

In this chater, a brief introduction to the tool used for the modelling and simulation, DIgSILENT PowerFactory 2014 is given in Section 4.2; thereafter the EEP network models of the transmission lines, transformers, generators and loads are presented with explanations of the associated consoles of the software. The single line diagram of EEP's high voltage grid is built for simulating the grid behaviour prior to and during the disturbance. A review of the power flow and transient stability analysis of a power system is also discussed in Section 4.4 and Section 4.5 respectively. In section 4.6, simulations are carried out for selected blackouts to identify the root causes of the corresponding system collapses on the EEP grid.

4.2. DIgSILENT PowerFactory Software

DIgSILENT PowerFactory software is a computer aided engineering tool for the analysis of transmission, distribution, and industrial electrical power systems. **"DIgSILENT "** is an acronym for "**DIg**ital **SI**mu**L**ation of **E**lectrical **N**e**T**works".

To address users power system analysis requirements, **PowerFactory** was designed as an integrated engineering tool to provide a comprehensive suite of power system analysis functions within a single executable program. Key features include:

1. PowerFactory core functions: definition, modification and organization of cases; core numerical routines; output and documentation functions.
2. Integrated interactive single line graphic and data case handling.
3. Power system element and base case database.
4. Integrated calculation functions (e.g. line and machine parameter calculation based on geometrical or nameplate information).
5. Power system network configuration with interactive or on-line SCADA access.
6. Generic interface for computer based mapping systems

The software is also a time domain Root Mean Square (RMS) and Electromagnetic Transients (EMT) simulation tool used in analysing and controlling electrical power transmission and distribution in industrial

power systems [48]. The software provides an environment to implement operations of a real-life power system with all the calculations. Its huge single database supports all power system functions – load flow, time domain RMS simulation, modal analysis, fault calculation/analysis (IEC, ANSI, and VDE), protective relay coordination, reliability, etc. – to be executed.

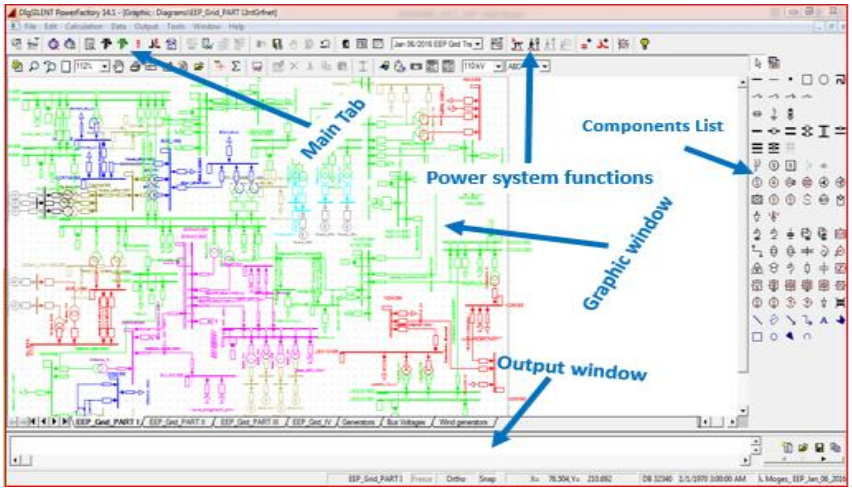

Figure 4-1 PowerFactory main window

PowerFactory is primarily intended to be used and operated in a graphical environment. That is, data is entered by drawing the network elements, and then editing and assigning data to these objects. Data is accessed from the graphics page by double-clicking on an object. An input dialogue is displayed and the user may then edit the data for that object. Figure 4-1 shows the PowerFactor Graphical User Interface (GUI) when a project is active.

4.3. EEP Network Models

The power system is made of more than a few parts: generators, transmission lines, transformers, loads, and shunt components. In this thesis however, the built-in models of transmission lines, transformers, generators, loads and shunt compensators are used along with the data that is obtained from EEP. These parts of the power system are implemented by way of modelling, simulation, and optimized for power flow calculation and transient analysis.

There are many possibilities to model electrical component, either in detail or in simple form in PowerFactory, but only basic modeling component and those options that are necessary for load flow and transient analyses are considered here. The power system component models of the EEP network in the PowerFactory software are explained as follows:

a) Generator: are modeled as voltage-controlled sources that control the voltage magnitude and active power injection into the busbar. The busbar connected to the generator is commonly referred as PV bus. In the network, at least one of the generators must be configured as reference machine, i.e., control the voltage magnitude and angle. The busbar connected to the reference machine is set as slack (SL) bus. Additionally, to investigate the loading and operation limit violation, it is required to set the active and reactive power maximum and minimum limits. The input data required for the generator models are indicated in Figure 4-2 and 4-3. Some of the generator data obtained from EEP are indicated in Table 4-1.

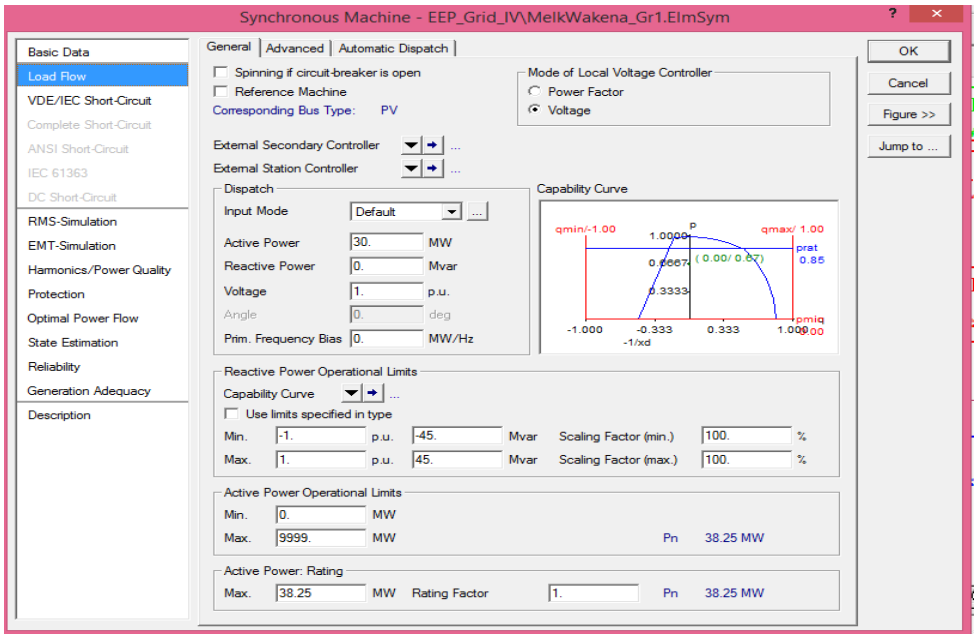

Figure 4-2 Load flow setting page of PowerFactory generator model

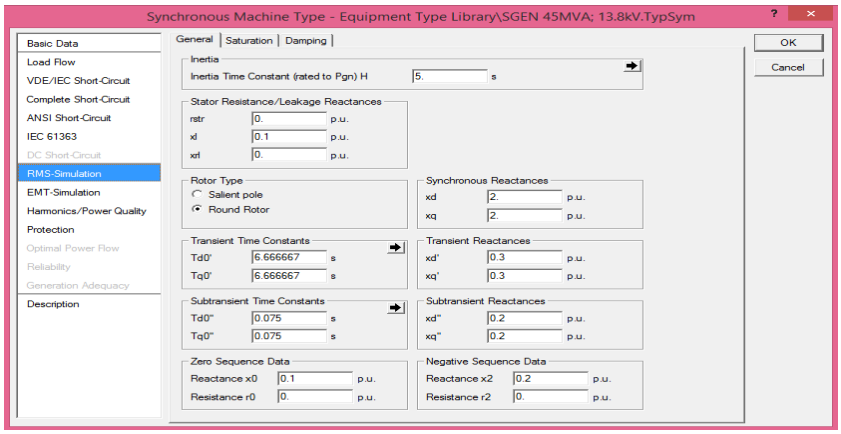

Figure 4-3 RMS simulation setting page of PowerFactory generator model

Table 4-1 Generators Data (snap shoot of July 17, 2016 @ 7:00 PM)

Gen. Name	Sn [MVA]	Un [kV]	R/X [p.u.]	P [MW]	cosphin [p.u.]	Pmin [MW]	Pmax [MW]	Qmin [MVAr]	Qmax [MVAr]
Fincha13.8 GR1	35	13.8	0.014	29	0.95	10	33.33	-16	14
Gilgel Gibe 13.8 GR1	73	13.8	0.0227	60	0.9	0	70	-21	21
Tis Abay II 10.5 GR1	40	10.5	0.018	27	0.9				
Tis Abay I 6.3 GR1	4.8	6	0.021	4	0.8	0	4	-2.9	2.9
Melka Wakena 13.8GR1	45	13.8	0.016	35	0.85				
Fincha 13.8 GR4	40	13.8	0.019	25	0.95	0	28	-34	23
Awash II GR2 10.5	20	10.5	0.022	6	0.9	3	15	-15	13
Melka Wakena 13.8 Gr4	45	13.8	0.016	35	0.85	0	38.25	-42	35
Melka Wakena 13.8 Gr3	45	13.8	0.016	35	0.85	0	38.25	-31.5	30.15
MelkaWakena 13.8 GR2	45	13.8	0.016	30	0.85	0	38.25	-31.5	30.15
Tis Abay I 6.3 GR2	4.8	6	0.021	4	0.8	0	4	-2.9	2.9
Tis Abay I 6.3 GR3	4.8	6	0.021	4	0.8	0	4	-3.84	3.84
Tis Abay Ii 10.5 GR2	40	10.5	0.018	27	0.9				
Awash II GR1 10.5	20	10.5	0.022	6	0.9	3	15	-15	13
Awash III GR2 10.5	20	10.5	0.022	9	0.9	3	15	-15	13
Awash III GR1 10.5	20	10.5	0.022	9	0.9	3	15	-15	13
Koka Hydro 10.5 GR2	18	10.5	0.032	10	0.9	0	13	-12	11.6
Koka Hydro 10.5 GR3	18	10.5	0.032	0	0.9	0	13	-18	13.5
Fincha 13.8 GR2	35	13.8	0.014	29	0.95	0	33.33	-16	14
Fincha 13.8 GR3	35	13.8	0.014	29	0.95	0	33.33	-16	14
Gilgel Gibe 13.8 GR2	73	13.8	0.0227	60	0.9	0	70	-21	21
Gilgel Gibe 13.8 GR3	73	13.8	0.0227	60	0.9	0	70	-21	21
TekUNIT1	86	13.8	0.1	66	0.9	0	78	-38	38
TekUNIT2	86.7	13.8	0.1	40	0.9	0	78	-38	38
TEKUNIT3	87.6	13.8	0.1	40	0.9	0	78	-38	38
TEKUNIT4	86.7	13.8	0.1	40	0.9	0	78	-38	38
Gilgel Gibe II UI	125	15	0.0227	95	0.85	0	105	-50	50
Gilgel Gibe II U2	125	15	0.0227	95	0.9	0	105	-50	50
Gilgel Gibe U3	125	15	0.0227	95	0.9	0	105	-50	50
Gilgel Gibe U4	125	15	0.0227	95	0.9	0	105	-50	50
Beles15B1	130	15	0.1		0.9				
Beles15B2	130	15	0.1		0.9				
Beles15B3	130	15	0.1		0.9				
Beles15B4	130	15	0.1		0.9				
GG III G1	220	15	0.0227	10	0.85	0	220	-100	100

b) Load: can be modeled in different ways such as constant impedance, constant current, or constant power. The modelling of system loads is not critical for the methodologies developed within this research and the use of a constant impedance representation is fully adequate for all the studies which have been performed, i.e., for load flow as well as RMS simulations. The load data for each blackout simulation were different as was indicated in Appendix C.

c) Line: Transmission line is modeled as $\boldsymbol{\pi}$ -network for calculation, and input data required by line are series resistance, series inductance, susceptance and shunt capacitance. Usually, these values are given in per km of length as it is indicated in Figure 4-5 and Figure 4-6 (b). The length of the line and the type of line model (i.e.,lamped or distributed parameter) should be specified as is indicated in Figure 4-6 (a). The line data for the HV EEP network is populated in Appendix A, Table A-1.

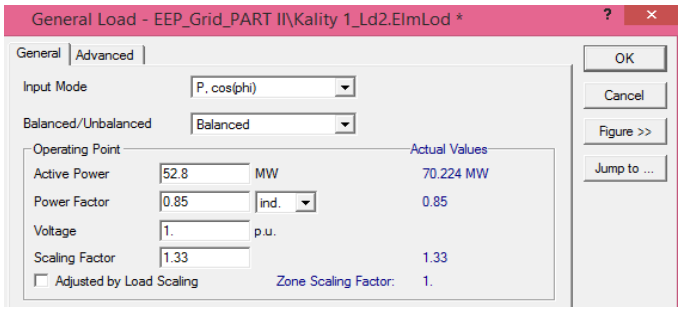

Figure 4-4 General load model in PowerFactory

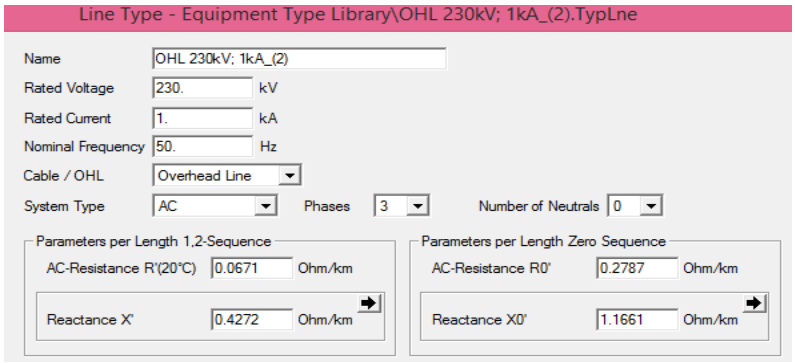

Figure 4-5 Line model in PowerFactory showing the ratings and other parameters of the line

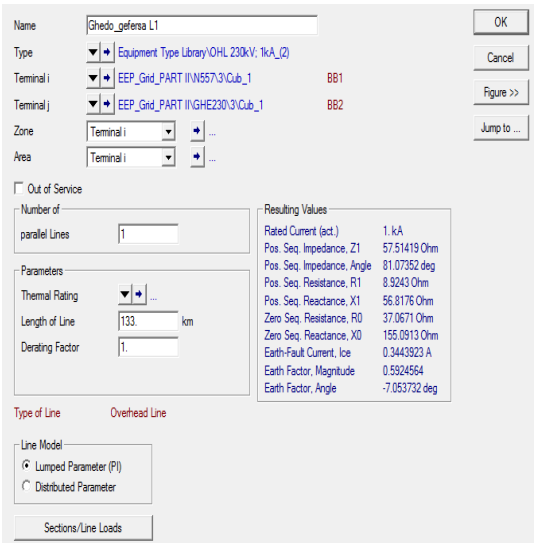

a) Length & line model of a line

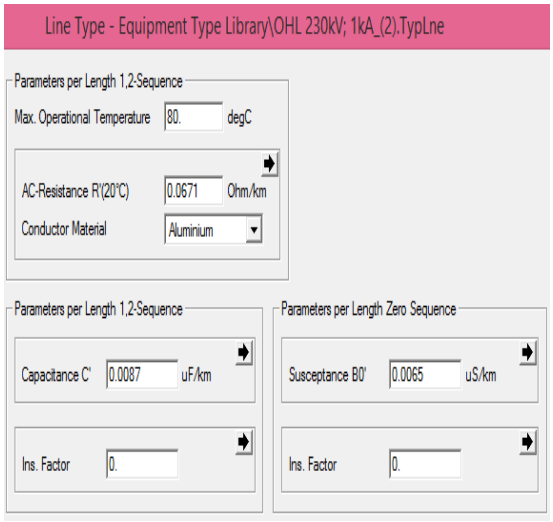

b) Shunt parameters of a line

Figure 4-6 Line model in PowerFactory including length, type of line model, shunt capacitance and susceptance

Since, transformers are also series branches in the network a similar model, i.e., a π − equivalent circuit representation is used in DIgSILENT PowerFactory. However, the transformers can be equipped with tap changers. The required input data for the transformers are rated MVA, primary and secondary voltage

levels, the numbers of phases, the short circuit voltage in percent, core loss in kW, the no load current, etc.., as it is indicated in Figure 4-7 (a) & (b).

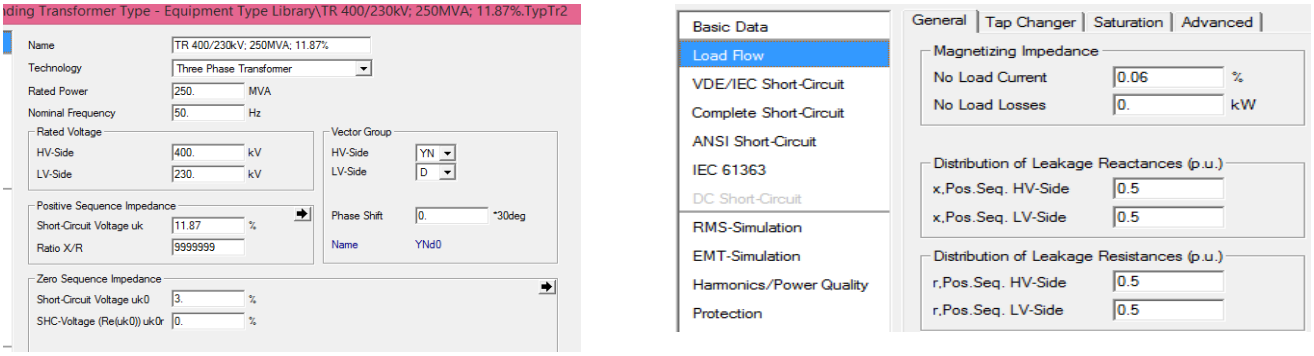

a) Rating of transformer

b) parameters of transformers

Figure 4-7 Transformer model in PowerFactory

The actual data obtained from EEP is then fed to the software. These data for the two-winding transformers are indicated in Table 4-2. The three-winding transformers' data is populated in Appendix A, Table A-3.

Table 4-2 Transformer Data (two-winding)

Node 1	Node 2	U_{n1} [kV]	U_{n2} [kV]	S_n [MVA]	S_{max} [MVA]	uk [%]	V_{fe} [kW]	i_0 [%]
Harar II 66	Harar II 15	66	15	9.6	12	7.216	8.3	0.13
G/Gibe Old 400kV	G/Gibe Old 230kV	400	230	250	250	10.3	20.7	0.26
Sebeta II 400kV	Sebeta II 33kV	400	230	250	250	9.85	20.7	0.11
Bahir Dar 400kV	Bahir Dar II 230 BB1	400	230	250	250	11.87	72.75	0.06
Beles15B1	Beles 400kV	15	400	133	133	10.3	7.703	0.26
D/Markos 400kV	Debre Markos 230kV	400	230	250	250	11.87	72.75	0.06
Sululta 400KV	Sululta 230KV	400	230	250	250	11.87	72.75	0.06
Sululta 230KV	Sululta 132KV	230	132	63	63	11.86	45	0.244
Bedele 230kV	Bedele 132	230	132	63	63	8.65	18.6	0.06
Sebeta 230kV BB1	Sebeta I 132kV	230	138	125	125	20.64	19	0.017
Gefarsa 230kV	Gefarsa 132kV BB1	230	138	125	125	20.64	19	0.017
Kaliti I 230kV BB1	Kaliti I 132kV BB1	230	138	125	125	20.64	19	0.017
Akaki 400	Akaki 230	400	230	500	500	12.5	20.7	0.19
Welayta Sodo 400 kv	Welyat sodo 132 new	400	132	250	250	9.85	20.7	0.11
Akaki 230	Akaki II 132	230	132	125	125	11.84	81.64	0.35
Akaki 400	Akaki 230	400	230	500	500	12.5	20.7	0.19
Gibe 3 400	N2269	400	15	441	441	13.37	85	0.15
hosaiena 230KV	Hosaina 132kV	230	138	45	63	6.371	20	0.23
JImma230KV	Jimma II 132kV	230	132	50.4	63	11.57	19	0.04
Sebeta 230 BB1	SEBETA I 132	230	138	125	125	20.64	19	0.017
Legetafo 230KV	lEGETAFO132KV	230	138	125	125	20.64	19	0.017
Sebeta 230 BB1	SEBETA I 132	230	138	125	125	20.64	19	0.017
G/Gibe Old 230KV	N2444	230	138	45	63	6.386	20	0.23
N2451	N2450	132	15	25	25	9.71	11.59	0.11
Metu166KV	metu33KV	66	33	6.3	6.3	7.6	6.5	0.7
Melka WakenaYougo	Melka Wakena You132kV	230	138	63	63	6.453	12	0.545

To sum up, DIgSILENT PowerFactory has an a built-in models of various power system components. For detail, it recommended to consult the user manual of the software [48].

4.4. Power Flow Analysis

The aim of the power flow analysis for this study is to determine the bus voltages and components overloading during prior to the disturbance, and to obtain the initial conditions for the transient analysis.

The nodal network equation formed, shown in equation (4.1) for a network with n buses, describes the relationship between system voltages **V** and points of current injection **I** [49].

$$\begin{bmatrix} I_1 \\ \vdots \\ I_i \\ \vdots \\ I_n \end{bmatrix} = \begin{bmatrix} Y_{11} & \dots & Y_{1i} & \cdots & Y_{1n} \\ \vdots & & \vdots & & \\ Y_{i1} & & Y_{ii} & & \vdots \\ \vdots & & \vdots & & \\ Y_{ni} & & \cdots & & Y_{nn} \end{bmatrix} \begin{bmatrix} V_1 \\ \vdots \\ V_i \\ \vdots \\ V_n \end{bmatrix} \qquad Or \quad \boldsymbol{I = YV} \tag{4.1}$$

In (4.1), subscripts i and j are bus numbers such that Y_{ii} is the self-admittance of bus i, and $Y_{ij}, i \neq j,$ is the mutual- admittance between buses i and j. Reduction of the network model is possible so that all zero-injection buses are neglected and the nodal network equation has much smaller dimension [50]. This lowers the computational burden during simulations and power system analysis. The active and reactive power injections are represented as [51, 13]:

$$P_i = V_i^2 G_{ii} + V_i \sum_{j=1, j\neq i}^{n} V_j\left(G_{ij}\cos(\theta_i - \theta_j) + B_{ij}\sin(\theta_i - \theta_j)\right) \qquad for\ i = 1,2,\dots.,n \tag{4.2}$$

$$Q_i = -V_i^2 B_{ii} + V_i \sum_{j=1, j\neq i}^{n} V_j\left(G_{ij}\sin(\theta_i - \theta_j) - B_{ij}\cos(\theta_i - \theta_j)\right) \qquad for\ i = 1,2,\dots.,n \tag{4.3}$$

Where, $\theta_{ij} = \theta_i - \theta_j$.

4.5. Transient Stability Analysis

A transient stability analysis is performed by combining a solution of the algebraic equations describing the network with a numerical solution of the system and thereby provides access to system voltages and currents during the transient period. In transient stability studies a load flow calculation is made first to obtain system conditions prior to the disturbance. Thereafter, a numerical solution of the system differential equation has to be solved. Utilizing the classical model of generators, the swing equation for generator i can be expressed as [52]:

$$\frac{2H_i}{\omega_s}\frac{\partial^2\delta_i}{\partial t^2} = P_{mi} - P_{ei}, \qquad i = 1, 2, \dots, m \tag{4.4}$$

$$H_i = \text{inertia constant in MJ/MVA}$$

The second order differential equation in equation (4.4) can be written as two simultaneous first order differential equations:

$$\frac{2H_i}{\omega_s}\frac{d\omega}{dt} = P_{mi} - P_{ei}, \qquad i = 1, 2, \dots, m \tag{4.5}$$

$$\frac{d\delta_i}{dt} = \omega_i - \omega_s \tag{4.6}$$

Before solving the above differential equations to determine the transient stability or instability of the system, it's necessary to compute the initial conditions.

Computation of Initial Conditions

Let us consider an '*n*' bus power system with '*m*' generators (*m* < *n*). Without loss of generality, it is assumed that the '*m*' generators are located at first '*m*' buses of the system. Towards computation of initial conditions, initially the load flow solution of the system is computed. From the load flow solution, following quantities are available:

(i) $V_i < \theta_i \qquad for\ i = 1, 2, \dots, n$
(ii) $P_{Li}, Q_{Li} \qquad for\ i = m+1, m+2, \dots., n$
(iii) $P_{Li}, Q_{Li}, P_{Gi}, Q_{Gi} \qquad for\ i = 1, 2, \dots., m$

Where $P_{Li}\ and\ Q_{Li}$ denote the real and reactive power load at bus 'i' respectively. Similarly, $P_{Gi}\ and\ Q_{Gi}$ denote the real and reactive power generation at bus 'i' respectively. Further, the quantities $V_i\ and\ \theta_i$ denote the voltage magnitude and angle of i^{th} bus respectively. With this information, following calculations are carriedout [53, 51];

a) At any bus 'i', the loads are converted to equivalent admittance as:

$$y_{Li} = \frac{P_{Li} - jQ_{Li}}{V_i^2} \qquad for\ i = 1, 2, \dots., n \tag{4.7}$$

b) Augment the $\mathbf{Y_{BUS}}$ matrix of the system as;

$$\mathbf{Y_{BUS}(i, i)} = \mathbf{Y_{BUS}^{Old}(i, i)} + y_{Li} \qquad for\ i = 1, 2, \dots, n \tag{4.8}$$

where, $\mathbf{Y_{BUS}(i, i)}$ is the original $\mathbf{Y_{BUS}}$ matrix of the system used in load flow calculation.

c) At the generator buses, the generators are represented as equivalent voltage sources behind the direct axis transient reactances as,

$$\mathbf{E_i} = \mathbf{V_i} + jx'_{di}\mathbf{I_i} = jx'_{di}\frac{\mathbf{P_{Gi}} - \mathbf{jQ_{Gi}}}{\mathbf{V_i^*}} = E_i < \delta_i \qquad for\ i = 1, 2, \ldots, m \tag{4.9}$$

In equation (4.9), the quantity x'_{di} denotes the direct axis transient reactance of the i^{th} machine. While performing the transient stability analysis, the magnitude $|E_i|$ is held constant. The equivalent diagram of the 'n' bus power system is shown in Figure 4-8.

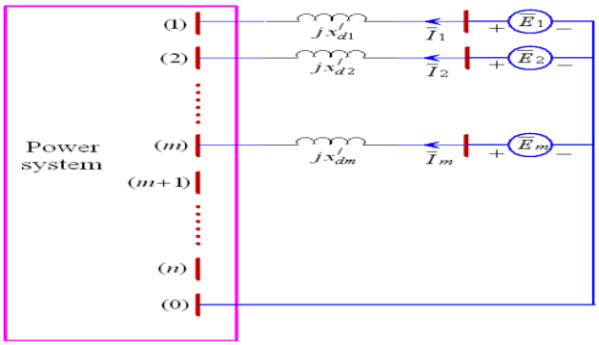

Figure 4-8 Equivalent representation of generators for transient stability analysis [54]

With the initial conditions computed as above, we are now ready to solve the transient stability problem. Basically, the transient stability problem is solved by two techniques [53, 51]: Partition explicit (PE) method and Simultaneous implicit (SI) method.

In the PE method, the network algebraic equations and the generator differential equations are solved separately. In the SI method, these algebraic and differential equations are solved together.

Network Algebraic Equations

The network algebraic equations are represented as in equation (4.1). In equation (4.1), $\mathbf{Y_{BUS}}$ is the bus admittance matrix of the system and

$$\mathbf{I_{BUS}} = [\,\mathbf{I_1}\ \mathbf{I_2}\ \ldots.\ \mathbf{I_m}\ \mathbf{I_{m+1}}\ \ldots.\ \mathbf{I_n}]^{\mathbf{T}}$$
$$\mathbf{V_{BUS}} = [\mathbf{V_1}\ \mathbf{V_2}\ \ldots.\ \mathbf{V_m}\ \mathbf{V_{m+1}}\ \ldots.\ \mathbf{V_n}]^{\mathbf{T}} \tag{4.10}$$

The voltage - current relationship of the generator reactance is given by,

$$u_k = jx'_{dk}i_k \quad => \ i_k = y_k u_k \tag{4.11}$$

In equation (4.11), i_k and u_k are the current through and voltage across the generator reactance respectively and $y_k = \frac{1}{jx'_{dk}} = -j\frac{1}{x'_{dk}}$. Now, at the generator terminals, $\mathbf{I_k} = i_k = y_k u_k; or\ \mathbf{I_k} = y_k(\mathbf{E_k} - \mathbf{V_k})\ as\ (u_k = \mathbf{E_k} - \mathbf{V_k})$. Or,

$$I_k + y_k V_k = y_k E_k \tag{4.12}$$

From equation (4.12), the voltages $V_1, V_2, \ldots, V_n$ can be solved, for known values of $E_1, E_2, \ldots, E_n$. With these known terminal voltages, the electrical power output of each generator can be calculated as;

$$\boldsymbol{P_{ei}} = \boldsymbol{Re}(\boldsymbol{E_i I_i^*}) \qquad for\ i = 1, 2, \ldots, m \tag{4.13}$$

Where

$$\boldsymbol{I_i} = y_i(\boldsymbol{E_i} - \boldsymbol{V_i}) \qquad for\ i = 1, 2, \ldots, m \tag{4.14}$$

With the above equations, the PE solution method is described below as it is used by the DIgSILENT PowerFactory software package for performing RMS simulation.

Partition Explicit Solution Scheme

In the PE method, the numerical integrations of the generator differential equations are carried out separately from the solution of the network algebraic equations. For numerical integration of differential equations, the total simulation time (t_T) is divided into *N* intervals, each interval being of duration Δt seconds. Thus, $\Delta t = \frac{t_T}{N}$. Now, the major steps for solving the transient stability problem, with PE method, are as follows [51, 54, 55].

1. Obtain the load flow solution of the given system. Thereafter, compute the internal voltages of all the generators ($E_i, for\ i = 1, 2, \ldots, m$) using equations (4.7)-(4.9). The magnitudes E_i would be kept constant at these calculated values throughout the simulation.
2. With the values of E_i obtained above, the equation set (4.12) is solved to obtain the terminal voltages at all the buses ($V_i,\ for\ i = 1, 2, \ldots, n$). Subsequently, the electrical power output of all the generators ($P_{ei},\ for\ i = 1, 2, \ldots \ldots, m$) are computed from equations (4.13) - (4.14).
3. Under steady state condition, mechanical power input to each generator is equal to its generator electrical output power (neglecting losses).Therefore, $P_{mi} = P_{ei},\ for\ i = 1, 2, \ldots, m$. Also, under steady state, all the generators are assumed to operate at synchronous speed (ω_s).
4. Thus, after the above three steps, at t = 0, the variables pertaining to generators ($E_i, \delta_i, \omega_i, P_{ei}$ for i = 1, 2, ……, m) and the network bus voltages (V_i, for i = 1, 2, ····· n) are all known.

5. The simulation process advances to $t = \Delta t$. At this instant, first the network equations given in the equation set (4.12) are solved to compute the bus voltages and subsequently, the output electrical power of each generator is calculated by using equations (4.13) - (4.14). Now, if the steady state condition is still maintained, i.e. if there is no change in the network (as compared to the network condition at t = 0), then the calculated values of P_{ei} would be again equal to the corresponding value of P_{mi}.

6. With the solution of the network equations at hand, we should now solve the generator differential equations for calculating the values of δ_i and ω_i at $t = \Delta t$. Towards that end, let us first re-write the swing equations of i^{th} machine for convenience in equations (4.5) - (4.6).

Now, from equation (4.5), as $P_{mi} = P_{ei}$, $\frac{d\omega_i}{dt} = 0$. In other words, there is no change in the speed of the generator and hence $\omega_i = \omega_s$. As a result, from equation (4.6), $\frac{d\delta_i}{dt} = 0$ and hence, the angle δ_i would also be maintained at the value calculated at t = 0. Therefore, under steady state condition, at $t = \Delta t$, both δ_i and ω_i would be maintained at the values calculated at t = 0.

7. Assume that the steady state condition continues from t = 0 to $t = (k - 1)\,\Delta t$, where, k is a positive integer. Following the arguments described at steps 5 and 6, it can be easily seen that at the end of $t = (k - 1)\,\Delta t$ sec., both δ_i and ω_i would still be maintained at the values calculated at t = 0.

8. Now, let us assume that a three phase to ground short circuit fault occurs in the system at $t = t_0 = k\Delta t$ at the l^{th} bus. To accommodate this fault condition in the network equations, the element $\boldsymbol{Y}_{ll}$ is increased manifold to reflect very high admittance from bus 'l' to ground. With this imposed condition, the network bus voltages are calculated from equation set (4.12). Subsequently, the output electrical power of each generator is calculated by using equations (4.13) - (4.14) corresponding to time $t = t_0$.

9. With the values of P_{ei} calculated in step 8, the swing equations (4.5) - (4.6) are integrated to obtain the values of δ_i and ω_i at $t = t_0$. Now, for integrating the swing equations, initial values of δ_i and ω_i are required. These initial values are taken to be equal to the values of δ_i and ω_i obtained at the end of $t = (k - 1)\Delta t$. For brevity, the value of δ_i (i = 1, 2, ····· m) calculated at $t = t_0$ is denoted as $\delta_i(t_0)$. With this value of $\delta_i(t_0)$, the voltage behind the transient reactance is updated as $E_i = E_i < \delta_i(t_0)$, for i = 1, 2, ····· m, where the magnitude E_i has been taken to be equal to the constant value calculated at step 1.

10. The simulation advances to $t = t_0 + \Delta t$. If the fault still persists, the values of P_{ei} are calculated as described in step 8. However, for this purpose, the values of E_i in equation set (4.12) are taken to be equal to the latest values calculated at the end of $t = t_0$ sec.

11. With the values of P_{ei} calculated at $t = t_0 + \Delta t$, step 9 is repeated to update the variables ω_i, δ_i and E_i at the end of $t = t_0 + \Delta t$. Again, for integrating the differential equations, the latest values of ω_i and δ_i (calculated at $t = t_0$) have been taken as the initial values.

12. Steps 10 and 11 are repeated to update the variables at $t = t_0 + 2\Delta t,\ t_0 + 3\Delta t,\ t_0 + 4\Delta t,\ \cdots\cdots$ till the fault clears.

13. At $t = t_{cl}$ ($t_{cl} = p\Delta t$, p being a positive integer and $p > k$), the fault clears. This condition is imposed in the network equations by restoring $\boldsymbol{Y}_{ll}$ to its original pre-fault value and subsequently, steps 8 - 12 are repeated to obtain the variations of δ_i and ω_i. By observing the variation of δ_i, the stability of the system is assessed.

In step 9, the generator differential equations are numerically integrated. There are two such numerical integration techniques used for RMS simulation of the power system, namely, modified Euler's method and 4*th* order Runga-Kutta technique.However, DIgSILENT PowerFactory software uses the R-K 4th order method. The detailed mathematical derivations of the R-K 4th order method is found in [54, 49, 51, 55].

Criteria for Stability

i) **Critical fault clearing times:** The critical clearing time is the maximum allowable time that a fault can be sustained without the synchronous generator becoming unstable. Typical fault clearing times are [56]:
   - For a three-phase fault, the typical maximum fault clearing time (including the relay operating time plus circuit breaker opening time) is 8 cycles.
   - For a double line to ground fault, the typical maximum fault clearing time, including the breaker failure is 17 cycles.
   - For a line-to-ground fault, the typical maximum fault clearing time (including the backup relay operating time plus circuit breaker opening time) is 30 cycles.

ii) **Assessment of the rotor angles for stability:** The generator will be stable for steady state rotor angles below 90 degrees and unstable for above 90 degrees ($\frac{\pi}{2}\ radians$). However, the rotor angles can swing into the unstable region during transient conditions and will be back in the stable-operating region. If the rotor angle swings around 90 degrees and decays very rapidly, then the generator is stable. If the rotor angle goes beyond 180 degrees in the first cycle, then the generator is unstable.

iii) **Voltage Swing during the disturbance:** During the fault, the bus voltage drops and upon fault clearing the voltage recovers. From the stability point of view, the voltage has to recover to the rated voltage immediately after fault clearing. If the voltage falls below 60% of the rated voltage and fails to recover (voltage collapse), such a condition is unacceptable.

4.6. Result Analysis and Discussions

In this part of the thesis, the following result analyses have been carried out to investigate root cause of the blackouts of 6th January 2016, 11th December 2015, 22nd December 2015, and 14th August 2015.

— Power flow simulations to analyse system performance under steady state conditions.
— RMS simulations to analyse system performance under transient conditions.

The selection of these blackouts is based on:

(1) The load, generation, and planned outage data available at the NLDC archive as shown in Appendix C and in [6], and the availability of the sequence of events recorded on the EMS found in [6] and hence a comparison can be made between the the sequence of events observed on the EMS and the simulation results. This helps us to corroborate whether the suggested cause could possibly have triggered the sequence of events that followed.
(2) To consider and study the impact of faults on different network levels (45 kV, 132kV, 230kV & 400kV) and to point out the system vulnerabilities of the national grid with respect to the faults on these different network levels.

In the existing network of EEP, nine uncompensated 400kV transmission lines, as indicated in Appendix A, are used to transfer bulk power from northwestern region of Beles HPP, southern and southwestern HPPs of G/Gibe III and G/Gibe II to big load centres of Addis Ababa and Central regions and further onwards. In addition to these lines, EEP has identified the 230kV and 132kV critical loaded lines which are responsible for the intra-power flows among the seven regional power systems [57]. Table 4-3 shows these lines.

Table 4-3 Critical loaded lines of EEP [57]

No.	Line	Interconnected Regions
1	230kV Sebeta I_Kality I	South and South western **With** Addis Ababa
2	230kV Koka_Dire Dawa III	Addis Ababa & Central **With** Eastern
3	230kV Alamata_Combolcha II_Legatafo	Addis Ababa & Central **With** Northern
5	230kV B/dar_Alamata	North Western **With** Northern
6	230kV Fincha HPP_Ghedo_Gefersa	Western **With** Central & Addis Ababa
7	230kV Sekoru_Ghedo	South western **With** Western and Central
8	132kV Gefersa_Sebeta I	Western and North Western **With** Addis Ababa, Central

This part of the thesis mainly focuses on performing computer simulations to corroborate whether the suggested initial event could possibly have triggered the sequence of events that were observed on the SCADA/EMS system.

4.6.1. January 6th 2016 Blackout

System Condition Prior to the Power Failure

On January 6th, the peak demand at 16:00 hrs was about 1.24 GW, the weather condition was windy as well as rainy in the southwestern region of the country (around GG II HPP). On the other parts of the country (northern & eastern parts), there was no sufficient rainfall to fed the reservoirs of Awash III & II, Koka and Tekeze HPPs. The system frequency was at its nominal value - 50 Hz. The total generation was over 1300 MW at 16:00 hrs, which consisted of 1200 MW of hydro power plant production and the remaining 100 MW was from wind turbine production. Of the total generation, G/Gibe II power plant constituted 27% of the total power production. The total transnational exchange was 15.8 MW, which was exported to Djibouti. Ghedo – Gefersa 230 kV transmission line I was in a planned maintenance outage.

The voltages at Kality I 230/132 kV, Sululta 400/230 kV, Sebeta I 230/132 kV, Bahir Dar II 400/230 kV, Akaki I 400/230 kV, Combolcha II 230/132 kV, and Ghedo 230/132 kV substations showed an increments from their nominal values as indicated in Figure 4-9. However, it was still in the acceptable range. These substation buses plays a vital role for the healthy power flow of the grid.

With this information, the steady state condition prior to disturbance has been simulated and the results are depicted below. The voltages at different buses that deviate (although the range is in the normal operating range) from the specified 1.0 pu are indicated in Figure 4-10. The power flow on the important transmission lines was indicated in Table 4-5 below. The total grid loss was 34.89 MW.

Table 4-4 Overloaded equipments prior to disturbance

Equipment name	Loading (%)
Gambela_Tr (230/66/33kV)	98.87 (ONAN[6])
Ghedo_Tr_1 (230/132/15kV)	95.5 (ONAN)
Koka_Tr_2 (132/15/10.5kV)	102.3(ONAN)
Koka_Tr_3 (132/15/10.5)	104 (ONAN)
Metu_Tr (230/66/15kV)	96 (ONAN)

As obtained from the load flow of the grid, some lines and transformers were already overloaded, the voltages of some critical buses were rising, and at some critical buses, it was declining as shown in Figure 4-9 and 4-10.

[6] *ONAN & ONAF: the type of cooling system for transformer. ONAN stands for **O**il **N**atural **A**ir **N**atural; where as ONAF stands for **O**il **N**atural **A**ir **F**orced.*

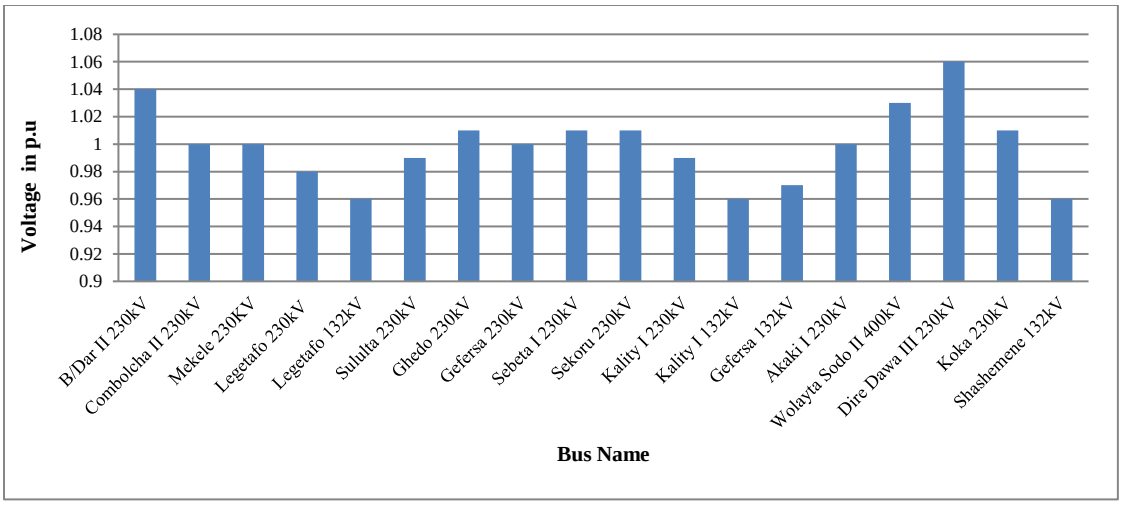

Figure 4-9 Voltages of critical buses prior to disturbance

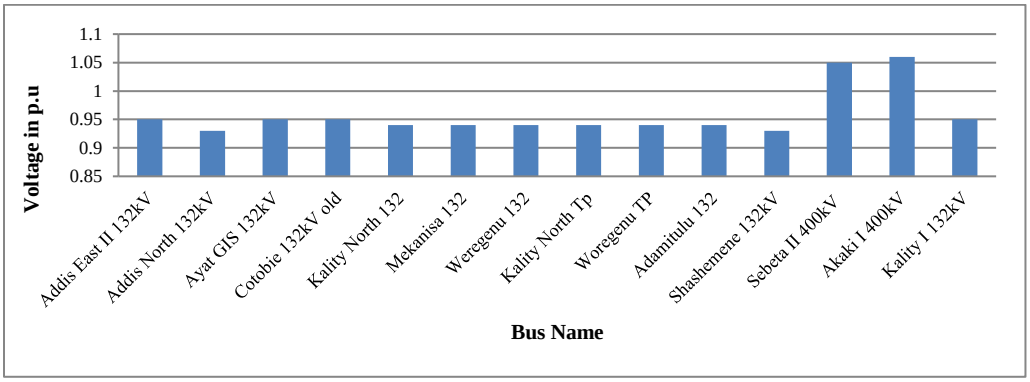

Figure 4-10 Voltage profiles of buses whose voltages deviate from 1 pu by $\pm 5\%$ or more.

In addition, some transformers were loaded above their limits and a disturbance under this condition would no longer be tolerated by the system. Table 4-4 depicted the situation.

Table 4-5 Power flows on important lines before the incident

No.	Important line(s)	MVA
1	Bahirdar II – Almata 230kV line	$72 + j50$
2	Sululta – D/Markos 400kV line	$192 + j77$
3	Sululta – Gefersa 230kV line I	$84 + j35$
4	Sululta – Gefersa 230 kV line II	$83 + j35$
5	Sebeta I – Kality I 230 KV line	$170 + j65$
6	Sebeta II – Gelan 400kV line	$221 + j22$
7	Sebeta II – G/Gibe II 400KV line	$326 + j7$
8	Gefersa – Ghedo 230 kV line II	$70 + j2$
9	Bahir Dar II – D/Markos 400kV line	$209 + j59$

Initiating Event

At 16:16 hrs GG II – Sekoru 400kV line was tripped by earth fault zone 1 protection due to a short circuit fault (LLL-G) at a distance of 7.8 km from Sekoru substation. With this initial event, a RMS simulation is performed to observe the characteristics of the system parameters before, during and after the fault has been cleared. From the simulation of the initiating events, the behaviour of the system before and immediately following a disturbance is graphically depicted in Appendix E, Figure E-22-26.

a) Before the disturbance

The rotor angles of HPP generators prior to the initiating events were at their steady values as shown in Table 4-6. The synchronous speed (ω_s) of all the HPP generators was 1.0 pu (50 Hz frequency). The terminal voltage of each generator was also synchronised to 1.0 pu as it is indicated in Appendix E, Figure E-23 (a).

Table 4-6 Rotor angles of HPP generators prior to the disturbance

HPP Generators	δ_{i0} (radians)
Beles (Gr_1, Gr_2, Gr_3, Gr_4)	-0.32
Fincha (Gr_1, Gr_2, Gr_3, Gr_4)	-0.382
GG III (Gr_1)	-0.738
GG II (Gr_1, Gr_2, Gr_3, Gr_4)	-0.738
Awash III (Gr_2)	-1.491
Koka (Gr1, Gr_2)	-1.041
Tekeze (Gr_1)	-0.777
GG I (Gr_1, Gr_2)	-0.635
Melkawakena (Gr_4)	-0.911

The reactive powers supplied by generators at steady state along with the maximum and minimum reactive power limit were indicated in Table 4-7 and it was indicated that all the generators' reactive power supplied prior to the initiating event were within the acceptable ranges.

The bus voltages were within limits (the minimum being 0.98 pu at Kality I 230kV bus and the maximum being 1.05 pu at Beles 400kV bus). There were no frequency deviations observed at critical buses. The current through GG II _Sebeta II 400kV line was 0.109 pu and the voltage across this line was around 1.037 pu and the current through GG I_Sekoru 230kV line was 0.114 pu and the corresponding voltage across this line was 1.010 pu. The turbine power (P_{mi}) input and electrical power (P_{ei}) output of each HPP generator is shown in Table 4-8 and therefore there was no overloaded generator.

Table 4-7 Reactive power supplied by each HPP generator prior to disturbance

HPP Generators	Reactive power supplied by each generator (MVAr)	Q_{Min}(rated) (MVAr)	Q_{Max} (rated) (MVar)
GG III (Gr_1)	-75.56	-100	100
Beles (Gr_1, Gr_2, Gr_3, Gr_4)	-33.01	-130	130
Tekeze (Gr_1)	-13.16	-38	38
GG I (Gr1, Gr2)	-7.83	-21	21
Awash III (Gr_2)	6.693	-15	13
Melkawakena (Gr_4)	0.532	-45	45
GG II (Gr_1, Gr_2, Gr_3, Gr_4)	-7.833	-50	50
Koka (Gr_1, Gr_2)	2.151	-12	11.6

Table 4-8 Turbine power input and electrical power output of HHP generators before the disturbance

HPP Generators	Turbine power (pu) (P_{mi})	Electrical power (pu) (P_{ei})
Beles (Gr_1, Gr_2, Gr_3, Gr_4)	0.796	0.796
Fincha (Gr_1, Gr_2, Gr_3, Gr_4)	0.94	0.94
GG III (Gr_1)	0.406	0.406
GG II (Gr_1, Gr_2, Gr_3, Gr_4)	0.807	0.807
Koka (G_1, Gr_2)	0.654	0.654
Tekeze (Gr_1)	0.521	0.521
Melkewakena (Gr_4)	0.782	0.782

b) During the fault

During the disturbance, the speed of generators was increased in general. Specially, the speed of GG I and GG II HPP generators were accelerating fast. The speed increment for GG III and Awash III HPP generators on the other hand were not that much as compared to GG I and GG II HPP generators. The speed of GG II and GG I HPP gnerators increased to 1.011 pu at the end of 150ms as indicated in Appendix E, Figure E-22. A very interesting characteristic observed on the generators is that the speed of generators increased as the generator is closer to the disturbance area (GG I & GG II HPPs are nearest plants to the faulted area). For instance, the speed of Beles, Fincha and Tekeze HPP generators was around 1.005 pu, and that of GG III and Awash III were 1.003 pu during disturbance. The rotor angles of Fincha and Beles was almost constant. The rotor angles of GG I and GG II HPP generators were increased to -0.516 rad and -0.616 rad respectively. The rotor angle of GG III HPP generator was decreased to -0.80 rad. The rest of the generator rotor angles were almost constant. The terminal voltages of GG I and GG II HPP generators were dipped below 0.4 pu and the voltages of GG III, Awash III and Melkawakena HPP generators were also dipped below 0.70 pu and that of Beles, Fincha, Tekeze and Koka HPP generators were sagged below 0.86 pu. The

behaviour of HPP generators (speed, rotor angle, terminal voltage, etc…) during the fault are depicted in Appendix E, Figure E-22-24.

The reactive power of GG III, GG II, GG I and Tekeze HPP generators exceed their limits. The reactive power supplied by GG III HPP generator was reached 192 MVAr and declined to 144.7 MVAr and that of GG II was reached to 144.7Mvar and returned to 94.62 Mvar at the end of the fault. The reactive power of GG I was reached to 29.9 Mvar as it is shown in Figure E-23 (b). Reactive power of Koka reached to 12.06 MVar which exceeded its maximum limit of 11.6 Mvar. The turbine power input (P_{mi}) of each generator was almost constant for the fault duration; the electrical power output (P_{ei}) of each HPP generator on the other hand was decreasing drastically.The active power supplied by each GG II HPP generator was almost equal to zero (0.057 pu). The power supplied by GG I HPP generators was around 0.115 pu each and that of GG III was around 0.129 pu. The power supplied by Beles and Melkawakena was depressed to 0.325 pu. As indicated in Figure E-24 (b) the power supplied by Tekeze and Fincha HPP generators were 0.158pu and 0.505 pu respectively. Therefore, as $P_{mi} > P_{ei}$ for each HPP generators, the aceelerating power is increased and as a result the generator's speed is increased as per the philosophy discussed in Section 4.1.6.

The voltage at Sekoru 400kV Bus was almost collapsed and that of GG II 400kV bus was dipped to 0.105 pu. The voltages at Fincha 230kV, Gefersa 230kV, Kality I 230kV, Legetafo 230kV, Sebeta II 400kV and Akaki 400kV buses were dipped below 0.60 pu. The voltages at Tekeze 230kV, B/Dar II 230kV and Beles 400kV buses were sagged to 0.84 pu. Figure E-25 in Appendix E depicted these conditions. The current through GG I _Sekoru 230kV line was shot to 0.478 pu at the start of the fault and decaying to 0.385 pu at the end of the fault and the corresponding voltage across it was dipped to 0.204 pu at the start of the fault and decreased to 0.181 pu at the end of the fault. The current through GG II_Sebeta II 400kV line was also shot to 0.375 pu at the start of the fault and decayed to 0.345 pu at the end of the fault and the voltage across it was dipped to 0.355 pu. These characteristics are depicted in Appendix E, Figure E-26 (a) & (b).

c) After the fault has cleared with a fault clearance time of 150ms and considering a RMS simulation of 10 seconds

Due to security reasons, it was difficult to obtain the protective relay settings of lines that were connected to Sekoru substations; hence, standard setting requirements for an earth fault proposed for EEP by SINO HYDRO Corporation Ltd., is taken from [58]. Therefore, according to [58], depending on the network levels, fault types and characteristics, the trip time for protective relays can be set to 0-10 seconds. Of course, for the three phase to ground fault, the maximum fault clearing time should not exceed 8 cycles (160ms) [56]. Hence, in this case a 150ms fault clearing time is taken to conduct a 10-second RMS simulation. The time domain transient simulations over a period of 10 seconds after initiation of a

disturbance are shown in Figure 4-11 to Figure 4-14. These simulations depict the dynamic performance of EEP system by representing profiles of generator rotor angles, speed and terminal voltage, turbine power, etc... The voltages of critical buses and their corresponding frequency deviations are also indicated in Figure 4-13(a) & (b), the voltages across and currents through GG II_Sebeta II 400kV and GG I_Sekoru 230kV lines are also shown in Figure 4-14.

After the fault has been cleared the speed of generators were recovered to the normal operating ranges with damped oscillations. The rotor angles of Beles, Fincha and Tekeze HPP generators were taking their steady state values with little and damped oscillations. The rotor angles of the remaining generators were transiently stable with sustained oscillations. The terminal voltages of all the generators were recovered to above 0.98 pu. The reactive power supplied by each generator was recovered to their steady state values. The other important characteristic observed on the generators was that as the terminal voltage was dipped, high reactive power was absorbed by the corresponding generators due to the high reactive current flow and this characteristic is shown in Figure 4-12. The reason is that the reactive power is highly dependent of the current flowing through the reactances of the generator [11].

The voltages at the critical buses were also returned to the normal operating condition range after the fault on the line has been cleared within 150ms. The frequency deviation observed on GG II 400kV substation was 0.5Hz and on other critical substations it was 0.4 Hz for 150ms and later the frequency deviations lowered to below 0.2 Hz after the line fault has cleared. Figure 4-13 shows these conditions.

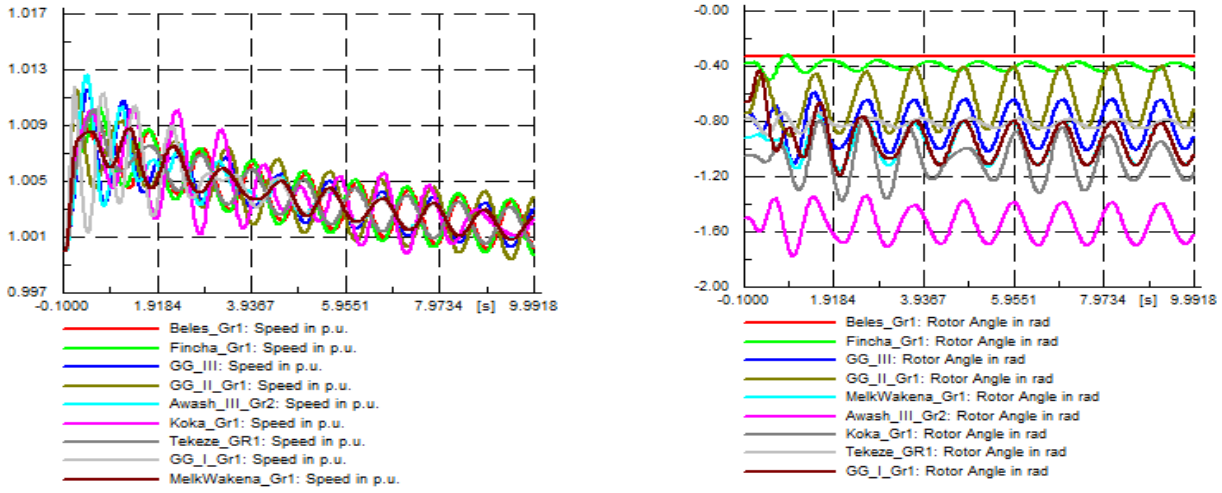

(a) Speed in pu

(b) Rotor angle in rad

Figure 4-11 Speed and rotor angle profiles of HPP generators

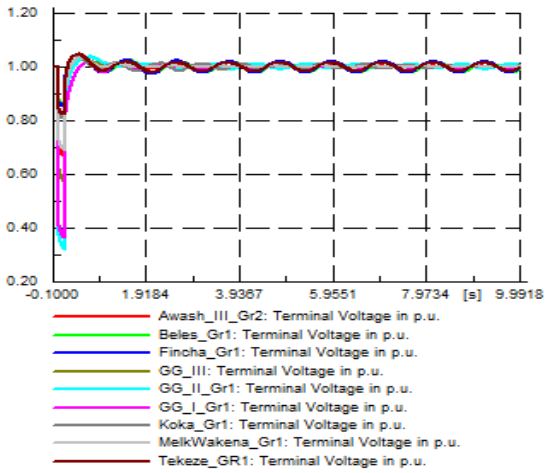

(a) Terminal voltage in pu

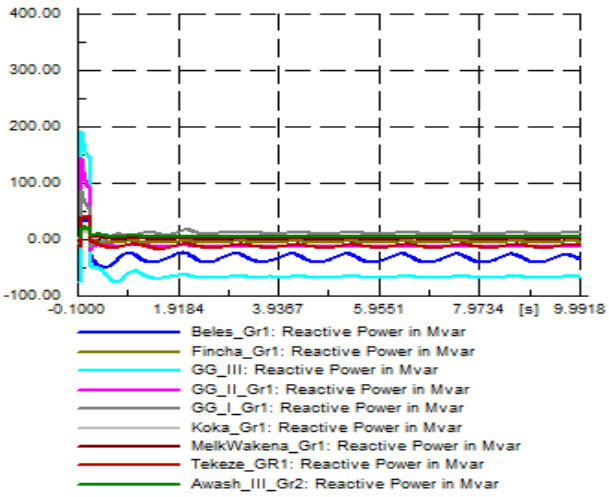

(b) Reactive power supplied Mvar

Figure 4-12 Terminal voltage and reactive power supplied by HPP generators

There was no overloaded equipment observed on the system and all the parameters of the power system were observed to be in the normal operating condition ranges.

The current through GG II_Sebeta II 400kV line was ramped up to 0.375 pu from the initial value of 0.125 pu during the fault and finally recovered to 0.242 pu at around 1.366 seconds with sustained oscillations. The current on GG I_Sekoru 230kV line on the other hand was shot to 0.482 pu during the fault and returned to 0.125 pu after the fault has been cleared with damped oscillations as shown in Figure 4-14 (a). The voltages across these lines are also indicated in Figure 4-14 (b). During the fault the voltages were dipped well below 0.34 pu and finally returned well above 1.0 pu after the fault has been cleared.

Therefore, from this analysis, the power system parameters of each component (generators, lines, etc) are within limits and the voltages at the critical buses were also recovered to their steady state values. Hence, we can say that if the fault clearance time setting of the protective relays of GG II_Sekoru 400kV line at both ends were 150ms or shorter than this the sequence of events observed on the SCADA would not be observed and hence the blackout of January 6th 2016 would not be happened.

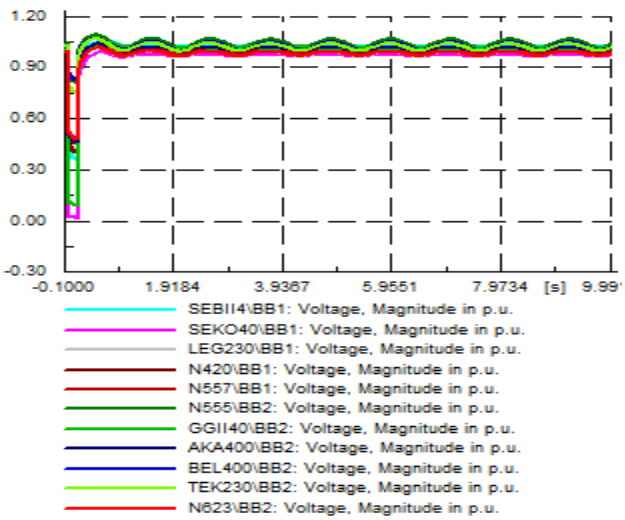

(a) Bus voltages in pu

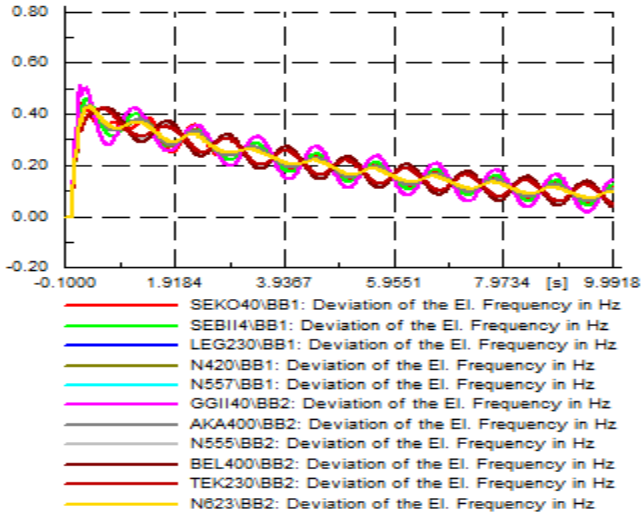

(b) Frequency deviations in Hz

Figure 4-13 Voltage profiles at critical buses

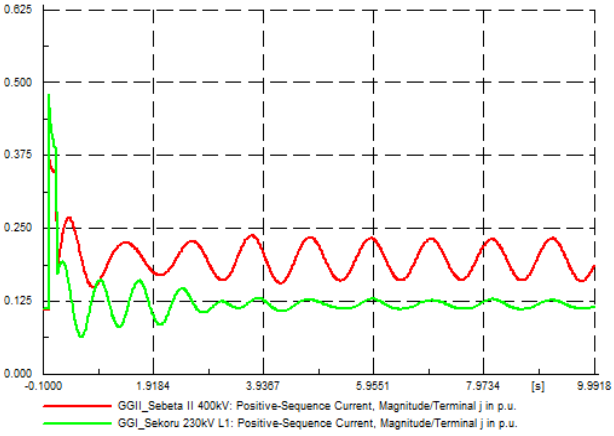

(a) Currents

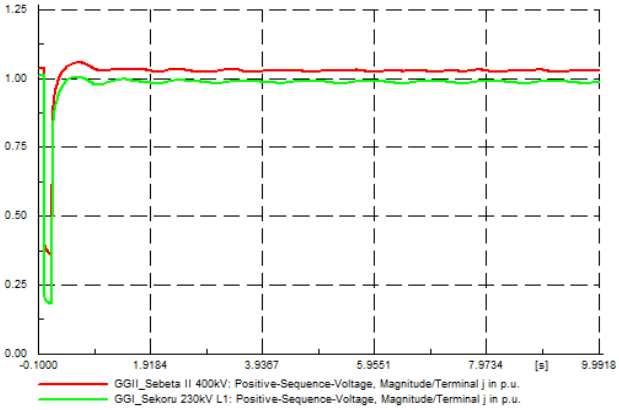

(b) Voltages

Figure 4-14 Currents through and voltages across GG II_Sebeta II 400kV and GG I_Sekoru 230kV lines

Cascading Events

As we have discussed above, the line fault on GG II_Sekoru 400kV line would not result in the blackout of January 6th 2016 if the fault was cleared with in 150ms. Of course the system survivability was up to a fault clearing time of 400ms (obtained from the simulation results). However, if the fault clearance time exceeded 450ms, then, the system would no longer be survived from cascaded trips. The sequence of cascading events observed on the SCADA and the simulation result obtained here are synonymous for a fault clearance time

of 450ms. The RMS simulation results for the fault clearance of 450ms are shown in Figure 4-15 to Figure 4-18.

Hence, from the above simulations, we observed that the speed (frequency) of GG II HPP generators was reached to 1.039 pu at around 0.532 seconds. In addition, the speed of Awash III & GG III HPP generators were increased to 1.037 pu and 1.039 pu respectively at around 0.718 seconds. In this case, the frequency of GG II power plant generators has been drastically increased and these generators lost synchronism and became monotonically unstable, the rotor angle swinging back and forth as it is indicated in Figure 4-15. And therefore the over frequency protection tripped all four units of GG II power plant. Let the tripping of GG II HPP generators at 0.532 seconds, Awash III & GG III HPP generators at 0.718 seconds be called as switching event 1 (SE-1) and therefore, applying these switching events (SE-1) with a time simulation of 10 seconds, the results are depicted in Figure 4-19-4-22.

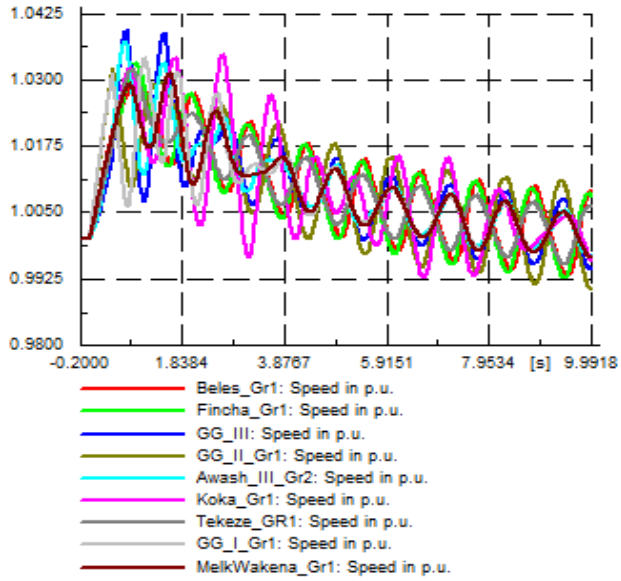

(a) Speed in pu

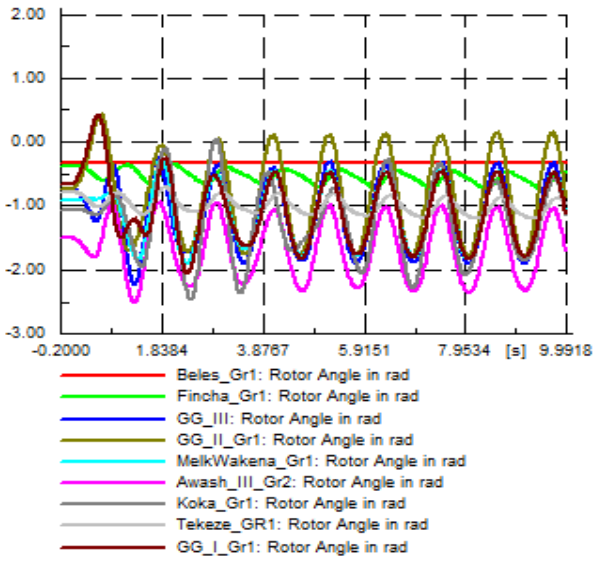

(b) Rotor angle in rad

Figure 4-15 Speed and rotor angle profiles of HPP generators for a fault clearing time of 450ms

The terminal voltages of the HPP generators were recovered to above 0.90 pu after the fault has been cleared with 450ms as was depicted in Figure 4-16 below. The turbine power input to the HPP generators were showing a decrease from the steady state value by their corresponding governor actions to compensate for the increase in the speed of generators. The electrical power output of these generators was unable to damp and recover to the steady values as was depicted in Figure 4-17.

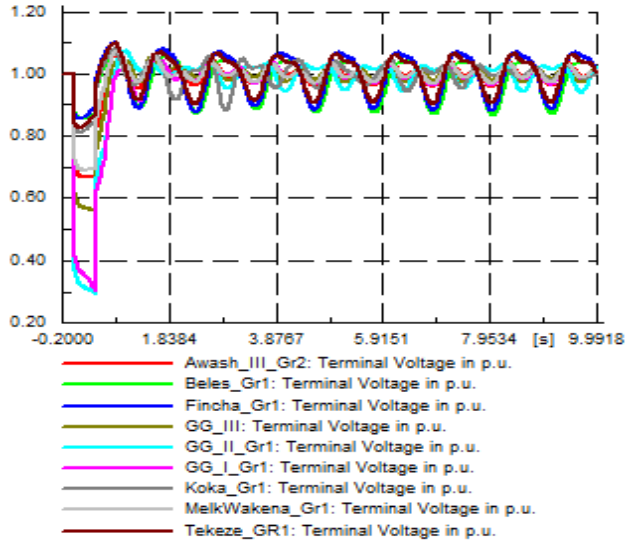

Figure 4-16 terminal voltage of the HPP generators for a fault clearing time of 450ms

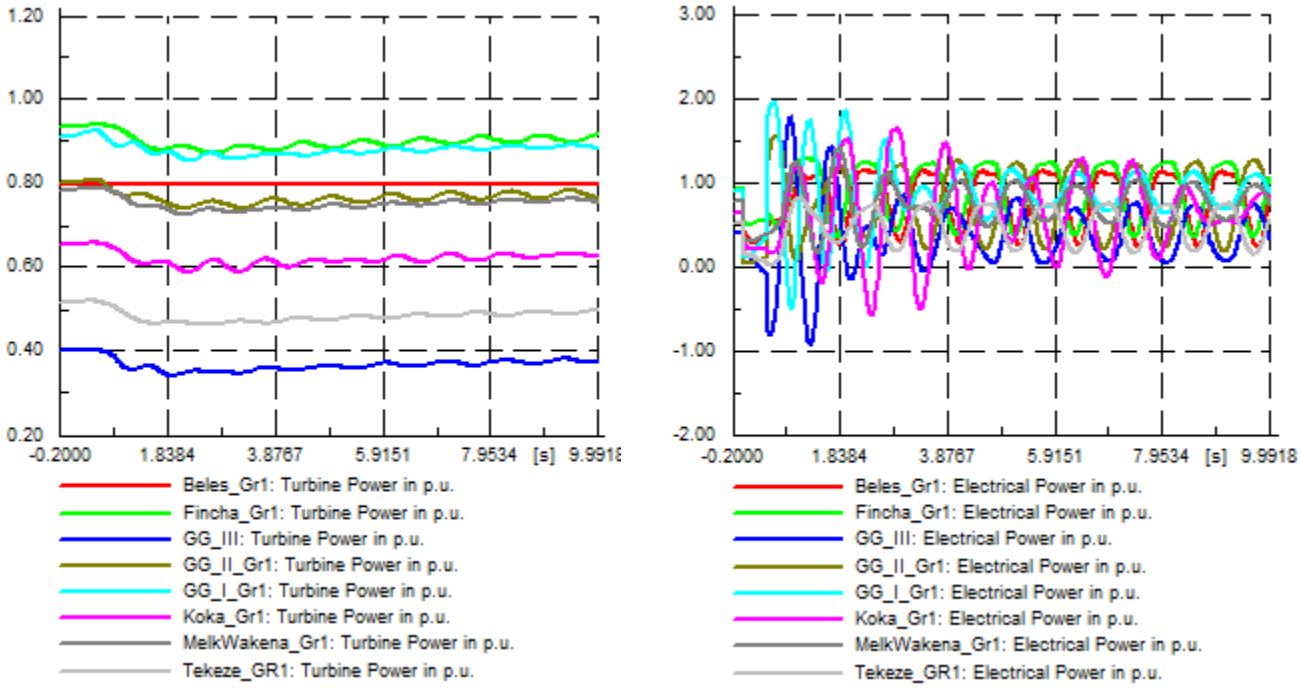

(a) Turbine power in pu (b) Electrical power output pu

Figure 4-17 Turbine power input to and electrical power output of HPP generators for a fault clearing time of 450ms

The bus voltages at critical buses of EEP were depicted in Figure 4-18. The voltage at Kality I 230kV bus was oscillating at around the lower limit of the voltage and the voltages at the rest of the critical buses were recovered well above 0.95 pu with damped oscillations after the fault has been cleared with 450ms.

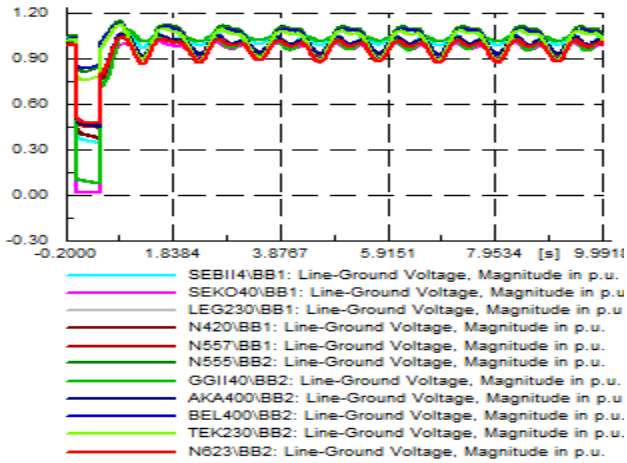

(a) Bus voltages in pu

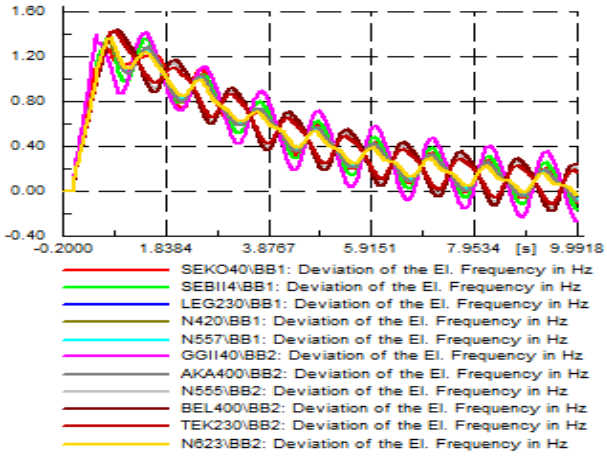

(b) Frequency deviations in Hz

Figure 4-18 Bus voltages and their corresponding frequency deviations at critical buses for a fault clearing time of 450ms

As GG II HPP generators had tripped, the system lost 27 % of the total generation, and the balance between the load demand and the generated power had been violated and the system frequency had been deteriorated. The voltages at the load buses (critical buses) were demolished and the system lost its consistency. The situation is depicted in Figure 4-22. After switching event 1 (SE-1), the speed of generators was continually depressed and went below 0.98 pu and the voltage across GG II _Sebeta II 400kV line was reached to 1.172 pu at around 1.651 seconds, as shown Figure 4-19 (a) and Figure 4-22 (b) respectively. Both conditions aggravated the situation and the remaining HPP generators were highly overloaded.

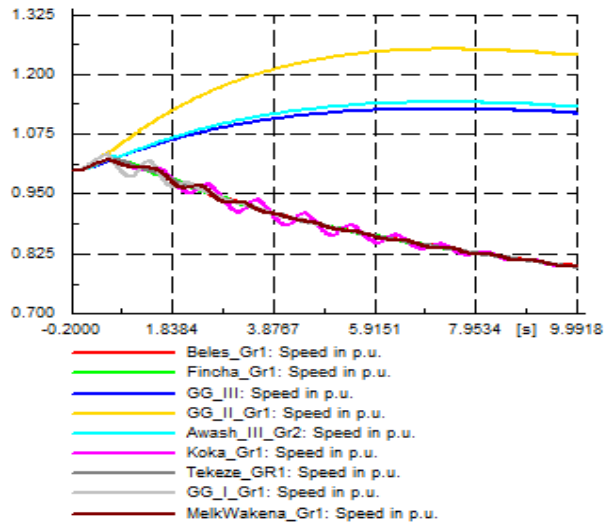

(a) Speed in pu

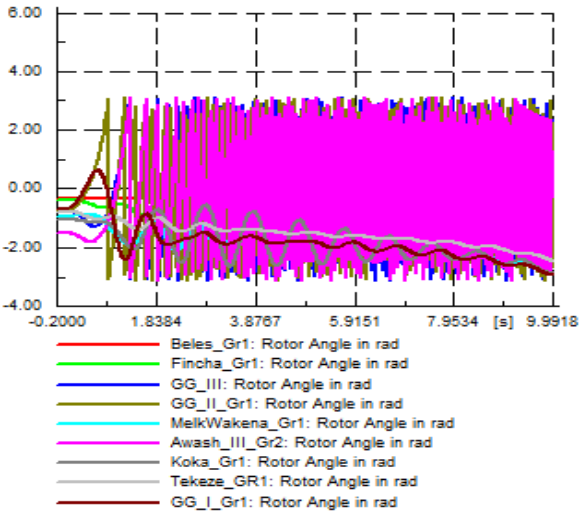

(b) Rotor angle in rad

Figure 4-19 Speed and rotor angle profiles of HPP generators after SE-1

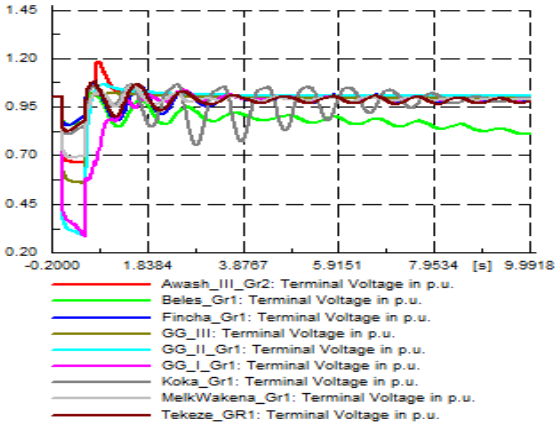

(a) Terminal voltage in pu

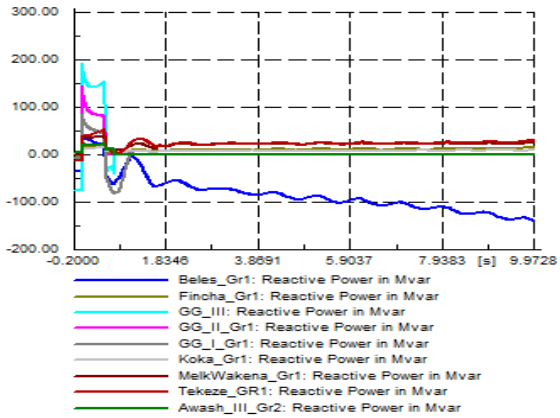

(c) Reactive power supplied in Mvar

Figure 4-20 Terminal voltage and reactive power supplied by HPP generators after SE-1

The terminal voltage of the each HPP generators, though there was a decrease in their magnitude, it was well above 0.90 pu with damped oscillations. There was a high reactive power deficit in the system and as a result, Beles HPP generators were forced to generate high reactive power upto their lower limits. These conditions are shown in Figure 4-20.

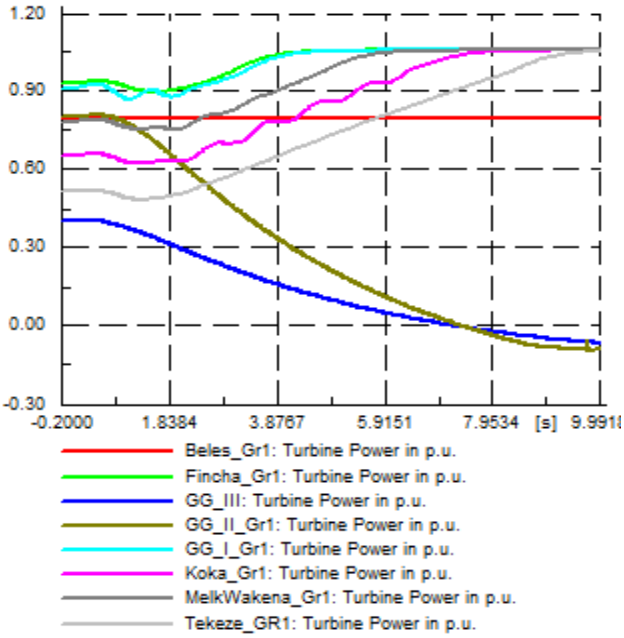

(a) Turbine power in pu

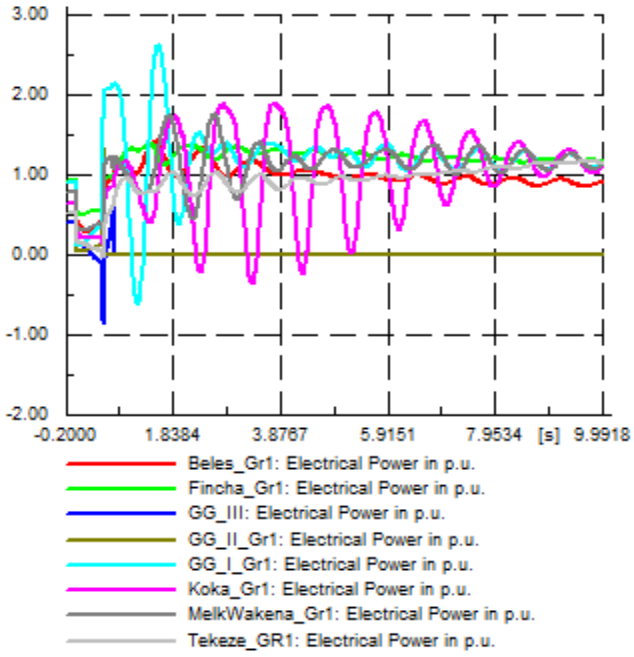

(b) Electrical power in pu

Figure 4-21 Turbine power input to and electrical power output of HPP generators after SE-1

As GG II and GG III HPP generators were tripped their corresponding turbine power input were decreased drastically to slash out the speed of the generators and on the other hand the turbine power input for the rest

of the generators were increased to 1.081 pu to supply the power deficit as was shown in Figure 4-21 (a). As the load was higher than the generation, the remaining generators' electrical power outputs were rising beyond 1.0 pu as was indicated in Figure 4-21(b) with damped oscillations to satisfy the load-generation balance. There was a reverse power flow (-0.616 pu) to the generators of GG I HPP at around 1.106 seconds.

Therefore, the tripping of components having an out of limit parameters were continued to be worsened and created a cascading event. Hence, SE-1 was followed by switching event 2 (SE-2) and includes:

- Tripping of GG I HPP generators with reverse power protections
- Tripping of GG II _Sebeta II 400kV line by overvoltage protections

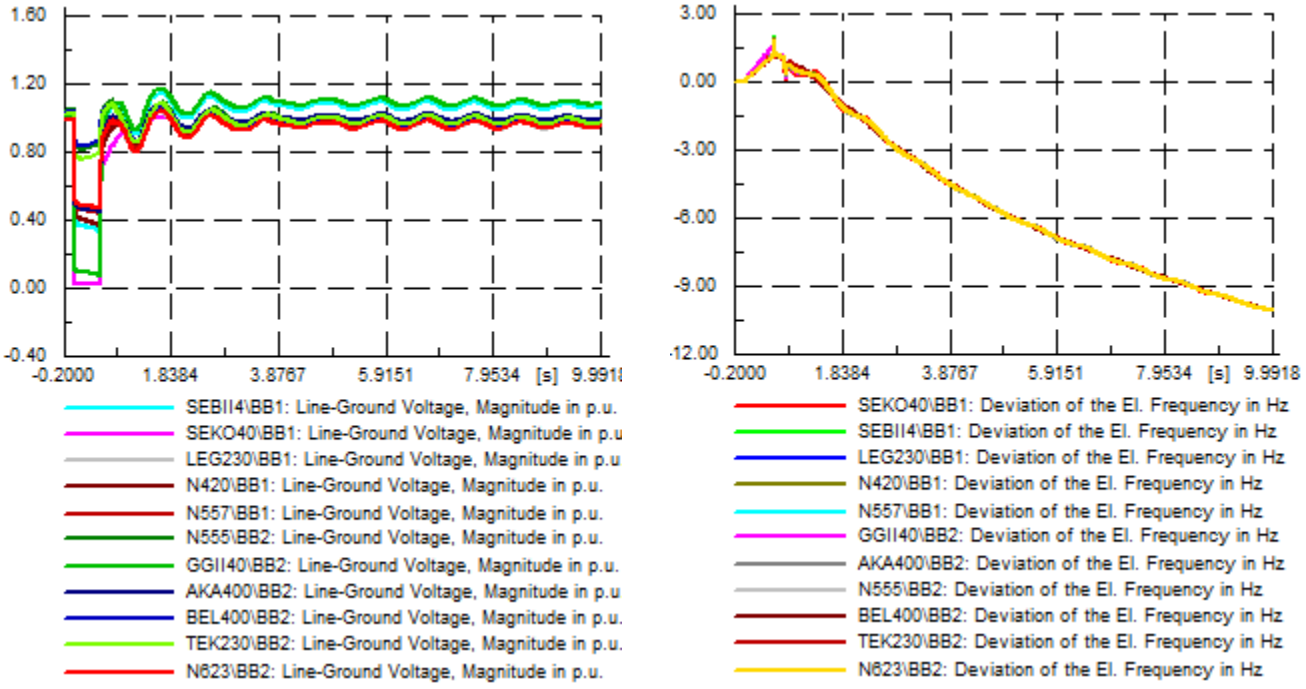

(a) Bus Voltages in pu

(b) Frequency deviations in Hz

Figure 4-22 Line to groung voltages and their corresponding frequency deviations at critical buses after SE-1

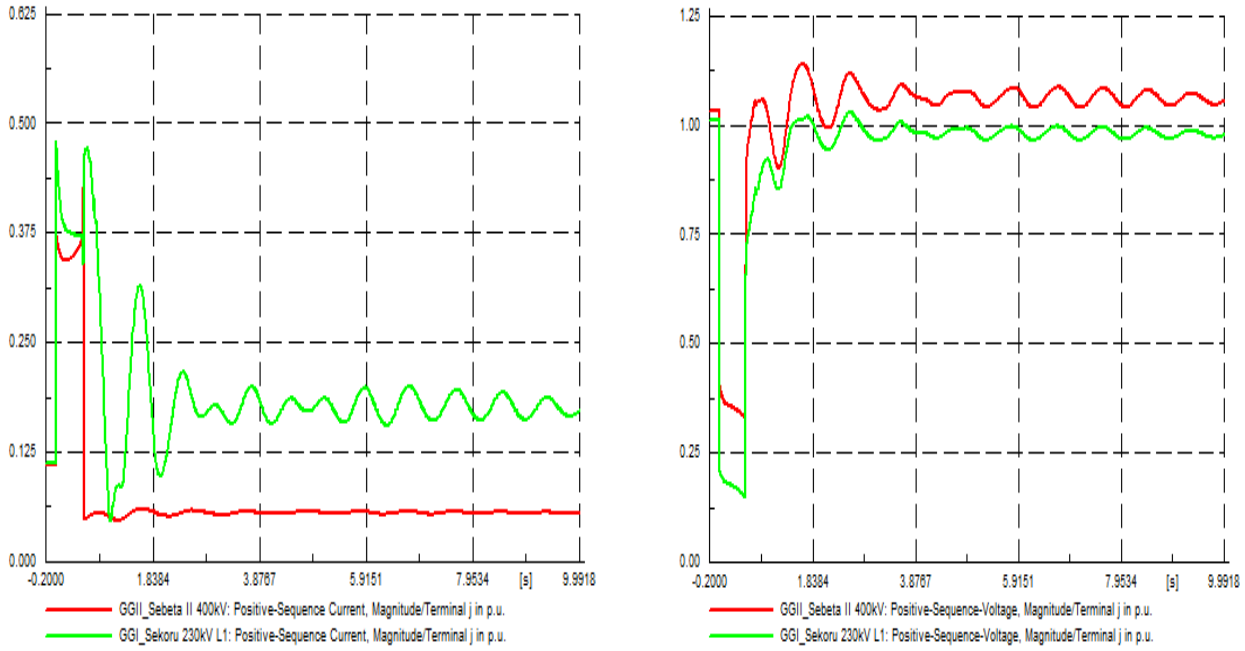

(a) Currents in pu

(b) Voltages in pu

Figure 4-23 Current through and voltage across GG II_Sebeta II 400kV and GG I _Sekoru 230kV lines after SE-1

After having SE-2, again a 10 second RMS simulation was performed and we have seen that the system was unable to recover from its weaknesses. The simulation results are depicted in Figure 4-24 to Figure 4-27. Accordingly, Melkewakena and Koka HPP generators were further overloaded and finally tripped by overcurrent and underfrequency protections. The terminal voltage of Beles HPP was depressed below 0.85 pu and the reactive power supplied by each generator was increased to -100 MVAr to support the reactive power deficit in the system. The speed of Tekeze HPP generator has been declined below 0.925 pu at around 3.314 seconds. The speed of Fincha, Beles, Awash II & III, and Koka HPP generators were also decreased drastically and the overloading of HPP generators were increased. These conditions are indicated in Figure 4-24 – 4-26.

Following the tripping of G/Gibe II – Sebeta II 400kV line and G/Gibe I power plant generators, the load flow was forced to change to the remaining generating plants and nearby transmission lines. This further aggravated the situation and G/Gibe I – Sekoru 230 kV line was became overloaded and finally tripped by overcurrent protection.

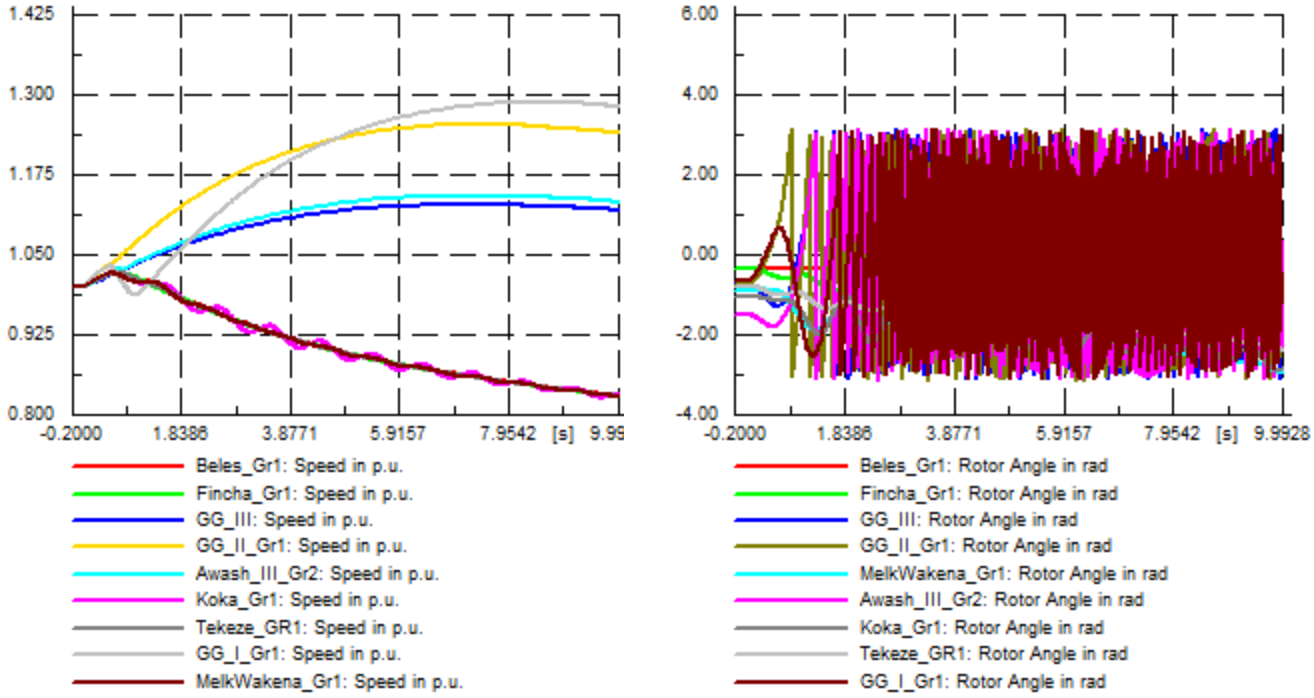

(a) Speed in pu

(b) Rotor angle in rad

Figure 4-24 Speed and rotor angle profiles of HPP generators after SE-2

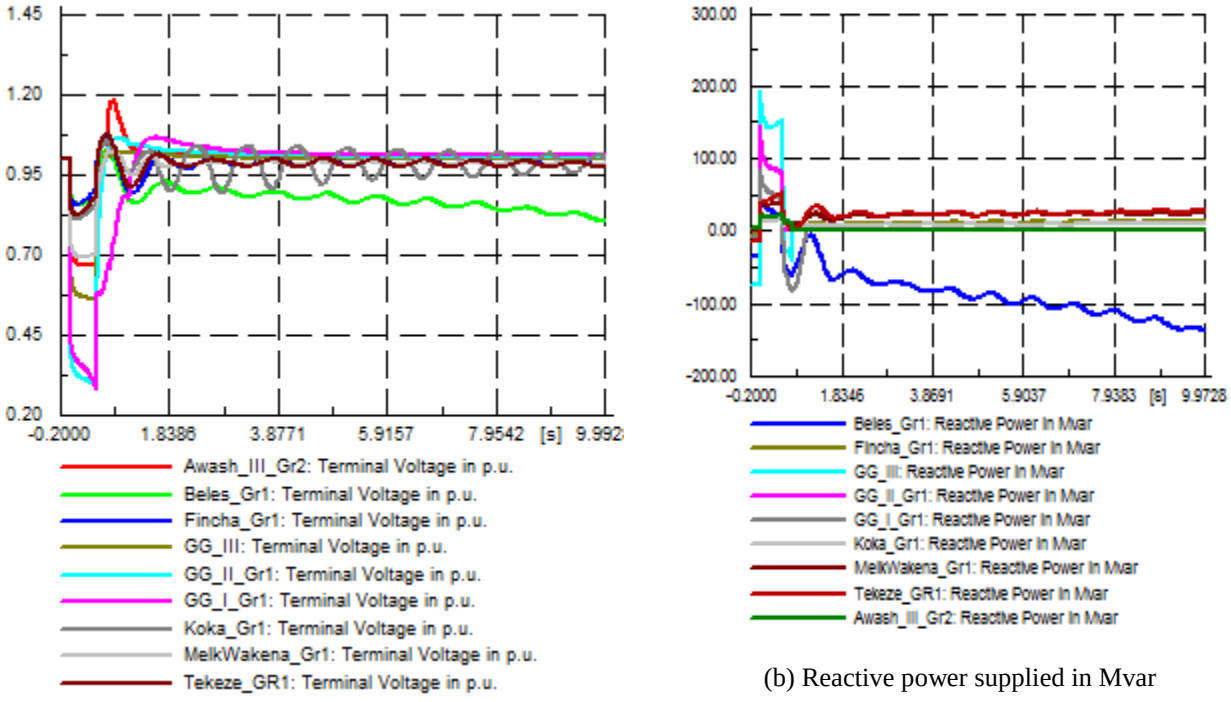

(a) Terminal voltage in pu

(b) Reactive power supplied in Mvar

Figure 4-25 Terminal voltage and reactive power supplied by HPP generators after SE-2

The remaining power plants (Fincha, Amertinesh, Awash II &III, Tekeze, Koka, and MelkaWakena) were became overloaded and most of them tripped by under frequency protection relays as indicated in Figure 4-24 (a). As the frequency of Fincha, Awash II, Koka, and other power plant generators were decreased, the governor was acting and the turbine power was increased as indicated in Figure 4-26(a). However, the frequency collapse was not easily recovered by governor actions and the cascade tripping of the HPP plant generators, transmission lines and transformers were continued.

In addition, after SE-2, the critical bus voltages (Kality I 230kV, Legetafo 230kV, Sekoru 400kV, etc) were deteriorated below 0.90 pu and their corresponding frequencies were further declining to 41 Hz (Frequency collapse has occurred.) as shown in Figure 4-27 (a)&(b).

Therefore, there was no way to recover the system to its normal state and the system cascade tripping continued till the system was totally collapsed within 60 seconds.

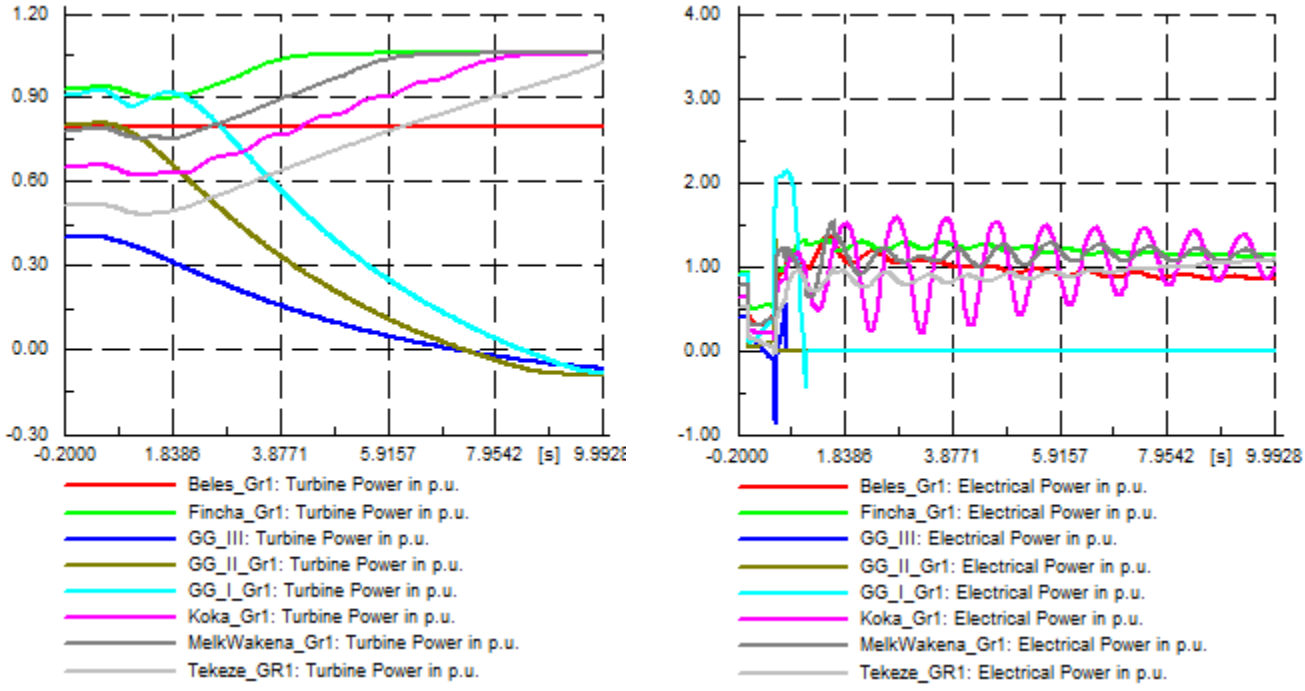

(a) Turbine power in pu

(b) Electrical power in pu

Figure 4-26 Turbine power input to and electrical power output of each HPP generator after SE-2

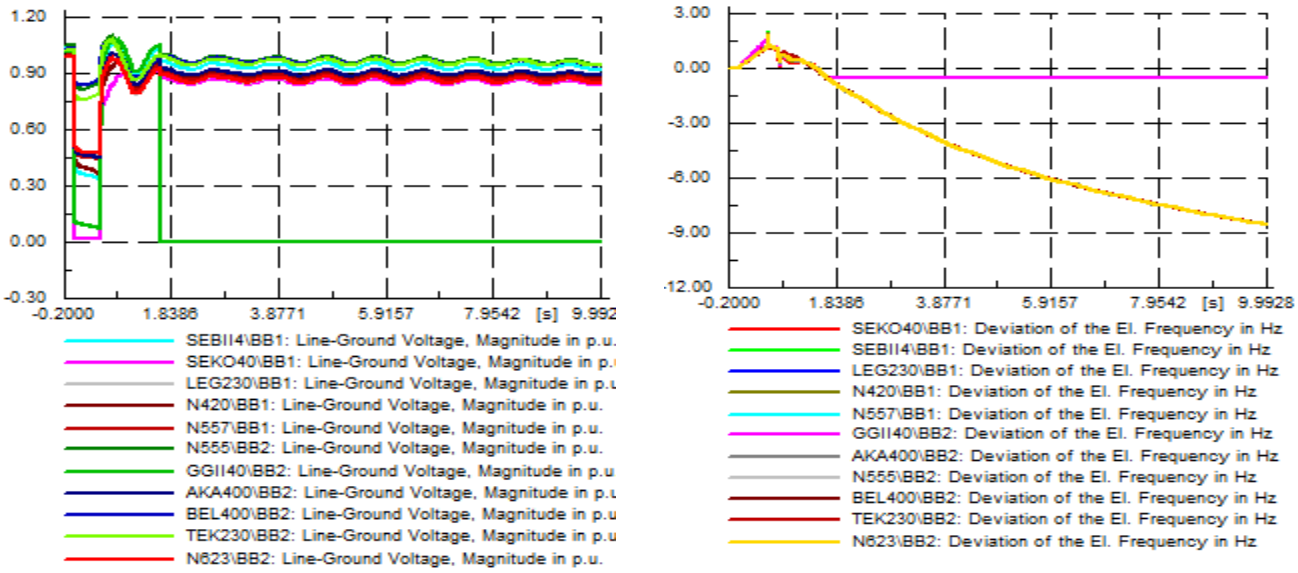

(a) Bus voltages in pu

(b) Ferequency deviations in Hz

Figure 4-27 Voltage and their corresponding frequency deviations at critical buses after SE-2

Final State of the System

The blackout affected the whole country except some parts of North Western region (Beles HPP generators were operating with 44.4 Hz frequency as the under frequency protection of this plant was not operating). The interrupted load was not supplied for a time interval ranging from 20 min to 2.5 hrs.

Process of the January 6th 2016 Blackout

The process of the 6th January 2016 can be summarised as shown below.

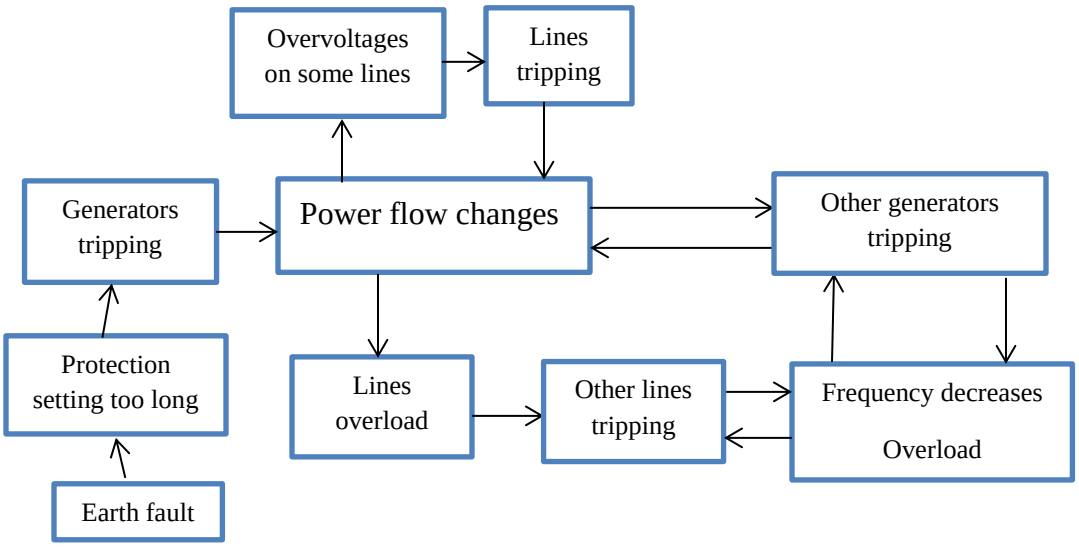

Figure 4-28 Process of the January 6, 2016 blackout – showing the cascading events

4.6.2. December 22nd 2015 Blackout

System Condition Prior to Collapse

On December 22nd 2015 at 15:00 hrs the total system generation were 1349.43 MW from which 1159 MW was from hydro generations, 145.43 MW was from wind generations and the remaining 45 MW was from diesel plants installed at Dire Dawa and Awash 7 killo substations. The system load at the time was 1295 MW. The transnational exchange was 19.56 MW exported to Djibouti and the system frequency observed on the EMS was around 50 Hz. Due to lack of rainfall around some hydro plants' reservoir, Koka, Awash II & III, Tis Abay I & II, and Tekeze HPPs were not capable of supplying power to their full capacity. Tis Abay I HPP was completely down at the time and Tekeze HPP was generating 45 MW only (15 % of its capacity). Sululta_Gefersa 230kV line II and Ghedo_Gefersa 230kV line III were in a planned outage though the reason were not justified.

The above steady state system condition prior to disturbance has been simulated and the results have been depicted in Figure 4-29. The voltages of important substations like, Combolcha II 230kV, Legetafo 230kV, Kality I 230kV, Kality I 132kV and Sululta 132kV substations were deteriorated and hence a further disturbance on the system could affect the steady state stability of the system. Over voltages were also observed on Akaki I 400kV, Hurso 230kV, Adigala 230kV and Dire Dawa III 230kV substations.

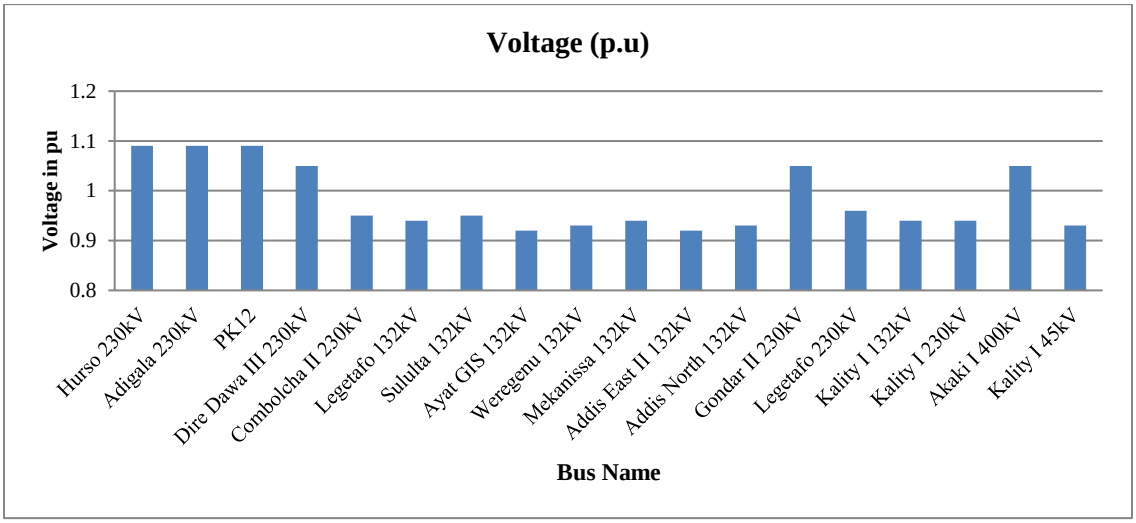

Figure 4-29 Voltages of some buses prior to system collapse

There was no overloaded equipment under this steady state conditions. The power flows on important lines that interconnect the regional power systems are indicated in Table 4-9. The total grid loss was 44.64 MW.

Table 4-9 Flows on important lines affected by the event

Line Name	MVA flow
Bahir Dar II_Alamata 230kV line	$70 + j50$
Sululta_D/Markos 400kV line	$211 + j90$
Sululta_Gefersa 230kV line I	$81 + j34$
Sebeta I_Kality I 230kV line	$148 + j66$
Sebeta II_Akaki I 400kV line	$191 + j17$
Sebeta II_GG II 400kV line	$278 + j76$
Gefersa_Ghedo 230kV line I	$63 + j11$
Gefersa_Ghedo 230kV line II	$63 + j11$
Sekoru_Ghedo 230kV line	$42 + j32$

From the steady state conditions, the rotor angles, the synchronous speed, the terminal voltages, the active and reactive power supplied by each generator was obtained and it was observed that all these parameters were within the limits.The synchronous speed (ω_s) and the terminal voltages of each generator were synchronised to 1.0 pu. The steady state value of the rotor angles of each HPP generator (δ_{i0}) was given in Table 4-10.

Table 4-10 Rotor angles of HPP generators at steady state

HPP Generators	δ_{i0} (radians)
Beles	-0.352
Fincha	-0.465
GG III	-0.677
GG II	-1.0
Awash III	-1.8
Tekeze	-0.777
GG I	-1.0
Melkewakena	-1.192

Table 4-11 Reactive power supplied by each HPP generator at steady state

HPP Generators	Reactive power (MVAr)
GG III	-54.84
Beles	-24.60
Tekeze	-12.32
GG I	-6.38
Awash III	9.388
GG II	-4.64
Fincha	-3.71
Melkawakena	-0.762

The reactive power supplied by each generator was also within the normal operating ranges prior to the disturbance and is indicated in Table 4-11.

The turbine power input (P_{mi0}) and the electrical power output (P_{ei0}) prior to the disturbance were equal and there was no accelerating power and the generators run at their synchronous speed as is indicated in Table 4-12.

Table 4-12 Turbine power input and electrical power output of HPP generators at steady state

HPP Generators	Turbine power (pu) (P_{mi0})	Electrical power (pu) (P_{ei0})
Beles	0.918	0.918
Fincha	0.908	0.908
GG III	0.404	0.404
GG II	0.623	0.623
Koka	0.135	0.135
Tekeze	0.584	0.584
Melkewakena	0.659	0.659

Initiating Event

The initiating event that caused the total system collapse was the occurrence of the earth fault (SLG) on Ghedo_Gefersa 230kV line I at 15:07 hrs with the fault current of $I_b = 2.193kA$. The fault location was 49.01 km from Gefersa substation. Having this information, the effects of the initiating disturbance on the behaviour of EEP system have been studied in a systematic manner by performing the following dynamic simulations and analyses:

- ✓ The maximum fault clearing time for a SLG fault is 600ms [56]. Therefore, here we are taking the fault clearing time of 300 ms to better visualize whether the suggested initiating event could possibly have triggered the cascading events observed on the SCADA (Table 4-13) and could have resulted system collapse of the December 22nd 2015.
- ✓ The generators speed, rotor angles, terminal voltages and their corresponding reactive power drawn are traced and analysed.
- ✓ The voltages of important buses that contributed a lot for the safe operation of the system are observed with their corresponding frequency deviations.
- ✓ The fault currents of incoming and outgoing lines and 230/132kv transformers of Gefersa substation are also simulated to further observe the characteristics of the system for the sequence of events observed on the SCADA/EMS.

During the disturbance, the speed of HPP generators was increased. Specifically, the speed of Beles, Fincha and Tekeze HPP generators were accelerating fast. The speeds of Beles HPP generators were increased to 1.014 pu at the end of the fault, Fincha HPP generators' speed was reached to 1.013 pu, and that of Tekeze was 1.012 pu. The rotor angles of Fincha and Beles HPP generators were almost constant. The rotor angles of GG I and GG II were increased to -1.163 rad. Similarly, the rotor angle of GG III HPP generator was increased to -1.0 rad and that of Melkawakena HPP was increased to -1.365 rad. Awash III and Koka HPP generators' rotor angles were also increased to -2.087 and -2.299 radians respectively and became unstable at the first swing. The behaviour of the power system during the disturbance (before the fault has cleared) is shown in Appendix E, Figure E-27 to Figure E-32.

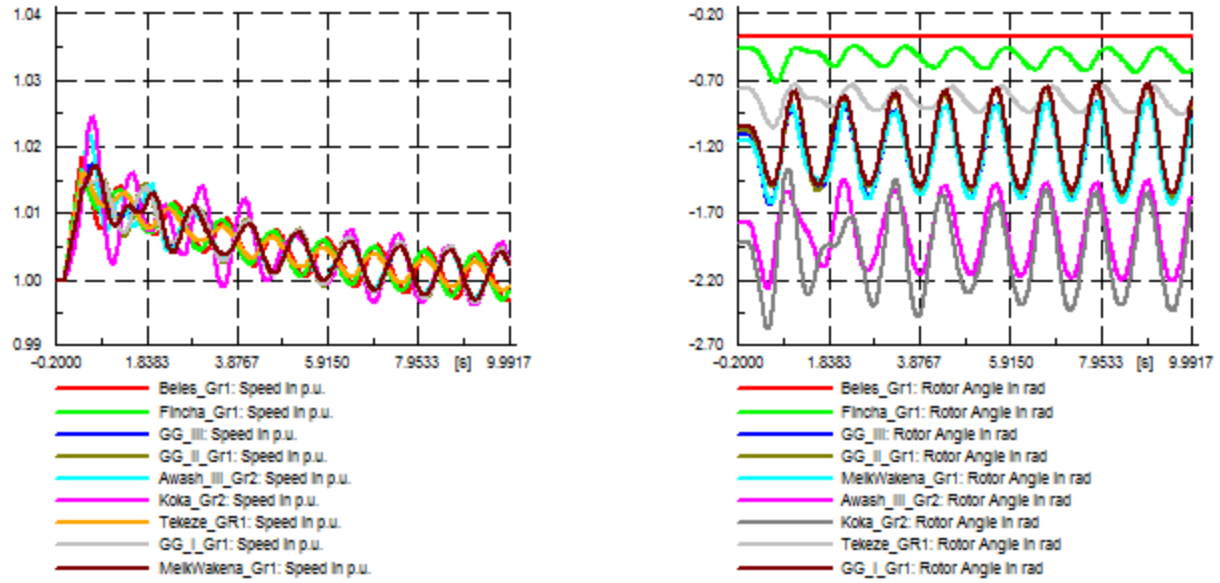

(a) Speed in pu (b) Rotor angles in rad

Figure 4-30 Speed and rotor angle profiles of HPP generators after the fault has cleared

After the fault has been cleared, the rotor angle of Koka HPP generators were swinging between -2.74 radian and -1.4 rad and after 750ms the rotor angles of these HPP generators were over damped as indicated in Figure 4-30 (b). The rotor angles of Fincha, Tekeze & Beles HPP generators were almost constant though little and damped oscillations were observed on Fincha & Tekeze HPP generators. The rotor angles of GG I and GG II HPP generators were oscillating between -1.506 rad and – 0.685 rad till 400ms. After 400 ms the rotor angles of these generators became over damped. After the fault has been cleared the speed of generators were recovered to the normal operating ranges with damped oscillations as can be seen in Figure 4-30 (a).

The terminal voltages of Melkawakena, GG I and GG II HPP generators were dipped below 0.8 pu where as that of GG III, Beles, Tekeze and Awash III HPPs were sag to 0.90 pu for the fault duration as shown in Figure 4-31 (a). Under this condition, the reactive power drawn from GG III HPP generator was increased to 147.3 MVAr. The reactive power drawn from GG II was also increased to 90.11 MVAr. Of course, for the fault duration of 300ms, the reactive power drawn from most of the HPP generators was increased beyond their limits. After the fault has been cleared, their corresponding reactive powers were returned to the steady state value as depicted in Figure 4-31 (b). The terminal voltages of Beles, Fincha & Tekeze HPP generators were decaying with over damped oscillations. The reactive powers supplied by each generator were recovered to the original values with small oscillations. The turbine power of each HPP generator was almost constant and their corresponding electrical power output was oscillating with centred at their original values.

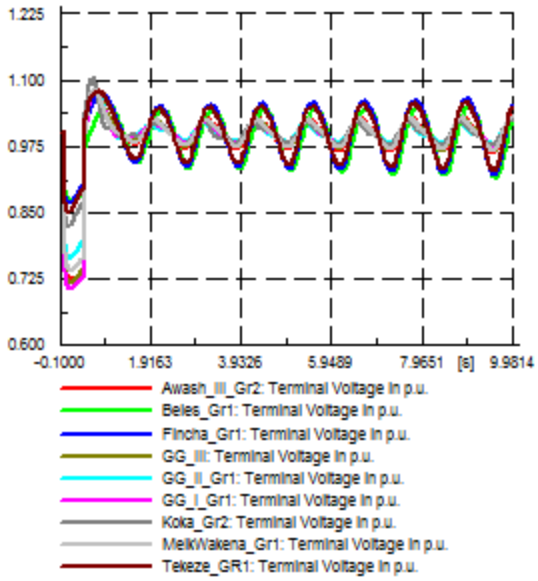

(a) Terminal voltages in pu

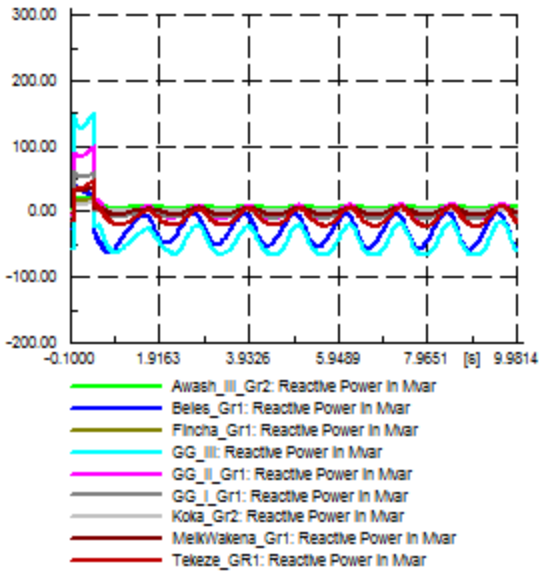

(b) Reactive power supplied in Mvar

Figure 4-31 The terminal voltages and the reactive power supplied by HPP generators after the fault has cleared

However, the electrical power supplied by Koka HPP generators were became -0.649 pu (motoring action-reverse power) at around 521ms. Awash III HPP generator was also supplying a negative power and therefore acts as a motor due to the reverse power flow. The reverse power is -0.334 pu at around 493 ms as depicted in Figure 4-32.

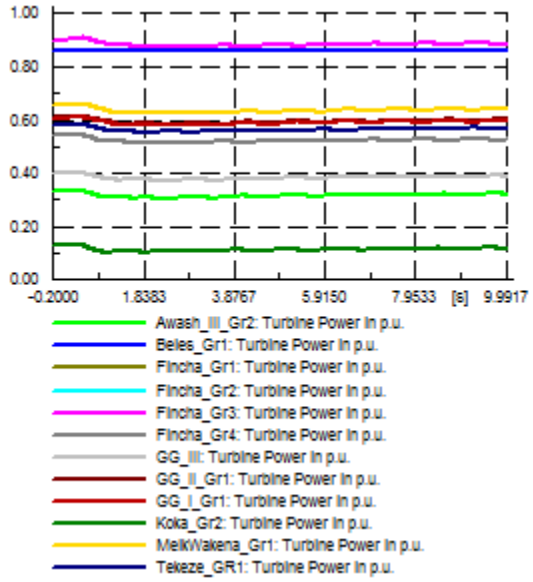

(a) Turbine power in pu

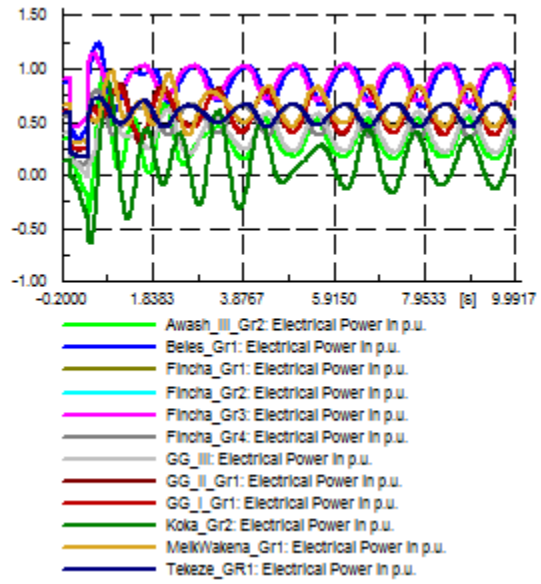

(b) Electrical power in pu

Figure 4-32 Turbine power input to and electrical power output of HPP generators after the fault has cleared

During the disturbance, the voltages at Ghedo 230kV, Legetafo 230kV, Kality I 230kV (N623), Gefersa 230kV (N557) and Fincha 230kV (N420) were dipped below 0.6 pu. The voltages at B/Dar II 230kV (N555), Akaki I 400kV and Sebeta II 400kV buses were sagged to 0.85 pu. When the fault has been cleared, the bus voltages at Legetafo 230kV and Kanlity I 230kV buses were recovered to their critical value of 0.94 pu. The voltages at the remaining critical buses were recovered back to their steady state values. The corresponding frequency deviations at these critical buses were decreased to 0.25 Hz with damped oscillations as is depicted in Figure 4-33 (a) & (b). The voltages at Kality I 230kV bus was later sagged to 0.835 pu with sustained oscillations after 1.607 seconds.

The voltage across Sululta 400/230kV transformers (I & II) was sagged to 0.893 pu at around 2.763 seconds with sustained oscillations and the corresponding currents were reached to 1.051 pu at around 1.649 seconds with over damped oscillations as is depicted in Figure 4-34 (a) & (b). The currents on Gefersa 230/132kV transformers were well below their rated values.

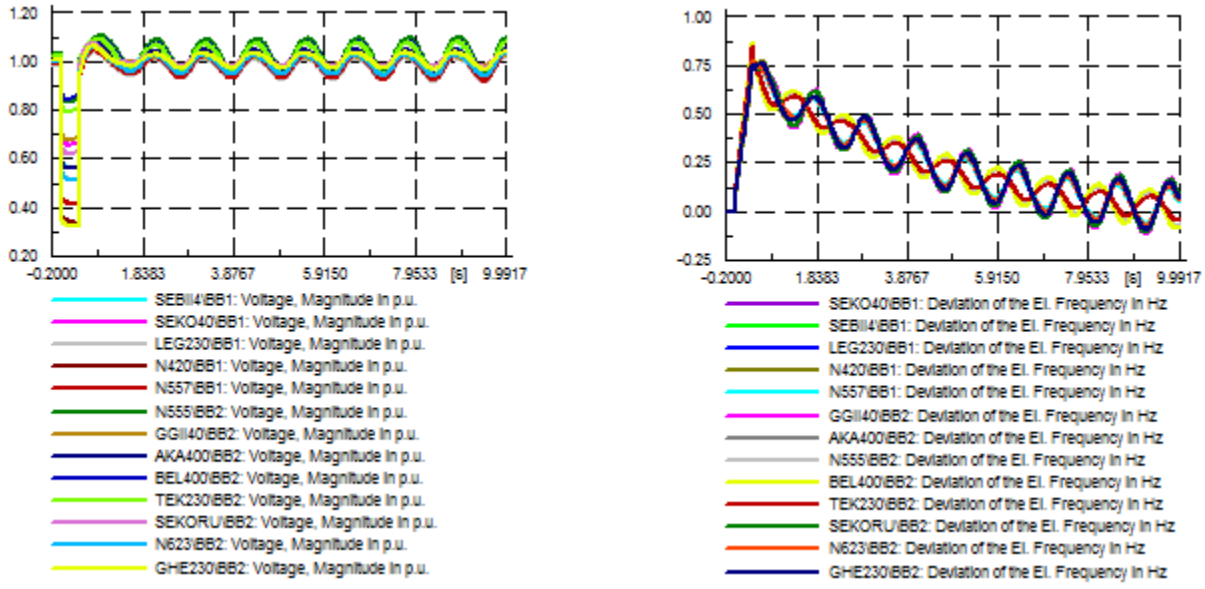

(a) Bus voltages in pu

(b) Frequency deviation in Hz

Figure 4-33 The bus voltages and their corresponding frequency deviations at critical buses after the fault has cleared

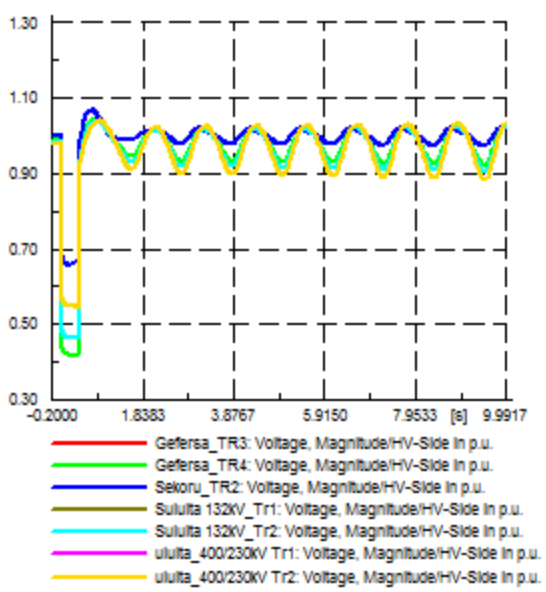

(a) Voltages in pu

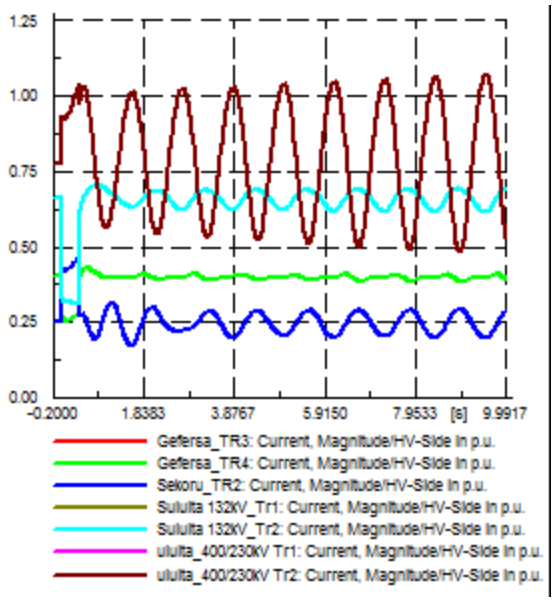

(b) Currents in pu

Figure 4-34 Voltages across and currents through transformers after the fault has cleared

As indicated in Figure 4-35, though the voltage across Sebeta I_Mekanisa 132kV line was recovered to 0.986 pu after the fault has been cleared, later the voltage across this line had been decayed to 0.895 pu at around 1.619 seconds with sustained oscillations. The current through Sululta_Gefersa 230kV line was reached to 1.097 pu at around 1.644 seconds with overdamped oscillations.

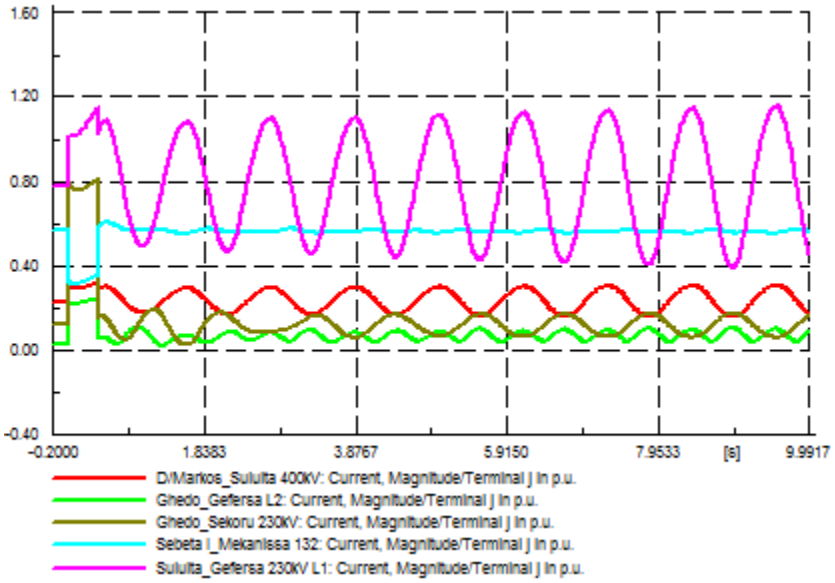

(a) Currents in pu

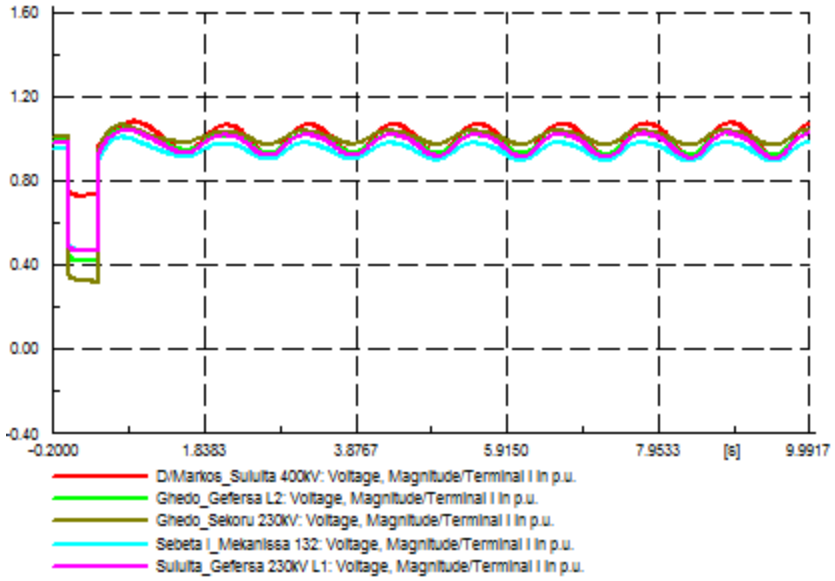

(b) Voltages in pu

Figure 4-35 The currents through and voltages across the incoming and outgoing lines of Gefersa substation

Cascading Events

As observed from the the simulation results above, Awash II & III and Koka HPP generators were became overloaded and later they acted as a motor. Therefore, the protection relays installed at these power plants tripped the corresponding generators and the cascaded tripping started and let we call these trippings as switching event 1 (SE-1) to describe them shortly. Hence, the cascading event started from SE-1 and includes:

- Awash II HPP generator (Gr2) & Awash III HPP generator (Gr2) were tripped at 493ms by overcurrent protections
- Koka HPP generators (Gr1 & Gr2) were tripped at 521 ms by reverese power protection & overcurrent protections respectively.

Therefore, by performing a 10-second time domain simulations for SE-1, the out of limit system parameters of components are depicted in Figure 4-36 to Figure 4-38. After SE-1, the speed of the HPP generators were decreased and synchronised to 0.995 pu as indicated in Figure 4-36 (a).

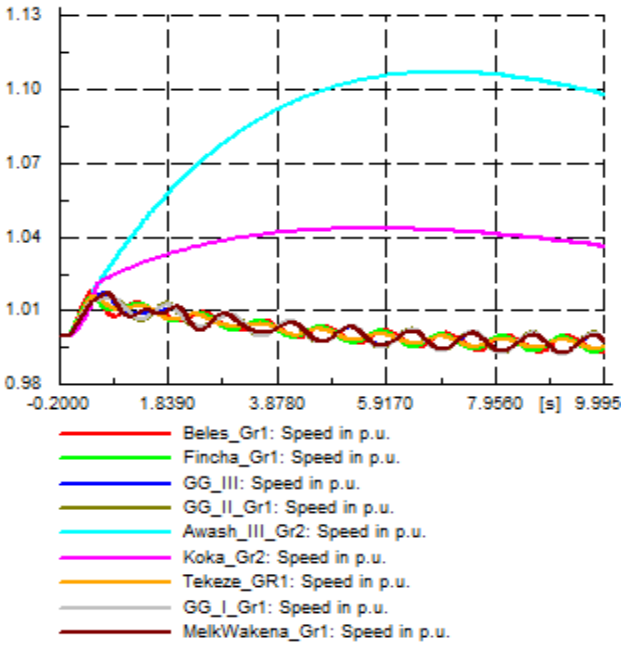

(a) Speed in pu

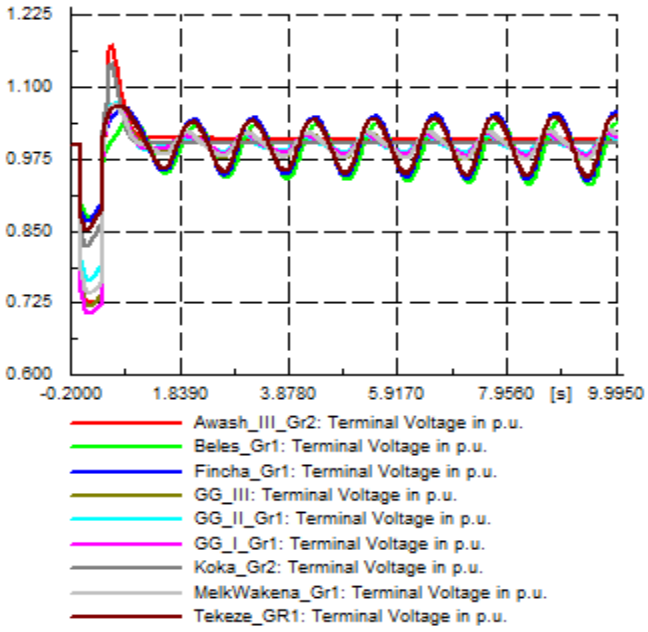

(b) Terminal voltage in pu

Figure 4-36 The speed and terminal votages of HPP generators after SE-1

The tripping of Awash III and Koka HPPs put further stress on the remaining generators and therefore the terminal voltages of Fincha, Beles & Tekeze HPP generators were sagged below 0.952 pu as shown in Figure 4-36 (b).

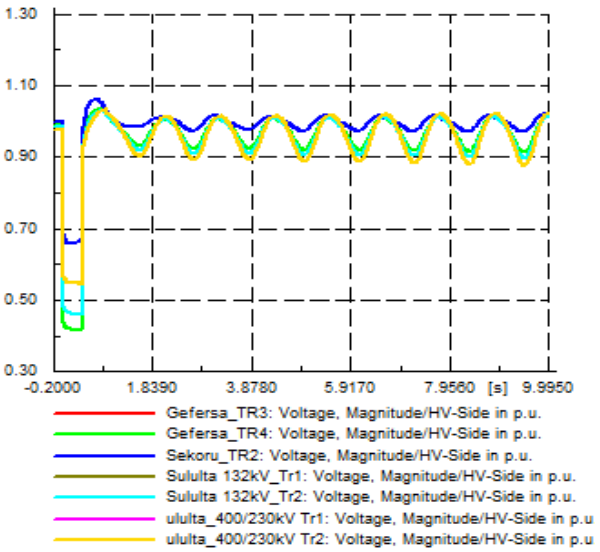

(a) Voltages in pu

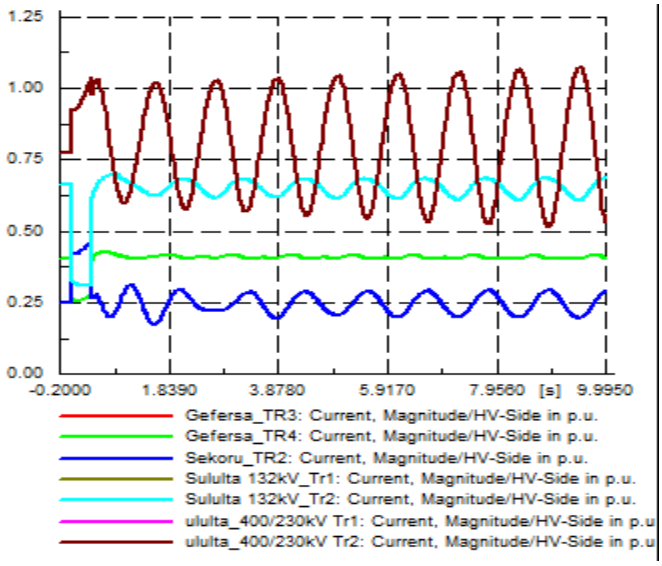

(b) Currents in pu

Figure 4-37 Voltage across and current through trasformers after SE-1

After Awash II & Koka HPP generators had been tripped, the voltages across Sululta 400/230kV transformers I & II were sagged to 0.906 pu at around 1.643 seconds and became overdamped after wards. The current through these transformers were rising to above 1.034 pu with over damped oscillations. The voltages across and currents through Sekoru 400/230kV transformer, Gefersa 230/132kV transformers were within limits as shown in Figure 4-37 (a) & (b).

After SE-1, the current flowing through Sululta _Gefersa 230kV line I was reached to 1.086 pu at around 1.609 seconds with over damped oscillations. The voltage across this line on Gefersa 230kV bus side was observed to be 0.932 pu as shown in Figure 4-38. Therefore, Sululta_Gefersa 230kV line I was tripped by overcurrent protections and let we call this tripping as switching event 2 (SE-2).

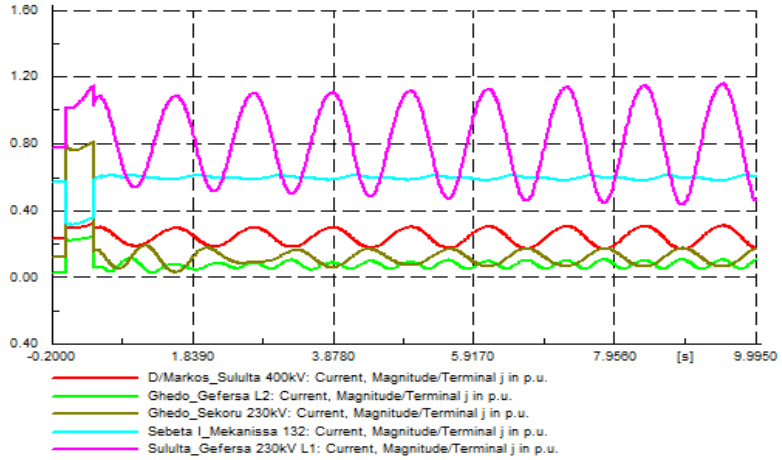

(a) Currents in pu

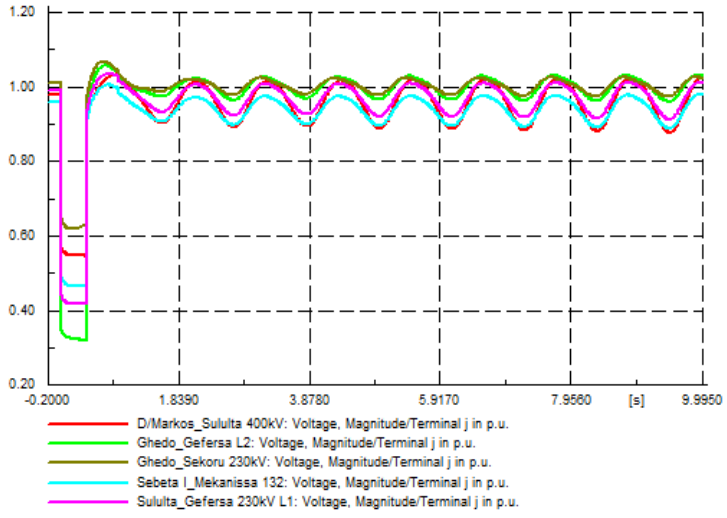

(b) Voltages in pu

Figure 4-38 Current through and voltage across transmission lines of the disturbance area after SE-1

As depicted from Figure 4-38, the current on Sululta_Gefersa 230kV line I was drastically increased due to the earth fault on nearby substation. Therefore, the cascading event continued when Gefersa_Sululta 230kV Line I was tripped at 1.609 seconds. Some of the sequence of events observed on the SCADA/EMS was indicated in Table 4-13.

Table 4-13 Sequence of tripping with time observed on the SCADA

Line/Gen/Transformer	Outage time	Reason
Ghedo_Gefersa 230kV line I	15:07	Earth fault, Ia = 119.8 A, Ib = 2.193kA, Ic = 57.16 A. Fault location = 49.01 km
Sululta_Gefersa 230kV line I	15:07	Earth fault, Ia = 79.46 A, Ib = 80.09 A, Ic = 57.16 A, In = 216.1 A
Ghedo_Gefersa 230kV line II	15:07	Earth fault, Ia = 519.5 A, Ib = 709.09 A, Ic = 405.1 A, zone 3
Sekoru_Ghedo 230kV line	15:07	No signal, Fault location = 96.3 km
Gefersa 230/132kv transformers III & IV	15:07	Earth fault, Ia = 207 A, Ib = 287 A, Ic = 292.7 A, In = 199.5 A
Sekoru 400/230kV transformer I	15:07	Overcurrent
Koka Unit I, Unit II	15:07	Reverse power
Adama wind I	15:07	Loss of voltage
Awash II & III, Melkawakena HPPs	15:07	Overcurrent
Kality I_Sebeta I 230kV	15:08	Earth fault
Suluta 400/230kv transformers I, II, III	15:08	Earth fault
Fincha HPP	15:08	Underfrequency
GG I HPP	15:08	Reverse power
GG II & GG III HPP	15:08	Underfrequency
Tekeze HPP	15:08	No signal

As Gefersa_Sululta 230kV line I was tripped, the EEP grid was split into two isolated areas as indicated in Figure 4-39 (a). Gefersa_Suluta 230kV line II was on a planned outage. Therefore, the high power transfer between these two substations was interrupted after Sululta_Gefersa 230kV line I had been tripped by an earth fault and overcurrent protections. This condition further put stress on the remaining lines and transformers which were connected to Gefersa substation. The rotor angles of generators were swinging each other as shown in Figure 4-39(b). The system was split into two parts with Fincha, Tekeze and Beles HPPs with one part and supplied the north western, western & northern regions and GG I, GG II, GG III, Melkawakena, Koka, Awash II and Awash III HPPs on the other part and supplying the remaining regions for few seconds.

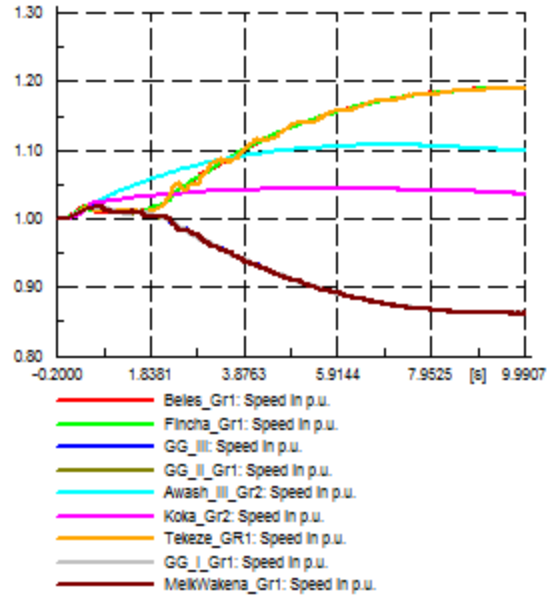

(a) Speed in pu

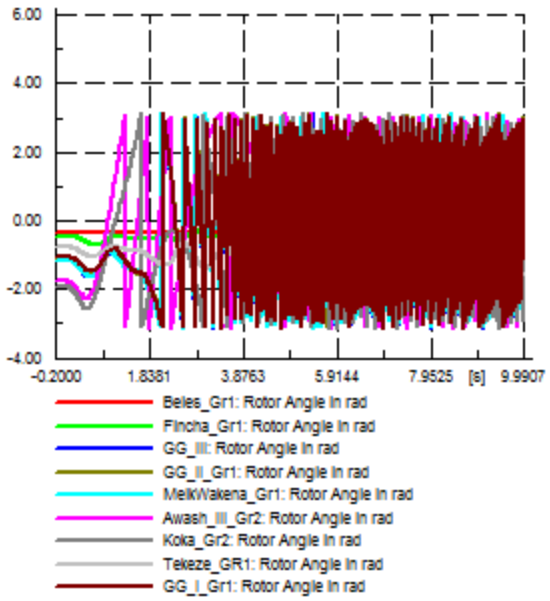

(b) Rotor angle in rad

Figure 4-39 Speed and rotor angle profiles of HPP generators after SE-2

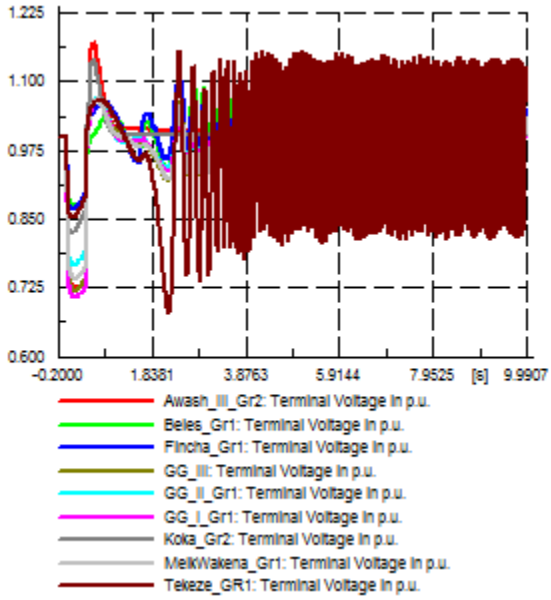

(a) Terminal voltage in pu

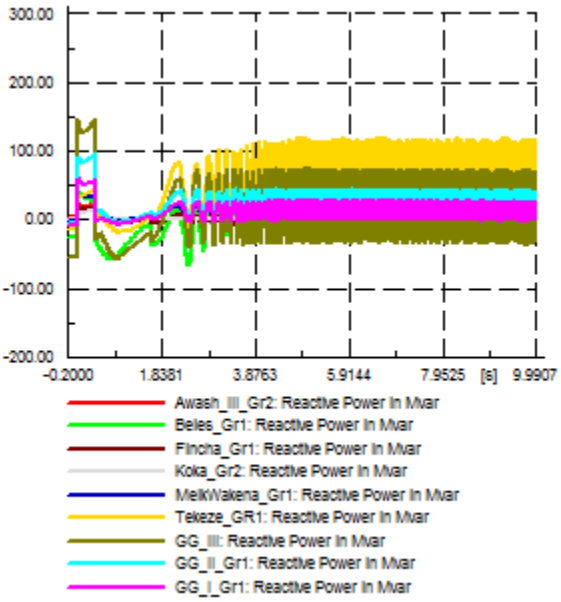

(b) Reactive power in Mvar

Figure 4-40 Terminal voltage and reactive power supplied by HPP generators after SE-2

The generators at Fincha, Tekeze and Beles HPPs were accelerated and their frequency was drastically increased and reached 1.1 pu at 3.8763 seconds. The speed of the other generators (for instance, GG I, GGII, GG III, Koka, Melkawakena) on the other hand were decreased to 0.95 pu. Figure 4-39 (a) depicted these results.

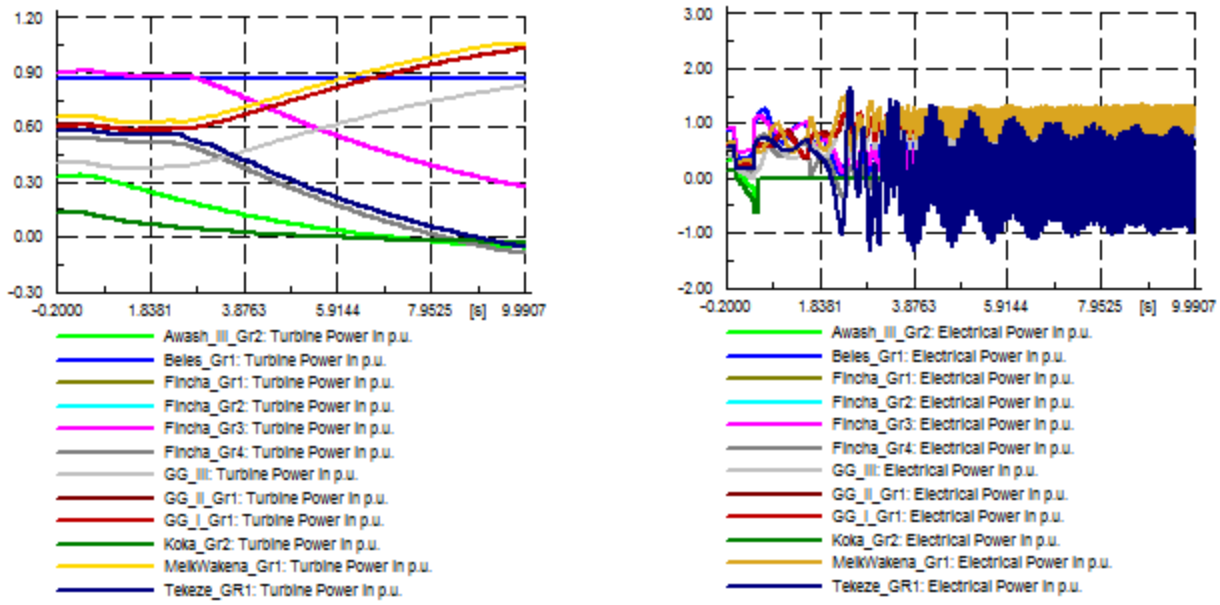

(a) Turbine power in pu

(b) Electrical power in pu

Figure 4-41 The turbine power input to and electrical power output of HPP generators after SE-2

The terminal voltage of Tekeze HPP generator was dipped well below 0.85 pu whereas that of Beles HPP generators were increased 1.08 pu at around 2.01 seconds. The turbine power for generators whose speed was decaying fast was increased to return their corresponding speed backed to the nominal value though it was impossible. High reactive power was supplied by these generators to supply the high reactive power demanded by the system load. As a result, the electrical power supplied by these generators was decreased. Figure 4-41 (a)-(b) depicted these situations.

The voltages of Kality I 230kV and Legetafo 230kV buses were dipped below 0.80 pu whereas the voltages at Tekeze 230kV buses were oscillating between 0.65 pu and 1.162 pu at around 2.188 seconds as shown in Figure 4-42 (a). The frequency deviations observed on some of these critical buses were around $\pm 6\ Hz$ at 3.99 seconds with over damped oscillations. The frequency on Fincha 230 kV, Beles 400kV, B/Dar II 230kV and Tekeze 230kV buses was increased above 55 Hz and on the other hand the frequency at the remaining critical buses was decreased below 45 Hz as shown in Figure 4-42 (b).

The voltages and currents of lines and transformers that emanated from Gefersa and Sululta substations were indicated in Figure 4-43 and Figure 4-44. The current flowing on Gefersa 230/132kV, Sululta 400/230kV & Sekoru 400/230kV transformers were in the acceptable range. However, the voltages across Sululta 400/230kV transformers were rising beyond 1.131 pu at around 2.416 seconds.

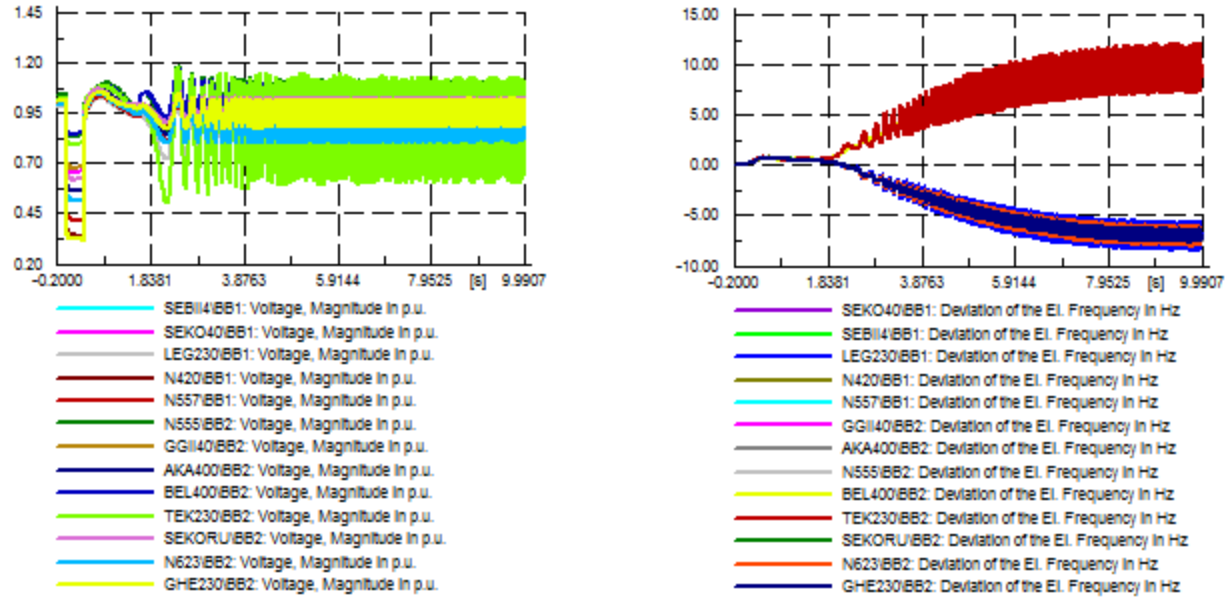

(a) Bus voltage in pu

(b) Frequency deviations in Hz

Figure 4-42 The voltages and their corresponding frequency deviations at critical buses after SE-2

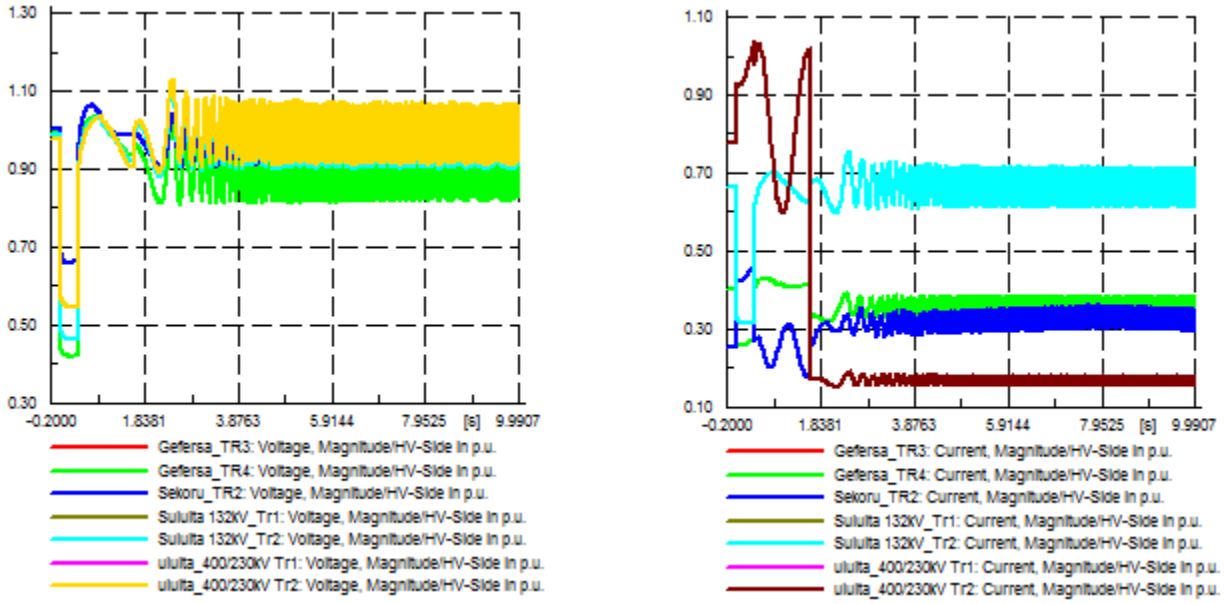

(a) Voltages in pu

(b) Currents in pu

Figure 4-43 Voltage across and the current flowing through transformers after SE-2

The currents on D/Markos_Sululta 400kV line, Ghedo_Gefersa 230kV line II, Ghedo_Sekoru 230kV, and Sebeta I_ Mekanisa 132kV lines were well below their rated values. However, the voltage across D/Markos_Sululta 400kV line was rising to 1.124 pu at around 2.425 seconds and that of Sebeta I _Mekanisa 132kV line was sagged below 0.87 pu at around 1.856 seconds as indicated in Figure 4-44.

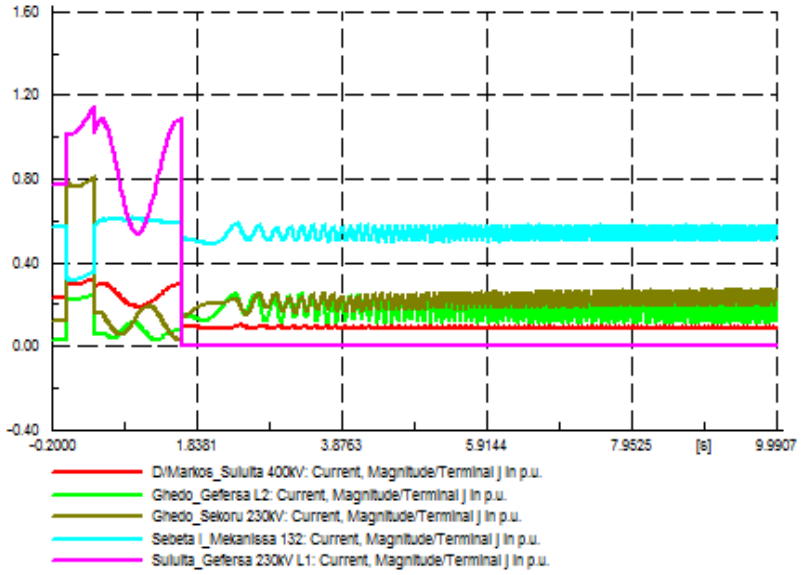

(a) Currents in pu

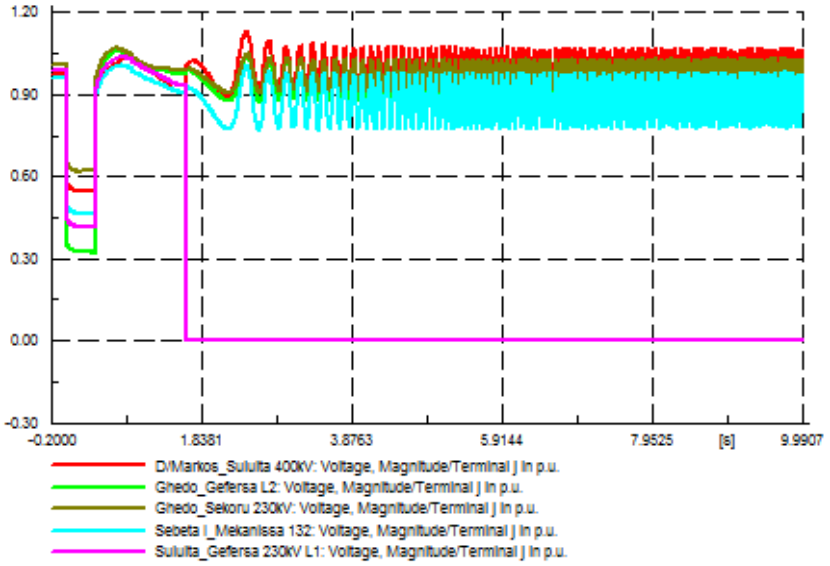

(b) Voltages in pu

Figure 4-44 The current flowing through and voltage across the incoming & outgoing lines of Gefersa s/s after SE-2

After SE-2, the sequence of events would not be stopped as the following components would be tripped by their corresponding protection systems.

- Undervoltage was observed across Sebeta I_Mekanisa 132kV line and would be tripped by Undervoltage protections.
- Overvoltage was seen across Sululta 400/230kV transformers and later they would be tripped by overvoltage protections.

— There was overvoltage across D/Markos_Sululta 400kV line and it could be tripped by overvoltage protections at at around 2.42 seconds.
— Tekeze HPP was tripped by Undervoltage protections at 2.017 seconds

Therefore, after SE-2, the system components had out of limit parameteres, the cascade tripping was continued, and the health of the system was paralysed.

Results of Analyses Identifying Constraints that Caused System Collapse

The operation of the Ethiopian Electric Power (EEP) system in general follows the criterion that under N-1 outage condition, i.e., the outage of any generating unit, transmission line or transformer etc…, the system should remain stabilised and continued to operate within limits [23]. This N-1 contingency provision, prior to system collapse on 22nd December 2015 had already been availed as one of the double line of Sululta_Gefersa 230kV line II was under shut down (planned outage). Moreover, the remaining line was transferring bulk hydro generation from Beles HPP in northwestern region through Sululta substation to the mid-country load centres, was loaded close to its stability limit and there was no margin in the system to handle the outage condition of Ghedo_Gefersa 230kV lines by an earth fault.

The steady state and dynamic analyses depicting system performance after disturbance clearly indicated that the system was not able to survive the earth fault, which was occurred on Ghedo_Gefersa 230kV line I. This line is the vital line that transferred bulk hydro generation from Fincha, GG I and GG II HPPs through Fincha HPP_Ghedo 230kV and Sekoru_Ghedo 230kV lines respectively.

Final State of the System

As seen from the above discussions the sequence of tripping continued as a result of out of limit parameters of generators (frequency, terminal voltage, electrical power output and reactive power supplied by), buses, lines and transformers. The high-speed cascade took only 2 minutes and finally the total system has collapsed at 15:08 hrs. Some of the major sequences of events are indicated in Table 4-13.

4.6.3. December 11th 2015 Blackout

Status of the Network Prior to the Disturbance

The December 11th 2015 blackout was occurred during the off-peak hours of the system. At 5:45 hrs, the total load was around 740MW. The total generation was around 880MW with no transnational exchange. The following major activities were performed before the occurrence of the system disturbance, which of course affected the stability of the grid to any disturbance that could arise on it.

- Planned activity at Ghedo substation for replacement of 230kV circuit breaker. Due to this, the 230kV lines from Fincha HPP_Ghedo_Gefersa were out of service.
- Gefersa-Sululta 230kV line I was out of service due to the upgrading and rehabilitation work at Gefersa substation.
- 400kV and 230kV bus bar of Gelan substation were dead due to planned interruption (to avoid overvoltages) from mid-night to morning of the following day.

Steady State Simulation & Analysis

Having all the above information, the load flow program was performed to see the steady state performance of the EEP grid before disturbance. The steady state power flow of the major lines that interconnected the different regional power systems is shown in Table 4-14 below. There was no overloaded component observed on the system. The total system power loss was 43.45 MW.

Prior to the disturbance, there were voltage deviations on some buses and therefore a disturbance under such condition would result in a deteriorated and failed system. Such voltage deviations could arise due to the uneven distribution of loads, poor planned outages, and poor dispatch schedules of the generating plants. For instance, the voltages on most of the buses in the Eastern region were rising, as there was no transnational exchange with Djibouti. It was observed that the voltage at Dire Dawa III 230kV bus was 1.08 and that of PK12 (to Djibouti) was 1.1 pu.

On the other hand, the voltages on the Addis Ababa and Central regions (these regions were the high load centres) were decreasing. For example, the voltage at Kality I 132kV and Legetafo 132kV buses were 0.95 pu. Figure 4-45 depicted these conditions.

Table 4-14 Power flows on important lines before the disturbance (5:45 hrs.)

Line name	MW flow	MVAr flow	Loading of the line (%)
B/Dar II_Alamata 230kV	86.4	-33.72	22.26
D/Markos_Sululta 400kV	325	4.57	19.49
Sebeta I_Kality I 230kV	143	0.91	39.89
Legtafo _Kality I 230kV	6.044	-1.67	1.52
B/Dar II_D/Markos 400kV	223	-40.88	13.05
Sekoru-Ghedo 230kv	16.53	-26.26	8.35
Gefersa_Sebeta I 230kV	111.17	-77.19	37.73
G/Gibe II_Sebeta II 400kV	88.11	-63.06	6.91
Tekeze_Mekele 230kV L1 & L2 each	37.07	10.50	11.84
Mekele_Alamata 230kV	26	-47.79	11.87
Combolcha_Legetafo 230kV	68.42	-8.44	19.95

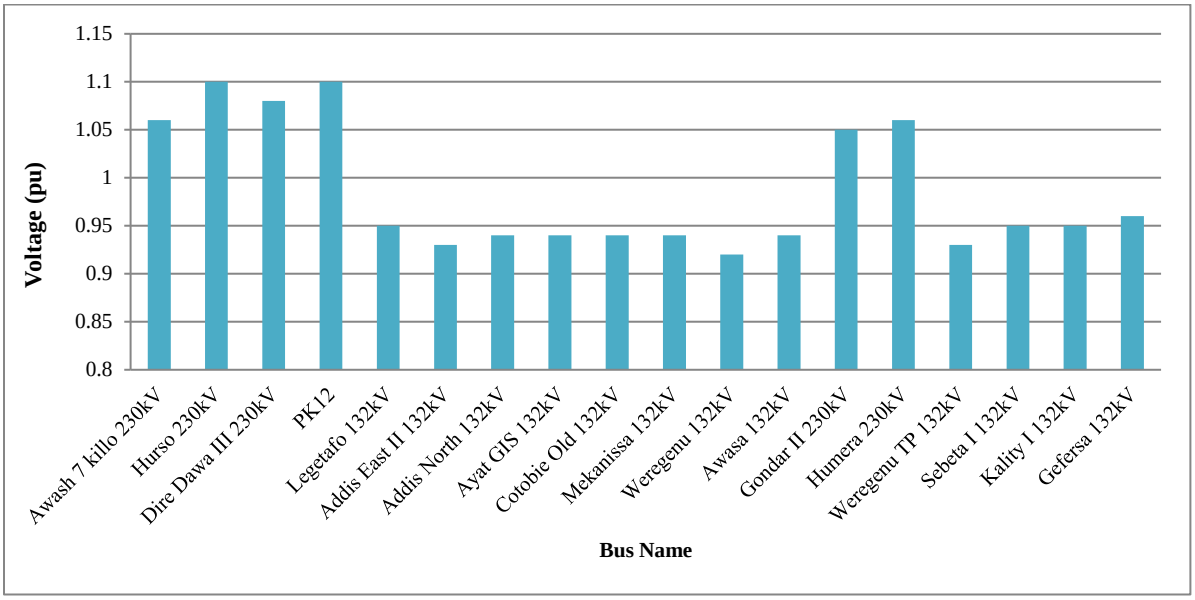

Figure 4-45 Voltage profiles of buses that deviate from 1.0 pu

Sequence of Events and Dynamic Simulations

The initiating event for the December 11th 2015 blackout was the short circuit fault (B phase of the line dropped on to the bus bars) at 5:58 hrs on Kality I _Mekanisa 132kV line inside Kality I 132kV switchyard. The sequence of events leading to blackout began just after 5:58 hrs when Mekanisa_Kality I 132kV line was tripped by an earth fault (LLG). This resulted in overloading and subsequent tripping of critical lines.

The RMS simulation results over a period of 10 seconds after initiation of disturbance are shown in Figure 4-46 to Figure 4-49. The simulation results depicted the dynamic performances of EEP system by

representing profiles of generator speed and their corresponding rotor angles, terminal voltages, reactive power supplied, the mechanical input power & their corresponding electrical output power of the HPP generators. The voltages of critical buses and their corresponding frequencies, the voltage across and current flowing through the lines and transformers that were directly or indirectly connected to the disturbed substation are also depicted in the simulations. The effects of the disturbance on the performance of EEP system with a fault clearing time of 160ms is summarised as:

- As indicated in Figure 4-46 (a), the speed and angle profiles of generators indicate that the system was transiently stable (except GG III HPP generator) but with sustained oscillations which indicates the presence of poorly damped oscillatory modes.
- The terminal voltages of generators of Koka, Melkewakena, and Tekeze & Awash III HPPs were dipped below 0.7 pu during the fault and recovered well above 0.98 pu with damped oscillations after the fault has cleared. On the other hand, the terminal voltages of the generators that were farthest[7] from the disturbance, for instance, GG III and Fincha HPPs were not sagged below 0.90 pu. Figure 4-46 (c) depicted these conditions.
- The reactive power supplied by each HPP generator was within limits and their corresponding turbine power was almost constant as indicated in Figure 4-46 (d) & (e).
- The voltages of most of the critical buses were dipped below 0.5 pu and recovered well above 0.95 pu and their corresponding frequency was increased to 50.2 Hz and returned to the nominal value with sustained oscilations as shown in Figure 4-47 (a) & (b).
- The currents flowing through Sebeta I_Mekanisa 132kV, Gefersa_Kality I 132kV, Sebeta I _Kality I 230kV and Akaki I_Kality I 132kV lines were drastically increased above 2.0 pu
- The voltages across Kality I 132/45kV transformers, Kality I 230/132kV transformers, Gefersa 230/132kV transformers, Sebeta I 230/132kV transformers, and Sululta 230/132kV transformers were dipped below 0.6 pu and recovered to above 0.95 pu after the fault has been cleared. Whereas the currents through these transformers were increased to 1.5 pu during the fault and returned well below their rated currents after the fault has been cleared by tripping Kality I_Mekanisa 132kV line.

[7] When we talk about distance in this case, we mean the electrical distance and is expressed in angle. The electrical length of a line can be expressed as $\theta = \beta l$ where l is the length of a line and β is the phase constant given by: $\beta = \omega\sqrt{LC} = 2\pi f\sqrt{LC}$, L & $C = inductance\ and\ capacitance\ of\ the\ line\ per\ unit\ length, respectively$ [9].

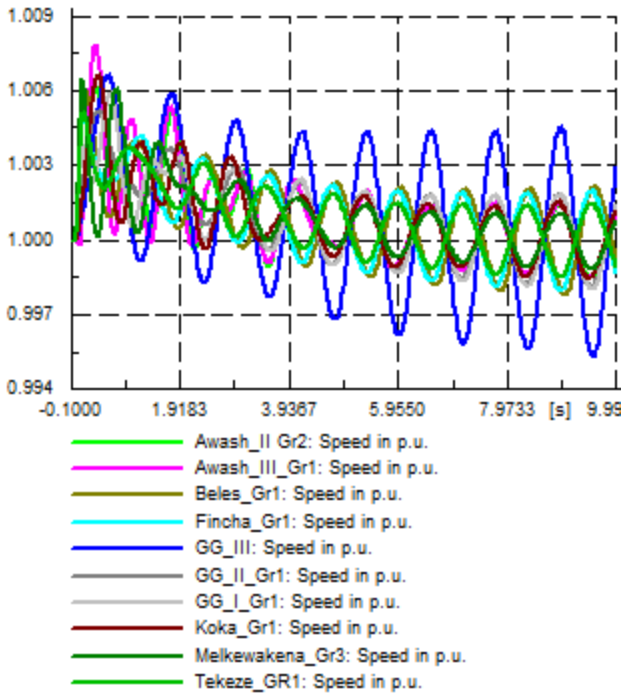

(a) Speed in pu

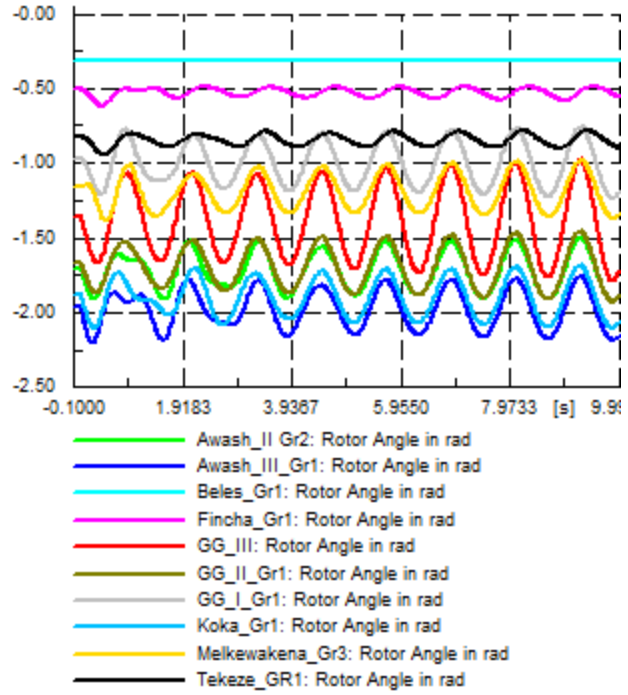

(b) Rotor angles in rad

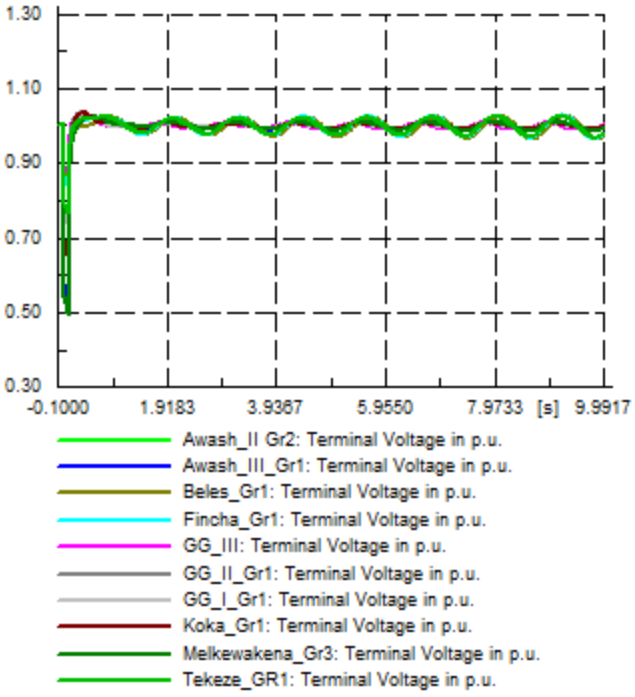

(c) Terminal voltage in pu

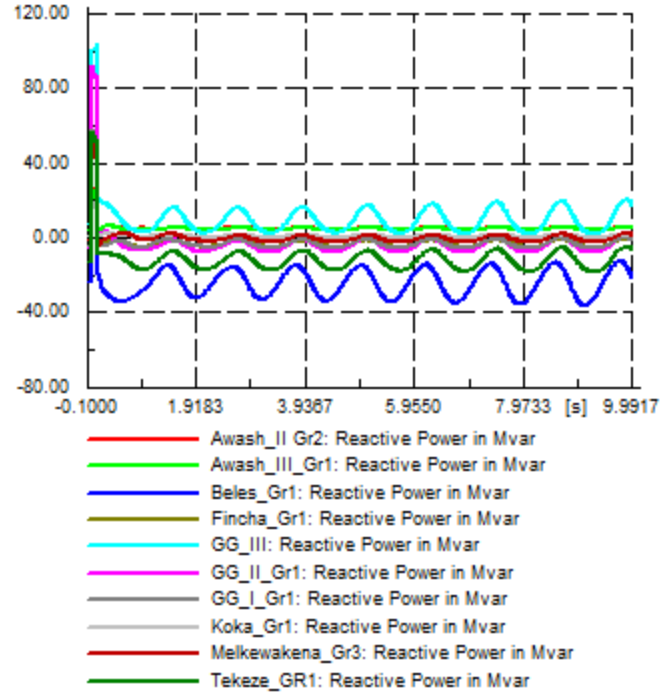

(d) Reactive power in Mvar

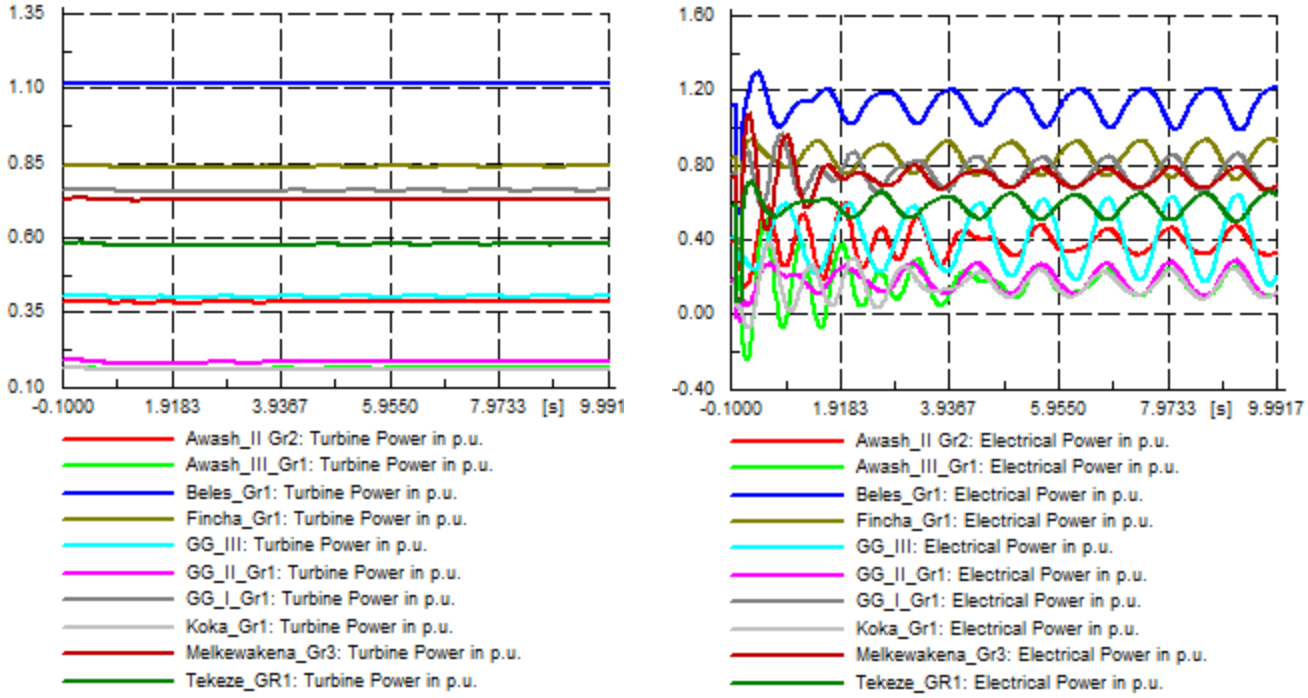

(e) Turbine power in pu

(f) Electrical power in pu

Figure 4-46 Profiles of HPP generators after the fault has cleared.

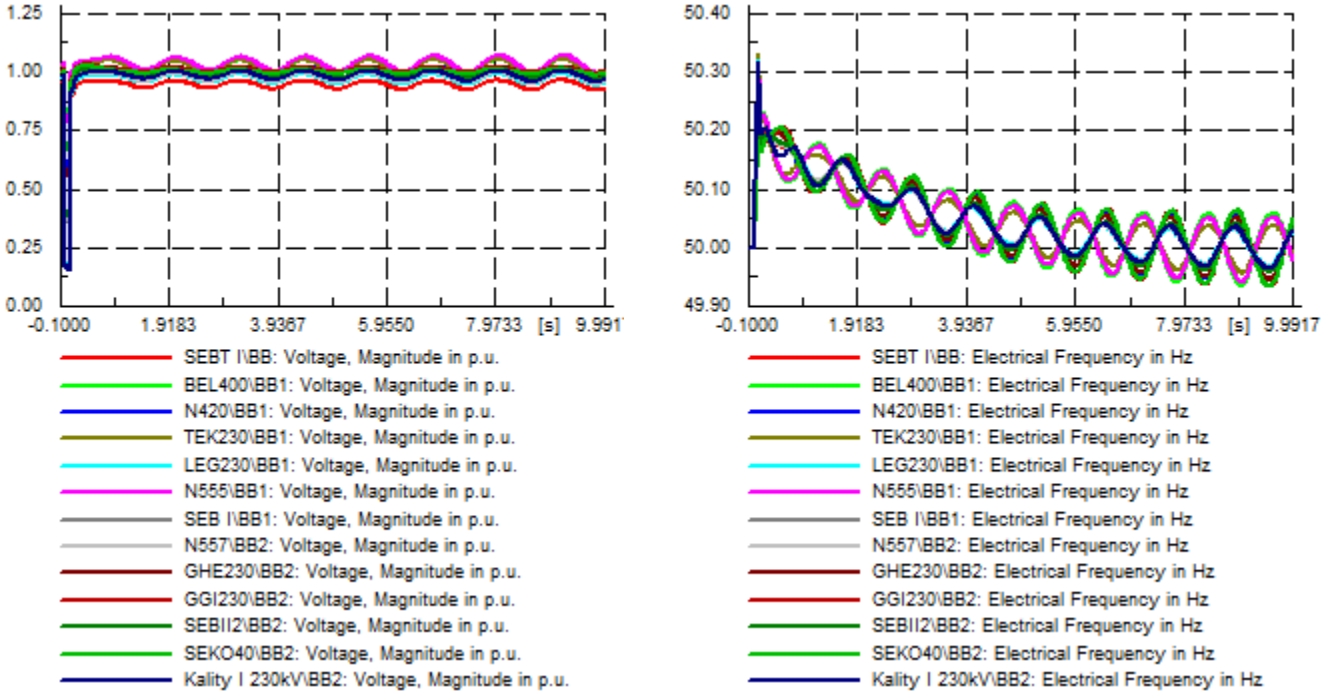

(a) Voltages in pu

(b) Frequency in Hz

Figure 4-47 The voltages and their corresponding frequencies at critical buses after the fault has cleared

As depicted in Figure 4-48, when Mekanisa_Kality I 132kV line was tripped by its protection system, the lines that were connected to Mekanisa and Kality I substations became overloaded. For instance, as the power flow from Kality I 132kV to Mekanisa 132kV was interrupted the load on Mekanisa 132kV bus was supplied only through Sebeta I_Mekanisa 132kV line and the line became overloaded as a result of the earth fault on near by transmission line.

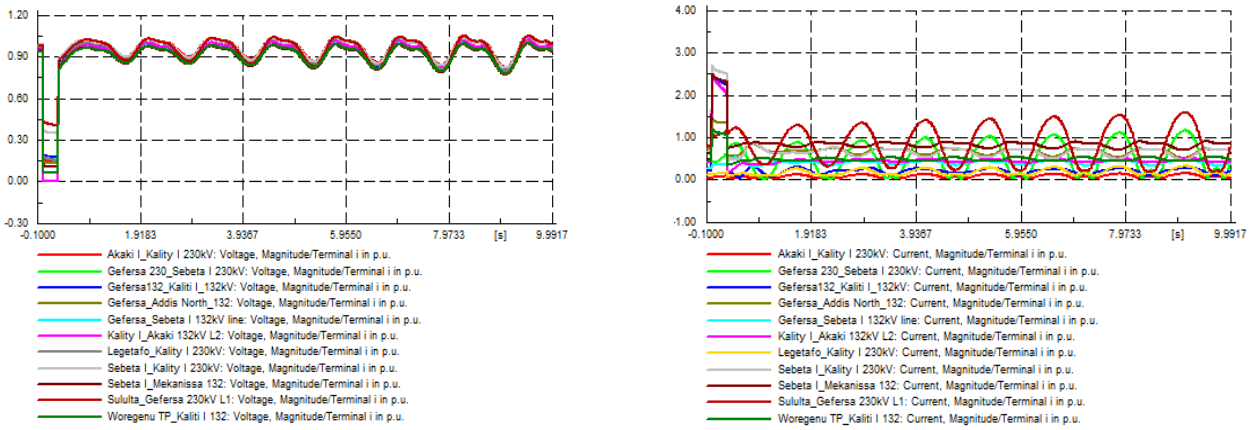

(a) Voltages in pu (b) Currents in pu

Figure 4-48 The voltages across and currents flowing through the transmission lines after the fault has cleared

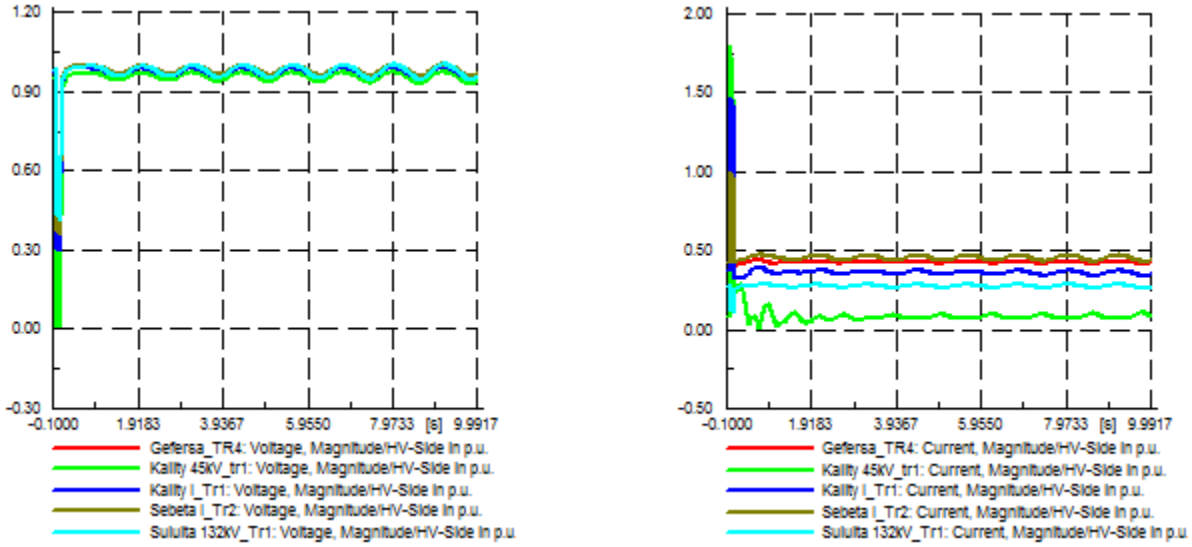

(a) Voltages in pu (b) Currents in pu

Figure 4-49 The voltages across and currents flowing through the transformers after the fault has cleared

The bulk hydro generations of GG I & GG II HPPs were supplying the high load centres of the capital Addis Ababa through Sebeta I_Kality I 230kV, Sebeta I_Gefersa 230kV and Sebeta I_Mekanisa_Kality I 132kV lines. But as Mekanisa _Kality I 132kV line was tripped due to short circuit fault on it, the bulk

hydro generations of GG I and GG II HPPs were supplying the high load centres only through Sebeta I_Kality I 230kV and Sebeta I_Gefersa 230kV lines. In addition, since the fault had happened near to Kality I substation, Sebeta I_Kality I 230kV line was highly overloaded and would be tripped by its protection system. Similarly, Gefersa_Kality I 132kV line was also became overloaded as high power was transferred through this line to support the loads that were connected to Kality I substation.

As observed from the dynamic simulations above, the currents through Sebeta I _Mekanisa 132kV, Kality I _Akaki I 132kV line I & II, Sebeta I _Kality I 230kV and Gefersa_Kality I 132kV lines were reached over 2.0 pu at around 1 second. And therefore, these lines were tripped by overcurrent protective relays (let we call it as switching event 1 (SE-1) to illustrate it shortly). As a result, the following phenomena were taken place:

— The system was split into two isolated areas and Fincha, Tekeze & Beles HPP generators were accelerating together and supply the loads of the Western, Northern and North-western regions of EEP. And the remaining HPP generators were decelerating and the frequencies of Awash II & III, GG I, GG II, GG III, Koka & Melkawakena HPP generators were collapsed drastically as it is depicted in Figure 4-50 (a). It was difficult to synchronize these generators.

— The terminal voltages of HPP generators were also decaying. For example, the terminal voltage of Tekeze HPP generator was dipped below 0.8 pu at around 2 seconds after the event. Figure 4-50 (c) shows the terminal voltages of the HPP generators that were affected by the disturbance.

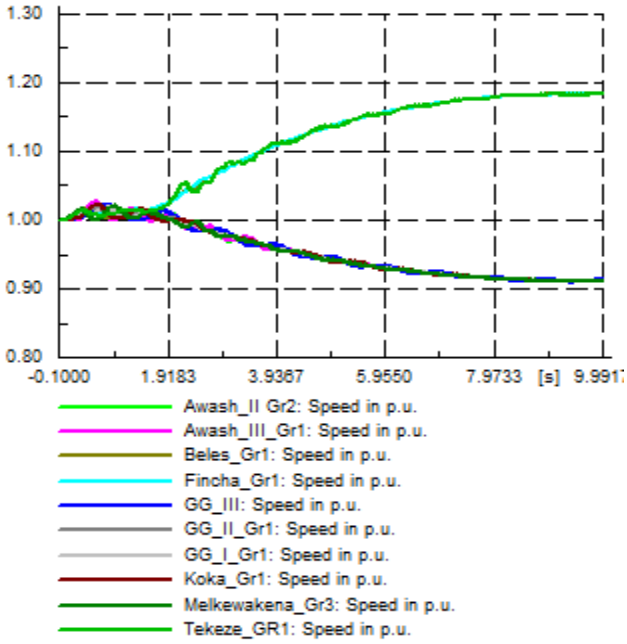

(a) Rotor speed in pu

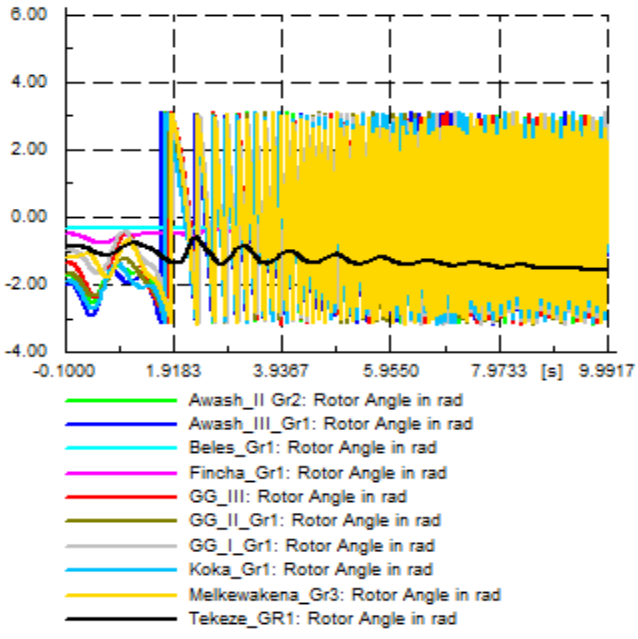

(b) Rotor angles in rad

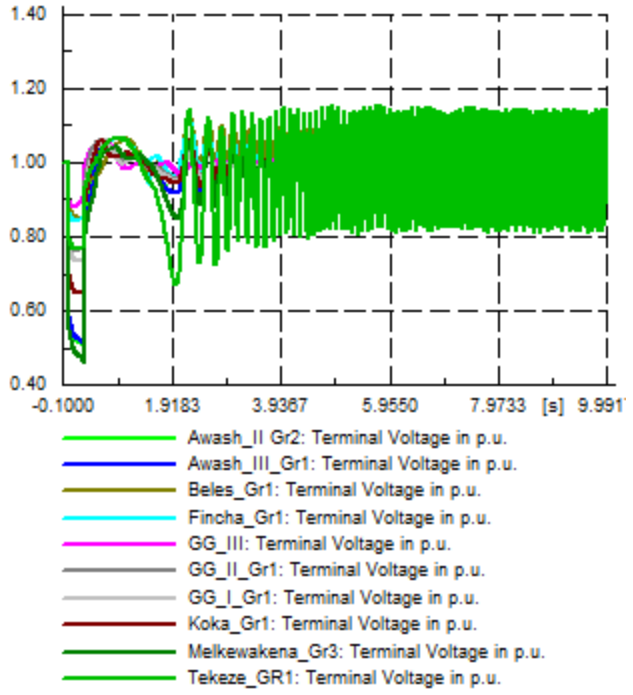

(c) Terminal voltage in pu

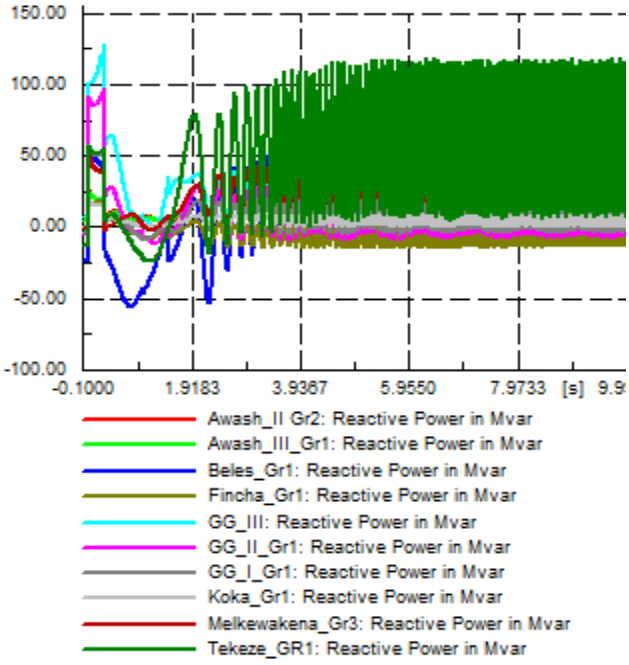

(d) Reactive power in Mvar

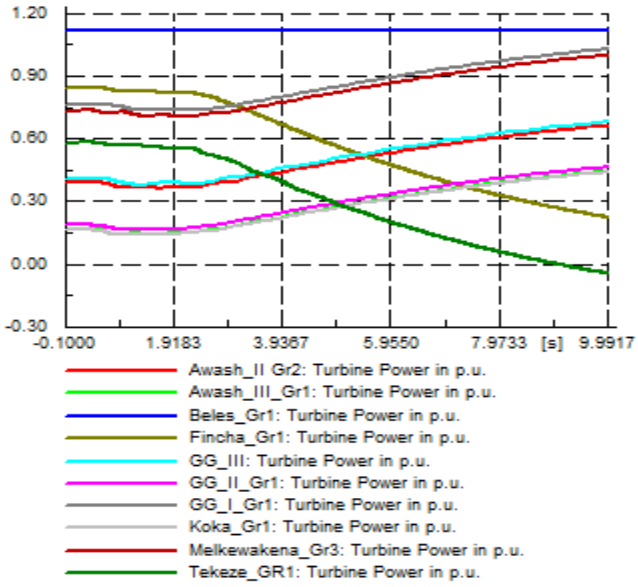

(e) Turbine power in pu

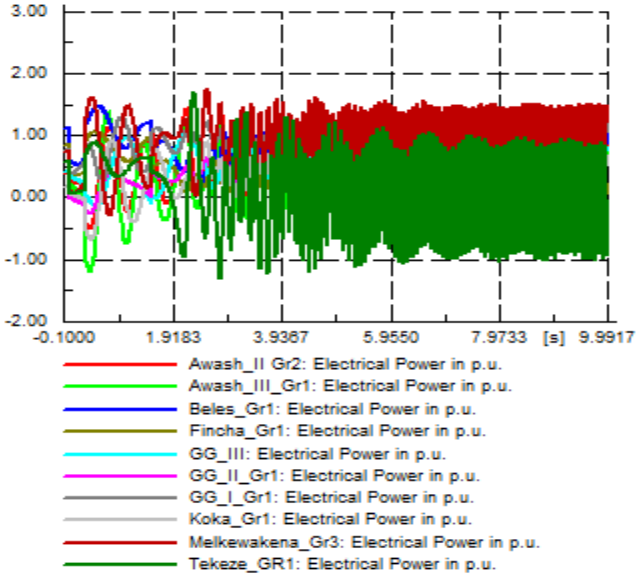

(f) Electrical power in pu

Figure 4-50 Profiles of HPP generators after SE-1

The voltages on critical buses were also deviating from the nominal value. The voltages at Legetafo 230kV, Kality I 230kV, and Tekeze 230kV buses were declined to 0.75 pu and oscillating back and forth as it is indicated in Figure 4-51 (a). On the other hand, the voltage at B/Dar 230kV bus was increased to 1.1 pu

and its corresponding frequency was rising above 51 Hz. Figure 4-51 (a) and (b) show the voltage and their corresponding frequencies at some important buses.

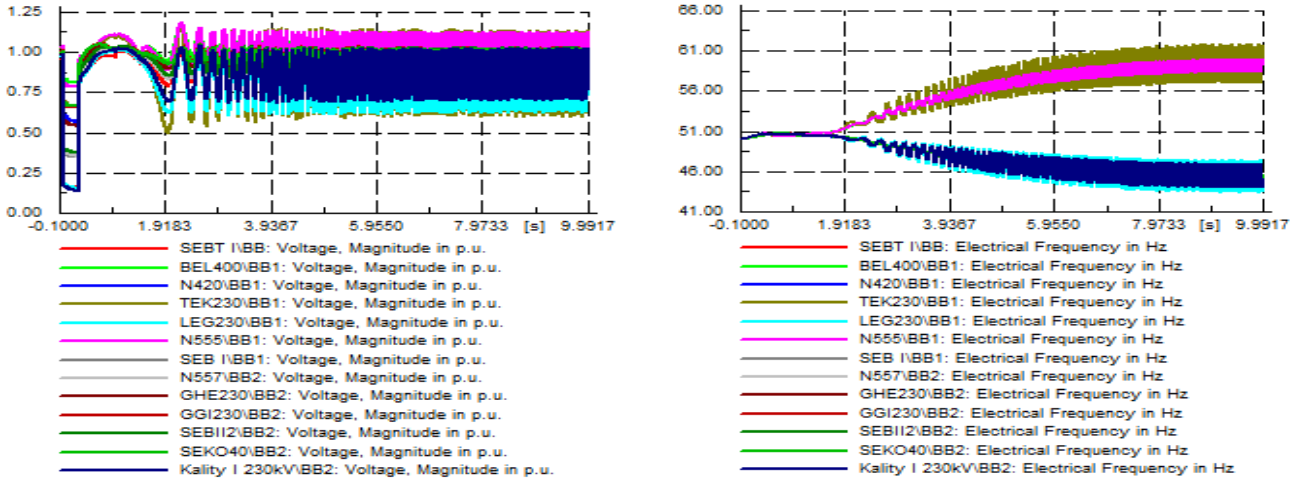

(a) Voltage in pu (b) Frequency in Hz

Figure 4-51 Voltages and their corresponding frequencies at critical buses after SE-1

The tripping of Sebeta I_Mekanisa 132kV, Sebeta I _Kality I 230kV and Gefersa_Kality I 132kV line put further stress on Gefersa_Addis North 132kV line and on Sululta_Gefersa 230kV lines. After SE-1, the currents flowing through Gefersa_Addis North 132kV line were reached to 1.34 pu at 2.07 seconds and sustained this value and the voltages across Suluta 230/132kV transformers (TR1 & TR2) were rising to 1.12 pu at 2.23 seconds after the disturbance had happened. Figure 4-52 and Figure 4-53 shows these conditions.

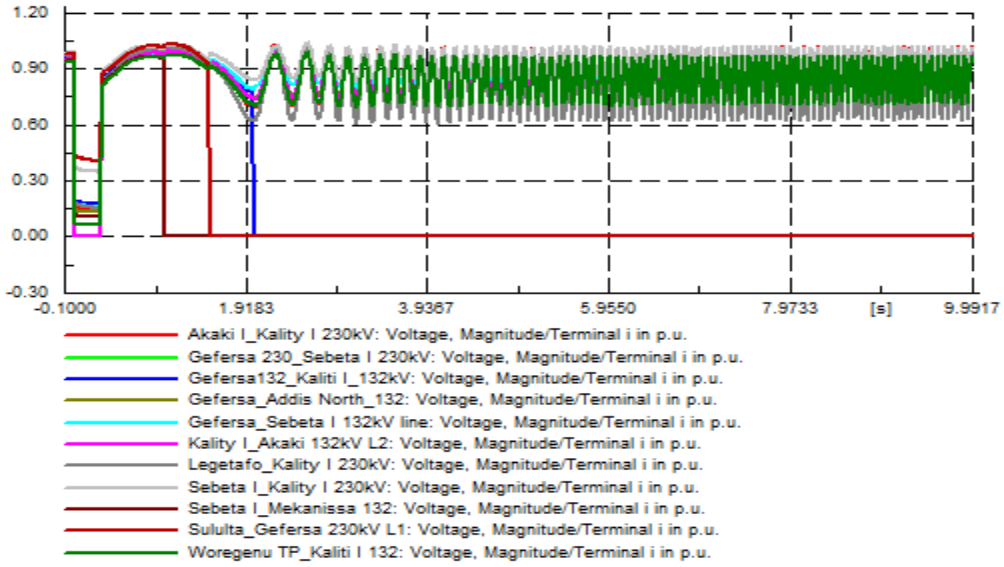

(a) Voltages in pu

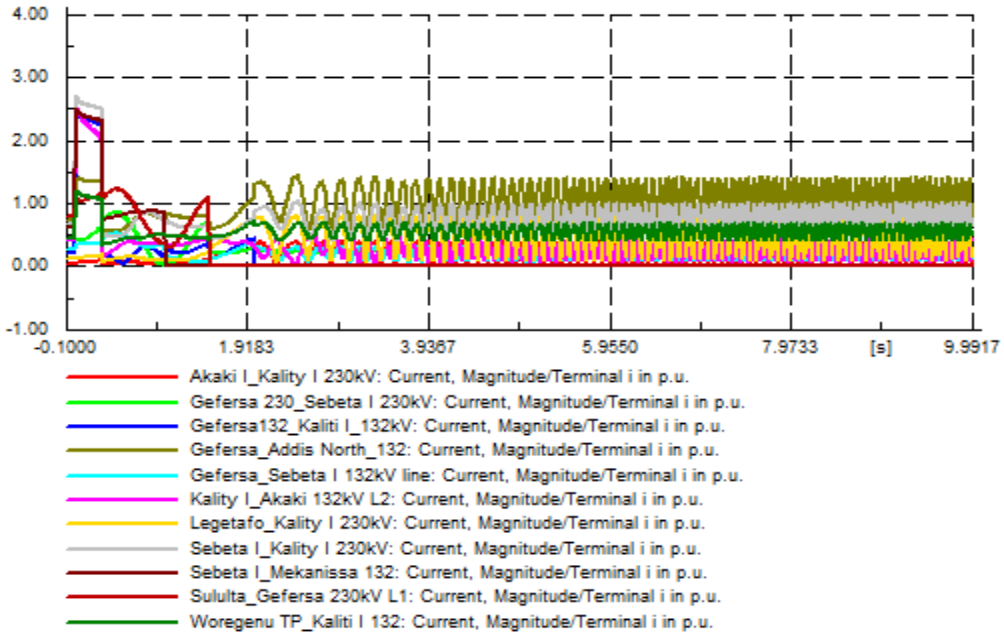

(b) Currents in pu

Figure 4-52 The voltages across and currents flowing through the transmission lines after SE-1

The voltage profiles of buses at which the wind plants were connected to are indicated in Figure 4-54, and the voltage profile of the bus that Ashegoda wind plant was connected to, was dipped below 0.6 pu at around 1.98 seconds. On the other hand, the voltage profile of Adama wind_I bus was sagged to 0.85 pu and was oscillating back and forth.

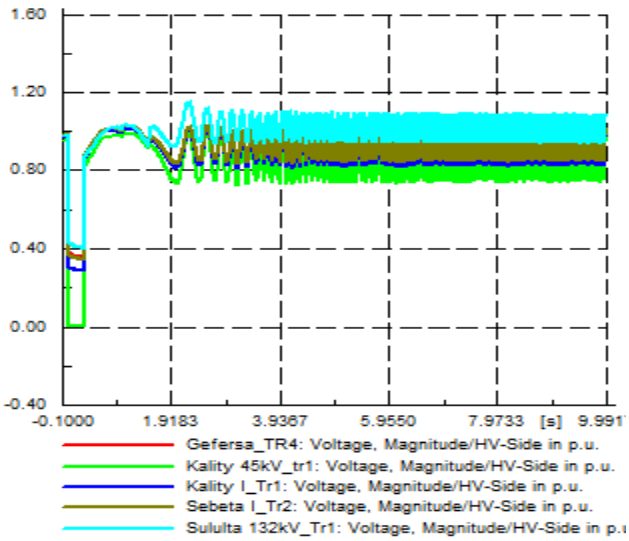

(a) Voltages in pu

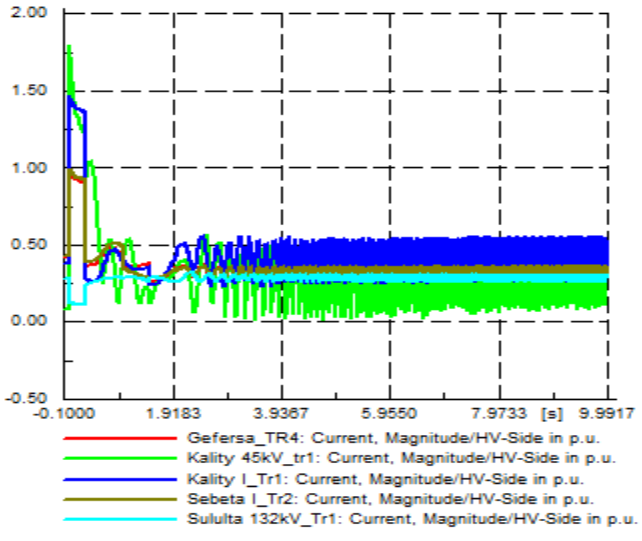

(b) Cureents in pu

Figure 4-53 Voltages across and currents flowing through the transmission lines after SE-1

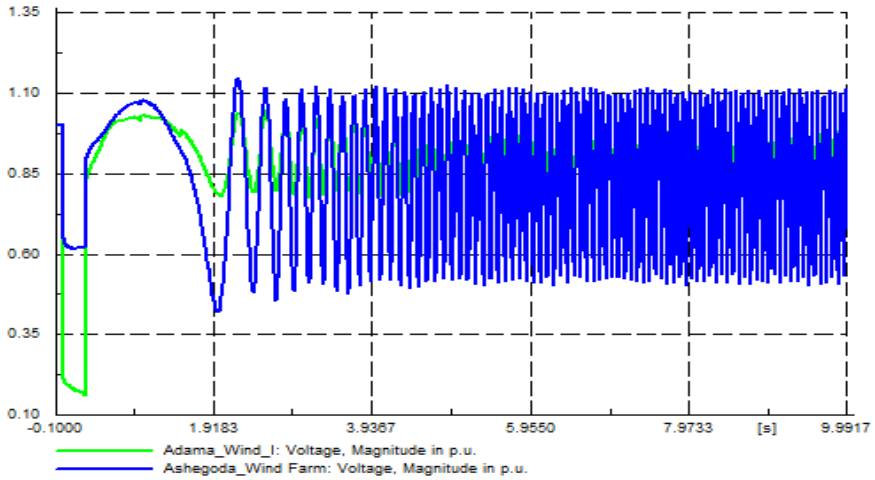

Figure 4-54 Voltage profiles of wind plants after SE-1

Therefore, the sequence of events continued as out of limits components tripped. As we have discussed from the simulation results above, the following components had out of limit parameters and were tripped by their corresponding protection systems (SE-2):

- ✓ Gefersa _Addis North 132kV line was overloaded and the current flowing through it was reached to 1.34 pu after 2.07 seconds and was tripped by overcurrent protection system.
- ✓ The terminal voltage of Tekeze HPP was dipped below 0.80 pu after 2 seconds and was tripped by Undervoltage protections
- ✓ Over voltages were observed on Sululta 230/132kV transformers (1.12 pu) and after 2.23 seconds and were tripped by overvoltage protection system.
- ✓ The wind plants were also tripped by loss of voltage protections.

To sum up, the tripping of these components had further aggravated the system collapse. After SE-2, the generators at Fincha and Beles HPPs tripped by overfrequency protections, the voltages at critical buses were dipped below 0.7 pu, Awash II & III, Koka, GG I, GG II & Melkawakena HPP generators were tripped by underfrequency protections. Most of these generators have gotten "Generator out of step (pole slip)" conditions as it is depicted in Appendix E, Section E.2.1. The simulation results after SE-2 that shows the speed, rotor angle, and terminal voltage of HPP generators are depicted in Appendix E, Figure E-18 (a)-(d). The voltage profiles of critical buses and their corresponding frequencies are also in indicated in Figure E-19, the voltages and currents on transformers and lines of the disturbance area are indicated in Appendix E, Figure E-20 & E-22.

4.6.4. August 14th 2015 Blackout

System Condition Prior to Disturbance

On August 14th 2015 at 9:45 hrs the total generation was 1419.9 MW and the transnational exchange was 31.55 MW to Djibouti with a system frequency of 50 Hz. The total system demand at 9:45 hrs was 1347 MW and GG II and Beles HPPs were met 56 % of the total system demand and mainly fed the 400kV system by generating 370 MW and 423 MW respectively. Tekeze, GG I and Fincha HPPs that mainly fed the 230kV network were generating 180 MW each and 105 MW respectively. The share of the wind generation was only 2.5 % of the total system power production. High load was observed on Gefersa 45kV feeder and the operators took no action. There was no SCADA/EMS system installed at this substation and as a result, online monitoring and operation of the power system components at Gefersa substation was impossible. With these load and generation dispatch pattern, GG I & Beles HPP generators were loaded above 90% and Gefersa 132/45/15kV transformer was loaded to 107.5 % of their rated capacity as shown in Figure 4-55.

Power Flow Simulations and Analysis

Figure 4-55 depicted the loading of equipments under steady state condition. It showed that Gefersa_Addis Alem 45kV line was loaded to 114.72 %, Weregenu TP_Weregenu 132kV line was loaded to 99.66 %, Koka 10.5/15/132kV transformers Tr1 & Tr2 were loaded to 98.5 %, and therefore there was no capacity margin on these equipments to further coped additional loading and any disturbance on the power system components around them would accelerate the system collapse.

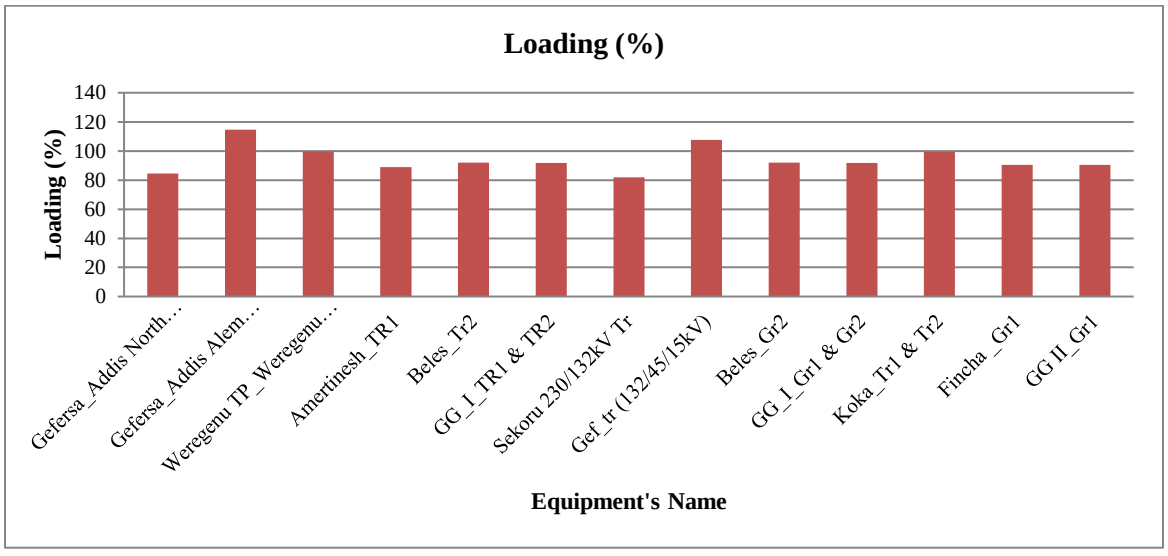

Figure 4-55 Equipment's loading prior to disturbance

The voltages at some critical buses were deteriorated, for instance, the voltages at Sebeta I 132kV, Kality I 132kV & Combolcha II 230kV were sagged to 0.94 pu. Figure 4-56 depicted these conditions.

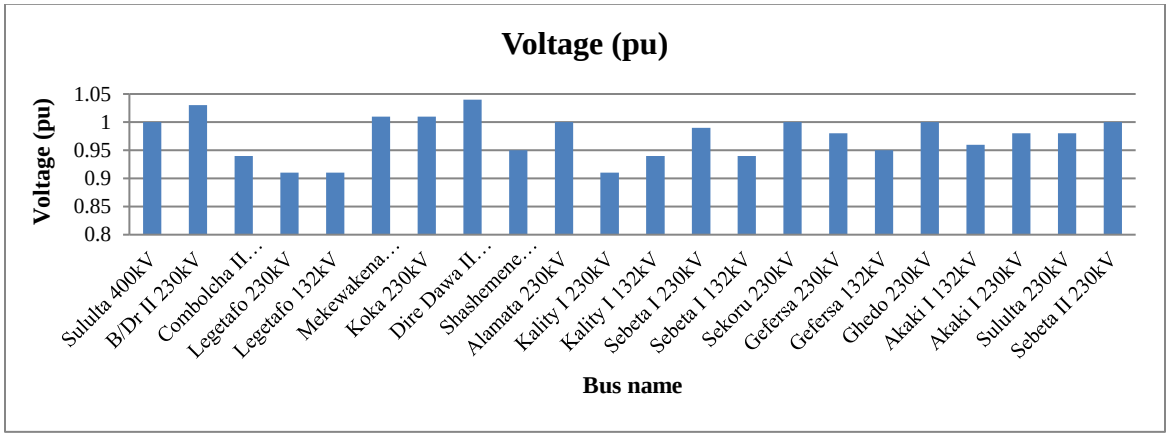

Figure 4-56 Voltages of important buses prior to disturbance

The power flows on lines that interconnected the load centres to the generations and were crucial for the intra-power flow among regional power systems is indicated in Table 4-15 below. There were no overloaded lines in this case and their loading was below 50 % for most of the lines. The total grid loss was observed to be 60.85 MW.

Table 4-15 MVA flows on important lines

Line Name	MVA
B/Dar II_Alamata 230kv line	$40 - j40$
Sululta_D/Markos 400kV line	$256 - j83$
Sebeta I _Kality I 230kV line	$185 - j14$
Sebeta II_Akaki I 400kV line	$259 - j116$
Kality I_Legetafo 230kV line	$10 - j60$
B/Dar II_D/Markos 400kV line	$294 - j50$
D/Markos _Fincha 230kV line	$41 - j16$
Sululta_Gefersa 230kV line I	$105 + j24$
Sululta_Gefersa 230kV line II	$104 + j24$

The synchronous speed prior to the fault was 1.0 pu and the rotor angles, reactive power supplied and the terminal voltages of HPP generators were within limits. The rotor angles (in radians) and the reactive power (MVar) supplied by each HPP generators are indicated in Table 4-16 and Table 4-17 respectively.

The terminal voltage of each HPP generator was synchronised to 1.0 pu. The turbine power input to and electrical power output of Fincha, Beles and GG I HPP generators were reached above 90 % of their corresponding rated values and a disturbance under this condition would not be tolerated. The turbine power and electrical power output of HPP generators are indicated in Table 4-18.

Table 4-16 Rotor angles of HPP generatotrs at steady state

HPP generators	δ_{i0} (radians)
Fincha HPP-G1	-0.377 rad
Beles HPP-G1	-0.837 rad
GG II – G1	-0.685 rad
Melkawakena Gr4	-1.106 rad
Koka	-0.968 rad
Tekeze	-0.603 rad
GG I	-0.713 rad

Table 4-17 Reactive power supplied by HPP generators at steady state

HPP Generators	Reactive power (MVar)
Awash III Gr2	7.466 MVar
Melkawakena Gr4	6.051 MVar
Koka Gr1	2.690 MVar
GG II Gr1	0.921 MVar
Fincha Gr1	-3.855 MVar
Tekeze Gr1	-10.75 MVar
Beles Gr1	-27.20 MVar

Table 4-18 Turbine power input to and electrical power output of HPP generators at steady state

HPP Generators	Turbine power (P_{mi0}) (pu)	Electrical Power (P_{ei0}) (pu)
GG I_Gr1	0.917	0.917
Beles –Gr2	0.921	0.921
Fincha_Gr1	0.905	0.905
GG II _Gr1	0.895	0.905
Melkawakena _Gr4	0.787	0.791
Tekeze _Gr1	0.520	0.523
Awash III_ Gr2	0.338	0.336
Beles_Gr1	0.257	0.268
Awash III _Gr1	0.215	0.222

The voltages at the critical buses were within the acceptable operating ranges and their corresponding frequency deviations were zero Hz.

Sequence of Events & Dynamic Simulations

The sequence of events leading to blackouts began just after 9:55 hrs. When T phase of Gefersa_Addis Alem 45kV line was cut and fallen on Gefersa switchyard due to overload. The overcurrent protection relay did not respond to this condition at the time. The time domain dynamic simulations over a period of 10 seconds after initiation of disturbance were performed to elaborate the sequence of events taken place on the EEP system and analysed the cause of collapse of the system.

The voltage on Gefersa_Kality I 132kV line was sagged below 0.85 pu by the end of 0.58 seconds and sustained this value as a result of the permanent earth fault on Gefersa_Addis Alem 45kV line in the switchyard of Gefersa substation, as it is shown in Appendix E, Figure E-7(b). Hence, Gefersa_kality I 132kV line was tripped and this situation put further stress on Sebeta I_Gefersa 132kV line. Fincha HPP was supplying power to the loads of Addis Ababa region by Ghedo_Gefersa 230kV lines through Gefersa_Kality I 132kV line and Gefersa_Sebeta I 132kV lines. Even the bulk hydro generation of Beles HPP was reached to load centres of the central & AA regions through these lines (it means that through Sululta_Gefersa 230kV lines). Therefore, the tripping of Gefersa_Kality I 132kV line resulted in

overloading and subsequent tripping of Gefersa_Sebeta I 230 kV line, Gefersa_Addis North 132kV line, Ghedo_Gefersa 230kV lines and Sululta_Gefersa 132kV lines. This is depicted in Appendix E, Figure E-12.

In addition, as the earth fault was permanent the voltages across 230/132kV transformers (TR1_TR4) of Gefersa substation were dipped to below 0.85 pu at the initiation of the disturbance and recovered to only 0.88 pu by the end of 0.712 seconds and tripped by the corresponding protective relays, as it is shown in Appendix E, Figure E-6. After all, the high load supplied by Gefersa substation was disconnected as all 230/132kV transformers were tripped. As a result, the voltages on Ghedo_Gefersa 230kV and Sululta_Gefersa 230kV lines reached over 1.1pu and tripped by overvoltage protections, as indicated in Appendix E, Figure E-12 (a). This sequence of events pulled the EEP system to split into isolated areas, and the HPPs on the Eastern, Southern and Southwestern regions were overloaded as the lines that interconnected the northern, north western and western HPPs, i.e., Tekeze, Fincha & Beles HPP were tripped. Addis Ababa & Central regions, Southern, South-western and Eastern regions were supplied mainly by GG I, GG II, Koka, Awash II & III, Melkewakena and Adama Wind I & II power plants. However, this condition could not be continued as the load was higher than the generated power. The frequencies and terminal voltages of these power plant generators were decaying as is depicted in Appendix E, Figure E-13 and Figure E-14.

On the other hand, the power generated by Fincha, Tekeze & Beles HPPs was higher and the load supplied by these plants was not much. As a result, the frequencies of these HPP generators were drastically increased. The voltages across transmission lines and transformers were beyond their limits, the cascade tripping continued for about 5 minutes, and finally the system has collapsed.

Results of the Analyses

The operation procedures proposed by NLDC (as was tried to mention in Section 3.1) states that any feeder outage that has supplied less than 10 MW could not result in system collapse and the system should remain stabilised and continue to operate within limits [57]. However, the earth fault on 45kV feeder of Gefersa substation had caused the total collapse of the entire EEP system.

Therefore, we can conclude that the major cause of the blackout was the incapability of the line protection to trip as the current flowing through the line exceeded its limit. If the overcurrent protection of the feeder were acting correctly, the 14th August 2015 blackout would not be happened as will be illustrated in Section 5.3. To sum up, the protection coordination settings of power system components has a vital role for blackout defence as well as prevention. The restoration times and other parameters of this blackout & many more are indicated in Appendix C.

Chapter 5

Identification of System Vulnerabilities and Mitigation Techniques

5.1. Introduction

As observed from the simulation result analysis and discusions in Section 4.6 and the blackout data analyses, the EEP system supported disturbances that initiated a cascading event that caused total or partial blackouts, even the SLG fault on its 45kV feeder was caused the total collapse of the system.

The degree of the vulnerability of a node or line is defined to be the decrease in the level of network performances after the node or line is removed intentionally from the network. The aim is to identify the most critical faults threatening the operation of the power system, and thus to take effective actions for preventions and adjustments. For this purpose, two indices, called performance indices (PI_s), that reflect the health of the system, are calculated. The indices allow assessing two different symptoms of system stress such as voltage instability and overloads. The combination of these indices yield a vulnerability index (VI). The vulnerability assessment and ranking can be used to coordinate and focus control actions that mitigate the consequences of the disturbances and reduce the risk of cascading events and system blackouts [59].

5.2. Identification of Vulnerable Areas

The identification of areas likely to cause major problems on the grid is done by means of contingency analysis. Contingency analysis is generally related to the analysis of abnormal system conditions [48]. This is a crucial problem, both in planning and in daily operation. A common criterion is to consider contingencies as a single outage of any system element (generator, transmission line, transformer or reactor) and evaluate the post-contingency state. This is known as the **N** - 1 security criterion.

In power systems operation, the network must remain within predefined margins during normal conditions as well as following a contingency. This work focuses on the Ethiopian electric power grid ability to operate inside these margins during outages of components. This ability to withstand disturbances is commonly referred to as "security" [26]. While there are multiple stages at which security can be analysed, namely, static, dynamic, and transient security analysis, this part of the work focuses on the static security. Static

security is defined as the ability of the system to return to a steady state within the specified limits of safety following a contingency [59]. One of the main tools used in static security analysis is the load flow, which is used to verify that electrical and thermal constraints are not being violated. The constraints of interest are the voltages at each bus and the power flowing through the lines, which are based on the stability limits of the system and the physical properties of the transmission lines respectively.

The process of vulnerability analysis involves studying the effect of the removal of a system component on the system, particularly the power flows and the bus voltages. This component can be a generator, transmission line, transformer, and so on. This work however focuses on outages on the transmission network. The reason is that most of the previous partial and total blackouts, as can be seen in Chapter 3 & 4, were happening because of the faults on the transmission lines. As can be seen from Appendix F, the Ethiopian Electric Power grid, which is the main area of interest, is heavily dependent on transmission lines from all regional power systems. What follows is a quantitative evaluation of which contingencies (line outages) lead to the most issues with regard to voltage limit and line loading violations.

As was noted in Appendix A, the network model used consists of 142 lines. An exhaustive analysis would require that an outage on each line and its effects are simulated using the load flow. One of the most popular load flow methods which is also used here, is the Newton-Raphson method.

It is true that the most severe contingencies vary by time of day as the load changes [38]. To overcome the need to study the worst line outages at different times of the day, the system was analysed at peak hours that is, the hours at the maximum consumption of electricity recorded by the system. In Ethiopia, this occurs at around 18:00 to 21:00 hrs [60]. At peak load, the system experiences the most stress because the lines are heavily loaded, and the generators are running at high capacity such that the loss of any component could spell serious trouble for the system. Consequently, studying the system at peak load accounts for the worst-case scenario, which is the practice in power system planning studies.

The method used to rank vulnerabilities is taken from [38, 61, 62]. This method computes *system performance indices (PI*) which indicate the severity of an outage based on the number of out of limit voltages and line flows that result from it. Two different indices are specified, one related to voltage violations and the other to line loading violations.

5.2.1. Performance Indices

The system performance index is a measure that can be used to evaluate the relative severity of a contingency [63]. System performance indices are not unique and take on different forms depending on the parameters that are of most importance to the engineer. The most common form of system performance

indices gives a measure of the deviation from rated values of system variables such as line flows, bus voltages, bus power injections, etc. The index to quantify problems related to loading and voltage limit violations are described in equations (5.1) and (5.2).

i) **Active Power performance index (PI_P):** This index is used to measure the degree of line over loads and is given by [37].

$$PI_P = \sum_{l=1}^{N_l} \left(\frac{W}{2n}\right)\left(\frac{P_l}{P_l^{max}}\right)^{2n} \tag{5.1}$$

Where

P_l is the MW flow of line l

P_l^{max} - is the MW capacity limit of line l

N_l - The number of overloaded lines in the system

W – Real power weighting factor (in general, W = 1)

n- a positive number (n = 1, 2, 3… etc...). If n is a alrge number, the PI_P will be a small number if flows are within limits and it will be large if one or more lines are overloaded

The summation is carriedout on overloaded lines only to avoid the masking problem reported in [37, 38, 62, 63].

ii) **Voltage performance index (PI_v):** The voltage level performance index chosen to quantify system deficiency due to out-of-limit bus voltages is defined by [37]:

$$PI_v = \sum_{i=1}^{N_B} ({}^{w}/_{2n}) \left\{\frac{\left(|V_i| - |V_i^{sp}|\right)}{V_i^{sp}}\right\}^{2n} \tag{5.2}$$

Where

V_i is the voltage magnitude corresponding to bus i

V_i^{sp} Specified voltage magnitude corresponding to bus i

n- a positive number and usually its value is 1 (n = 1, 2, 3… etc...).

N_B - Number of buses in the system whose voltage magnitude either below a specified minimum or above a specified maximum

w - Real non-negative weighting factor (in general $w = 1$)

Thus, this index measures the severity of the out-of-limit bus voltages and provides a direct means of comparing the relative severity of the different line outages on the system voltage profile [38].

Ranking is performed for all branch outages against their rated power carrying capacity (i.e., a loading of 100%), and considering voltage violations outside the range 0.9 pu to 1.1 pu which is the provided emergency voltage in the Ethiopian Electric Power system [57]. The most severe line outages and the performance indices for the two criteria are shown in descending order in Figure 5-1 and 5-2. Figure 5-1shows the ranking of line outages in terms of the performance index calculated based on the branches overload. It can be seen that the most dangerous line outage is the disconnection of the line D/Markos_Sululta 400kV line that leads to overloading of B/Dar II 400/230kV transformers (TR1 & TR2) and finally lead to the disconnection of Beles HPP, which is the main actor of EEP grid for system synchronisation.

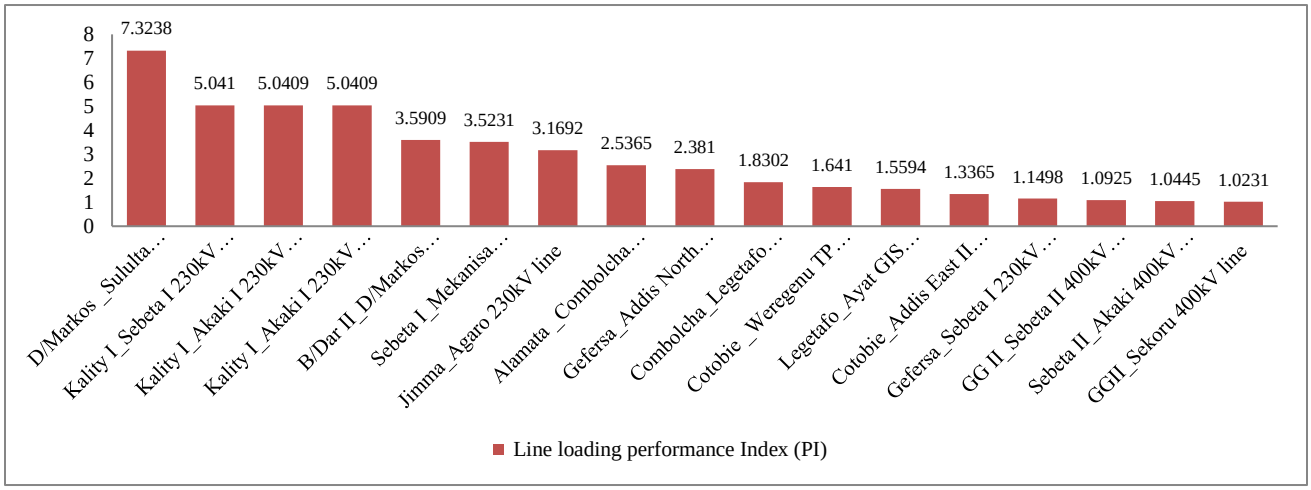

Figure 5-1 Line outages ranked in terms of performance index calculated for power flows

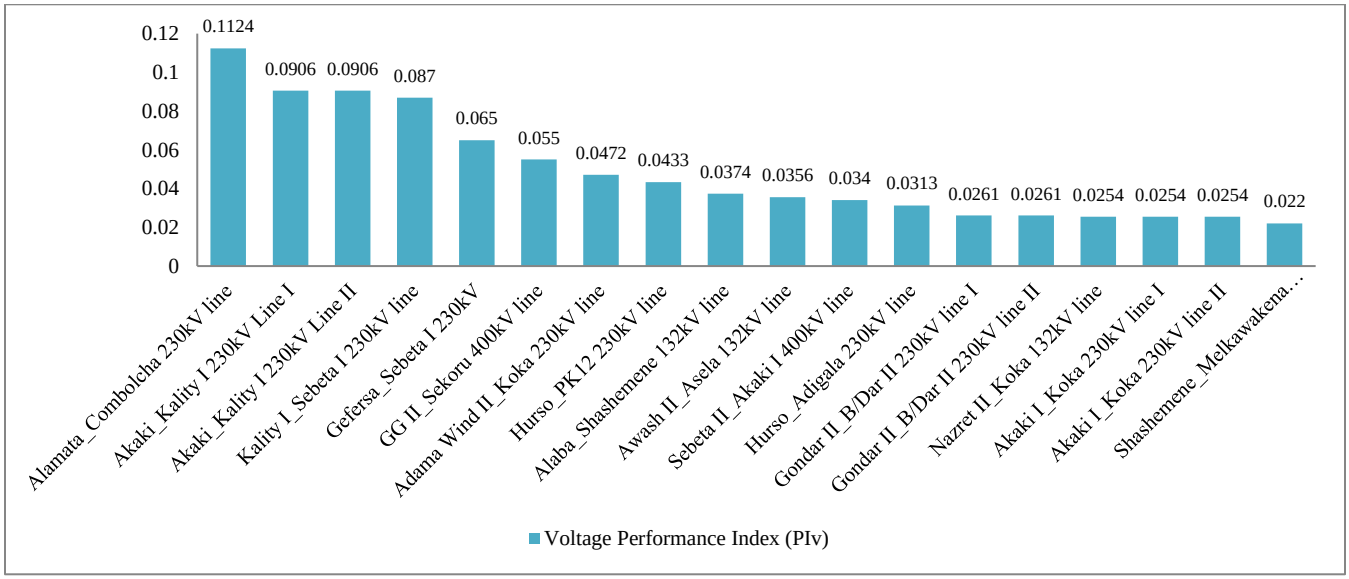

Figure 5-2 Line outages ranked in terms of performance index calculated for bus voltages

On the other hand, Figure 5-2 shows the line outages ranking based on the performance index calculated in terms of the bus voltage. It is easy to observe that the most dangerous line outages from the voltage point of view are the disconnections of lines, viz., Alamata_Combolcha 230kV, Akaki I_ Kality I 230kV line I & II and Sebeta I_Kality I 230kV lines.

5.2.2. Analyses Results for the most Severe Contingencies (Line Outages)

Now we use the above-proposed algorithm to analyse a snapshot of the Ethiopian Electric Power grid at 19:00 on July 17, 2016. At this snapshot, the system contains 63 synchronous generators, 104 load buses, 134 substations, 99 two-winding transformers, 26 three-winding transformers, 3 shunt capacitor banks, 45 shunt reactors and 142 transmission lines as it is indicated in Appendix F. The detailed system data can be found at Appendix A-D. For this case, the grid was loaded to 1539.74 MW from which 100 MW was exported to Sudan and 50 MW was exported to Djibouti. The full AC power flow is run to get the steady state results, such as bus voltages and line flows. Next, contingency analysis is done by considering a load-scaling factor of 1.33 by using DIgSILENT PowerFactory Software package as this factor is used by the planning and operation department of NLDC for daily peak load forecasting and generation dispatch scheduling.

It is found that there are 28 severe line outages whose active power flow performance indices are greater than 1.0 pu and voltage level performance indices are greater than 0.02 pu. Table 5-1 and Table 5-2 shows the results of the power flows in the overloaded elements and out of limit bus voltages of the network in case of the most severe line outages.

The ends of the transmission lines associated with the most severe line outages are labelled in Figure 5-4. It is evident that most of these line outages are predominantly along the highest voltage transmission lines (400kV & 230kV) connecting the regional power systems of the country to the capital, Addis Ababa. Almost all of the contingencies affect the high load centre, i.e., Addis Ababa region, as can be seen in Table 5-1 & 5-2. This knowledge implies that, as far as the transmission network is concerned, the main weakness is on the lines feeding Addis Ababa region from the rest of the regional power systems.

Simulation of these contingencies begins with ascertaining a steady state solution of the system. From the steady state simulation (considering the load scaling factor), some components were overloaded as was indicated in Figure 5-3. These components' capacity should be upgraded during rehabilitation projects in

the future[8]. No voltage violations exist in the base case simulation. In addition, all generators are operating at, or close to their specified voltage.

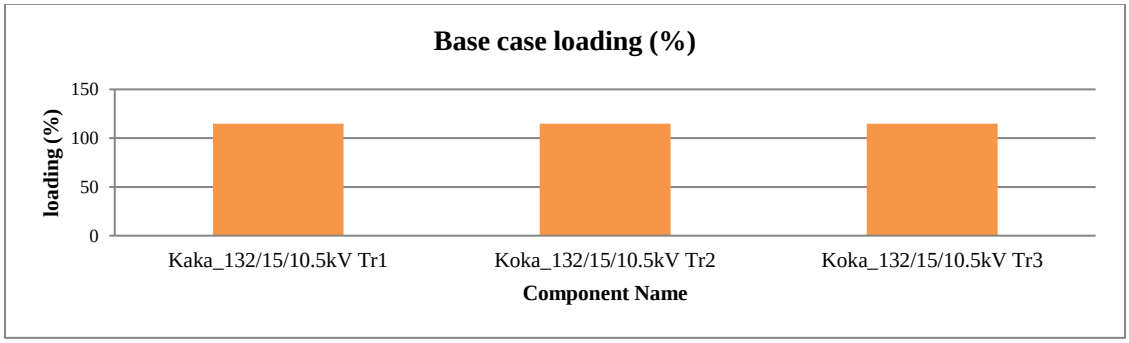

Figure 5-3 Overloading components during the base case simulation

Table 5-1 Loading violations per case

Contingency Name	Overloaded Component(s)	Loading (%)		
		Continuous loading	Short time loading	Base case
D/Markos_Sululta 400kV line	Combolcha_Tr (230/132kV)	204.1	204.1	98.6
	Alamata_Combolcha 230kV line	149.7	149.7	39.8
	Legetafo_Ayat GIS 132kV line	137.6	137.6	92.9
	Cotobie_Ayat GIS 132kV line	137.0	137.0	92.3
	Ghedo_Tr (230/132/15kV)	110.9	110.9	98.2
	Combolcha_Legetafo 230kV line	107.7	107.7	17.2
	BDR_TR1 (400/230kV)	102.0	102.0	35.2
	BDR_TR2 (400/230kV)	102.0	102.0	35.2
Kality I_Sebeta I 230kV line	Sebeta I_Mekanisa 132kV line	164.2	164.2	81.4
	Cotobie_Weregenu TP 132kV line	141.9	141.9	90.7
	Gefersa_Addis North 132kV line	120.3	120.3	85.3
	Kality I_Akaki I 132kV L1, L2	119.9	119.9	96.1
	Combolcha _Tr (230/132kV)	113.4	113.4	98.6
	Gefersa_Kality I 132kV line	109.6	109.6	25.5
Kality I_Akaki I 230kV L1, L2	Sebeta I_Mekanisa 132kV line	164.2	164.2	81.4
	Cotobie _Weregenu TP 132kV line	141.9	141.9	90.7
	Gefersa_Addis North 132kV line	120.3	120.3	85.3
	Kality I_Akaki I 132kV L1, L2	119.9	119.9	96.1
	Combolcha_Tr (230/132kV)	113.4	113.4	98.6
	Gefersa_Kality I 132kV line	109.6	109.6	25.6
BDR II_D/Markos 400kV line	D/Markos 400/230kV Tr	135.7	135.7	43.6
	Combolcha_Tr (230/132kV)	109.3	109.3	98.6
	Legetafo_Ayat GIS 132kV line	103.0	103.0	92.9
	Cotobie_Ayat GIS 132kV line	102.4	102.4	92.3
	BDR_TR1 & TR2 (400/230kV)	100.9	100.9	35.2
Sebeta I_Mekanisa 132kV line	Mekanisa_Kality I 132kV line	122.4	122.4	35.8
	Kality I_Akaki I 132kV L1, L2	110.9	110.9	96.1

[8] Koka 132/15/10.5kV transformers (Tr1, Tr2, and Tr3) are the most vulnerable equipments as it was indicated in the blackout analyses of January 6th 2016 and 14th August 2015. The capacities of these transformers did not match with that of their corresponding generator capacities. The transformers got overloaded prior to the generators did.

	Cotobie_Weregenu TP 132kV line	103.9	103.9	90.7
	Gefersa_Addis North 132kV line	102.7	102.7	85.3
	Combolcha_Tr (230/132kV)	101.4	101.4	98.6
Jimma_Agaro 230kV line	Ghedo_Tr (230/132/15kV)	213.7	213.7	98.2
	Sekoru_230/132kV Transformer	133.1	133.1	72.6
Alamata_Combolcha 230kV line	Sululta_400/230kV Tr1& Tr2	117.6	117.6	80.7
	Kality I_Akaki I 132kV L1, L2	107.4	107.4	96.1
Gefersa_Addis North 132kV line	Cotobie_Addis East II 132kV line	124.4	124.4	36.0
	Kality I_Akaki I 132kV L1, L2	105.0	105.0	96.1
	Combolcha_Tr (230/132kV)	104.1	104.1	98.6
	Sebeta I_Mekanisa 132kV line	101.4	101.4	81.4
Combolcha_Legetafo 230kV line	Combolcha_Tr (230/132kV)	128.7	128.7	98.6
	Akaki I_Kality I 132kV L1	100.1	100.1	96.1
	Akaki I_Kality I 132kV L2	100.1	100.1	96.1
Cotobie_Weregenu TP 132kV line	Weregenu TP_Kality 132kV line	147.2	147.2	52.6
	Kality I_Akaki I 132kV L1, L2	105.6	105.6	96.1
Legetafo_Ayat GIS 132kV line	Gefersa_Addis North 132kV line	130.4	130.4	85.3
	Kality I_Akaki I 132kV L1, L2	119.1	119.1	96.1
Cotobie_Addis East II 132kV line	Gefersa_Addis North 132kV line	129.9	129.9	85.3
	Cotobie_Weregenu TP 132kV line	104.3	104.3	90.7
Gefersa_Sebeta I 230kV line	Kality I_Akaki I 132kV L1, L2	109.7	109.7	96.1
	Combolcha_Tr (230/132kV)	104.7	104.7	98.6
GG II _Sebeta II 400kV line	Sekoru_230/132kV Tr1	106.6	106.6	72.6
	Combolcha_Tr (230/132kV)	102.4	102.4	98.6
Sebeta II_Akaki I 400kV line	Combolcha_Tr (230/132kV)	102.7	102.7	98.6
	Kality I_Akaki I 132kV L1, L2	101.7	101.7	96.1
GG II_ Sekoru 400kV line	Metu_230/66/15kV Tr	101.5	101.5	95.5
	Combolcha_Tr (230/132kV)	100.8	100.8	98.6

The resultant state of the system is successfully computed, and the result shows several violations as shown in Table 5-1 and Table 5-2 above. With these violations, it is unlikely that the system would be able to operate. Voltages outside their limits could lead to widespread instability, failures, and damage of equipment while overloads could permanently damage equipment also leading to instability [37]. Normally, procedures need to be in place to prevent the system from reaching such an operating point and may require that parts of the system get shut down in a coordinated way to save the system from damage, at the cost of cutting off supply to some customers. These types of blackouts are too common in the Ethiopian electricity sector and have been widely reported by NLDC [6, 60], even though scientific publications on this issue are not available.

Table 5-2 Voltage limit violations of buses for a load scaling factor of 1.33

Contingency Name	**Bus name(s)**	**Voltage (p.u)**		
		Actual	Step	Base case
Alamata_Combolcha 230kV line	Akaki I 132kV	0.90	0.02	0.92
	Sululta 230kV	0.89	0.04	0.93
	Kality I 230kV	0.89	0.04	0.93
	Legetafo 230kV	0.88	0.04	0.92
	Sululta 400kV	0.88	0.05	0.93
	Gefersa 132kV	0.87	0.04	0.91
	Kality I 132kV	0.87	0.03	0.90
	Shehedi 230kV	0.87	0.03	0.90
	Sululta 132kV	0.87	0.04	0.91
	Combolcha 230kV	0.82	0.12	0.94
	Combolcha 132kV	0.81	0.12	0.93
	D/Berhan 132kV	0.84	0.07	0.91
Akaki I_kality I 230kV L_1, L_2	Kality I 230kV	0.89	0.04	0.93
	Legetafo 230kV	0.89	0.03	0.92
	Shashemene 132kV	0.89	0.03	0.92
	Debrezeit TP 132kV	0.88	0.04	0.92
	Debrezeit II132kV	0.88	0.04	0.92
	Akaki I 132kV	0.88	0.04	0.92
	Shoarobit 132kV	0.88	0.03	0.91
	Sululta 132kV	0.87	0.04	0.91
	Awasa 132kV	0.87	0.03	0.90
	Gefersa 132kV	0.87	0.04	0.91
	D/Berhan 132kV	0.87	0.04	0.91
	Kality I 132kV	0.86	0.04	0.90
Kality I_Sebeta I 230kV line	Kality I 230kV	0.89	0.04	0.93
	Legetafo 230kV	0.89	0.04	0.93
	Shashemene 132kV	0.89	0.03	0.92
	Debrezeit TP 132kV	0.89	0.03	0.92
	Debrezeit II 132kV	0.89	0.03	0.92
	Akaki I 132kV	0.88	0.04	0.92
	Shoarobit 132kV	0.88	0.03	0.91
	Sululta 132kV	0.88	0.03	0.91
	Awasa 132kV	0.87	0.03	0.90
	Gefersa 132kV	0.87	0.04	0.91
	D/Berhan 132kV	0.87	0.04	0.91
	Kality I 132kV	0.86	0.04	0.90
Gefersa_Sebeta I 230kV line	Sululta 400kV	0.89	0.04	0.93
	Gefersa 230kV	0.89	0.05	0.94
	Kality I 132kV	0.88	0.02	0.90
	Shoarobit 132kV	0.88	0.03	0.91
	Sululta 230kV	0.88	0.05	0.93
	Kality I 230kV	0.88	0.05	0.93
	Legetafo 230kV	0.88	0.05	0.93
	Gefersa 132kV	0.88	0.03	0.91
	Sululta 132kV	0.86	0.05	0.91
	D/Berhan 132kV	0.88	0.03	0.91
GG II _ Sekoru 400kV line	Gambela 230kV	0.89	0.06	0.95
	Nekemte 132kV	0.90	0.04	0.94
	Sululta 132kV	0.89	0.02	0.91

	Ghimbi 132kV	0.89	0.04	0.93
	Gefersa 132kV	0.89	0.02	0.91
	Metu 66kV	0.89	0.06	0.95
	Gambela 66kV	0.85	0.05	0.93
Adama Wind II_Koka 230kV line	Akaki I 132kV	0.90	0.02	0.92
	Shoarobit 132kV	0.89	0.02	0.91
	Sululta 132kV	0.89	0.02	0.91
	D/Berhan 132kV	0.88	0.03	0.91
	Gefersa 132kV	0.88	0.03	0.91
	Kality I 132kV	0.88	0.02	0.90
	Harar III 132kV	0.87	0.05	0.92
Hurso_PK12 230kV line	Adigala 230kV	0.89	0.11	1.0
	Harar III 132kv	0.86	0.06	0.92
	Harar III 66kV	0.85	0.05	0.90
	PK12	0.82	0.16	0.98
Alaba_Shashemene 132kV line	Adamitulu 132kV	0.87	0.05	0.92
	Shashemene 132kV	0.84	0.08	0.92
	Awasa 132kV	0.82	0.08	0.90
Awash II _Asela 132kV line	Shashemene 132kV	0.89	0.03	0.92
	Awasa 132kV	0.87	0.03	0.90
	Adamitulu 132kV	0.86	0.06	0.92
	Assela 132kV	0.85	0.08	0.93
Sebeta II_Akaki I 400kV line	Shoarobit 132kV	0.89	0.02	0.91
	D/Berhan 132kV	0.89	0.02	0.91
	Sululta 132kV	0.88	0.03	0.91
	Gefersa 132kV	0.88	0.03	0.91
	Kality I 1323kV	0.88	0.02	0.90
Hurso_Adigala 230kV line	Harar III 132kV	0.88	0.04	0.92
	PK12	0.85	0.13	0.98
	Adigala 230kV	0.84	0.06	1.0
Gondar II_BDR II 230kV L_1, L_2	Gondar II 230kV	0.89	0.06	0.95
	Gondar II 66kV	0.88	0.06	0.94
	Shehedi 230kV	0.84	0.06	0.90
Nazret II _Koka HPP 132kV line	Koka HPP 132kV	0.89	0.06	0.95
	Debrezeit TP 132kV	0.89	0.04	0.93
	Debrezeit II 132kV	0.89	0.04	0.93
	Kality I 132kV	0.88	0.03	0.91
Akaki I_Koka 230kV L_1, L_2	Kality I 132kV	0.88	0.02	0.90
	Sululta 132kV	0.89	0.02	0.91
	D/Berhan 132kV	0.89	0.02	0.91
	Gefersa 132kV	0.89	0.02	0.91
Shashemene _Melkawakena Yougo 132kV line	Adamitulu 132kV	0.90	0.02	0.92
	Shashemene 132kV	0.88	0.04	0.92
	Awasa 132kV	0.86	0.04	0.90

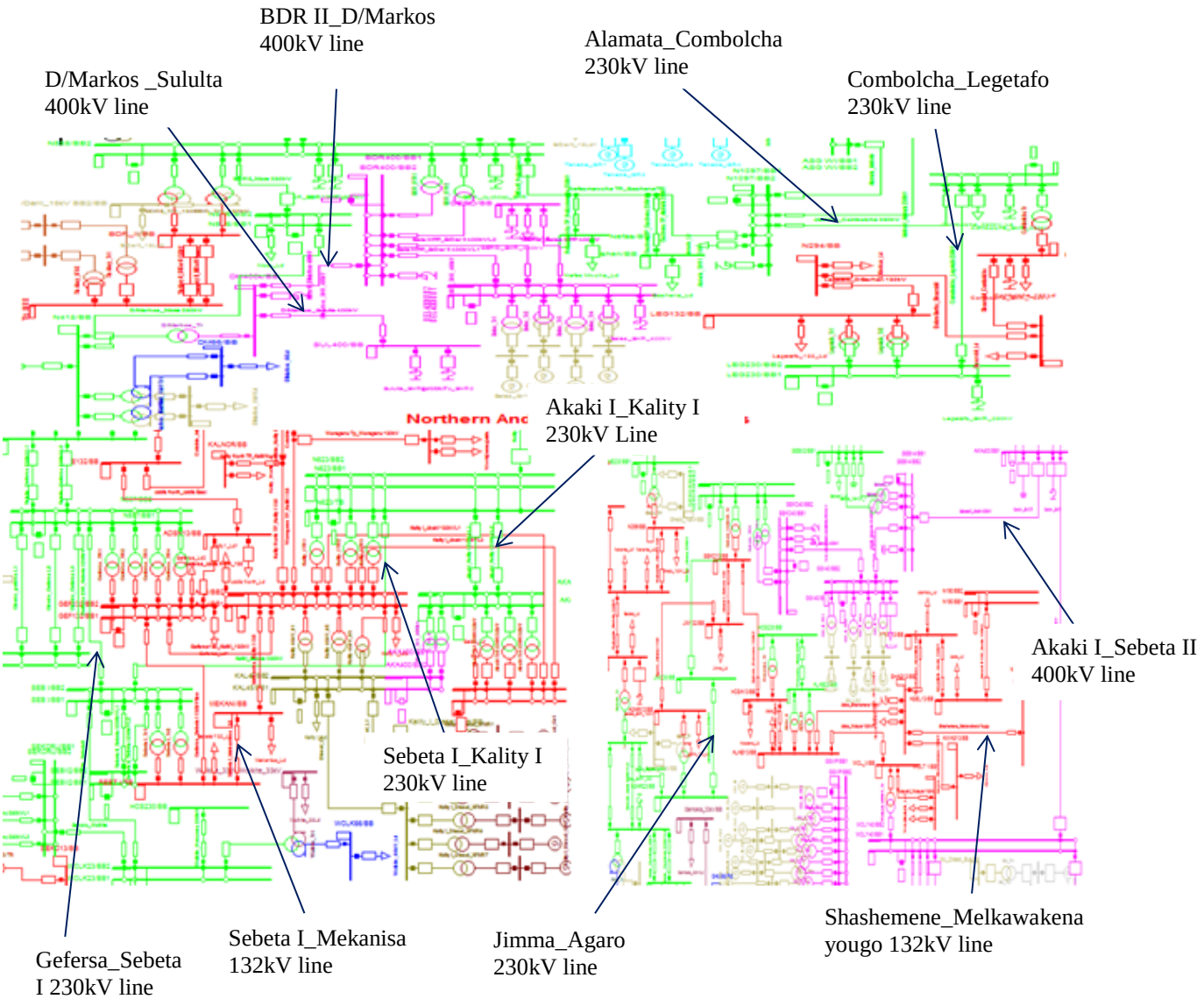

Figure 5-4 Portion of the EEP grid showing points of interest

5.2.3. Determination of Vulnerable Lines and Buses

Generally, results of contingency analysis gives an idea about vulnerable buses whose voltages must be maintained within limits by transmission and substation rehabilitation and upgrading (TSRUP) projects. For instance, by installing static shunt compensators at high load buses, by implementing intelligent under voltage load shedding (UVLS) protection schemes or adding parallel lines and increasing the capacities of the vulnerable lines to withstand contingencies, and to ensure secure operation during contingencies. Network vulnerabilities with respect to buses are those buses that have out of limit bus voltages in case of different line outages. Accordingly, the network most vulnerable buses are Sululta & Gefersa 132kV buses and 11 different outage cases led them to have out of limit bus voltages. The highest percentage voltage

deviations for these buses are $-14\ \%, and\ -13\ \%$, respectively. The second most vulnerable buses are Kality I 132kV and D/Berhan 132kV buses where 9 different outage cases led them to have out of limit bus voltages. Figure 5-5 shows the network's most vulnerable buses ranked based on the number of outages that caused voltage limit violations starting from the most vulnerable buses.

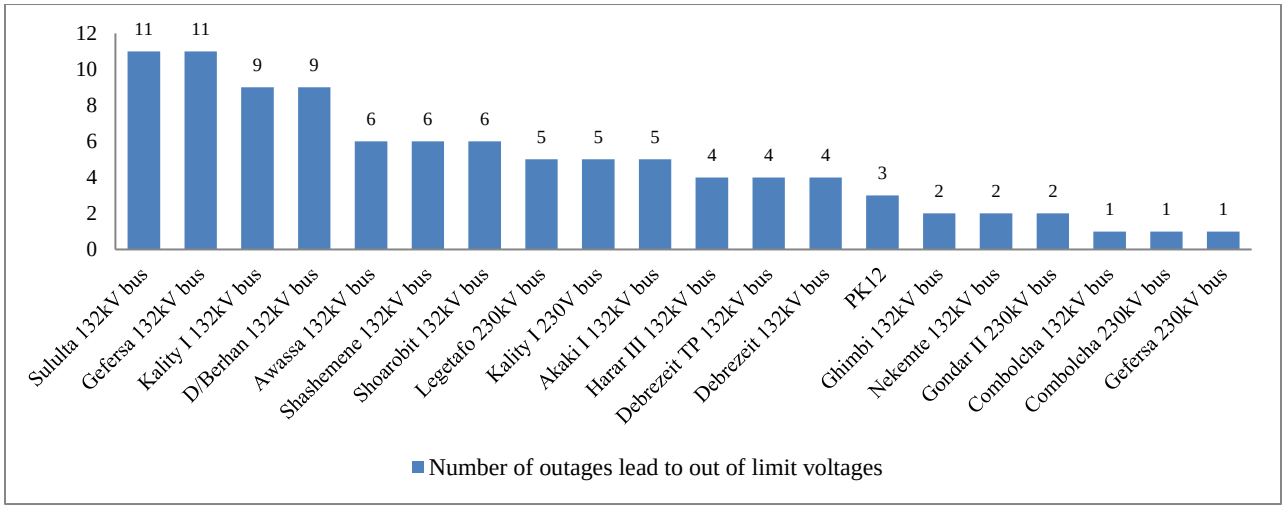

Figure 5-5 Vulnerabilities ranked based on number of outages that lead to voltage limit violations of buses

Similarly, results of contingency analysis can also give us an idea about the vulnerable equipments (lines, transformers or generators) whose capacity must be increased by transmission and substation rehabilitation and upgrading (TSRUP) projects to withstand contingencies, and to ensure secure operation during contingencies. Network vulnerabilities with respect to equipments overloading are the lines/generators or transformers which always become overloaded in case of different outages. Based on the probability of outage occurrence, the network most vulnerable element is the transformer at Combolcha II 230/132kV substation, 12 different outage cases lead this transformer to overload. It is found that the highest percentage loading for this equipment is (204.1%). Table 5-3 shows the network vulnerabilities ranked based on number of outages lead to lines overload starting with the most vulnerable element besides each element highest percentage loading. The second most vulnerable element which is the transmission lines connecting Kality I 132kV and Akaki I 132kV buses, where 12 different outage cases lead to these lines overload with highest percentage loading equal to (119.9 %). Gefersa_Addis North 132kV, Cotobie_Weregenu TP 132kV, and Sebeta I_Mekanisa 132kV lines are the next most vulnerable elements, where 6,5, and 4 different outage cases lead them to overload respectively.

Table 5-3 Vulnerabilities ranked based on number of outages lead to overloads

Overloaded elements	Number of outages lead to overload	Highest percentage loading
Combolcha _Tr (230/132kV)	12	204.1
Kality I_Akaki I 132kV line I	12	119.9
Kality I_Akaki I 132kV line II	12	119.9
Gefersa_Addis North 132kV line	6	129.9
Cotobie_Weregenu TP 132kV line	5	141.9
Sebeta I_Mekanisa 132kV line	4	164.2
Gefersa_Kality I 132kV line	3	109.6
Ghedo_230/132/15kV Tr	2	213.7
Legetafo_Ayat GIS 132kV line	2	137.6
Cotobie_Ayat GIS 132kV line	2	137
Sekoru_230/132kV Tr	2	133.1
Alamata_Combolcha 230kV line	1	149.7
D/Markos 400/230kV Tr	1	135.7
Cotobie_Addis East II 132kV line	1	124.4
Sululta 400/230kV Tr1	1	117.6
Sululta 400/230kV Tr2	1	117.6
Combolcha_Legetafo 230kV line	1	107.7
BDR_TR1 (400/230kV)	1	102
BDR_TR2 (400/230kV)	1	102
Metu_230/66/15kV Tr	1	101.5

Whereas based on the worst transmission capacity selected during the network design, the vulnerabilities can be considered in the manner of the largest value of percentage loading. According to that, the network most vulnerable element is the Ghedo_230/132/15kV transformer. Figure 5-6 shows the network vulnerabilities ranked based on the largest percentage loading starting with the most vulnerable element.

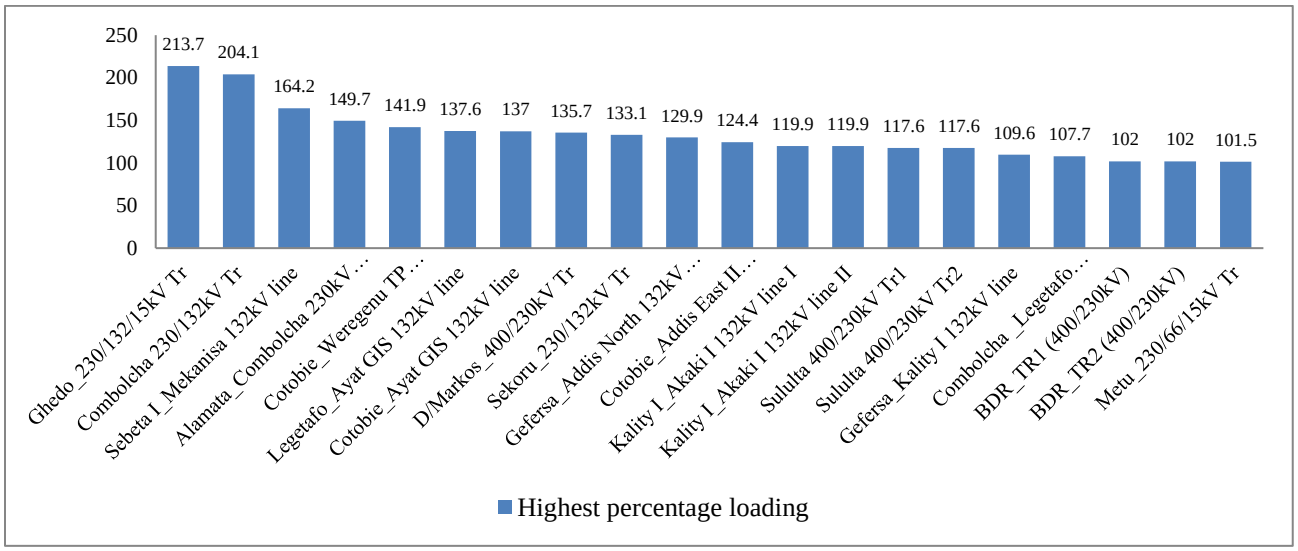

Figure 5-6 Vulnerabilities ranked based on the highest percentage loading

To sum up, most of the network vulnerabilities with respect to bus voltage violations are occurred on those buses found at high load centres, i.e., Addis Ababa region. In addition, the network most vulnerable elements with respect to equipment overloading are those elements either found at Addis Ababa or those elements interconnecting the regional power systems to each other or they are paths to supply the high load centres.

5.3. Proposed Mitigation Techniques

As can be seen from the simulation studies in Chapter 4 and from the analysis of blackouts in Chapter 3, the cause of the disturbance that resulted for the outage of power system equipments were linked to the following specific system weaknesses:

- Poor protection system coordinations
- Breaker not fast enough to clear the fault
- Poor planned outages
- Not adhering to the security standards while planning and operating the power system (e.g., not using SCADA/EMS at major substations like Sebeta I & Gefersa s/s. SCADA system is crucial for the quick access of network configuration during day to day operation and under emergency condition; Beles HPP generators were operating beyond their frequency range).
- Violation of the N-1 criterion and the security rules outlined in the operating policy guidelines of EAPP (for instance, not having additional paths for the tie lines and for lines that interconnect the major HPP generation to the national grid)

Therefore, this section focuses on techniques that can be used to coordinate and focus control actions that mitigate the consequences of the disturbances and reduce the EEP system's vulnerability to cascading events and system blackouts.

5.3.1. Fine Protection System Coordination

As was observed in Section 4.6, the August 14th 2015 blackout would be preventable if the protection system coordination for the equipments, primarily for lines and transformers, of the fault area were set systematically with detailed power system planning studies. Additional blackouts whose initiating events were associated with the poor protection coordination & settings are indicated in Appendix C and Section 3.5, Table 3-20. Fine protection system coordination is the proper selection of protective devices for correct sequential operation.

The overcurrent protection of Gefersa_Addis Alem 45kV feeder did not responding to the overloads which was arising on it. The feeder was loaded to 114%. This overload led T- phase of the conductor to be broken

and fallen on the ground in the switchyard of Gefersa substation and a SLG fault had happened. The protection system for Gefersa 132/45/15 kV transformer did not also respond to the SLG fault on its 45kV side. These conditions were the triggering events for the overloading of Gefersa_Kality I 132kV line. The voltage across the line was sagged to 0.85 pu at around 0.58 seconds as was discussed in Section 4.2.4. As a aresult, Gefersa_Kality I 132kV line was tripped by undervoltage protection. This event on the other hand aggravated the system collapse and cascaded tripping of lines, transformers and generators as was discussed in Section 4.6.4. Since the disturbance was happened on the 45kV feeder, the relays that control the breakers of this feeder had to be coordinated so that selective system protection could be achieved.

Here, a fault clearing time of 400ms is used for the SLG fault on Gefersa_Addis Alem 45 kV feeder to better visualize the the importance of proper protection system coordination. By doing so, we made the protective relay installed for the feeder to respond prior to the protective relays of Gefersa_Kality I 132kV line did. For this case, the voltage across Gefersa_Kality I 132kV line was 0.941 pu and the current through this line was reached to only 0.65 pu during the fault and then recovered to 0.23 pu after the fault has been cleared. In addition, the current on Gefersa_Sebeta I 132kV line was shot only to 0.8 pu during the fault and then returned to 0.23 pu after the fault has been cleared. The voltages across and the currents through the incoming and outgoing lines of Gefersa substation were within limits as depicted in Figure 5-7 (a) & (b).

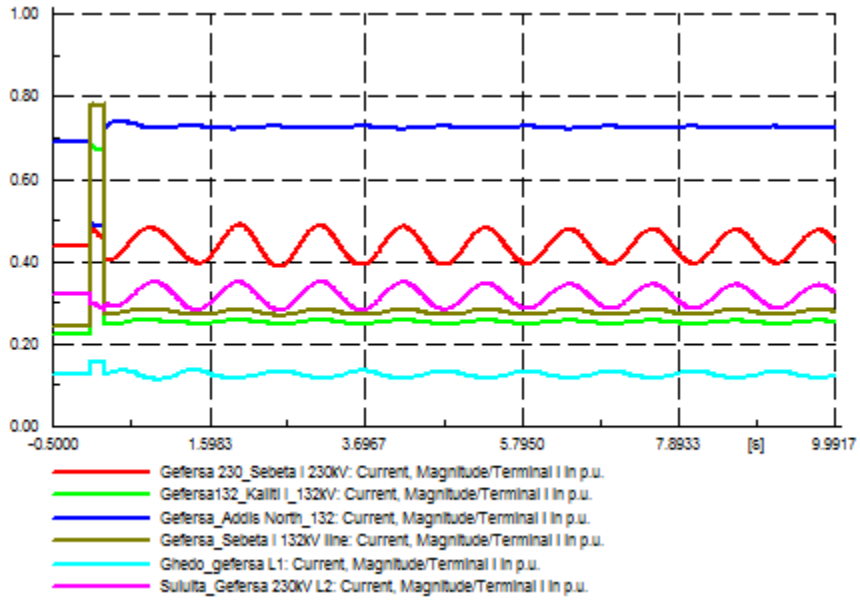

(a) Currents in pu

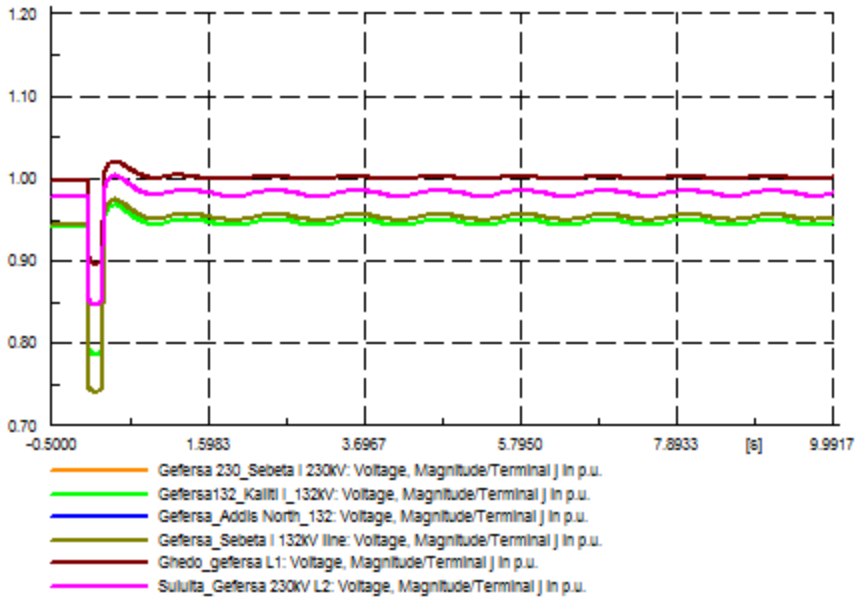

(b) Voltages in pu

Figure 5-7 The currents flowing through and voltage across the transmission lines after the fault was cleared within 400ms

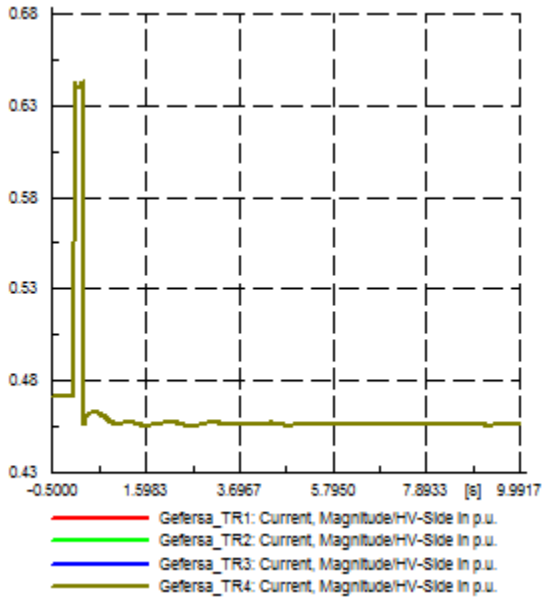

(a) Currents in pu

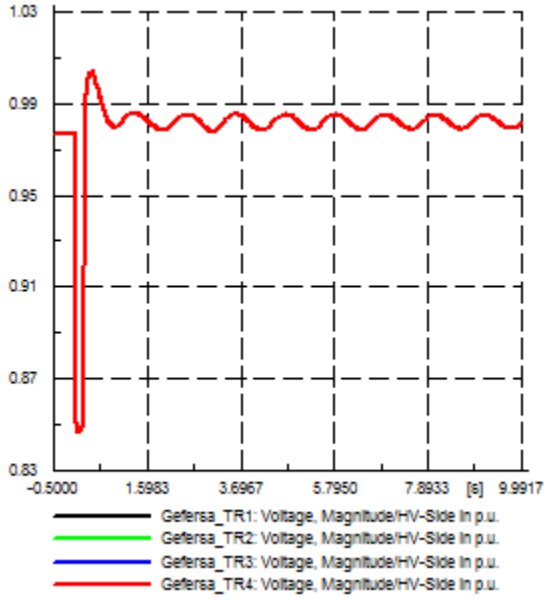

(b) Voltages in pu

Figure 5-8 The currents through and voltages across the transformers after the fault was cleared within 400ms

The currents through and the voltages across Gefrsa 230/132kV transformers (TR1, TR2, TR3, & TR4) were also within limits for the SLG fault on Gefersa_Addis Alem 45kV feeder with a fault clearing time of 400ms. This situation is depicted in Figure 5-8 (a) & (b).

Therefore, proper coordination of the protective devices can help us to selectively isolate the faulted line and avoids the cascading events that will arise on the system. The balckouts of August 8th 2014, June 17th 2014, September 3rd 2014 and November 28th 2015 were happened as a result of poor protection system coordination as was indicated in Appendix C.

5.3.2. High-Speed Fault Clearing

The amount of kinetic energy gained by the generators during a fault is directly proportional to the fault duration. The quicker the fault is cleared the less the disturbance it causes [9]. Circuit breakers do not have their own tripping intelligence and must be used in conjunction with relays. It is the relays that provide the intelligence and control logic for tripping the circuit breakers. Two-cycle breakers, together with high-speed relays and communication, are now widely used in locations where rapid fault clearing is important [11, 64].

As was observed from the discussions in Section 4.6.1, the blackout of January 6th 2016 was happened due to the slow fault clearing time settings of the protective relays of the faulted line. The fault that was happened on GG II_Sekoru 400kV line was a three phase to ground fault. For the three phase to ground fault the maximum fault clearing time should not exceed 8 cycles (160ms). With these informations, the system is simulated with a fault clearing time of 150 ms. The simulation results depicted that the speed of GG I and GG II HPP generators were increased to only 1.012 pu during the fault and returned to 1.001 pu with damped oscillations after the fault has been cleared as indicated in Figure 5-9 (a). the same is true for Awash III and GG III HPP generators.

The reactive power generated from and the electrical power output of the HPP generators were within limits after the fault has been cleared as was indicated in Figure 5-9 (b) & (d). There was no reverse power flow to any of the HPP generators as shown in Figure 5-9 (b). The terminal voltages of all HPP generators were returned to 1.0 pu after the fault has been cleared as indicated in Figure 5-9 (c).

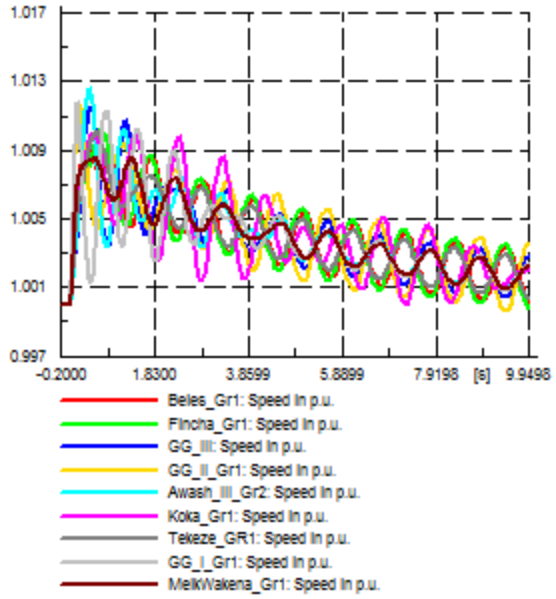

(a) Speed in pu

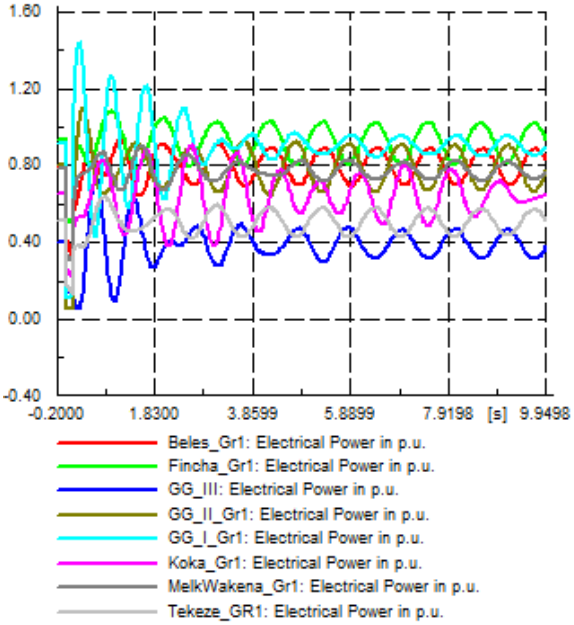

(b) Electrical power in pu

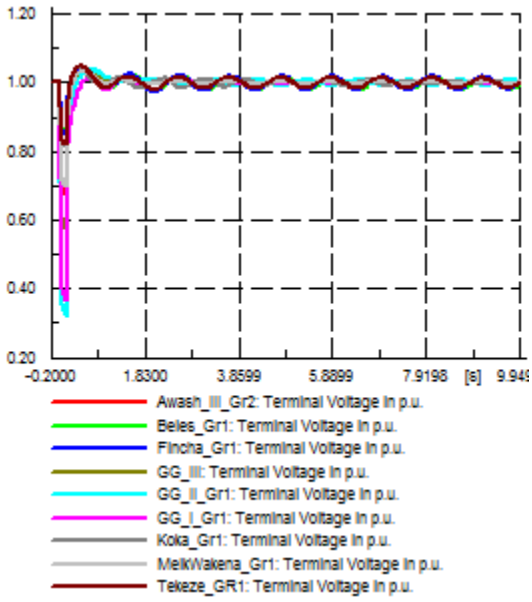

(c) Terminal voltage in pu

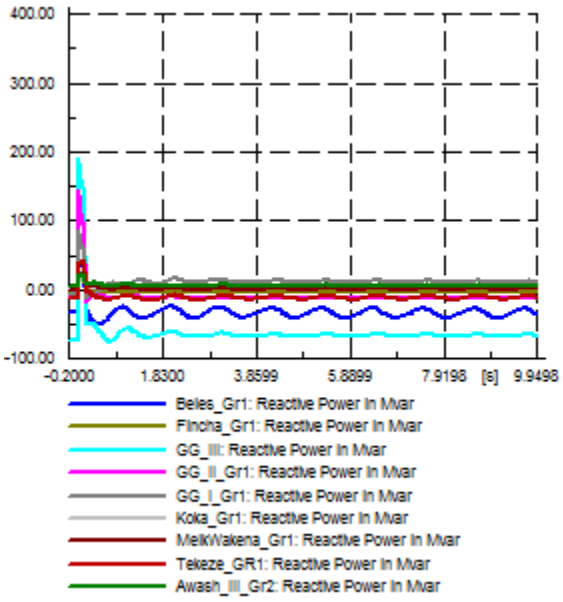

(d) Reactive power supplied in MVAr

Figure 5-9 Profiles of HPP Generators for a fault clearing time of 150 ms

The voltages at critical buses were also returned to above 0.97 pu after the fault has been cleared. The frequency deviations were not exceeding 0.45 Hz during the fault and returned to below 0.2 Hz after the fault has been cleared. This is depicted in Figure 5-10. The currents through GG II_Sebeta II 400kV and GG I_Sekoru 230kV lines were far below their rated capcity after the fault has been cleared. The voltages

across GG I_Sekoru 230kV line was recovered to 0.99 pu and that of GG II_Sebeta II 400kV line was recovered to 1.031 pu as was indicated in Figure 5-11.

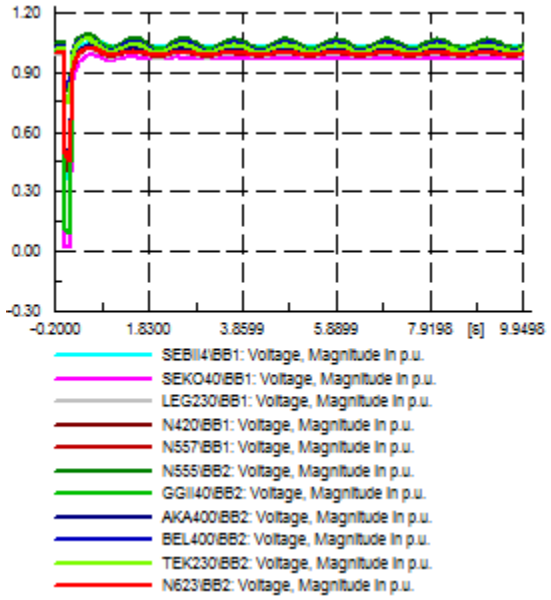

(a) Bus voltages in pu

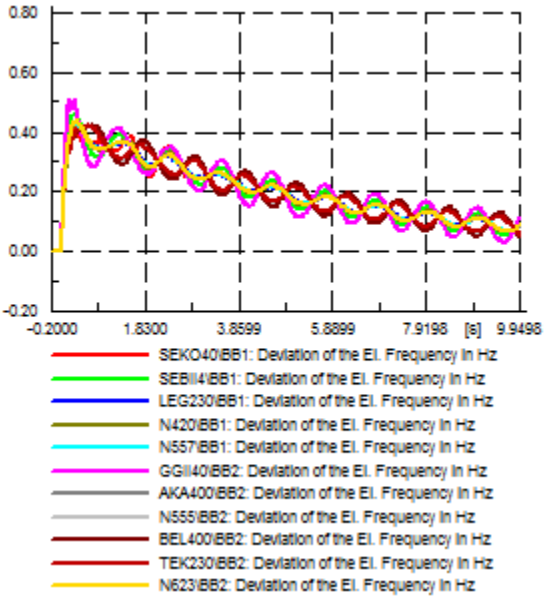

(b) Frequency deviations in Hz

Figure 5-10 Voltages and their corresponding frequency deviations at critical buses for a fault clearing time of 150ms

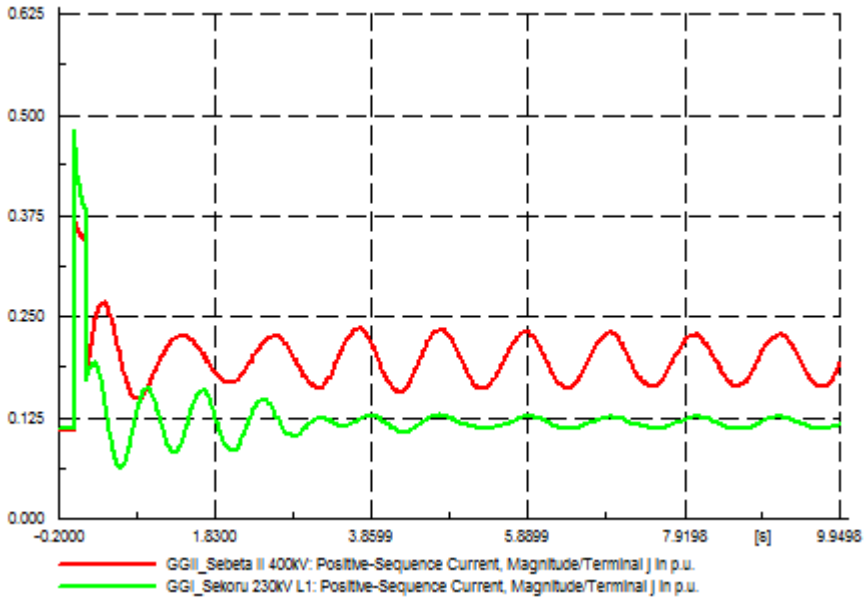

(a) Current in pu

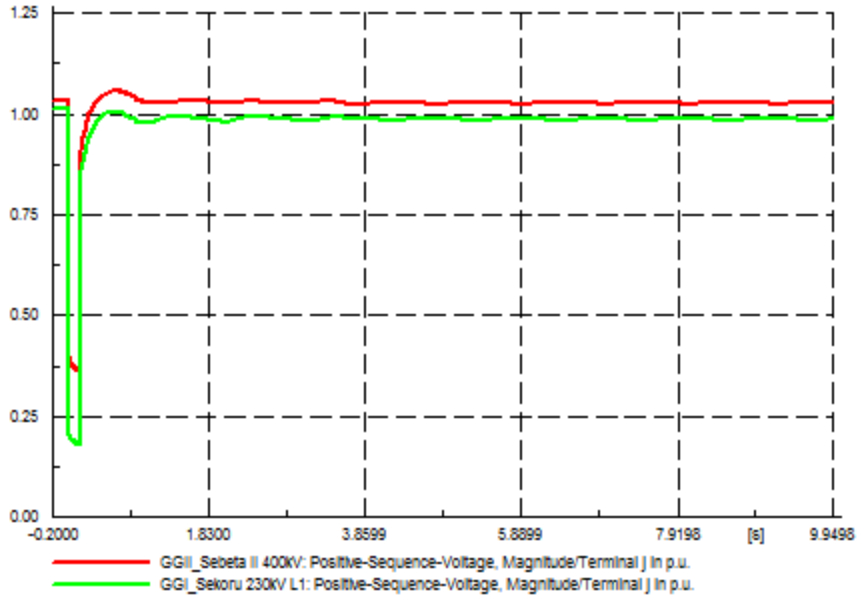

(b) Voltages in pu

Figure 5-11 the currents through and voltages across GG II_Sebeta II 400kV and GG I_Sekoru 230kV lines

Therefore, from the above analysis, we can conclude that the blackout of January 6th 2016 could be preventable if the the fault was cleared wthin 150 ms or faster than this.

5.3.3. Carry out Planned Outages Based on Power System Studies

Planned outages are important to maintain the system intact if and only if they are carried out with detailed power system studies and does not affect the security and stability of the system. However, the planned outages of 11th December 2015 and 22nd December 2015 were hazardous for the stability and operation of the electric power system of EEP. These planned outages caused EEP to pay price for the total collapses of the system on these days. As mentioned in Section 4.2.3, the following planned outages were done before the occurrence of the system disturbance, which of course affected the stability of the grid to any disturbance that could arise on it.

- Fincha HPP_Ghedo_Gefersa 230kV lines were out of service with the aim of replacing the 230kV circuit breaker at Ghedo substation.
- Gefersa-Sululta 230kV line I was out of service due to the upgrading and rehabilitation work at Gefersa substation.
- 400kV and 230kV bus bar of Gelan substation were dead due to planned interruption from mid-night to morning of the following day. The aim of this interruption was intended to avoid system overvoltage.

Of course, the first two outages were done for maintenance reasons but the planned interruptions of Gelan (Akaki I) 400kV and 230kV busbars were carriedout with the aim of voltage regulation [6]. The planned interruptions of Gelan 230kV and 400kV busbars were not logical and were not based on power system planning studies. As observed from Section 4.6.3, the short circuit fault on Mekanisa_Kality I 132kV line was resulted the overdamping of GG III HPP generator and the overloading of Sebeta I_Mekanisa 132kV, Gefersa_Kality I 132kV and Sebeta I_Kality I 230kV lines. As a result, the cascade tripping were happened as was discussed in Section 4.6.3.

Here, a simulation is run with the 230kV and 400kV busbars of Gelan substation energised. The simulation results depicted that the speed of HPP generators were increased during the disturbance and later returned to their normal operating ranges after the fault has been cleared. There was no overdamped oscillation on GG III HPP generator. The rotor angle of each HPP generator was with in the the operating ranges. The terminal voltages of all the HPP generators and their corresponding reactive power generated from them were within limits, as indicated in Figure 5-12.

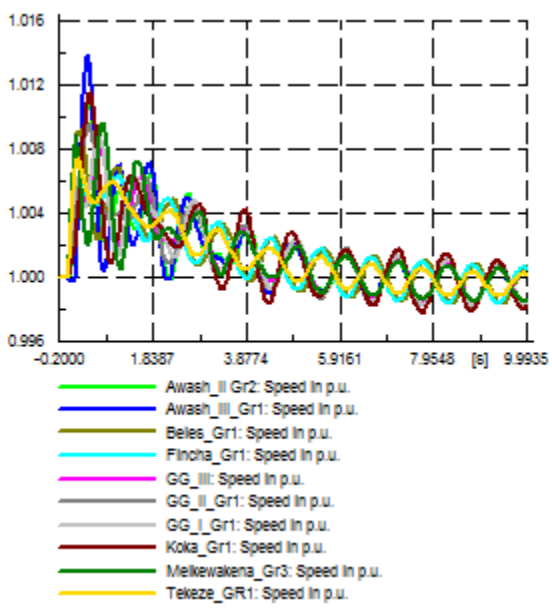

(a) Rotor speed in pu

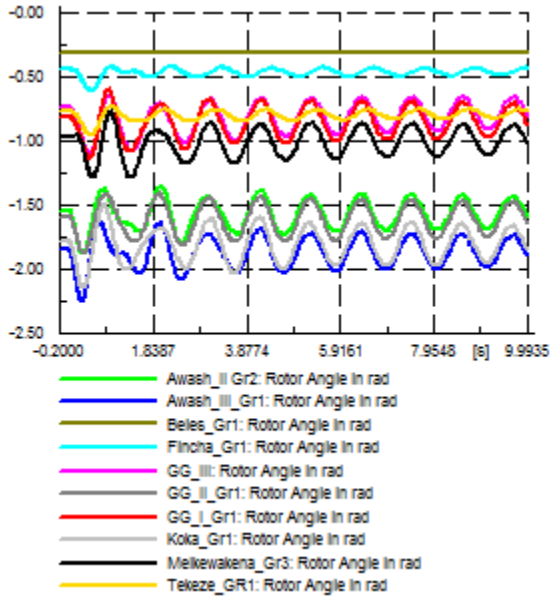

(b) Rotor angles in rad

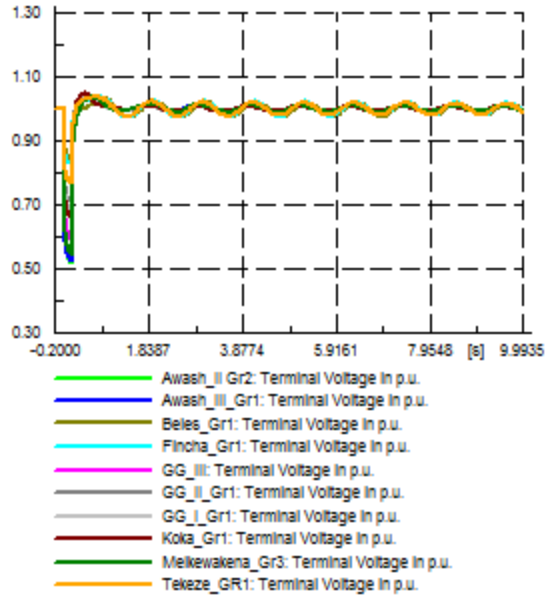

(c) Terminal voltages in pu

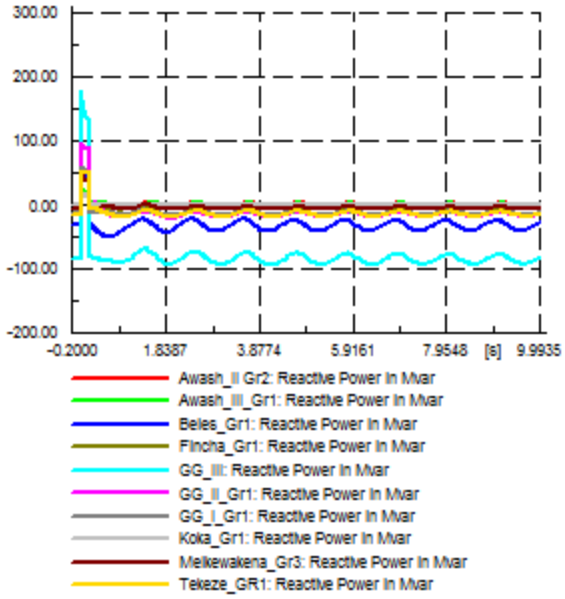

(d) Reactive power in Mvar

Figure 5-12 Profiles of the HPP generators after the planned interruptions were energised.

As can be seen from Figure 5-13, the voltages at critical buses were also well above 0.95 pu after disturbance. Their corresponding frequencies were increasing not above 50.45 Hz during the disturbance and returned to 49.95 Hz after the fault has been cleared.

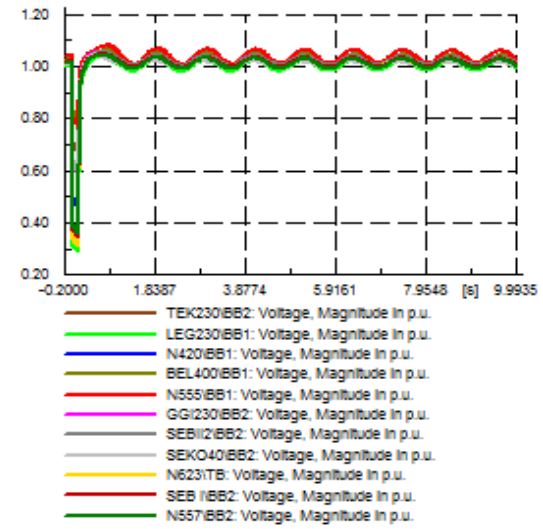

(a) Voltages in pu

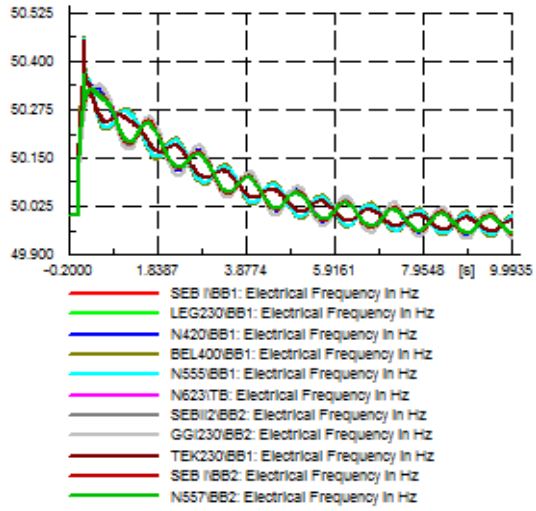

(b) Frequencies in Hz

Figure 5-13 Voltages and their corresponding frequencies at critical buses after the fault has been cleared

The voltages across lines once dipped below 0.5 pu during the fault on Mekanisa_Sebeta I 132kV line and returned to well above 0.92 pu. During the disturbance, the currents through Sebeta I_Mekanissa 132kV and Akaki I_Kality I 132kV lines were rising above 2.50 pu and returned to 0.85 pu after the fault has been cleared. The currents through and voltages across Gefersa_Kality I 132kV and Sebeta I_Kality I 230kV lines were returned to their steady state values after the fault has been cleared. Figure 5-14 (a)-(b) depicted these conditions.

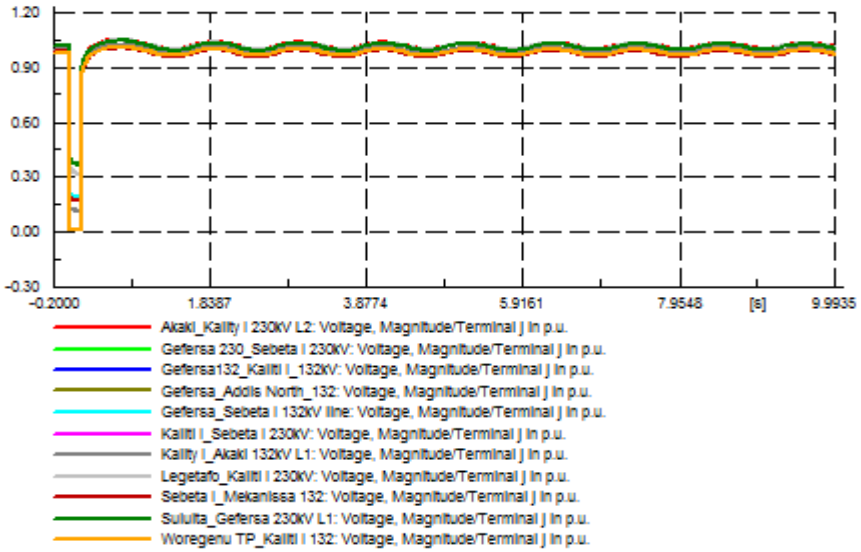

(a) Voltages in pu

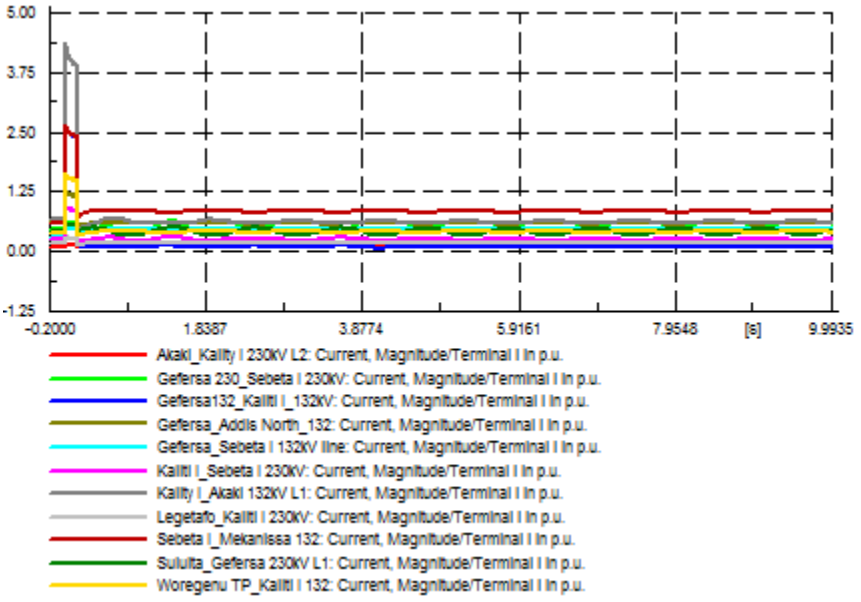

(b) Currents in pu

Figure 5-14 The voltages across and the currents through the transmission lines after the fault has been cleared

As indicated in Figure 5-15 (a)-(b) the power system parameters, i.e., the voltages across and currents through the transformers were within the normal operating ranges.

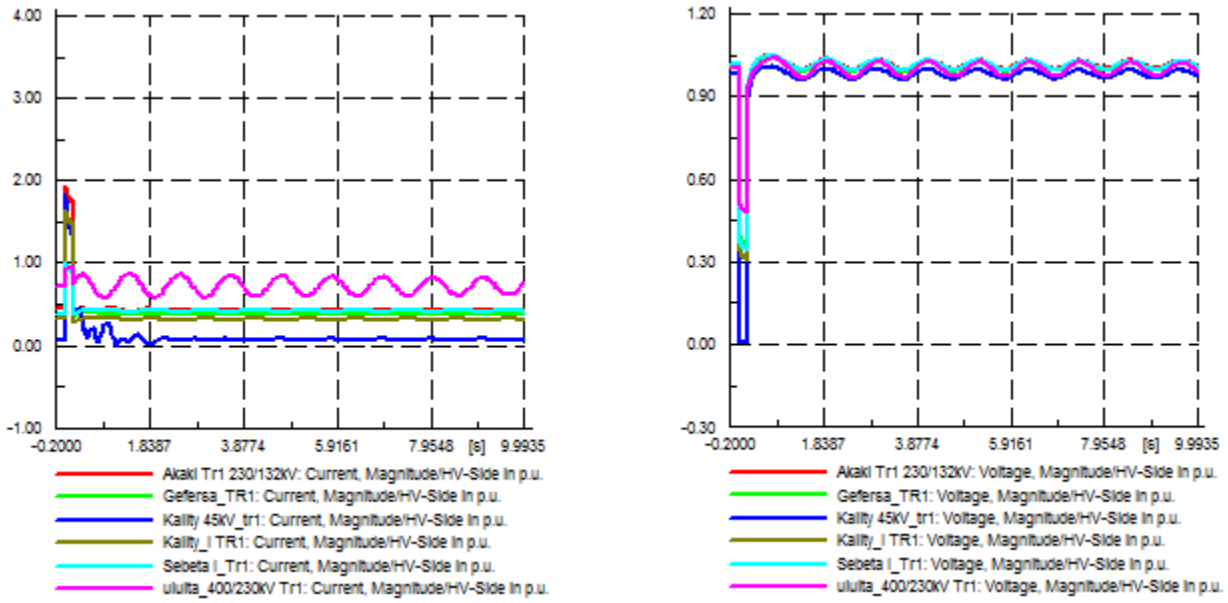

(a) Voltages in pu

(b) Currents in pu

Figure 5-15 The voltages across and currents flowing through the transformers after the fault has been cleared

To sum up, the above simulation results prove that the planned interruptions of Gelan 230kV and 400kV busbars were not carried out based on the knowledge of power system planning studies (operators' misjudgement) and therefore, these planned interruptions were the major causes for the cascading events that were observed during the system collapse of the 11th December 2015. The December 25th 2015 and January 17th 2016 blackouts were also caused by operator misjudgements as was indicated in Section 3.3 and Appendix C. Operator misjudgement while operating the power system can be mitigated through intensive trainings.

5.3.4. Adhering to the Security Standards

In 2014, EEP and EEU were ratifying the operating policy guidelines with regard to the security and operation of the electric power system. In order to maintain the security of the National power system on a day-to-day basis, it is important that the planned outages of generations & transmission systems are properly coordinated. It is necessary to carry out power system studies in order to assess the grid security and network stability while finalizing the annual outage plan of these important elements. In the guideline it was mentioned that every high voltage substation has to be equipped with the energy management system (EMS/SCADA) so that the operators of the corresponding stations can easily monitor and operate the power system. The SCADA system is also crucial for the quick access of network configuration during day-to-

day operation and under emergency condition. In addition, the lines that interconnect the major power plants to the national grid and the lines that interconnect the regional power systems have to have additional paths for the power flows (double circuit lines).

Though many efforts have been done and are going to be done, the security standards outlined on the policy guidelines and what has been practiced on the ground during the operation and planning of the Ethiopian Electric Power system are non-aligned. This has in turn affected the stability of the system during minor disturbances. For instance, Gefersa (230/132 kV) and Sebeta I (230/132 kV) substations are the major actors for interconnecting the different regional power systems to the high load centres and are the backbone of the national grid. Gefersa (230/132kV) substation is interconnecting the western and southwestern regional power systems to the central and Addis Ababa regions through Ghedo_Gefersa 230kV lines. It also helps to interconnect the northwestern region to the high load centres through D/Markos_Sululta 400kV line and Sululta_Gefersa 230kV lines. On the other hand, Sebeta I substation connects the high load centres with the bulk hydro generations of GG I, II & III HPPs in the southern and southwestern regions. However, these two crucial substations are not equipped with SCADA systems, and there is no way for the quick access of network configuration during day-to-day operation and under emergency condition. If there was such a system at Gefersa substation, the operators would be able to notice the overload on Gefersa_Addis Alem 45kV feeder and they would take actions (either shed some loads or trip the line safely) before the conductor was broken and fallen on the ground. Therefore, the blackout of August 14th 2015 would not be happened.

The other most important security rule but not completely practiced by EEP is that the major power plants and the regional power systems have to be connected to the national grid through additional paths (double circuits). This enhances the N-1 security of the power system. For instance, as was observed in Section 5.2, D/Markos_Sululta 400kV line was the most severe line as was indicated in Figure 5-1. It was so because this line was a single circuit line and there was no additional path for the power flow that transmits the bulk hydro generations of Beles HPP to the high load centres. If it was a double circuit line, for instance, the line would no more be a severe line. The same is true for the following transmission lines:

- ✓ Alamata_Combolcha 230kV line
- ✓ Combolcha_Legetafo 230kV line
- ✓ B/dar_Alamata 230kV line
- ✓ D/Markos _Sululta 400kV line
- ✓ B/Dar II _D/Markos 400kV line
- ✓ GG II _Sekoru 400kV line
- ✓ GG II _ Sebeta II 400kV line
- ✓ Sekoru_Jimma II 230kV line

Hypothetical lines with the same rating as the existing lines were used to corroborate whether the above-suggested means could possibly have reduced the severity of these line outages. A contingency analysis is used in the same procedures as in Section 5.2 and the result showed that there was no overloaded equipment

and out of limit bus voltages for the N-1 contingency conditions of the proposed lines. This is depicted in Table 5-4 & 5-5.

Table 5-4 Line loading for the contingencies of severe lines after the hypothetical lines are installed

Contingency Name	Component name	Loading (%)		
		Cont. 2[9]	Cont. 1	Base case
D/Markos_Sululta 400kV line	Combolcha_230/132kV Tr	66.66	204.1	98.6
	Alamata_Combolcha 230kV line	20.22	149.1	39.8
	Legetafo_Ayat GIS 132kV line	93.65	137.6	92.9
	Cotobie _Ayat GIS 132kV line	93.06	137.0	92.3
	Ghedo_230/132/15kV Tr	98.2	110.9	98.2
	Combolcha_Legetafo 230kV line	13.19	107.7	17.2
	BDR_TR1 (400/230kV)	21.88	102	35.2
	BDR_TR2 (400/230kV)	21.88	102	35.2
Alamata _Combolcha 230kV line	Sululta_400/230kV Tr1	70.46	117.6	80.7
	Sululta_400/230kV Tr2	70.46	117.6	80.7
	Kality I_Akaki I 132kV line I	86.24	107.4	96.1
	Kality I_Akaki I 132kV line II	86.24	107.4	96.1
Combolcha_Legetafo 230kv line	Combolcha_230/132kV Tr	73.02	128.7	98.6
	Kality I_Akaki I 132kV line II	87.6	100.1	96.1
	Kality I_Akaki 132kV line II	87.6	100.1	96.1
GG II _Sekoru 400kV line	Metu_230/66/15kV Tr	94.23	101.5	95.5
	Combolcha_230/132kV Tr	66.84	100.8	98.6

As can be seen from Table 5-5, no bus voltage violation was occurred for the contingencies of Alamata_Combolcha 230kV line and GG II_Sekoru 400kV line after hypothetical lines of the same capacity as the existing lines were installed.

[9] *"Cont.2" is the loading of components for the corresponding contingency if the major lines were doubled. "Cont. 1" is the loading of components for the corresponding contingency for the current topology of EEP*

Table 5-5 Bus voltages for the contingencies of severe lines after the hypothetical lines are installed

Contingency Name	Bus name	Voltage (pu)		
		Cont. 2	Cont. 1	Base case
Alamata_Combolcha 230kV line	Akaki I 132kV	0.97	0.90	0.92
	Sululta 230kV	1.0	0.89	0.93
	Kality I 230kV	0.99	0.89	0.93
	Legetafo 230kV	0.99	0.88	0.92
	Sululta 400kV	1.03	0.88	0.93
	Gefersa 132kV	0.96	0.87	0.90
	Kality I 132kV	0.95	0.87	0.90
	Shehedi 230kV	0.95	0.87	0.90
	Sululta 132kV	0.96	0.87	0.91
	Combolcha 230kV	1.02	0.82	0.94
	Combolcha 132kV	1.02	0.81	0.93
	D/Berhan 132kV	0.98	0.84	0.90
GG II _Sekoru 400kV line	Gambela 230kV	0.96	0.89	0.95
	Nekemte 132kV	0.96	0.90	0.94
	Sululta 132kV	0.96	0.89	0.91
	Ghimbi 132kV	0.96	0.89	0.93
	Gefersa 132kV	0.96	0.89	0.90
	Metu 66kV	0.96	0.89	0.95
	Gambela 66kV	0.91	0.85	0.90

As was observed in Section 5.2, the most vulnerable equipment was the transformer at Combolcha 230/132kV substation and the most vulnerable buses were Sululta 132kV and Gefersa 132kV buses. However, by using the methods proposed here, i.e., by adding additional transmission line, the vulnerability of Combolcha_230/132kV transformer to overloads for the severe line outages is highly reduced. Similarly, the vulnerability of Sululta and Gefersa 132kV buses to bus voltage violations are highly improved for the severe line outages. For instance, the outage of Alamata_Combolcha 230kV line was resulted the voltage at Sululta 132kV bus to be 0.87 pu. However, for the hypothetical line installed, the voltage at Sululta 132kV is 0.96 pu for the same line outage conditions.

In addition, the outage of D/Markos _Sululta 400kV line was caused the overloading of Combolcha_230/132kV transformer (a loading of 204.1 %) as was discussed in Section 5.2, but when the hypothetical line having the same capcity as the existing line is installed the loading of Combolcha _230/132kV transformer is o 66.56 % for the same line outage conditions.

Chapter 6

Conclusions, Recommendations and Future Work

6.1. Conclusions

In simple terms, what have been accomplished in this thesis are firstly the analyses of the causes and the mechanisms of previous blackouts of the Ethiopian electric power system and identification of the system vulnerabilities and weaknesses of the national grid. Then, based on the identified blackout causes and system weaknesses, some methods that can help mitigate system blackouts are proposed. This goal was achieved by modelling and simulating the national grid by using DIgSILENT PowerFactory software.

From the blackout simulation studies, it is shown that the causes of the blackouts were linked to:

- the poor protection system coordination,
- poor planned interruptions,
- slow breaker actions (not clearing the fault as fast as possible), and
- violations of the security rules while planning and operating the power system

From the vulnerability analysis, it is found that the most severe line outage was the disconnection of D/ Markos_Sululta 400kV line (PI_p = 7.3238 pu), which leads to overloading of B/Dar II 400/230kV transformers (TR_1 and TR_2) and hence leads to the disconnection of Beles HPP which is the main actor of EEP grid for system synchronisation. Based on the probability of outage occurences, the network's most vulnerable element was Combolcha_230/132kV transformer and 12 different line outage cases lead this element to overload. It is found that the highest percentage loading for this equipment was 204.1 %. The other most vulnerable elements are Kality I_Akaki I 132kV line I & II, Gefersa_Addis North 132kV line, Cotobie_weregenu TP 132kV line, and Sebeta I_Mekanisa 132kV lines. On the other hand, the most dangerous line outages with respect to the voltage level performance index (PI_v) are the disconnections of Alamata_Combolcha 230kV line (PI_v = 0.1124 pu), Akaki I_Kality I 230kV lines I & II (PI_v = 0.0906 pu), and Sebeta I_Kality I 230kV line (PI_v = 0.087 pu), respectively. Based on the line outage occurences, the network's most vulnerable buses are Sululta and Gefersa 132kV buses and 11 different line outage cases lead these buses to have out of limit voltages.

Generally, it is observed that most of the network vulnerabilities with respect to bus voltages violations and element overloadings are occurred on those buses and elements found at the high load centres, i.e., Addis Ababa region.

Finally, the study puts the different methods that can help to reduce the likelihood of disturbances that will arise in the future. The study also puts the method that can help to cease the vulnerability of the EEP system. Some of the proposed techniques are:

- Fine protection system coordination
- High-speed fault clearing
- Carryout planned interruptions based on the knowledge of power system planning studies and
- Adhering to the security criterions while planning and operating the power system.

Moreover, the simulation results of these proposed methods indicated that the past blackouts of 14th August 2015, 11th December 2015, 6th January 2016 and many more could be preventable. The vulnerability of the system can also be reduced by installing additional lines in parallel with the most severe lines. Moreover, the vulnerabilities with respect to bus voltage violations and component overloadings of those buses and components found on the high load centres are significantly reduced by installing parallel circuit lines that fed Addis Ababa region from the rest of the regional power systems.

6.2. Recommendations

As can be seen from Appendix D & F, the Ethiopian electric power grid consists of more than 45 mechanically switched (with manual breakers and isolators) shunt reactors, one fixed capacitor bank having 90 Mvar capacity installed at Akaki I 400kV bus, two mechanically switchable capacitor banks having 45 and 90 Mvar capacities installed at Sebeta II 230kV & 400kV buses respectively. It is to be noted that these fixed and mechanically switched capacitors and reactors can achieve steady state voltage regulation. However, as far as no automatic control is implemented on these devices, fast voltage regulation is impossible to prevent voltage instabilities during transient conditions. As already seen from the blackout and vulnerability analyses, these fixed and mechanically switched shunt compensators could not be able to prevent system collapses. Therefore, a means is required, i.e., replacing these mechanically switched capacitors and reactors by FACTS devices, to increase the power transfer and to solve the problem of voltage collapse caused by contingency conditions at buses, such as Sululta 132kV, Gefersa 132kV and Kality I 132kV buses.

6.3. Suggestions for Future Work

The work explored here has highlighted solutions that should be explored by EEP to deliver reliable power to the customers and therby contributes its part for the industrial and socio-economic development of the nation. Future work on blackouts and their mitigation techniques is necessary, as this is only a preliminary study. Future work should also consider other solutions cases, like, installing FACTS devices. However, the work on FACTS devices should consider the performance analysis of the device under different fault conditions. In addition, different methods of optimal placement of FACTS device should be investigated and analysed by different analytical tools with higher level of accuracy.

References

[1] W. N. G. E. Getamesay Bekele, “Energy Poverty in Addis Ababa City, Ethiopia,” *Journal of Economics and Sustainable Development*, 2015.

[2] World Bank Group- International Development Association, “International Development Association Project Paper on a Proposed Additional Credit to the Federal Democratic Republic of Ethiopia for the Electricity Network Reinforcement and Expansion Project,” World bank, Ethiopia, May 6, 2016.

[3] World Bank Group-International Development Association, “International Development Association Roject Appraisal Document on a Proposed Credit in the Amount of SDR 114 million and a Proposed SCF-SREP Grant in the Amount of US$24.5 million to the FDRE for a Geothermal Sector Development Project (GSDP),” World_Bank, Addis Ababa, Ethiopia, April 4, 2014.

[4] R. C. T. C. Andrew Herscowitz, “Power Africa: Investment Brief for the Energy Sector in Ethiopia,” Power Africa, Pretoria, South Africa, 2014.

[5] FDRE National Planning Commission, “The Federal Democratic Republic of Ethiopia The Second Growth and Transformation Plan (GTP II),” Addis Ababa, September, 2015.

[6] National Load Dispatch Centre of Ethiopia, “"Partial and Total Blackouts Report" - National Load Dispatch Center, Ethiopian Electric Power, Ethiopia,” EEP, Addis Ababa, 2013-2015.

[7] N. Ethiopian Electric Power, “Grid Disturbance report,” 2015.

[8] WorldBank, “"Africa’s Power Infrastructure: Investment, Integration, Efficiency",” Vivien Foster and Cecilia Briceño-Garmendia,Series Editors, Washington D.C, 2011.

[9] Tesfahun.A, “"Challenges of the Ethiopian manufacturing sector under the GTP II",” Addis Ababa, 2015.

[10] B. A. C. V. E. L. D. E. N. Ian Dobsona, “"Complex systems analysis of series of blackouts: Cascading failure, critical points, and self-organization",” *Chaos*, 2007.

[11] P.Kundur, " Power System Stability and Control ", New York: McGraw-Hill, 1994.

[12] Marvin Karugarama, Mitigation of Blackout in Kigali Using a Microgrid with Advanced Energy Storage and Solar Photovoltaics, Blacksburg, VA: MSc. thesis, 2015.

[13] Karel Perutka, MATLAB for Engineers-Applications inControl, Electrical Engineering, IT and Robotics, Rijecka, Croatia: InTech, 2011.

[14] J. E. Dagle, “Postmortem Analysis of Power Grid Blackouts,” *IEEE Power & Energy Magazine*, pp. 30-35, September/October 2006.

[15] M. D. Zhong, “"China's Protection Technique in Preventing Power System Blackout to World",” in *2011The International Conference on Advanced Power System Automation and Protection*, 2011.

[16] T. K. S. Arulampalam Atputharajah, “"Power System Blackouts - Literature review",” in *Fourth International Conference on Industrial and Information Systems, ICIIS*, sirilanka, 2009.

[17] Erik, “The Black-out in southern Sweden and eastern Denmark, September 23, 2003,” in *CIGRE- Large Disturbance Workshop*, Paris, 2004.

[18] U.S.-Canada Power System Outage Task_Force, “"Final Report on the August 14, 2003 Blackout in the United States and Canada: Causes and Recommendations",” Canada, 2004.

[19] P. D. R. F. N. H. I. K. P. K. G. Andersson, “"Causes of the 2003 major grid blackouts in North America and Europe, and recommended means to improve system dynamic performance",” *Power Systems, IEEE Transactions*, pp. 1922-1928, 2005.

[20] S. M. B. a. A. A. Girgis, “"Development of adaptive protection scheme for distribution systems with high penetration of distributed generation,",” *Power Delivery, IEEE Transactions on, vol. 19*, pp. 56-63, 2004.

[21] Z. D. Barkans J., "Protection Against Blackouts and Self-Restoration of Power Systems", Riga: RTU Publishing House, 2009.

[22] M. Shahidehpour, Handbook of Electrical Power System Dynamics : Modeling, Stability and Control, Piscataway: IEEE Press, 2013.

[23] National Load Dispatch Center of EEP, “Operating Procedures for National Load Dispatch Center,” Ethiopian Electric Utility, Addis Ababa, Ethiopia, April, 2014.

[24] N. E. D. Veropai, “Analysis of blackout development mechanisms in electric power systems,” in *IEEE PES General Meeting*, Pittsburgh, USA, 2008.

[25] N. E. D. Voropai, “Analysis of blackout development mechanisms in electric power systems,” *IEEE PES General Meeting*, 21–24 July 2008.

[26] W. T. a. F. Y. M. Shahidepour, “Impact of Security on Power Systems Operation,” *Proceddings of the IEEE, Vol. 93*, pp. 2013-2015, 2005.

[27] J. McCalley, “Operational defence of power system cascading sequences: probability, prediction, and mitigation,” *PSerc Seminar*, October 7, 2003.

[28] G. W. Stagg and A. H. El-Abiad, Computer Methods in Power Systems, new York: McGraw-Hill, 1968.

[29] J.B gupta, Transmission and Distribution of Electrical Power, New Delhi: S.K Kataria & Sons, July 2012.

[30] M. S. S. T. J. O. J. Duncan Glover, Power System Analysis and Design, Stamford, USA: Cengage Learning, 2012.

[31] O.T.S, Power system protection, Part II, Training Manual, April 2016.

[32] Li W, Risk Assessment of Power Systems: Models, Methods, and Applications, New York: Willey, 2005.

[33] M. S. W. Lu Q, "Vital basic research on modern power systems geared to the 21st Century," Progress in Natural Science, 2010.

[34] Z. J. i. W. L. Z. X. Wu Xu, "Power System Key Lines Identification Based on Cascading Failure and Vulnerability Evaluation," in *China International Conference on Electricity Distribution (CICED 2012)*, Shanghai, 2012.

[35] Bhatt N B, "August 14, 2003 US-Canada blackout," in *IEEE PES General Meeting*, Denver Co, 2004.

[36] L. Y. Venkatasubramanian V, "Analysis of 1996 Western American electric blackouts," *Bulk Power System Dynamics and Control-ė,* pp. 22-27, 2004.

[37] G. D. I. S. M. O. O. P. R. a. J. T. G. C. Ejebe, "Methods for contingency screening and ranking for voltage stability analysis of power systems," in *Power Industry Computer Application Conference Proceedings., 1995 IEEE*, 1995.

[38] G. C. E. a. B. F. Wollenberg, "Automatic Contingency Selection," *IEEE Transactions on Power Apparatus and Systems,* pp. 97-109, 1979.

[39] A. Y. M. Y. H. A. Salah Eldeen Gasim Mohamed, "Power System Contingency Analysis to detect Network Weaknesses," in *Zaytoonah University International Engineering Conference on Design and Innovation in Infrastructure 2012*, Amman Jordan, 2012.

[40] Q. Z. V. V. A. A Fouad, "System Vulnerability as a Concept to Assess Power System Dynamic Security," *IEEE Transactions on Power Systems,* vol. 9, May 1992.

[41] B. C. M. Winokur, "Identification of Strong and Weak Areas for Emergency State Control," *IEEE Transactions on Power Apparatus and Systems,* Vols. PAS-103, June 1984.

[42] X. Z. M. C. Shengwei Mei, Power Grid Complexity, Beijing: Springer, 2011.

[43] D. E. N. I. D. B. A. Carreras, "Determining the Vulnerabilities of the Power Transmission System," in *45th Hawaii International Conference on System Sciences*, Hawaii, 2012.

[44] V.Brandwajn and M.G. Lauby, "Complete bounding method for AC contingency screening," in *IEEE Transactions on Power Systems, Vol. 4, No.2*, May 1989.

[45] T. H. Y. W. M. C. Ettore Bombard, "Classification and trend analysis of threats origins to the security of power systems," *Electrical Power and Energy Systems,* vol. 50, pp. 50-64, 19 March 2013.

[46] R. M. R. J. B. M. El-werfelli, "Analysis of the National 8th November 2003 Libyan Blackout".

[47] Shirani, "Iranian Electric Power System Blackout on 31st of March 2003," in *CIGRE*, Paris, 2004.

[48] DIgSILENT GmbH, Power Factory User's Manual, DIgSILENT PowerFactory Version 14.0, Gomaringen, Germany: DIgSILENT PowerFactory , 2008.

[49] J. B. J. B. J. Machowski, Power System Dynamics and Stability, Chichester: John Wiley and Sons, 1997.

[50] A. F. P.M. Anderson, Power System Control and Stability, New York: IEEE Press, 1994.

[51] K R. Padiyar, Power System Dynamics: Stability and Control, New Delhi: BS Publications, 2008.

[52] D. Das, Electrical Power Systems, New Delhi: New Age International Publishers, 2006.

[53] A. H. E. A. Glenn W. Stagg, Computer Methods in Power System Analysis, McGraw-Hill, 1968.

[54] S. o. E. a. C. E. NPTEL, *Transient Stability Analysis*, lass lecture, 2013.

[55] Murad Ridwan, Class Notes on Analytical & Computational Methods (ECEG-6201), vol. Chapter 2, Addis Ababa University, AAiT, Addis Ababa: School of Electrical & Computer Engineering, Nov. 2012, pp. 12-29.

[56] Ramasamy Natarajan, Computer -Aided power System Analysis, New York: Marcel Dekker, 2002.

[57] Ethiopian Electric Power-NLDC, Operating Procedures for National Load Dispatch Centre, Addis Ababa, Ethiopia: NLDC, 2015.

[58] Sino Hydro Corporation Ltd., "Nifas Silk 132/15kV Substation Protection Relay Setting Manual - Calculation Note," 2015.

[59] O. Alsac and B. Stott, "Optimal Load Flow with Steady-State Security," *IEEE Transactions on Power Apparatus and Systems,* pp. 745-751, 1974.

[60] E. National Load Dispatch Centre, Operating Procedures for National Load Dispatch Centre, Addis Ababa, 2015.

[61] F. M. Gonzalez-Longatt, PowerFactory Applications for Power System Analysis, Stuttgart Und Umgebung, Deutschland: Springer, August 2014.

[62] B. F. W. Allen J. Wood, Power Generation, Operation, and Control, Second ed., Willey, 2013, pp. 415-436.

[63] A. B. B. H. F. Albuyeh, "Reactive Power Considerations in Automatic Contingency Selection," *IEEE transactions on Power Apparatus and Systems,* Vols. PAS-101, January 1982.

[64] Dr.M. El-Shimy, Dynamic Security of Interconeected Power Systems, vol. 1 & 2 , Cairo: LAMBERT, 2015.

Appendices

Appendix A: Line, Load and Transformer Data

Table A. 1 Line Data

Node 1	Node 2	Network Level	l [km]	r [Ω/km]	x [Ω/km]	c [nF/km]	Ith [kA]	r0 [Ω/km]	x0 [Ω/km]	c0 [nF/km]
GG OLD 230 kV	Wolkite 230kV	230	65.3	0.0597	0.4113	8.9	1.05	0.2029	1.3029	6
Gefarsa 132 BB1	Kaliti I 132 BB1	132	24.75	0.1906	0.434	8.4	0.49	0.3724	1.3217	5.6
Gefarsa 132 BB1	Sebeta I 132 TP	132	10.78	0.1906	0.434	8.4	0.49	0.3724	1.3217	5.6
MEKANISSA 132	Kaliti I 132 BB1	132	16.16	0.1906	0.434	8.4	0.49	0.3724	1.3217	5.6
Sebeta I 132	Mekanissa 132	132	7.81	0.1906	0.434	8.4	0.49	0.3724	1.3217	5.6
Gefarsa 132 BB1	Addis North 132	132	11.11	0.1906	0.434	8.4	0.49	0.3724	1.3217	5.6
Cotobie 132	Weregenu 132 TP	132	2.45	0.1906	0.434	8.4	0.49	0.3724	1.3217	5.6
Weregenu 132 TP	Weregenu 132	132	4.5	0.1906	0.434	8.4	0.49	0.3724	1.3217	5.6
Weregenu 132 TP	Kaliti I 132 BB1	132	17.51	0.1906	0.434	8.4	0.49	0.3724	1.3217	5.6
Cotobie 132	Kaliti North 132 TP	132	18.65	0.1906	0.434	8.4	0.49	0.3724	1.3217	5.6
Kaliti North 132 TP	Kaliti I 132 BB1	132	1.5	0.1906	0.434	8.4	0.49	0.3724	1.3217	5.6
Kaliti North 132 TP	Kaliti North 132	132	0.44	0.1906	0.434	8.4	0.49	0.3724	1.3217	5.6
Akaki II 132	Debre Zeit II 132 TP	132	28.54	0.1906	0.4264	8.6	0.49	0.3678	1.3413	5.6
Akaki II 132	Koka 132 BB1	132	61	0.1906	0.433	8.4	0.49	0.3717	1.3245	5.5
Debre Zeit II 132 TP	Debre Zeit II 132	132	0.05	0.1906	0.4333	8.4	0.49	0.3732	1.3226	5.6
Koka 132 BB1	Wonji DCP	132	7.36	0.1906	0.4264	8.6	0.49	0.3678	1.3413	5.6
Koka 132 BB1	Wonji TP	132	7.36	0.1906	0.4264	8.6	0.49	0.3678	1.3413	5.6
Gonder II 230	SHR Gonder II	230	0.01	0.0918	0.3205	11.4	1	0.2709	1.1482	6.9
Awash 7 230	Koka 230	230	128.8	0.0725	0.4089	8.9	0.92	0.2517	1.2465	5.9
Akaki 230	Koka 230	230	66.4	0.0739	0.4142	8.9	0.89	0.2466	1.2614	5.9
Akaki 230	Koka 230	230	66.4	0.0739	0.4142	8.9	0.89	0.2466	1.2614	5.9
Koka 230	Melka Wakena 230	230	163.9	0.0739	0.4142	8.9	0.89	0.2466	1.2614	5.9
Gefarsa 230	Sebeta 230 BB1	230	10.64	0.0725	0.408	8.9	0.92	0.2519	1.248	5.8
Addis North 132	Addis East II	132	8.707	0.1835	0.4237	8.6	0.51	0.3681	1.3395	5.4
Cotobie 132	Addis East II	132	4.223	0.1835	0.4237	8.6	0.51	0.3681	1.3395	5.4
KALITI I 230 BB1	N1925	230	3.565	0.0725	0.408	8.9	0.92	0.2519	1.248	5.8
Gefersa 230 kV	Ghedo 230kV	230	33.26	0.0671	0.4272	8.7	1	0.2787	1.1661	6.5
Mekele 230kV	Tekeze 230kV	230	103	0.0918	0.3234	11.3	0	0.2642	1.1007	6.9
GG Old 230kV	Gilgel Gibe I 230	230	2.5	0.0597	0.4113	8.9	1.05	0.2029	1.3029	6
Gilgel Gibe 400kV	Sebeta 2 400kV	400	185	0.0375	0.4259	8.7	0	0.286	1.0839	6.8
G/Gibe OLD 230KV	Gilgel Gibe I 230kV	230	2.5	0.0597	0.4113	8.9	1.05	0.2029	1.3029	6
Bahir Dar 400KV	Beles 400kV	400	62.8	0.0209	0.3096	12	0	0.2017	1.0341	7.7
Bahir Dar 400KV	D/Markos 400KV	400	193.7	0.0209	0.3034	12.2	0	0.2219	1.0075	7.9
D/Markos 400KV	Sululta 400KV	400	215.8	0.0209	0.3096	11.9	0	0.2017	1.0342	6.8
Sululta 230KV	Gefarsa 230	230	16.86	0.0599	0.4081	9.1	0	0.2456	1.1745	6.1
Finchaa II	Ghedo 230	230	69.73	0.0668	0.4211	8.7	0	0.2393	1.1985	5.8
Alamata 230	Combolcha 230KV	230	170.6	0.0919	0.3167	11.6	0	0.2593	1.115	6.4
Legetafo 230kV	Kaliti I 230 BB1	230	34.5	0.0918	0.3225	11.3	0	0.2634	1.0946	6.9
Combolcha 230kV	Semera230kV	230	177.1	0.0918	0.3206	11.4	0	0.2676	1.1005	6.9
Bedele230kV	Metu230kV	230	90.4	0.0919	0.3166	11.6	0	0.26	1.1224	7.1
Mekele 230	Mehoni	230	100	0.0919	0.3168	11.5	0	0.2619	1.1675	6.7
Hurso 230	Koka 230	230	313	0.0919	0.3168	11.6	0	0.2659	1.1619	6.9
Alamata 230	Combolcha 230kV	230	170.6	0.0919	0.3167	11.6	0	0.2593	1.115	6.4
Dire Dawa III 230	Awash 7 230	230	208.9	0.0725	0.4089	8.9	0.92	0.2517	1.2465	5.9
Sululta 230KV	Legetafo 230KV	230	21	0.0919	0.3167	11.6	0	0.2593	1.115	6.4
Sebeta 2 400KV	Akaki 400	400	33	0.019	0.3291	11.1	0	0.2108	0.9855	7
Welayta Sodo 400 kv	Akaki 400	400	267	0.0206	0.3082	12.5	0	0.2215	1.0163	7.1
Welayta Sodo 400 kv	Gibe 3 400	400	51	0.0206	0.3082	12.5	0	0.2215	1.0163	7.1

Table A. 3 Transformer Data (three winding)

Node 1	Node 2	Node 3	U_{n1} [kV]	U_{n2} [kV]	U_{n3} [kV]	S_{n12} [MVA]	S_{n23} [MVA]	S_{n31} [MVA]	uk_{12} [%]	uk_{23} [%]	uk_{31} [%]
Harar II 132 kV	Harar II 66kV	Harar II 33kV	132	66	33	20	9.6	9.6	8	2.41	6.89
Dire Dawa I 132	Dire Dawa I 66	Dire Dawa I 15	132	66	15	20	20	20	7.88	5.7	14.8
Koka 132 BB1	Koka Hydro 10.5 GR1	Koka Hydro 15	135	10.5	15	18	6	6	9.63	8	3.94
Finchaa 230	Finchaa 66	FINCHAA 15A	230	66	13.2	12.02	12.02	24.2	4.70	1.29	6.94
Bahir Dar II 230	Bahir Dar II 66	Bahir Dar II 15A	230	66	15	6.3	2.7	2.7	6.31	0.93	3.83
Gonder II 230	Gonder II 66	Gonder II 15	230	66	15	16	16	16	4.67	4.01	9.02
Bahir Dar II 230	Bahir Dar II 132	Bahir Dar II 15B	230	132	15	50	16.7	16.7	9.34	4.69	8.29
D/Markos 230	Debre Markos 66	Debre Markos 15	230	66	15	6.3	2.7	2.7	6.42	0.94	3.85
Awash II 132 BB1	Awash II 15A	Awash II GR110.5	142	15	10.5	4.2	4.2	14	2.91	5.89	7.26
Wolkite 230 BB1	WolkitE 66	Wolkite 33	230	66	33	16	16	16	5.56	2.76	8.68
Ghedo 230	GhedO 132	Ghedo 15	230	132	15	16	4	4	7.36	3.94	1.88
Gefarsa 132 BB1	Gefarsa 45	Gefarsa 15A	132	45	15	15	15	15	6.08	3.57	13.1
Dire Dawa III 230	Dire Dawa III 132 BB1	Dire Dawa III 15	225	132	15	37.8	11.34	11.34	4.54	2.24	3.8
Mekele 230	Mekele 132	Mekele 15	220	132	15	25	15	15	2.46	4.34	5.99
Harar II 132	Harar II 66	Harar II 33	132	66	33	20	9.6	9.6	8	2.4	6.93
Ghedo 230	Ghedo 132	Ghedo 15	230	132	15	16	4	4	7.27	3.93	1.89
Awash II 132 BB1	Awash II 15A	Awash II GR 10.5	142	15	10.5	6	6	20	4.06	7.77	10.4
Awash III 132BB1	Awash III 15	Awash III GR2 10.5	142	15	10.5	6	6	20	4.06	7.77	10.4
Koka 132 BB1	Koka Hydro 10.5 GR2	Koka Hydro 15	135	10.5	15	18	6	6	9.548	8	3.955
B/Dar II 230 BB1	B/Dar II 132	B/Dar II 15B	230	132	15	50	16.7	16.7	9.35	4.68	8.25
B/Dar II 230 BB1	B/Dar II 66	B/Dar II 15A	230	66	15	6.3	2.7	2.7	6.31	0.93	3.83
D/Markos 230	D/Markos 66	D/Markos 15	230	66	15	6.3	2.7	2.7	6.38	0.93	3.85
Finchaa II	Finchaa II 33kV	Finchaa II 15kV	230	33	15	20	10	10	22	8	13.9
Metu 230kV	Metu166kV	Metu15kV	230	66	15	40	20	20	22.5	8.16	13.8
Agaro 230kV	Agaro 132	Agaro15kV	230	132	15	63	63	23	41.4	10.0	28.4
Gambela 230kv	Gambela 66	Gambla33KV	230	66	33	32	16	16	11.9	11.6	11.6

Table A. 4 Load Data

Node 1	Element Name	Network Level	Load Flow Type	P [MW]	cosphi [p.u.]	fP
Harar II 33	Harar II 33	33	Z constant	4.89	0.95	1.33
JIJIGA I 15	JIJIGA I 15	15	Z constant	1.1	0.95	1.33
JIJIGA II 33	JIJIGA II 33	33	Z constant	5.1	0.95	1.33
HARAR II 15	HARAR II 15	15	Z constant	2.75	0.95	1.33
DIRE DAWA II 15	DIRE DAWA II 15	15	Z constant	2.2	0.95	1.33
DIRE DAWA I 15	DIRE DAWA I 15	15	Z constant	9.4	0.95	1.33
JIJIGA II 15	JIJIGA II 15	15	Z constant	5.41	0.95	1.33
DIRE DAWA III 15	DIRE DAWA III 15	15	Z constant	2.53	0.95	1.33
AWASH 7 KILO 15	AWASH 7 KILO 15	15	Z constant	2.2	0.95	1.33
AMIBARA 15	AMIBARA 15	15	Z constant	2.2	0.95	1.33
ASEBE TEFERI 15	ABESE TERFERI 15	15	Z constant	2.2	0.95	1.33
BEDESA 15	BEDESA 15	15	Z constant	2.31	0.95	1.33
METEHARA 15	METEHARA 15	15	Z constant	4.66	0.95	1.33
KALITI I 15	KALITI I 15	15	Z constant	6	0.95	1.33
AKAKI S.P FACTORY 1	AKAKI S.P FACTORY	15	Z constant	4.62	0.95	1.33
DEBRE ZEIT I 15	DEBREZEIT I 15	15	Z constant	1.87	0.95	1.33
DUKEM 15	DUKEM 15	15	Z constant	0.88	0.95	1.33

ABA SAMUEL 15	ABA SAMUEL 15	15	Z constant	0.88	0.95	1.33
KALITI II 15B	KALITI II 15B	15	Z constant	20	0.95	1.33
NEFAS SILK 15	NEFAS SILK 15	15	Z constant	12.65	0.95	1.33
ADDIS CENTER 15	ADDIS CENTER 15	15	Z constant	52.8	0.85	1.1
WEREGENU 15	WEREGENU 15	15	Z constant	13	0.95	1.33
KALITI NORTH 15	KALITI NORTH 15	15	Z constant	7.48	0.95	1.33
ADDIS EAST I 15	ADDIS EAST I 15	15	Z constant	10	0.88	1.2
ADDIS EAST II 15	ADDIS EAST II 15	15	Z constant	41	0.88	1.1
DEBRE BIRHAN 15	DEBRE BIRHAN 15	15	Z constant	3.12	0.95	1.33
SHOA ROBIT 15	SHOA ROBIT 15	15	Z constant	1.43	0.95	1.33
DEBRE ZEIT II 15	DEBRE ZEIT II 15	15	Z constant	16	0.95	1.33
ELALA GEDA 15	ELALA GEDA 15	15	Z constant	4.4	0.95	1.33
YESU FACTORY 15	YESU FACTORY 15	15	Z constant	3.3	0.95	1.33
KOKA 15	KOKA 15	15	Z constant	2.2	0.95	1.33
MODJO 15	MODJO 15	15	Z constant	2.2	0.95	1.33
NAZRETH I 15	NAZRETH I 15	15	Z constant	3.74	0.95	1.33
KOKA HYDRO 15	LO307	15	Z constant	0	0.95	1.33
METU 15	METU 15	15	Z constant	2.42	0.95	1.33
BEDELE 15	BEDELE 15	15	Z constant	4.18	0.95	1.33
NEKEMTE 15	NEKEMTE 15	15	Z constant	3.63	0.95	1.33
AGARO 15	AGARO 15	15	Z constant	3.12	0.95	1.33
GILGEL GIBE 15	GILGEL GIBE 15	15	Z constant	1.65	0.95	1.33
ARBAMINCH 15	ARBAMINCH 15	15	Z constant	6.05	0.95	1.33
WOLAYITA SODDO 15	WOLAYITA SODDO	15	Z constant	5.14	0.95	1.33
Alaba15KV	ALABA 15	15	Z constant	2.2	0.95	1.33
AWASA 15	AWASA 15	15	Z constant	7.8	0.95	1.33
SHASHEMENE 15	SHASHEME 15	15	Z constant	12.1	0.95	1.33
DILLA I 15	DILLA I 15	15	Z constant	4.29	0.95	1.33
YIRGA ALEM 15	YIRGA ALEM 15	15	Z constant	3.86	0.95	1.33
SHAKISSO 15	SHAKISSO 15	15	Z constant	7.04	0.95	1.33
NEGELE BORENA 15	NEGELE BORENA 15	15	Z constant	1.65	0.95	1.33
BUTAJIRA 33	BUTAJIRA 33	33	Z constant	1.29	0.95	1.33
ASELA 15	ASELA 15	15	Z constant	6.4	0.95	1.33
BUTAJIRA 15	BUTAJIRA 15	15	Z constant	2.2	0.95	1.33
MIZAN 15	MIZAN 15	15	Z constant	1.65	0.95	1.33
MIZAN 33	MIZAN 33	33	Z constant	0.88	0.95	1.33
GHIMBI 15	GHIMBI 15	15	Z constant	1.65	0.95	1.33
FINCHAA 15A	FINCHAA 15A	15	Z constant	1.1	0.95	1.33
GONDER I 15B	GONDER I 15B	15	Z constant	0.55	0.95	1.33
GONDER I 15A	GONDER I 15A	15	Z constant	0.55	0.95	1.33
DANGLA 15	DANGLA 15	15	Z constant	3.74	0.95	1.33
WERETA 15	WERETA 15	15	Z constant	2.53	0.95	1.33
BAHIR DAR II 15A	BAHIR DAR II 15A	15	Z constant	5.4	0.95	1.33
BAHIR DAR I 15	BAHIR DAR I 15	15	Z constant	4.4	0.95	1.33
DEMBI DOLO 15	DEMBI DOLO 15	15	Z constant	2	0.95	1.33
FINCHA SUGAR II 15	FINCHA SUGAR II 15	15	Z constant	2.2	0.95	1.33
FINCHA SUGAR I 15	FINCHA SUGAR I 15	15	Z constant	2.75	0.95	1.33
GAMBELA 15	GAMBELA 15	15	Z constant	2	0.95	1.33
GONDER II 15	GONDER II 15	15	Z constant	8.25	0.95	1.33
ADWA 15	ADWA 15	15	Z constant	6.82	0.95	1.33
MAYCHEW 15	MAYCHEW 15	15	Z constant	1.21	0.95	1.33
WUKRO 15	WUKRO 15	15	Z constant	2.2	0.95	1.33
ADIGRAT 15	ADIGRAT 15	15	Z constant	3.3	0.95	1.33
ENDASELASIE 15	ENDASELASIE 15	15	Z constant	1.5	0.95	1.33
MEKELE 15	MEKELE 15	15	Z constant	12	0.95	1.33
ADIGRAT 66	ADIGRAT 66	66	Z constant	0	0.95	1.33

Appendix B: Generators Data

Table B- 1 Generators Data

Gen. Name	Sn [MVA]	Un [kV]	R/X [p.u.]	P [MW]	Q [MVAr]	cosphin [p.u.]	Pmin [MW]	Pmax [MW]	Qmin [MVAr]	Qmax [MVAr]
Fincha13.8 GR1	35	13.8	0.014	29		0.95	10	33.33	-16	14
Gilgel Gibe 13.8 GR1	73	13.8	0.0227	60		0.9	0	70	-21	21
Tis Abay II 10.5 GR1	40	10.5	0.018	27		0.9				
Tis Abay I 6.3 GR1	4.8	6	0.021	4		0.8	0	4	-2.9	2.9
Melka Wakena 13.8 GR1	45	13.8	0.016	35		0.85				
Fincha 13.8 GR4	40	13.8	0.019	25		0.95	0	28	-34	23
Dire Dawa Diesel 15	12.5	15	0.1	10	7.5		0	10	-10	10
Dire Dawa Diesel 15	12.5	15	0.1	10	7.5		0	10	-10	10
Dire Dawa Diesel 15	12.5	15	0.1	10	7.5		0	10	-10	10
Awash II GR2 10.5	20	10.5	0.022	6		0.9	3	15	-15	13
Melka Wakena 13.8 GR4	45	13.8	0.016	35		0.85	0	38.25	-42	35
Melka Wakena 13.8 GR3	45	13.8	0.016	35		0.85	0	38.25	-31.5	30.15
Melka Wakena 13.8 GR2	45	13.8	0.016	30		0.85	0	38.25	-31.5	30.15
Tis Abay I 6.3 GR2	4.8	6	0.021	4		0.8	0	4	-2.9	2.9
Tis Abay I 6.3 GR3	4.8	6	0.021	4		0.8	0	4	-3.84	3.84
Tis Abay II 10.5 GR2	40	10.5	0.018	27		0.9				
Awash II GR1 10.5	20	10.5	0.022	6		0.9	3	15	-15	13
Awash III GR2 10.5	20	10.5	0.022	9		0.9	3	15	-15	13
Awash III GR1 10.5	20	10.5	0.022	9		0.9	3	15	-15	13
Koka Hydro 10.5 GR2	18	10.5	0.032	10		0.9	0	13	-12	11.6
Koka Hydro 10.5 GR3	18	10.5	0.032	0		0.9	0	13	-18	13.5
Fincha 13.8 GR2	35	13.8	0.014	29		0.95	0	33.33	-16	14
Fincha 13.8 GR3	35	13.8	0.014	29		0.95	0	33.33	-16	14
Gilgel Gibe 13.8 GR2	73	13.8	0.0227	60		0.9	0	70	-21	21
Gilgel Gibe 13.8 GR3	73	13.8	0.0227	60		0.9	0	70	-21	21
TekUNIT1	86	13.8	0.1	66		0.9	0	78	-38	38
TekUNIT2	86.7	13.8	0.1	40		0.9	0	78	-38	38
TEKUNIT3	87.6	13.8	0.1	40		0.9	0	78	-38	38
TEKUNIT4	86.7	13.8	0.1	40		0.9	0	78	-38	38
Gilgel Gibe II UI	125	15	0.0227	95		0.85	0	105	-50	50
Gilgel Gibe II U2	125	15	0.0227	95		0.9	0	105	-50	50
Gilgel Gibe U3	125	15	0.0227	95		0.9	0	105	-50	50
Gilgel Gibe U4	125	15	0.0227	95		0.9	0	105	-50	50
BELES15B1	130	15	0.1			0.9				
BELES15B2	130	15	0.1			0.9				
BELES15B3	130	15	0.1			0.9				
BELES15B4	130	15	0.1			0.9				
GG III G1	220	15	0.0227	10		0.85	0	220	-100	100

Appendix C: Blackout Data

Table C- 1. The 2013 blackouts

Blackout	Start time	Total generation (MW)	Lost Load (MW)	Affected Regions	Affected Customers ($\times 10^6$)	Type	Cause of the blackout	Initiating events	Acted relays	Restoration time
28-Jan-2013	16:57	1108.2	746	All except NW	1.6	A	Natural (self-initiated fire)	EF on Sebeta II-GGII 400kV TL	Distance Overcurrent Over-frequency Under-frequency	23 min to 3 Hrs.
17-Feb-2013	14:54	1108.3	-	All except NW	-	-	N.a	EF on Kality I-Koka 132kV line	Distance Overcurrent Overvoltage Over-frequency	
2-Mar-2013	16:31	907	542		1.38		Aged Circuit breaker	Tripping of Melka wakena HPP	Overcurrent Distance Under-frequency	2.5 Hrs. to 3.5 Hrs.
6-Mar-2013	21:04	1334	737	All	2.4		N.a	Temporary earth fault on Ghedo-Gefersa 230kV line	Distance Under-frequency Over-current Under-excitation	40 min to 2 Hrs.
22-Apr-2013	19:35	1247	713		2.1		Suicide (one person was trying to kill himself by touching the transmission line)	EF on B/Dar II-D/Markos 400kV line	Distance Under-frequency Reverse power	45 min to 2 Hrs.
26-Apr-2013	13:10	1036	694		2.08		N.a	Tripping of Tekeze HPP (by over-frequency)	Over-frequency Load –rejection overload	30 min t0 3.5 Hrs.
22-May-2013	06:01	868.1	476		1.32		Loosely re-joined conductors from previous maintenance	Tripping of Koka & Awash III HPPs	Under – frequency Distance Overcurrent Load-rejection Overload	15 min to 6 Hrs.
25-May-2013			930		2.1		System stressful due to peak load conditions (system peak load was)	Tripping of Alamata – B/Dar 230kV line & Gefersa-Kality I 132kV line by overload protections	Overcurrent Turbine-governor lock out relay Under-frequency Voltage-loss	12 min to 3.5 Hrs.
27-Jul-2013			1104.62	All	2.4	A				15 min to 2.25 Hrs.
13-Sep-2013	20:08	1247.82	967	All	2.35		Stressful condition (overload)	Tripping of Mekanisa-Sebeta 132kV line	Overcurrent Under – frequency Turbine-governor lock	45 min to 2.75 Hrs.
7-Oct-2013	20:08	1247.82	967	All	2.35	A	System stressful due to peak load conditions (system peak load was)	Tripping of Alamata – B/Dar 230kV line & Gefersa-Kality I 132kV line by overload protections	Overcurrent Turbine-governor lock out relay Under-frequency Voltage-loss	15 min to 3 Hrs.

24-Oct-2013	23:55	702	684	All	1.5	A	Collapse of tower	L – G fault on Fincha HPP – D/Markos 230kV line	Distance Under-frequency Under-voltage Overload	48 min to 2.25 Hrs
12-Nov-2013	16:53	1118.91	522.2	Addis Ababa & Central Regions	1.2		N.a	EF on Sebeta I – Sebeta II 230kV transmission line	Distance Overcurrent Under-frequency Voltage loss	25 min to 45 min
17-Nov-2013	12:20	1115.89		All		A	Broken conductor (Kality I-Kality II 132kV TL was broken and fallen on the busbar of Kality I 132kV s/s)	Short circuit fault on Kality I 132kV busbar	Backup relay Over-frequency Over-voltage Load rejection	N.a
6-Dec-2013	8:04	1105.74	959.97	All	2.19	A	N.a	EF on Fincha HPP – D/Markos 230kV transmission line	EF start (In>1) Under-frequency	50 min to 2 Hrs.

Table C- 2. The 2014 blackouts of EEP

Blackout	Time	Total generation (MW)	Lost Load (MW)	Affected Regions	Affected Customers ($\times 10^6$)	Type	Cause of the blackout	Initiating events	Acted relays	Restoration time
2-Feb-2014	19:55	1279.71	1259.71	All	3.01	A	Broken conductor (aged transmission line)	Short circuit fault on Kality I- Kality II 132kV line	N.a	40 min to 2 Hrs.
5-Apr-2014	9:24	1091.61	593.9	A.A & Central regions	1.23	A	N.a	EF on Kality I-Sebeta I 230kV line	EF start (In>1) Under-frequency Reverse power Over-frequency Over-voltage	30 min to 3.5 Hrs.
13-Apr-2014	12:02	1169.21	1169.21	All except NW region	2.9	A	Contact with tree (lack of trimming)	EF on Gefersa-Addis North 132kV line	Distance Over-voltage Over-frequency Under-frequency Load-rejection	38 min to 4 Hrs.
8-Mar-2014	21:26	1279.51	980.82	All	3.01	A	N.a	EF trip on Alamata-B/Dar II 230kV line	EF start (In>1) Distance Overcurrent Under-frequency	18 min to 2 Hrs.
7-May-2014	9:45	1085.15	989.25	North, South, A.A, Central and South western regions	2.73	B	N.a	Tripping of Sebeta I-Kality I 230kV line, Sululta-Gefersa 230kV line I, & Sebeta II-Sebeta I 230kV lines due to EF	N.a	37 min to 2.5 Hrs.

11-May-2014	7:25	970.06	542.12	N.a	1.42	N.a	N.a	Tripping of Sebeta I 230/132kV transformer due to EF and Gelan 400/230kV transformer tripped with differential protection (external fault)	EF start (In>1) Differential protection Over-voltage Over-frequency	27 min to 3.5 Hrs.
17-Jun-2014	12:57	1342.73	1127.43	-	2.5	-	Protection hidden failure (relay setting problems)	Tripping of Fincha HPP – Ghedo 230kV line without any reason	Overcurrent Under-frequency Under-voltage	31 min to 4.25 Hrs.
8-Aug-2014	23:17	882.07	872.07	All	3	A	Protection failure False teleprotection signal	Tripping of Beles HPP-B/Dar II 400kV line II with distance protection device fail and teleprotection fail signal	Distance Under-frequency overcurrent	56 min to 8.75 Hrs.
3-Sep-2014	23:17	1239.02	948.14	All	3.01	A	Protection failure False teleprotection signal	Tripping of Beles HPP-B/Dar II 400kV line II with distance protection device fail and teleprotection fail signal	Distance Under-frequency overcurrent	21 min to 11 Hrs.
24-Oct-2014	16:16	1079.71	1079.71	All	3.1	A	N.a	Tripping of B/Dar II – Beles HPP 400kV by overvoltage	N.a	26 min to 3.75 Hrs.
6-Nov-2014	23:57	826.5	789.68	All	2.9	A	Less reactive power reserve in the system System was stressful due to overloads	Gondar II-Shehedi 230kV line was tripped by under-voltage protection	Under-voltage Over-voltage Over-frequency Overcurrent	1 Hr. to 7 Hrs.

Table C- 3. The 2015 blackouts of EEP

Blackout	Time	Total generation (MW)	Lost Load (MW)	Affected Regions	Affected Customers ($\times 10^6$)	Type	Cause of the blackout	Initiating events	Acted relays	Restoration time
15-Jan-2015	16:11	1176.25	455	Western, 1st and 2nd stage of under-frequency loads at A.A region	1.6	B	N.a	N.a	N.a	15 min to 4 Hrs.
15-Mar-2015	14:30	983	983.31	All areas except B/Dar & Gondar	4		N.a	Tripping of B/Dar-D/Markos 400kV line with a loading of 318 MW by EF on phase A & phase B	Distance Overload Reverse power Under-frequency Phase-unbalance	50 min to 4 Hrs.
22-Apr-2015	20:20	1306.25	1308.95	All	4	A	N.a	Tripping of Fincha – D/Markos 230kV line due to EF on phase B with a fault level of 1.858kA	EF start (In>1) Under- frequency relays	1 Hr. to 8 Hrs.
8-May-2015	01:54	746.38	745.38	All	4	A	Natural (heavy rain and storm)	Transient earth fault on phase B of (B/DarII-D/Markos 400kV line)	Under-frequency Overcurrent Over-voltage	1.25 hrs. to 8 hrs.
26-May-2015	6:43	1077.1	509.1	A.A, Central, East, South, North and North East regions	2.4	B	Lack of trimming (contact with trees)	EF on G/Gibe II-Sebeta II 400kV line	Distance Over-frequency Overcurrent Under-frequency	43 min to 5 hrs.
27-Jul-2015	14:34	1261.21	1175.11	All except some NW regions	4.2	A	Lack of trimming (contact with tree)	Permanent EF on G/Gibe II-Sebeta II 400 kV line (L-G fault on phase C)	Distance Overcurrent (most lines) Under-frequency (most HPPs) Over-voltage (some lines)	44 min to 22 hrs.
14-Aug-2015	10:00	1419.9	1029	All areas except NW	4	A	Self-initiated fire as a result conductor broken and fallen on earth	Tripping of Gefersa-Addisalem 45kV line due to EF	Overcurrent EF Over-voltage Loss of voltage Under-frequency	28 min to 3.75 hrs.
28-Nov-2015	12:31	1318:04	1401.04	All	4.2	A	Natural & self-initiated fire Protection hidden failure	Tripping of GERD- Beles 400kV lines by EF; following this Beles HPP was tripped by false teleprotection signal	Teleprotection Under-frequency Overcurrent Loss of voltage	35 min to 8 hrs.

29-Nov-2015	19:27	1145.2	988.32	All	4	A	False teleprotection command	Tripping of Beles HPP	Under-frequency Overcurrent Loss of voltage	38 min to13.5 hrs.
11-Dec-2015	5:53	880.62	772.38	All	3.6	A	N.a	EF (L-G fault) on Mekanisa-Kality I 132kV line, following this Gefersa-Kality I and Gefersa-Mekanisa 132kV lines were tripped by overload	Earth fault start (In>1) Overcurrent Under-frequency	45 min to 5.25 hrs.
22-Dec-2015	15:07	1349.43	809.43	All	4	A	N.a	Tripping of Sululta- Gefersa 230kV line by EF	Distance Underfrequency Overfrequency	46 min to 3.5 hrs.
25-Dec-2015	4:34	838.96	874.05	All	4	A	Operator misjudgement (switching transient)	Tripping of 400/230kV transformers (I&II) at B/Dar II substation by overvoltage	Overvoltage Underfrequency Reverse power Undervoltage Overcurrent	31 min to 5.5 hrs.

Table C- 4. Some 2016 blackouts

Blackout	Time	Total generation (MW)	Lost Load (MW)	Affected Regions	Affected Customers ($\times 10^6$)	Type	Cause of the blackout	Initiating events	Acted relays	Restoration time
6-Jan-2016	16:16	1340.18	975	Except NW	3.8	B	N.a	Tripping of G/Gibe II-Sekoru II 400kV line by EF Tripping of Gibe II-Sebeta II 400kV line without reason	Distance Under-frequency Overvoltage Overcurrent	20 min to 2.5 hrs.
17-Jan-2016	07:59	1322.61	1300.81	All	4.2	A	Operator misjudgement (when the power plant maintenance team transfer the DC supply (excitation system and other auxiliary systems)from bank A to bank B)	Tripping of Beles HPP	Underfrequency Undervoltage Overload	25 min to 3 hrs.

Appendix D: Shunt Compensators

Table D- 1 Shunt Reactors

Node 1	Element Name	Network Level	Sn [MVA]	Vcu [kW]	Vfe [kW]	Un [kV]
DIRE DAWA III 132 BB1	DIRE DAWA III SHR	132	8	24	0	132
COMBOLCHA 132	COMBOLCHA SHR	132	10	30	0	132
AGARO 15	AGARO SHR	15	5	29.45	0	15
SHASHEMENE 132	SHASHEMENE SHR	132	12	49	0	132
BAHIR DAR II 230 BB1	BAHIR DAR II SHR	230	15	39.286	18.414	230
N1853	SHR1280	400	45	55.27	38.05	400
Bahir Dar 400KV	SHR1291	400	0	0	0	400
Sululta 400KV	SHR1305	400	45	118.2	0	400
endeselase230KV	SHR1316	230	15	60.3	0	230
N1892	SHR1318	230	15	60.3	0	230
N1948	SHR1321	230	15	60.3	0	230
HUMERA230KV	SHR1323	230	15	60.3	0	230
HUMERA230KV	SHR1324	230	15	60.3	0	230
N1922	SHR1346	230	15	80	0	230
N1923	SHR1347	230	15	80	0	230
SEMERA230KV	SHR1349	230	15	65	0	230
N1929	SHR1353	230	15	65	0	230
N1932	SHR1354	230	15	65	0	230
GG OLD 400KV	SHR1370	400	45	55.27	38.05	400
PK 12	SHR1400	230	15	65	0	230
Adigala	SHR1402	230	10	50	0	230
PK 12	SHR1405	230	10	50	0	230
Shehedi	SHR1456	230	15	70	0	230
GONDER II 230	SHR1457	230	15	70	0	230
Hurso 230	SHR1513	230	15	28.51	23.24	230
KOKA 230	SHR1515	230	15	28.51	23.24	230
Hurso 230	SHR1518	230	15	28.51	23.24	230
KOKA 230	SHR1520	230	15	28.51	23.24	230
Hurso 230	SHR1526	230	15	65	0	230
Gambela-Metu	SHR1670	230	15	39.296	18.414	230
METU230KV	Metu 230	230	15	39.296	18.414	230
D/Markos 400KV	SHR1674	400	45	118.2	0	400

Table D- 2 Shunt Capacitors

Node 1	Element Name	Network Level	Sn [MVA]	Vdi [kW]	Un [kV]
SEBETA 2 400KV	SHC1282	400	90	0	400
SEBETA 2 33	SHC1284	230	45	10	230
Gelan	SHC1283	400	90	0	400

Appendix E: Simulation Results

E.1 Dynamic Simulation Results of August 14th 2015 Blackout

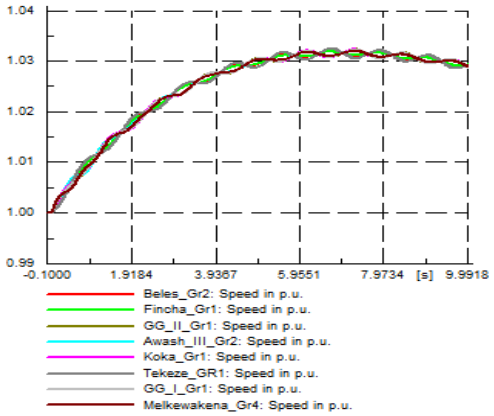

(a)

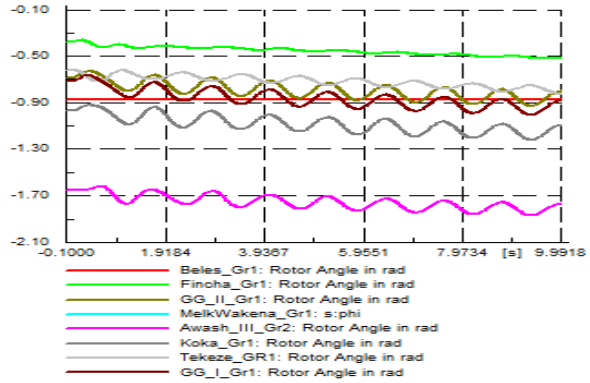

(b)

Figure E- 1 (a) speed and (b) rotor angles of HPP generators during the fault

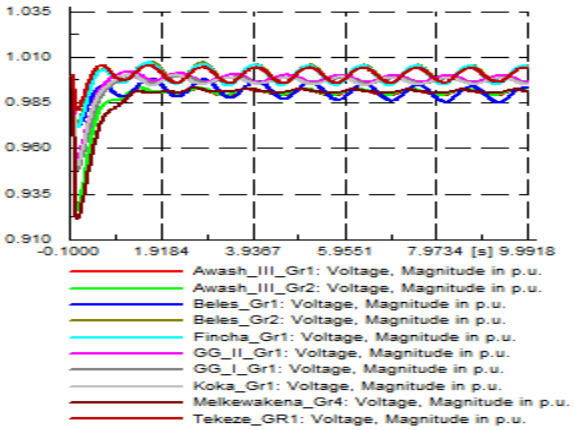

(a)

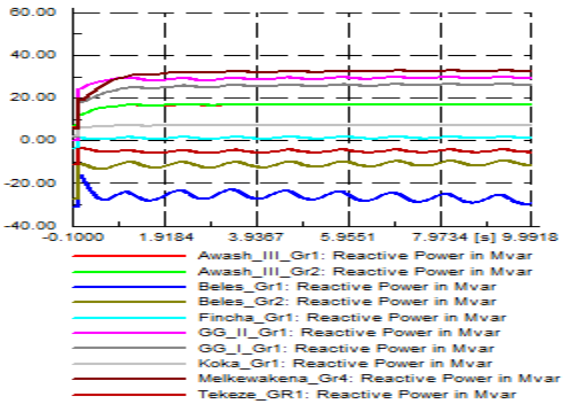

(b)

Figure E- 2 (a) terminal voltages and (b) reactive power drawn from generators during the fault

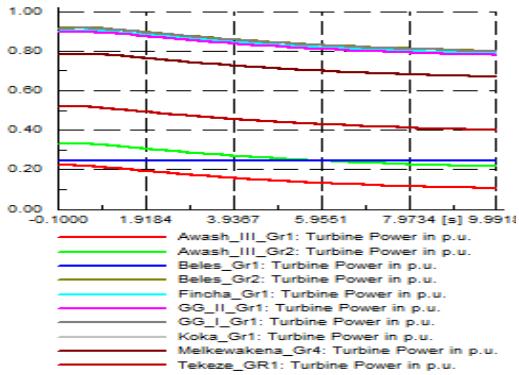

(a)

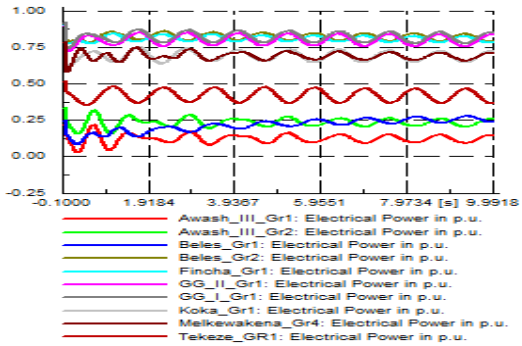

(b)

Figure E- 3 (a) mechanical input power, (b) electrical power output of generators during the fault

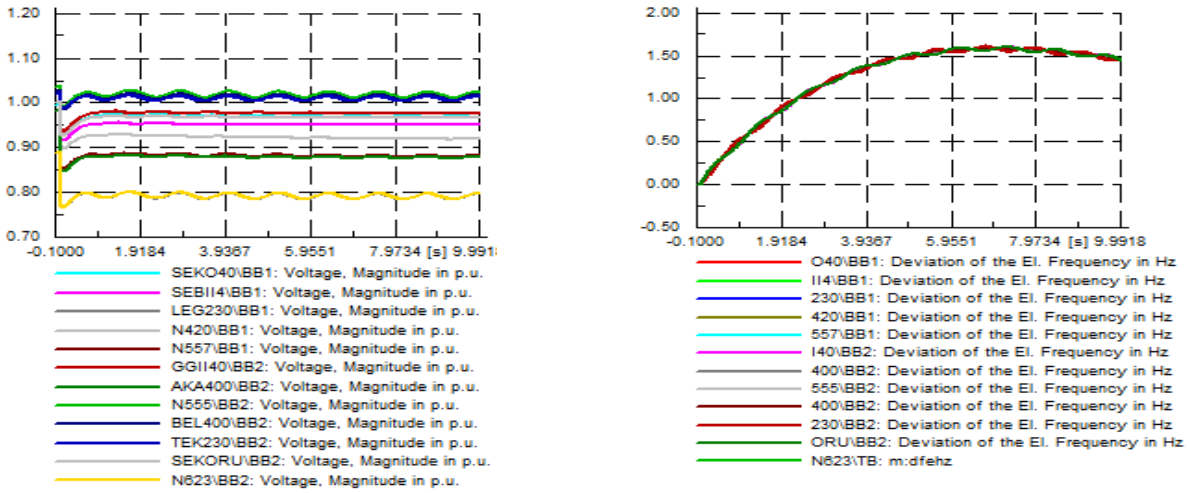

(a) (b)

Figure E- 4 (a) voltages, (b) frequency deviations at important substation buses during the fault

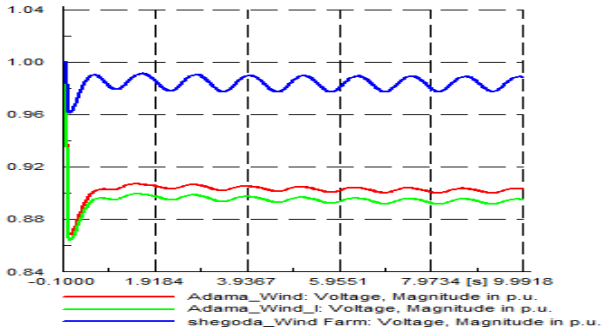

Figure E- 5 Voltages at wind power plant buses during the fault

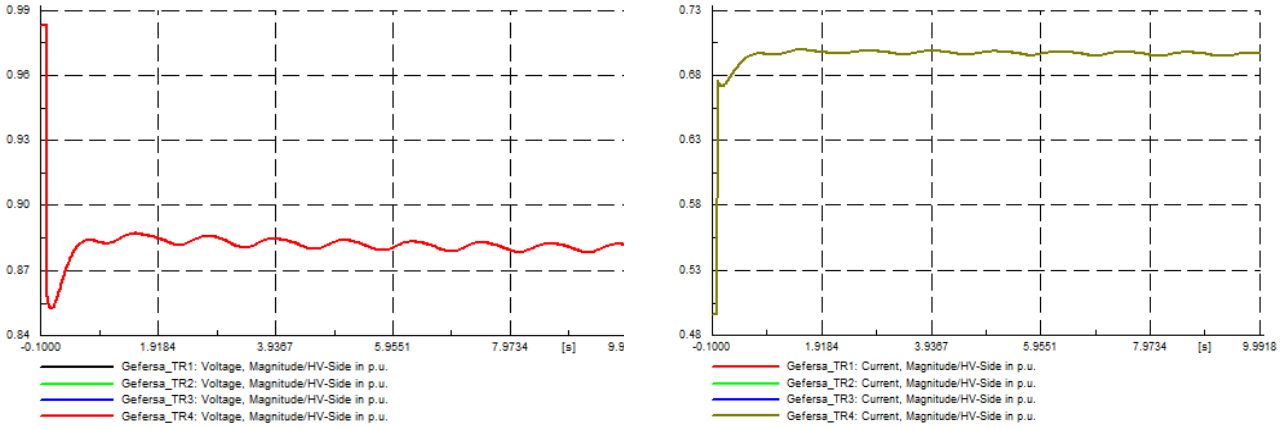

(a) (b)

Figure E- 6 (a) voltage, (b) currents of Gefersa 230/132kV transformers during the fault

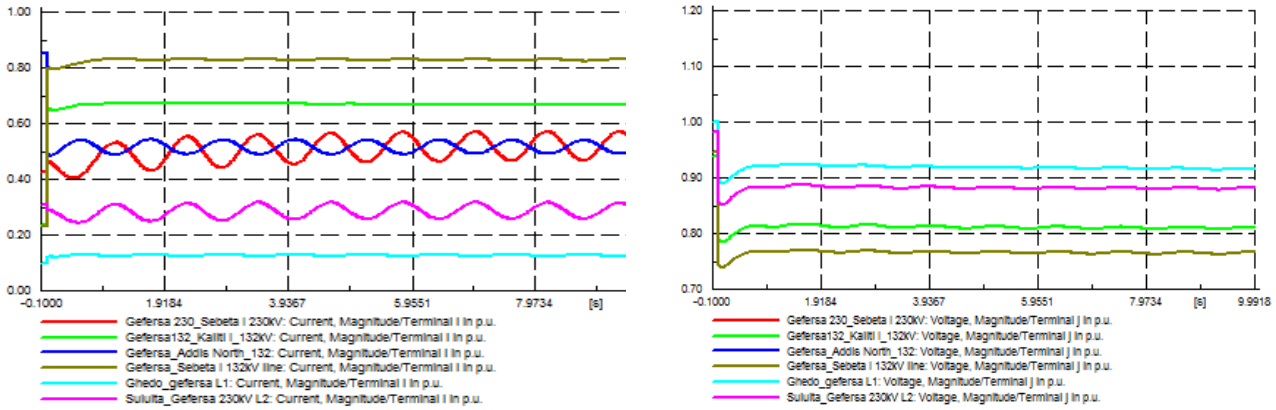

(a) (b)

Figure E- 7 (a) currents, (b) voltages on lines the come in and out of Gefersa substation during the fault

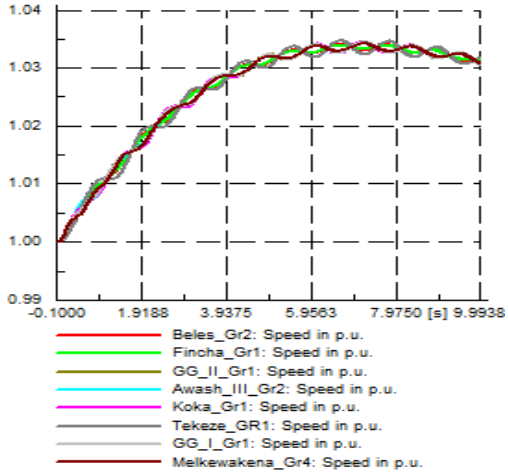

(a)

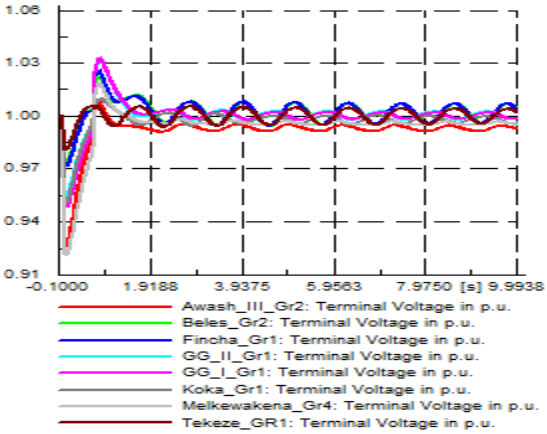

(c)

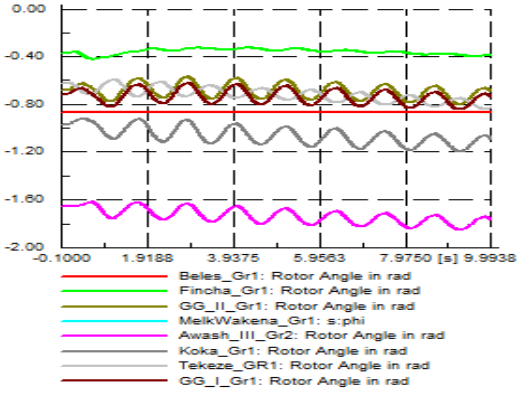

(b)

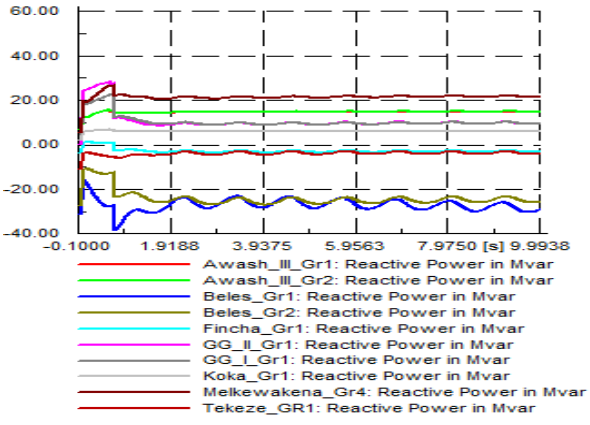

(d)

Figure E- 8 (a) speed, (b) rotor angle, (c) terminal voltage, and (d) reactive power drawn from generators after SE-1

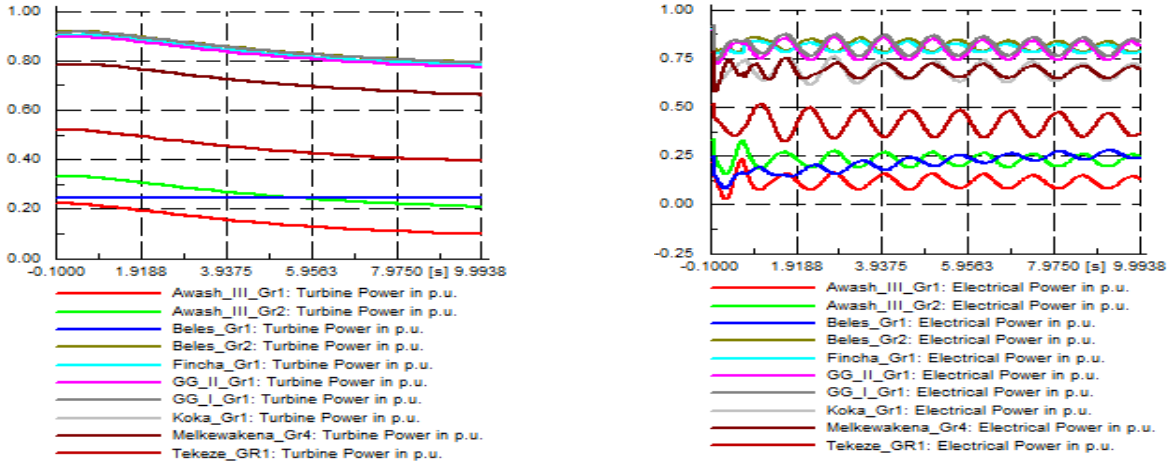

(a) (b)

Figure E- 9 (a) mechanical power inputs, (b) electrical power outputs of generators after SE-1[10]

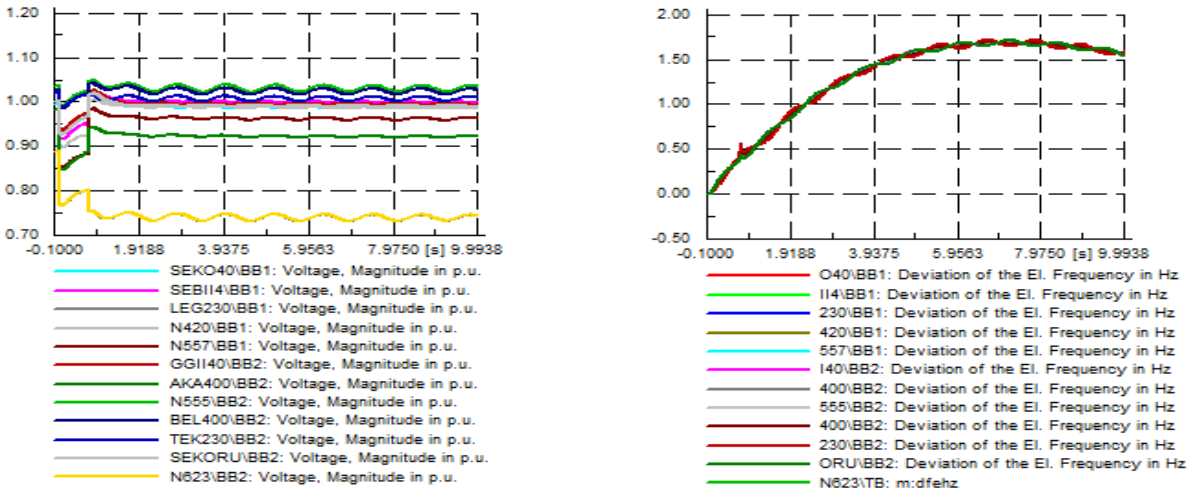

(a) (b)

Figure E- 10 (a) voltages at critical buses and (b) their corresponding frequency deviations after SE-1

[9]*SE-1: includes tripping of Gefersa 230/132kV transformers (TR1_TR4), Sebeta I_Gefersa 132kV line & Kality I_Gefersa 132kV line.*

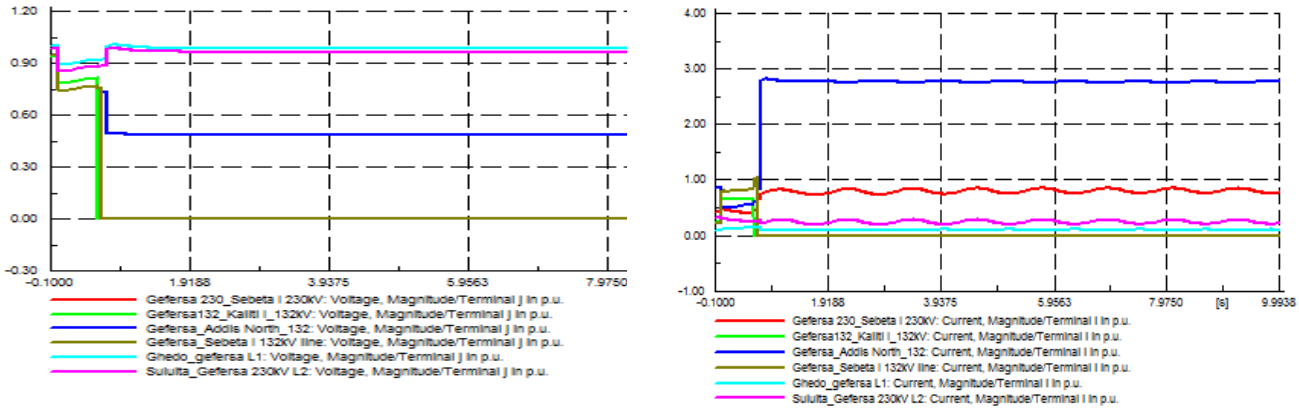

(a) (b)

Figure E- 11 (a) voltages, (b) currents of incoming and outgoing lines of Gefersa substation after SE-1

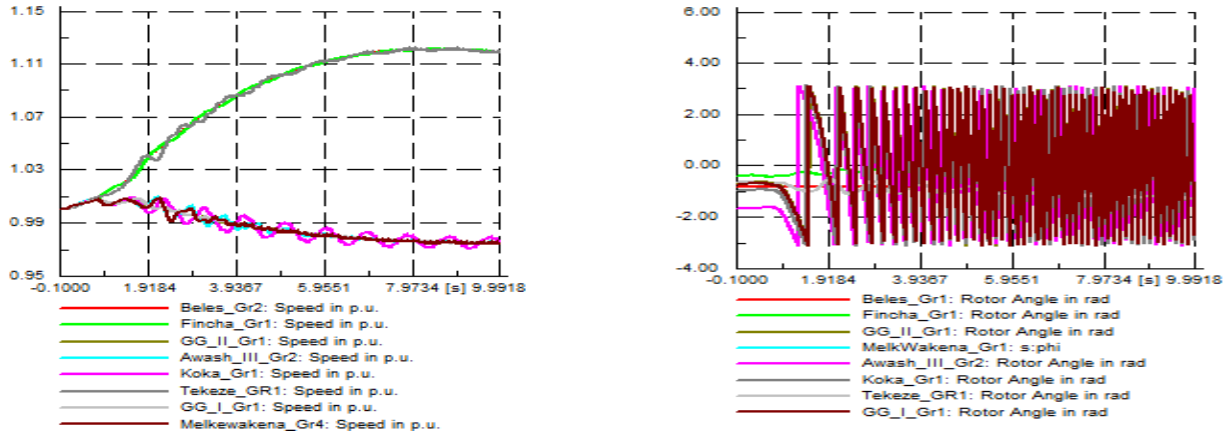

(a) (b)

Figure E- 12 (a) speed, (b) rotor angles of HPP generators after SE-2

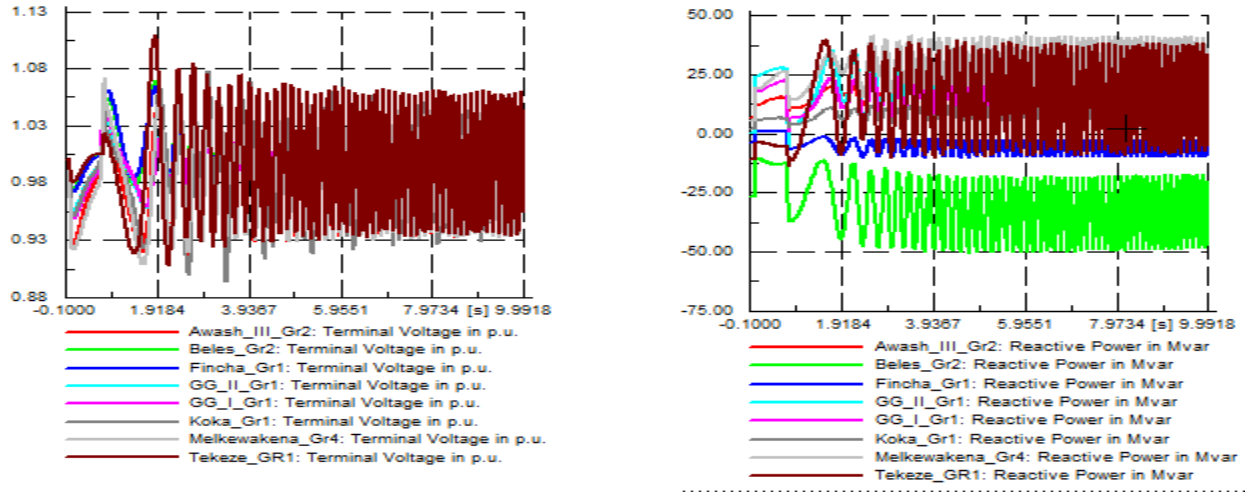

(a) (b)

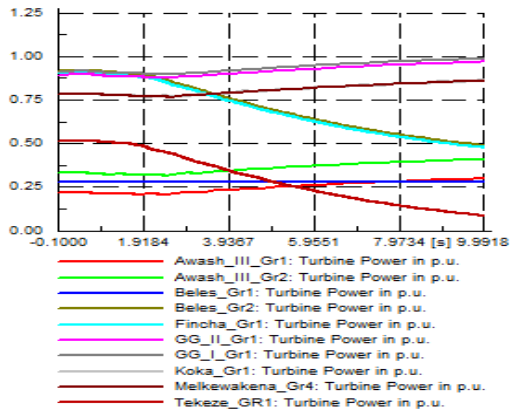

(c)

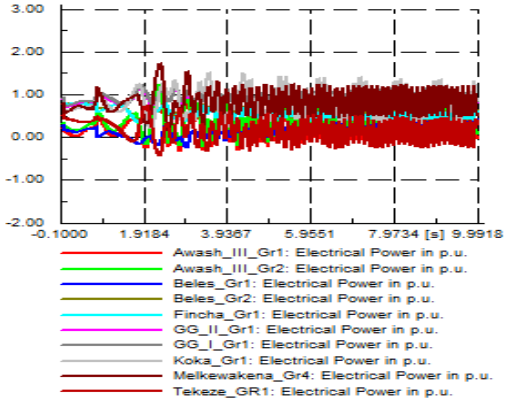

(d)

Figure E- 13 (a) terminal voltages, (b) reactive power, (c) turbine power, (d) electrical power output of HPP generators after SE-2

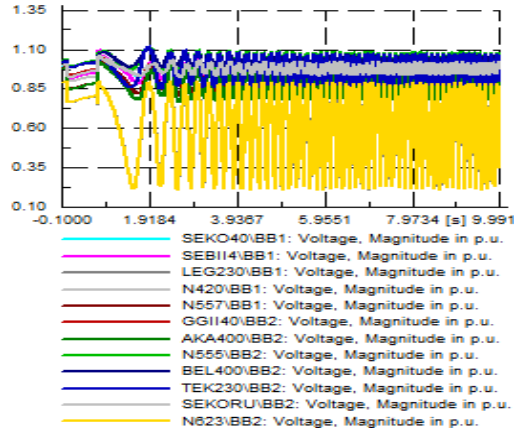

(a)

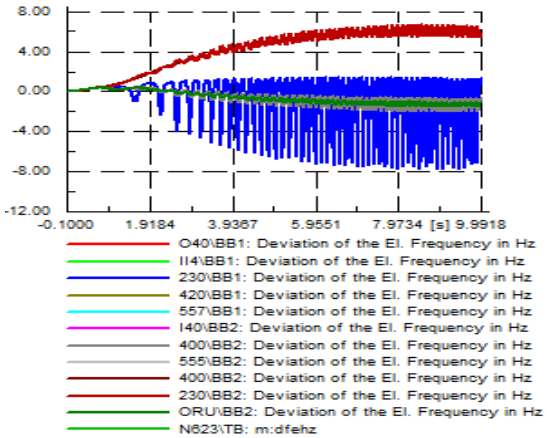

(b)

Figure E- 14 (a) voltages of important substation buses, (b) their corresponding frequency deviations after SE-2

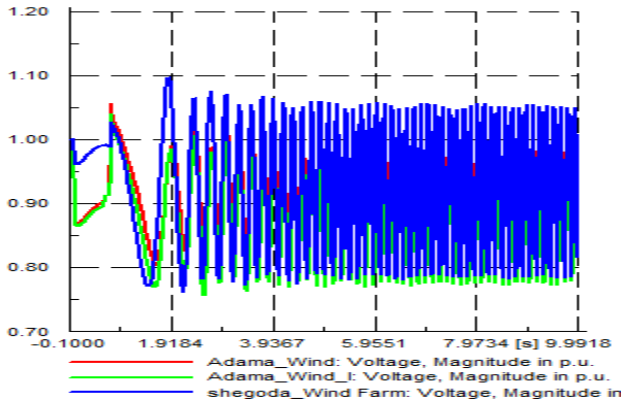

Figure E- 15 voltage at wind plant buses after SE-2

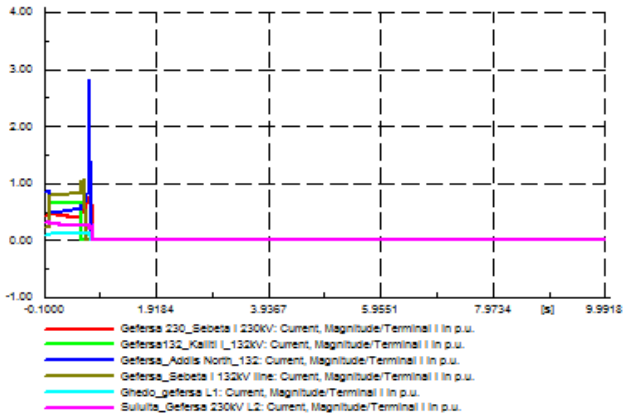

(a)

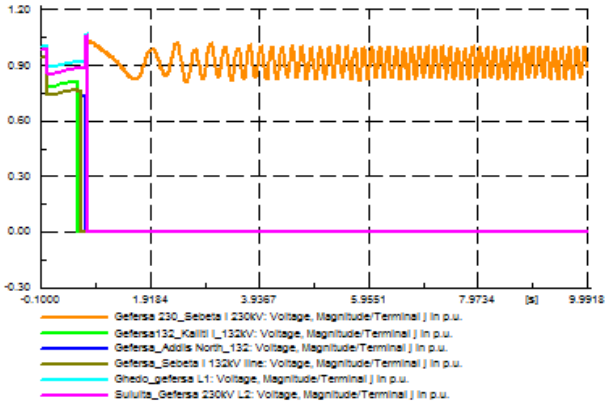

(b)

Figure E- 16 (a) Currents, (b) voltages of incoming and outgoing lines at Gefersa substation after SE-2[11]

E.2 Dynamic Simulations Results of December 11th 2015 blackout

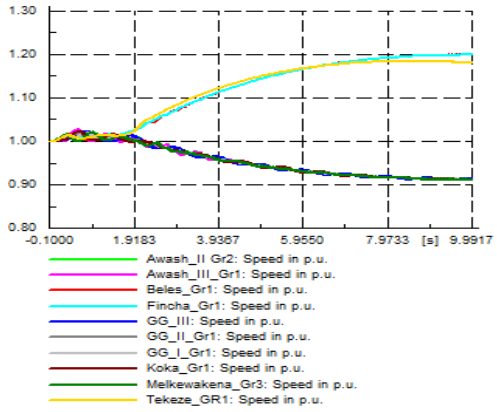

(a)

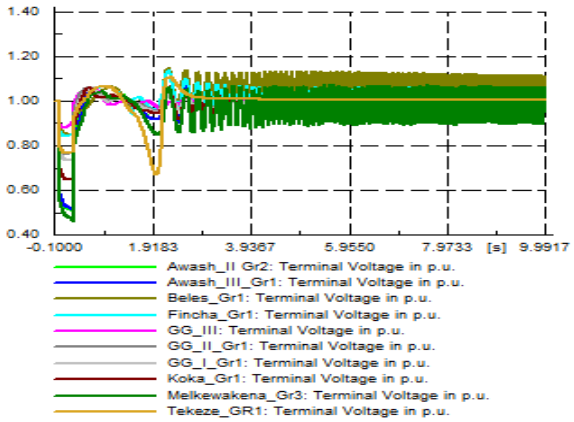

(c)

(b)

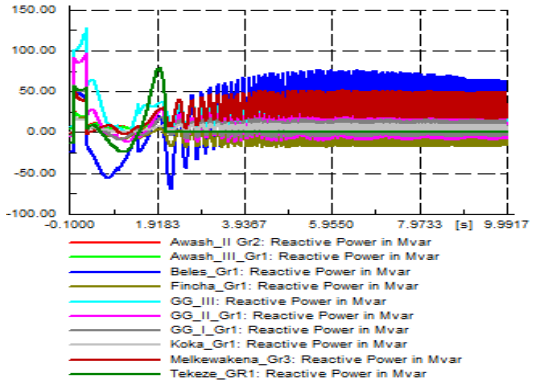

(d)

[11] *SE-2 includes the tripping of Sululta_Gefersa 230kV line I, Ghedo_Gefersa 230kV line and Gefersa_Addis North 132kV line*

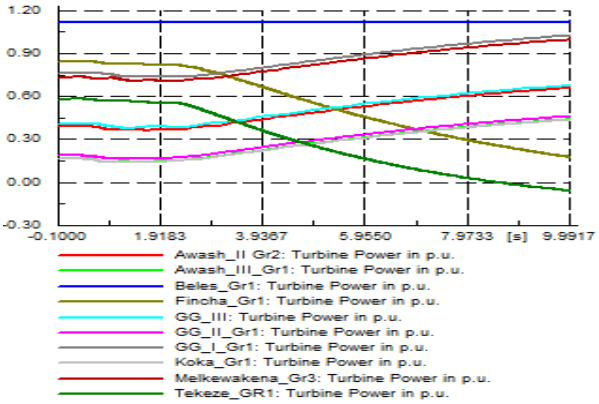

(e)

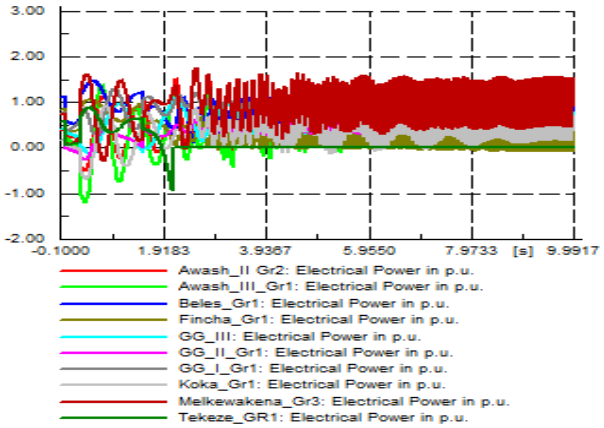

(f)

Figure E- 17 (a) speed, (b) rotor angles, (c) terminal voltage, (d) reactive power supplied by, (e) turbine power input to, (f) electrical power output of each HPP generators after SE-2

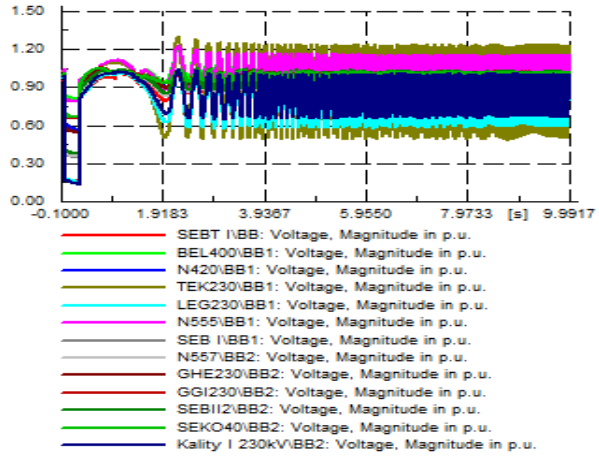

(a)

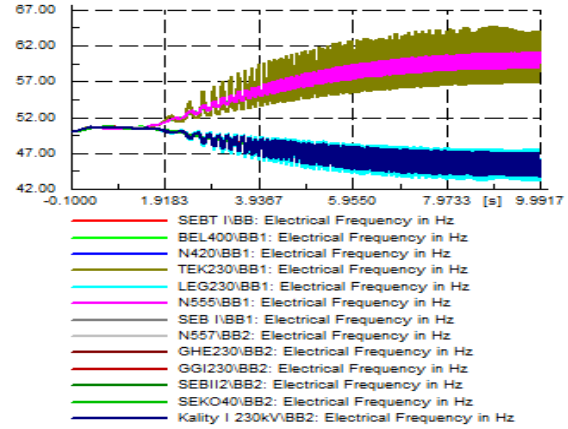

(b)

Figure E- 18 (a) bus voltages, (b) their corresponding frequencies at critical buses after SE-2

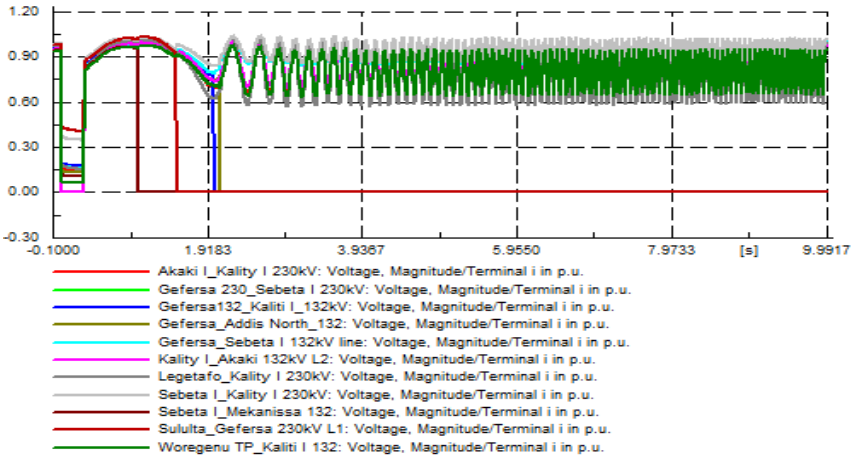

(a)

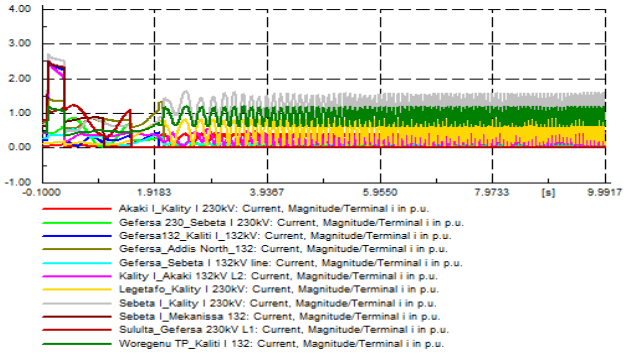

(b)

Figure E- 19 (a) voltage across, (b) current through transmission lines after SE-2

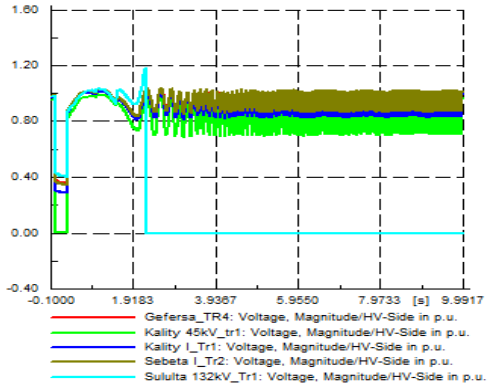

a)

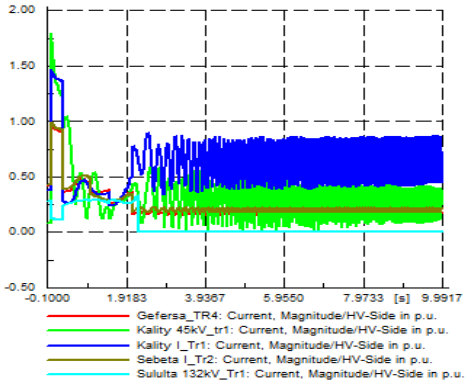

b)

Figure E- 20 (a) voltage across, (b) current through transformers after SE-2

E.2.1 Generator out of step (pole slip) conditions

```
DIgSI/pcl  - (t=02:542 s) 'EEP_Grid_IV\Awash_III_Gr2.ElmSym':
DIgSI/pcl  - (t=02:542 s) Generator out of step (pole slip).
DIgSI/pcl  - (t=02:552 s) ------------------------------------------------------
DIgSI/pcl  - (t=02:552 s) 'EEP_Grid_IV\Awash_II Gr2.ElmSym':
DIgSI/pcl  - (t=02:552 s) Generator out of step (pole slip).
DIgSI/pcl  - (t=02:562 s) ------------------------------------------------------
DIgSI/pcl  - (t=02:562 s) 'EEP_Grid_IV\Koka_Gr1.ElmSym':
DIgSI/pcl  - (t=02:562 s) Generator out of step (pole slip).
DIgSI/pcl  - (t=02:562 s) ------------------------------------------------------
DIgSI/pcl  - (t=02:562 s) 'EEP_Grid_IV\Koka_Gr2.ElmSym':
DIgSI/pcl  - (t=02:562 s) Generator out of step (pole slip).
DIgSI/pcl  - (t=02:572 s) ------------------------------------------------------
DIgSI/pcl  - (t=02:572 s) 'EEP_Grid_PART II\Amertinesh_Gr1.ElmSym':
DIgSI/pcl  - (t=02:572 s) Generator out of step (pole slip).
DIgSI/pcl  - (t=02:572 s) ------------------------------------------------------
DIgSI/pcl  - (t=02:572 s) 'EEP_Grid_PART III\GG_II_Gr2.ElmSym':
DIgSI/pcl  - (t=02:572 s) Generator out of step (pole slip).
DIgSI/pcl  - (t=02:572 s) ------------------------------------------------------
DIgSI/pcl  - (t=02:572 s) 'EEP_Grid_PART III\GG_II_Gr3.ElmSym':
DIgSI/pcl  - (t=02:572 s) Generator out of step (pole slip).
DIgSI/pcl  - (t=02:572 s) ------------------------------------------------------
DIgSI/pcl  - (t=02:572 s) 'EEP_Grid_PART III\GG_II_Gr4.ElmSym':
DIgSI/pcl  - (t=02:572 s) Generator out of step (pole slip).
DIgSI/pcl  - (t=02:572 s) ------------------------------------------------------
DIgSI/pcl  - (t=02:572 s) 'EEP_Grid_PART III\GG_II_Gr1.ElmSym':
DIgSI/pcl  - (t=02:572 s) Generator out of step (pole slip).
DIgSI/pcl  - (t=02:572 s) ------------------------------------------------------
DIgSI/pcl  - (t=02:572 s) 'EEP_Grid_PART III\GG_III.ElmSym':
DIgSI/pcl  - (t=02:572 s) Generator out of step (pole slip).
DIgSI/pcl  - (t=02:582 s) ------------------------------------------------------
```

```
DIgSI/pcl  - (t=02:582 s) ---------------------------------------------
DIgSI/pcl  - (t=02:582 s) 'EEP_Grid_IV\Melkewakena_Gr3.ElmSym':
DIgSI/pcl  - (t=02:582 s) Generator out of step (pole slip).
DIgSI/pcl  - (t=02:592 s) ---------------------------------------------
DIgSI/pcl  - (t=02:592 s) 'EEP_Grid_PART II\GG_I_Gr2.ElmSym':
DIgSI/pcl  - (t=02:592 s) Generator out of step (pole slip).
DIgSI/pcl  - (t=02:592 s) ---------------------------------------------

DIgSI/pcl  - (t=02:602 s) ---------------------------------------------
DIgSI/pcl  - (t=02:602 s) 'EEP_Grid_PART II\GG_I_Gr1.ElmSym':
DIgSI/pcl  - (t=02:602 s) Generator out of step (pole slip).
DIgSI/pcl  - (t=02:602 s) ---------------------------------------------
DIgSI/pcl  - (t=02:602 s) 'EEP_Grid_PART II\GG_I_Gr3.ElmSym':
DIgSI/pcl  - (t=02:602 s) Generator out of step (pole slip).
DIgSI/pcl  - (t=03:482 s) ---------------------------------------------
DIgSI/pcl  - (t=03:482 s) 'EEP_Grid_PART I\Tekeze_GR1.ElmSym':
DIgSI/pcl  - (t=03:482 s) Generator out of step (pole slip).
```

E.3 Dynamic Simulation Results of January 6th 2016 Blackout

E.3.1 Behaviour of the power system before and during the fault

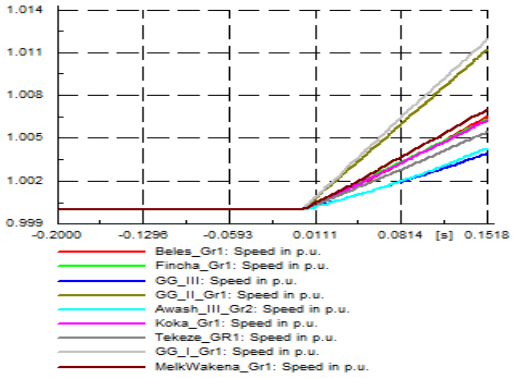

(a)

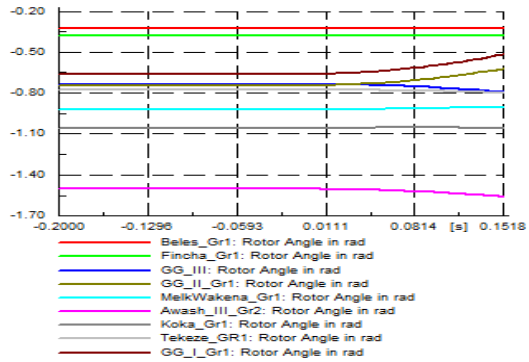

(b)

Figure E- 21 (a) the speed and (b) rotor angles of generators before and during the fault

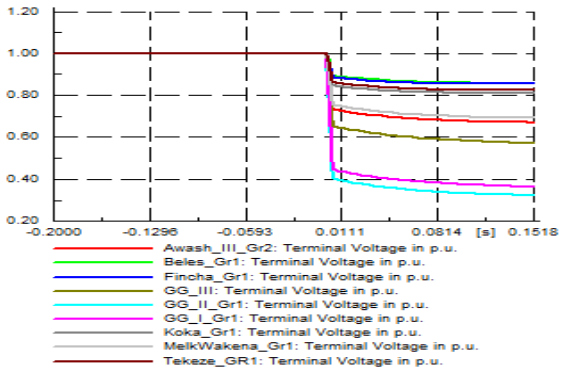

(a) Terminal voltage in pu

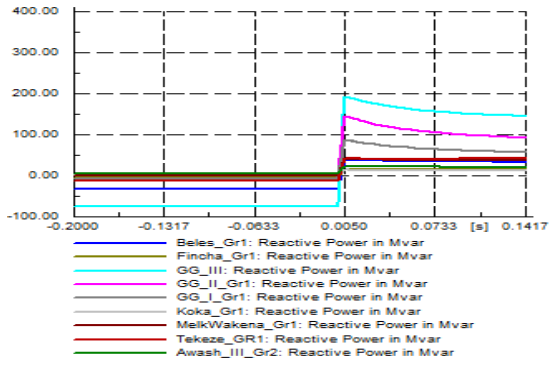

(b) Reactive power in MVar

Figure E- 22 (a) terminal voltage, (b) reactive power supplied by generators before and during disturbance

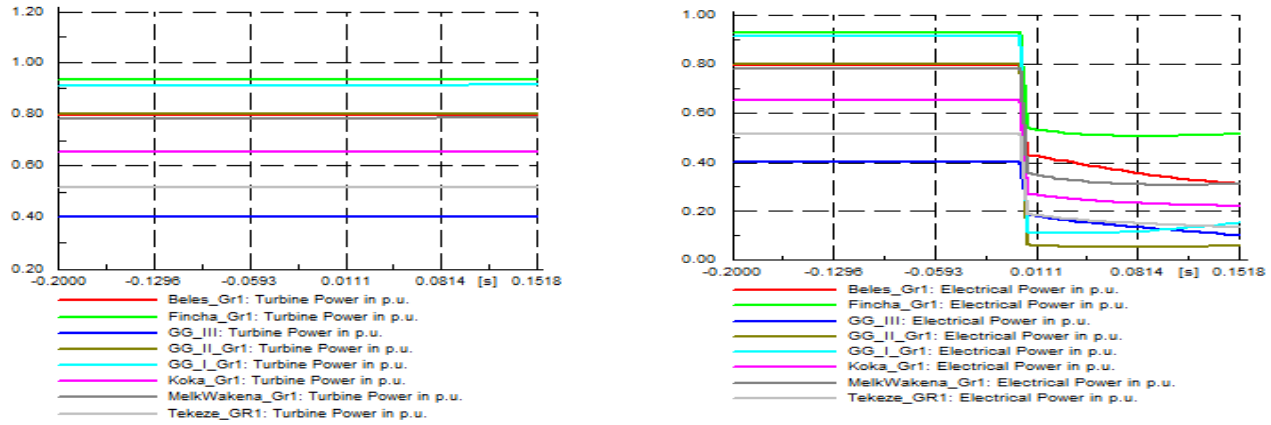

(a) (b)

Figure E- 23 (a) turbine power input to, (b) electrical output of generators before and during disturbance

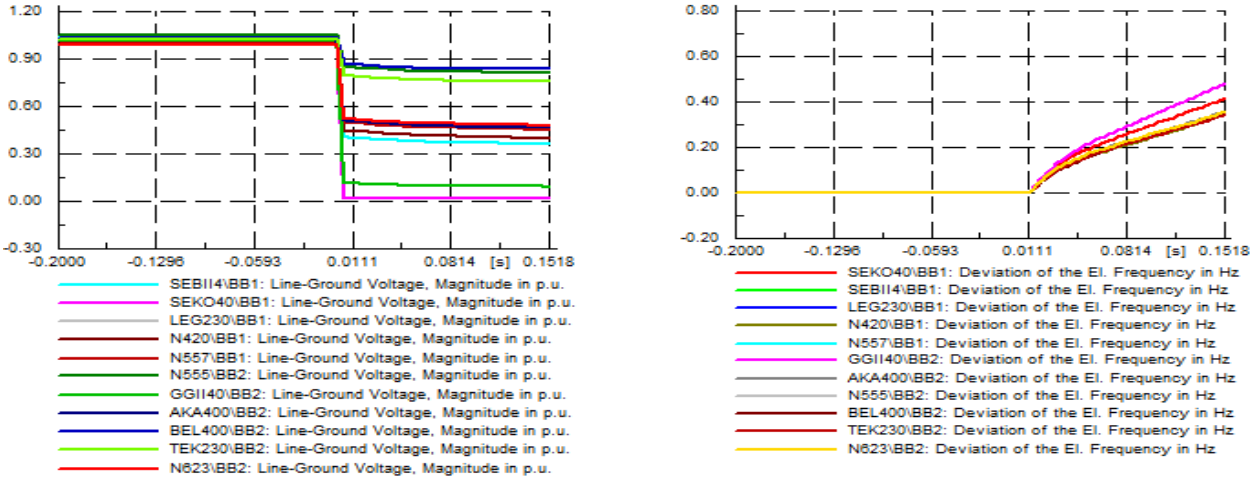

(a) (b)

Figure E- 24 (a) bus voltages, (b) frequency deviations at critical buses before and during disturbance.

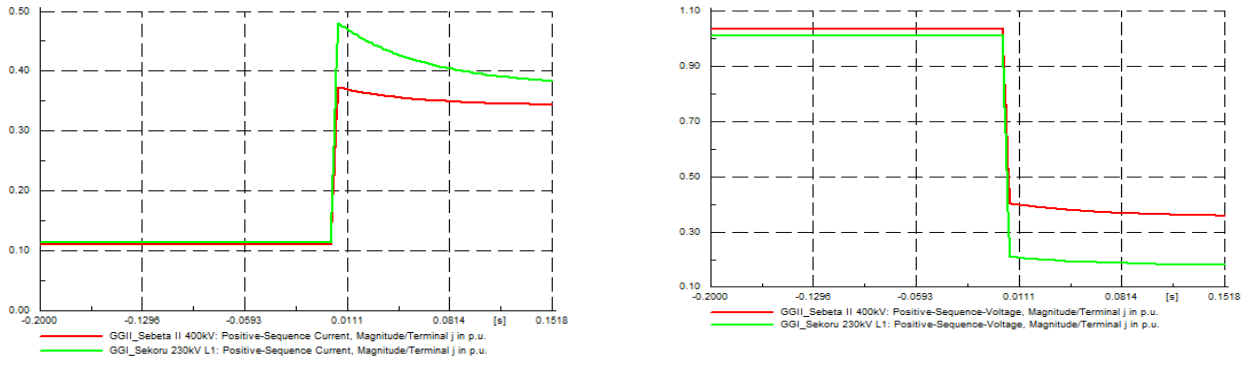

(a) (b)

Figure E- 25 (a) current through, (b) voltage across lines before and during disturbance

E.4 Dynamic Simulation Results of December 22nd 2015 Blackout

E.4.1 Behaviour of the power system before and during the fault

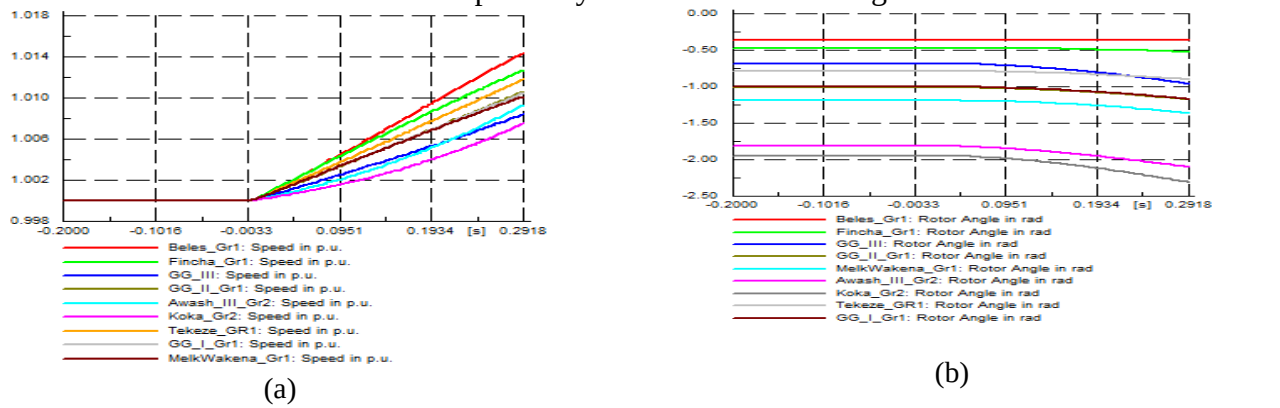

(a) (b)

Figure E- 26 (a) speed, (b) rotor angles of HPP generators before and during the disturbance

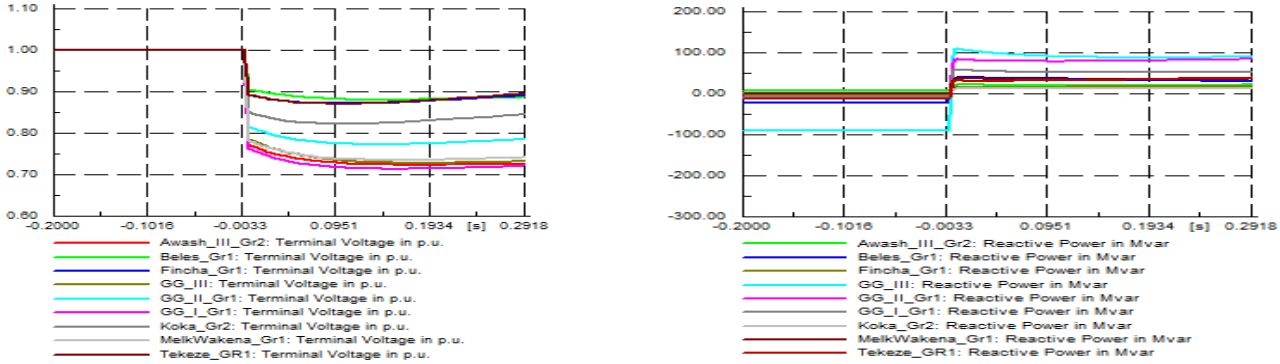

(a) (b)

Figure E- 27 (a) terminal voltage, (b) reactive power supplied by HPP generators before and during disturbance

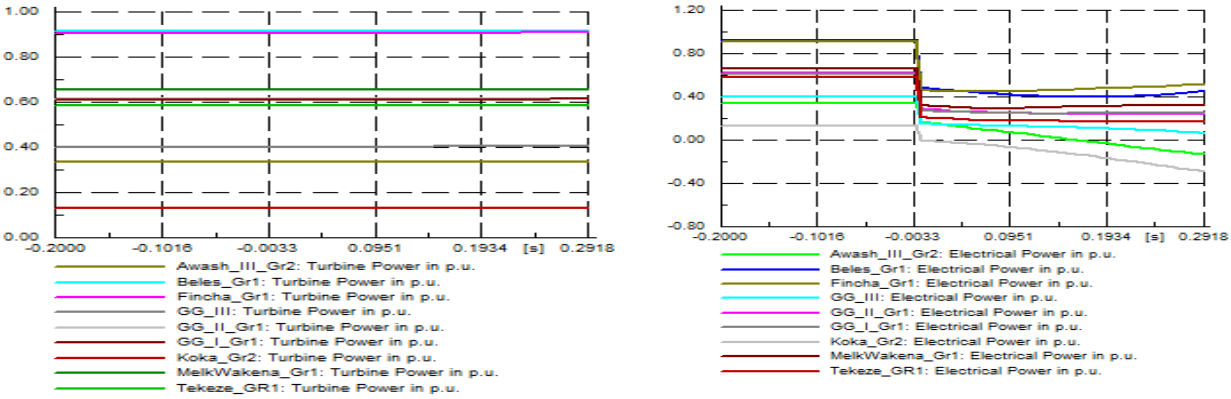

(a) (b)

Figure E- 28 (a) turbine power input, (b) electrical power output of each HPP generator

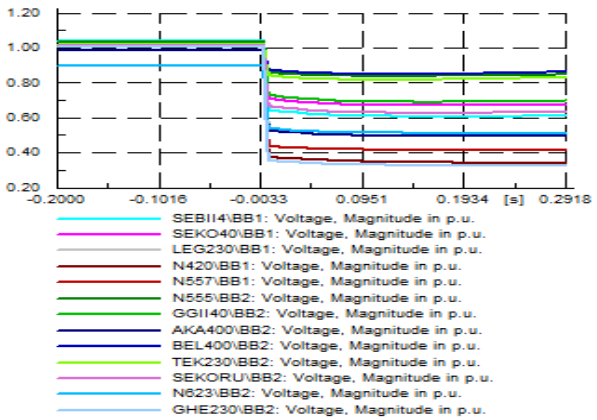

(a)

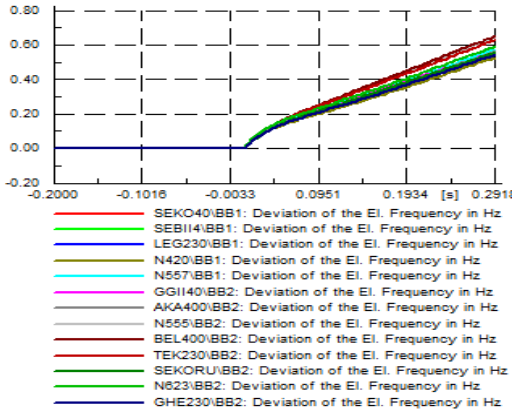

(b)

Figure E- 29 (a) bus voltages, (b) their corresponding frequency deviations at critical buses

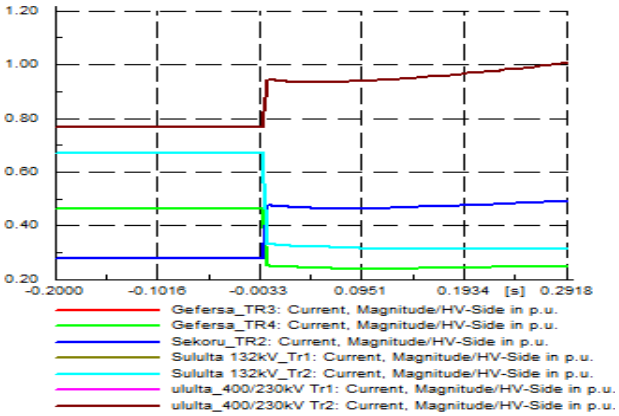

(a)

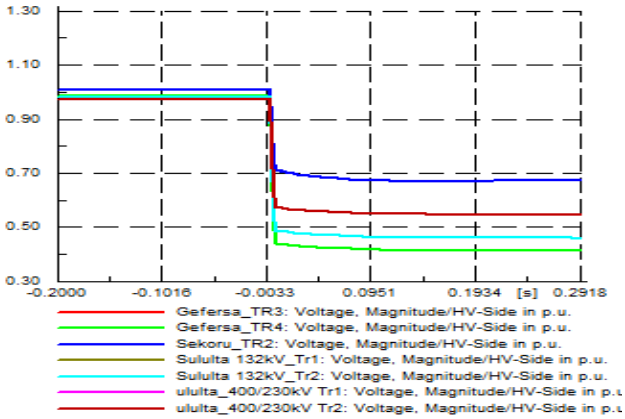

(b)

Figure E- 30 (a) current through, (b) voltage across each transformer of the disturbance area

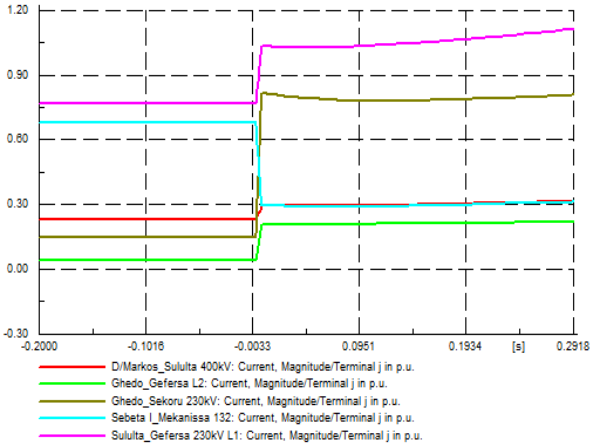

(a)

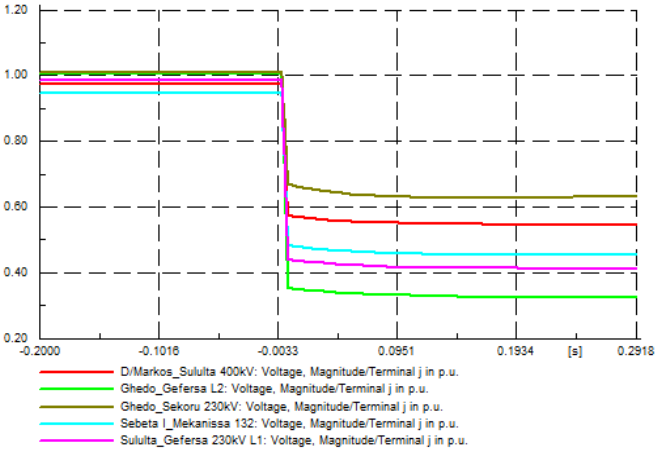

(b)

Figure E- 31 (a) current through, (b) voltage across each line of the disturbance area.

Appendix F: EEP Grid

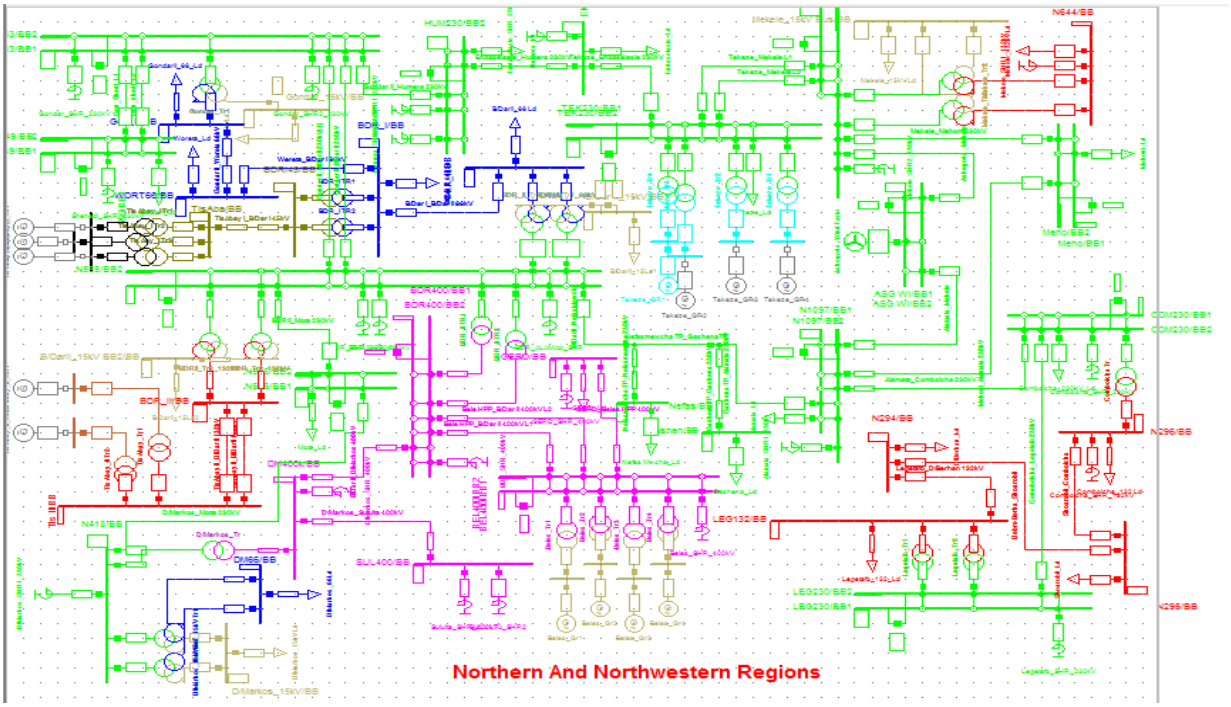

Figure F- 1 North and Northwestern regions

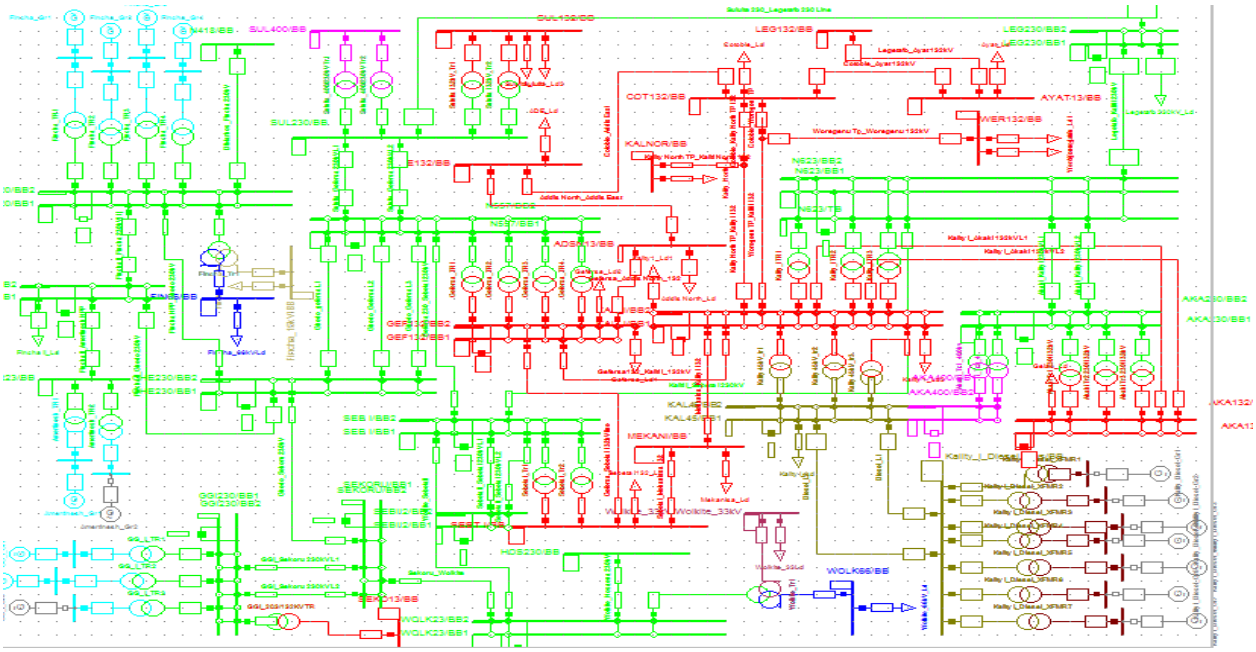

Figure F- 2 Addis Ababa, Central and Some parts of western regions

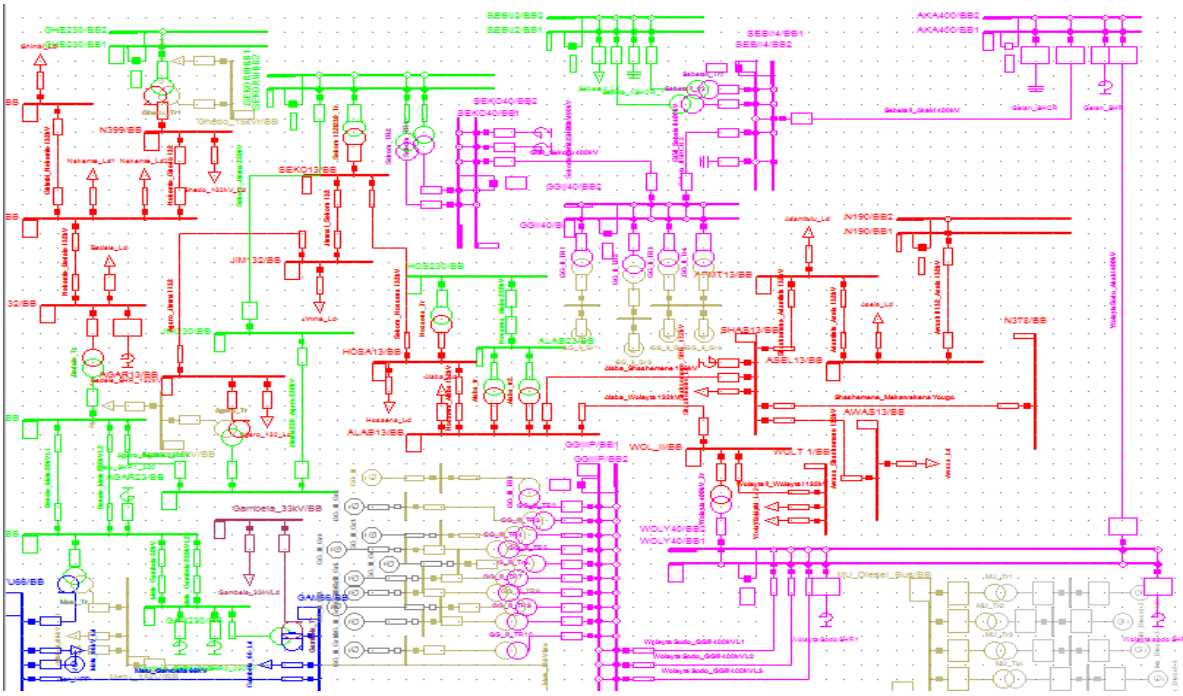

Figure F- 3 South and South Western Regions

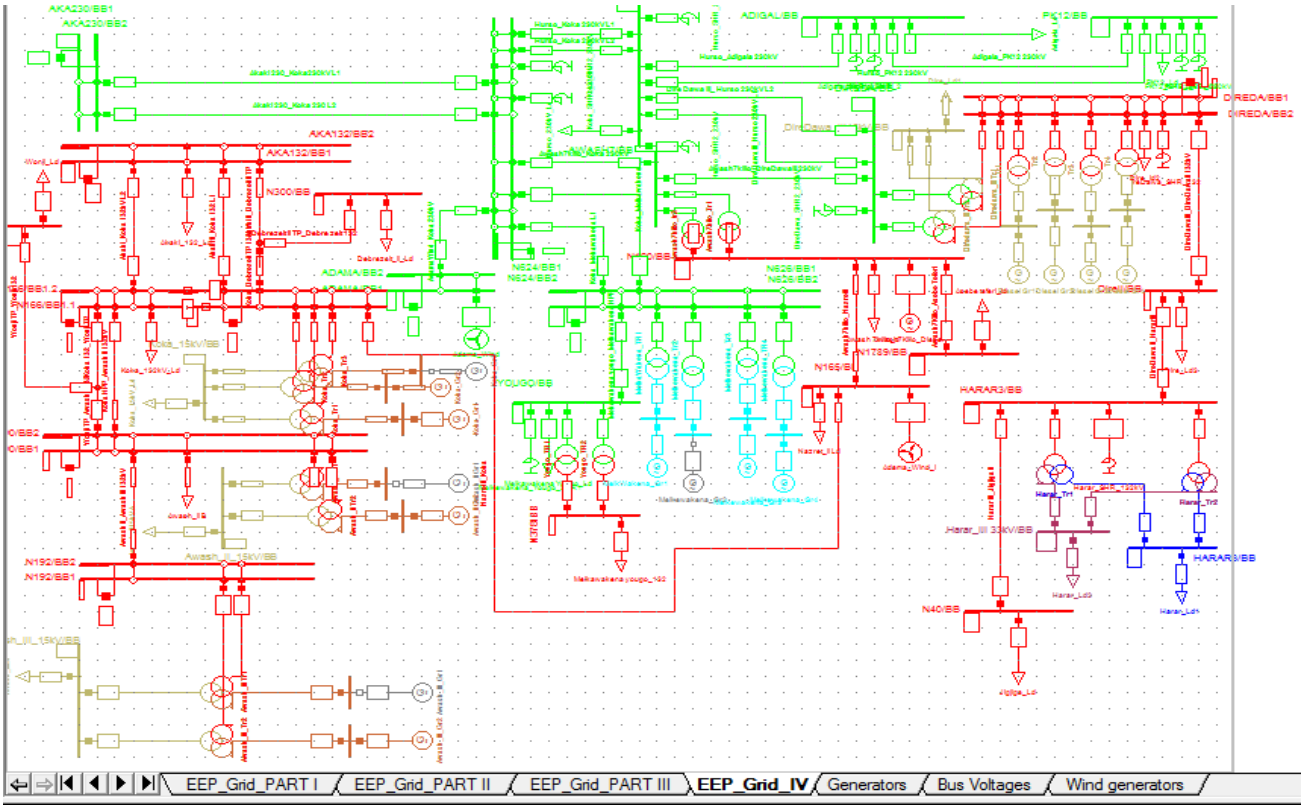

Figure F- 4 Eastern Region